Microscopía confocal de reflectancia *in vivo* en dermatología: Aplicación en el diagnóstico de tumores cutáneos

Sonia Segura Tigell

Aquesta tesi doctoral està subjecta a la llicència ***Reconeixement- NoComercial 3.0. Espanya de Creative Commons***.

Esta tesis doctoral está sujeta a la licencia ***Reconocimiento - NoComercial 3.0. España de Creative* Commons**.

This doctoral thesis is licensed under the ***Creative Commons Attribution-NonCommercial 3.0. Spain License***.

UNIVERSITAT DE BARCELONA
Facultat de Medicina

IDIBAPS
Línia Investigació Oncologia i Hematologia

TESIS DOCTORAL

MICROSCOPÍA CONFOCAL DE REFLECTANCIA *IN VIVO* EN DERMATOLOGÍA: APLICACIÓN EN EL DIAGNÓSTICO DE TUMORES CUTÁNEOS

SONIA SEGURA TIGELL
Abril 2011

Directora:
Dra. Susana Puig Sardà

IDIBAPS Institut D'Investigacions Biomèdiques August Pi i Sunyer

UNIVERSITAT DE BARCELONA

A la meva família,
als meus amics,
als meus mestres

AGRAÏMENTS

Vull agrair a la Dra. Susana Puig i al Dr. Josep Malvehy la seva amistat, suport i dedicació durant aquest llarg procés. Gràcies al Dr. Giovanni Pellacani i al seu equip per introduir-me en el camp de la microscopia confocal i per la seva càlida acollida durant la meva estància a Modena. Gràcies també al Dr. Salvador González pels seus ànims i suport a la darrera etapa d'aquest camí i per ser un mestre i referent tan excepcional. També estic en deute amb tots els adjunts del servei de dermatologia de l'Hospital Clínic per tot el que em van ensenyar durant el meu període formatiu. Vull recordar especialment als meus companys de la residència pels moments inoblidables compartits durant aquells anys. Finalment agrair al Dr. Pujol de l'hospital del Mar el seu suport a aquest projecte des del primer moment i molt especialment a tot l'equip del servei de dermatologia de l'hospital del Mar per fer del meu dia a dia a la feina un moment especial.

PRESENTACIÓN DE LA TESIS

Esta tesis es el resultado de un esfuerzo iniciado en la segunda mitad del año 2005 tras la cesión de un ejemplar de microscopio confocal de reflectancia a la Unidad de Melanoma del Servicio de Dermatología del Hospital Clínic y la concesión de una beca de final de residencia para la implementación de esta herramienta en la práctica clínica dermatológica.

El presente trabajo reúne cuatro estudios realizados con el fin de demostrar la utilidad clínica de la técnica de microscopía confocal de reflectancia *in vivo* en el estudio y manejo clínico de las neoplasias cutáneas.

Para ello, en primer lugar, se presentan los resultados de un estudio realizado de forma prospectiva con 154 tumores cutáneos con la finalidad de establecer qué parámetros de microscopía confocal se relacionan con cada diagnóstico, analizar si estos criterios son reproducibles y finalmente evaluar la correlación de estos criterios con la dermatoscopia y la histología convencional.

En segundo lugar, se estudian de forma más detallada los parámetros de microscopía confocal en melanomas gruesos y melanomas nodulares. En un tercer artículo se profundiza en las características por microscopía confocal del carcinoma basocelular pigmentado.

Finalmente, en un cuarto artículo, estudiamos la aplicabilidad de la microscopia confocal en el diagnóstico y seguimiento de pacientes con genodermatosis de alto riesgo de desarrollar cáncer cutáneo (síndrome de Gorlin i Xeroderma pigmentoso) afectos de carcinomas basocelulares múltiples y tratados con terapia fotodinámica.

ÍNDICE

1. INTRODUCCIÓN

1.1. El cáncer cutáneo en el siglo XXI

El cáncer cutáneo representa en la actualidad un problema de salud pública importante debido al progresivo aumento en su incidencia[1,2]. Dos motivos fundamentales podrían explicar esta tendencia: el envejecimiento de la población debido al aumento de la esperanza de vida y la generalización de los hábitos de recreo vinculados a la exposición solar entre la población general. En algunas áreas geográficas, como es el caso de Australia o en el sur de Chile[3], cobra un papel relevante la disminución del grosor de la capa de ozono, el principal filtro del que dispone nuestro planeta para obviar los efectos nocivos de la radiación ultravioleta.

El cáncer cutáneo más frecuente es el carcinoma basocelular, seguido del carcinoma escamoso cutáneo y del melanoma maligno. Estos tres tipos de tumores representan más del 95% de los tumores malignos de la piel. Otros tumores malignos menos frecuentes que afectan la piel incluyen los linfomas, el carcinoma de Merkel y los tumores anexiales malignos.

1.1.1. La realidad del melanoma maligno

Dentro del cáncer cutáneo, el melanoma maligno, sin ser el más frecuente tiene un interés especial debido al riesgo de producir enfermedad invasiva y la ausencia de tratamiento eficaz en estadios avanzados de la enfermedad.

La incidencia del melanoma maligno (MM) se ha incrementado en los últimos 30 años. Entre todos los cánceres en los EEUU el MM es el quinto en incidencia entre los hombres y el sexto entre las mujeres[4] pero es la segunda causa de pérdida de años productivos[5,6] y la causa más frecuente de cáncer en las mujeres entre 20 y 29 años[7]. En Europa central ha aumentado en las últimas décadas de forma similar a los EEUU, pasando de 3-4 casos a 10-15 casos por 100,000 habitantes y año. Los estudios de Cohortes de varios países parecen indicar que esta tendencia al alza se mantendrá al menos en las próximas dos décadas, por lo tanto se espera que la incidencia se doble de nuevo[8]. La incidencia más alta de melanoma se registra en Australia y Nueva Zelanda oscilando entre 40 y 60 casos por 100,000 habitantes y año. Mientras la mortalidad por melanoma aumentó en EEUU y Europa en las décadas de los 70 y 80, a partir de 1990 en muchos países puede detectarse una disminución de la mortalidad que es paralela a la disminución del Breslow y por tanto una mejoría en el diagnóstico del MM en fase inicial[8].

Un estudio reciente realizado en Cataluña[1] pone de manifiesto que al igual que en el resto del mundo, la incidencia del MM se ha incrementado en los últimos 20 años a mayor velocidad que cualquier otro tumor, especialmente en mujeres y se especula que esta tendencia probablemente se mantendrá en los próximos años. En contraposición, la mortalidad por

melanoma probablemente se mantendrá estable gracias a un diagnóstico en fases más iniciales. En dicho estudio se calcula que la incidencia cruda por 100.000 habitantes y año en el periodo 2005-2009 fue de 10,4 en los hombres y 15,7 en las mujeres. Se estima que esta incidencia aumente en los próximos 5 años a 12 y 19,7 casos por 100.000 habitantes y año en hombres y mujeres respectivamente, alcanzando dentro de 10 años valores de 13,9 en el caso de los hombres y 24,9 en las mujeres[1]. Según los datos del registro de la *Xarxa Catalana de Melanoma* la incidencia cruda de melanoma en Cataluña en el año 2007 alcanza los 10,13 casos/100000 habitantes/año, siendo la tasa ajustada por edad de 8,64 casos (datos pendientes de publicación).

Debido a la dramática disminución de la supervivencia en función del estadiaje de la enfermedad, cobra un especial interés el diagnóstico precoz de este tumor para garantizar la supervivencia de los pacientes diagnosticados de melanoma. De este modo, si la supervivencia a los 10 años en melanomas delgados (Estadio IA) es superior al 90%, cae al 80% en Estadio IB (casos con Breslow de 1 a 2 mm [o menos a 1 mm con ulceración o más de 1 mitosis/mm^2]). En estadios localmente avanzados (Breslow superior a 4mm) aún en ausencia de afectación ganglionar o metastásica en el momento del diagnóstico (Estadio IIC) la supervivencia no llega al 40%[9] (Fig. 1).

Fig. 1. Curvas de supervivencia del melanoma maligno según el grosor medido en índice de Breslow **(A)** y el estadio clínico **(B)**[9].

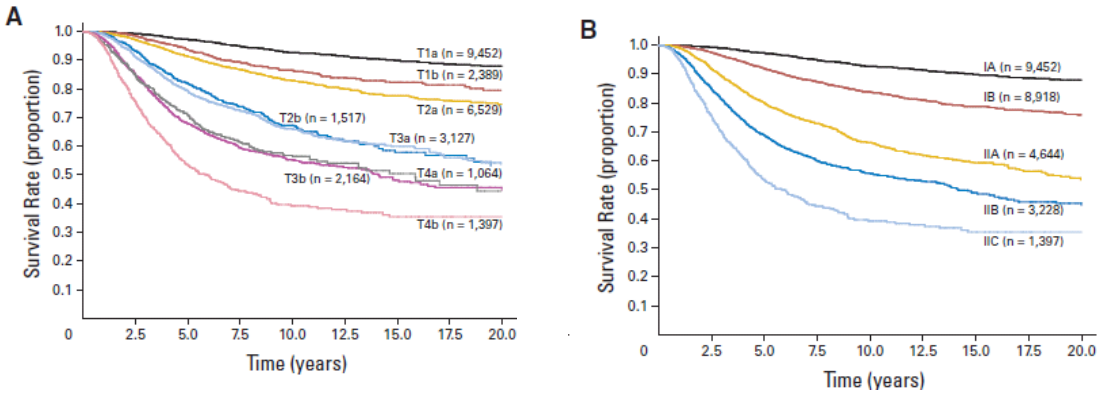

Hay básicamente dos maneras de incidir en el diagnóstico precoz del melanoma y incidir por tanto en una mejor supervivencia: las campañas poblacionales de educación y detección precoz; y sobre todo la mejora en el diagnóstico por parte de los profesionales sanitarios.

El diagnóstico precoz del melanoma es probablemente uno de los retos más importantes de la práctica diaria de cualquier dermatólogo. Sin embargo, la sensibilidad del dermatólogo clínico en el diagnóstico de melanoma se estima del 60-70%[10-12] lo cual resulta insuficiente para garantizar el correcto despistaje de un tumor potencialmente mortal.

Para ello, en las últimas décadas se han desarrollado nuevas técnicas diagnósticas con el objetivo de mejorar la precisión diagnóstica pre quirúrgica del cáncer cutáneo y especialmente

el melanoma, entre ellas destaca la microscopía de epiluminiscencia o dermatoscopia y más recientemente la microscopía confocal de reflectancia.

1.1.2. Cáncer cutáneo no melanoma. Nuevos tratamientos no invasivos

El cáncer cutáneo no melanoma (CCNM) ha experimentado una incidencia creciente en la actualidad, debido fundamentalmente al envejecimiento de la población. No existen registros oficiales ni estudios publicados sobre la incidencia del CCNM en España. Existe un estudio reciente sobre la incidencia de carcinoma basocelular (CBC) en el Barcelonés Norte[13] que obtiene una incidencia cruda de 253 casos por 100000 habitante y año (tasa ajustada por edad 195,5). En nuestra sociedad adquieren importancia técnicas de tratamiento no invasivo que garanticen un buen resultado cosmético con mínimo número de recidivas. Estos tratamientos se han ido desarrollando en los últimos 15 años y son aplicables al CBC y a los carcinomas espinocelulares (CE) intraepiteliales (enfermedad de Bowen así como las queratosis actínicas entendidas como lesiones precursoras de un carcinoma espinocelular). Si hasta los años 80 el tratamiento curativo más aceptado para el tratamiento del CBC y CE era la cirugía, en 1994 se consiguió por primera vez remisiones completas de CBC mediante un tratamiento médico, se trataba de la utilización del INF-alfa-2b intra y peritumoral[14]. Unos años más tarde, en 1998, Beuter y cols.[15] hicieron una aportación histórica, con la obtención de regresiones completas en el 80-90% de los CBCs mediante la utilización de una crema que contenía un derivado imidazólico, imiquimod 5%. Esta sustancia es capaz de inducir la apoptosis de las células tumorales mediante la producción de TNF-alfa, así como la actuación directa sobre los receptores *toll-like* 7. No tardaría en conseguirse la indicación terapéutica de la crema de imiquimod 5% en queratosis actínicas, CBC superficial y enfermedad de Bowen. Otro tratamiento en boga en los últimos años con las mismas indicaciones que el imiquimod pero con mecanismo de acción completamente distinto es la terapia fotodinámica[16-19] tal y como se desarrollará en esta introducción más adelante.

De más reciente conocimiento y aún en el campo de la investigación son las sustancias inhibidoras de la vía Hedgehog (HH). En los mamíferos existen tres homólogos HH, siendo la proteína más conocida la Sonic Hedgehog (SHH). La vía SHH es crucial para el desarrollo y mantenimiento del sistema nervioso central, esqueleto axial, pulmones y piel, entre otros. SHH se sintetiza como una proteína precursora que es secretada y ligada al receptor Patched-1 (PTCH-1), un receptor transmembrana que es responsable de la inhibición de la señal SHH. En la mayoría de los CBC existe una sobre activación de SHH, debido a una mutación inactivadora de la proteína PTCH-1[20,21]. La inhibición de la señal SHH por parte de PTCH-1 se produce mediante la inhibición de otro receptor trasmembrana denominado Smoothened (SMO). Tenemos así nuevas dianas terapéuticas para el tratamiento de los CBCs pero también de otros tumores extracutáneos como el meduloblastoma, el cáncer de páncreas y el de próstata[22].

Recientemente se ha utilizado una molécula inhibidora de SMO (Vismodegib) por vía oral en 33 pacientes afectos de CBCs avanzados o metastásicos, obteniendo respuesta en un 58% de

los casos[23]. Se están desarrollando inhibidores tópicos de esta vía para el tratamiento de CBCs en pacientes con síndrome de Gorlin en los que la vía SHH está activada por una mutación en PTCH-1.

Terapia fotodinámica

La terapia fotodinámica (TFD) se fundamenta en producir una respuesta terapéutica mediante la producción de radicales de oxígeno citotóxicos a partir de la fotoactivación de ciertas moléculas aplicadas tópicamente sobre una lesión[16-19]. Las sustancias fotoactivadoras más frecuentemente utilizadas son los derivados de las porfirinas: el ácido 5-aminolevulínico (ALA) (Levulan®, Dusa) y su forma esterificada metilaminolevulinato (MAL) (Metvix®, Galderma). Estos derivados de las porfirinas no son fotosensibilizantes por sí mismos sino que actúan como pro-fármacos que se aplican en preparados tópicos sobre la lesión durante 3-4 horas. Estas sustancias penetran a través de los epitelios dañados y son trasformados en protoporfirina IX (PpIX) que se acumula a nivel intracelular induciendo la destrucción celular. La irradiación de la lesión con una longitud de onda determinada dentro del espectro de la luz visible en presencia de oxígeno y de la PpIX produce la liberación de radicales de oxígeno que inducen la destrucción tumoral a través de distintos mecanismos, el más importante la destrucción de los lípidos de membrana. La PpIX se metaboliza en 48h, evitando por tanto una fototoxicidad prolongada. MAL ofrece ciertas ventajas respecto a ALA: 1) mayor especificidad (mayor apetencia por los tejidos neoplásicos); 2) mayor lipofilia, por tanto mayor penetración cutánea; 3) menor tiempo de aplicación (3h MAL respecto las 4 de ALA); 4) menor dolor, produce menor estimulación de las fibras nerviosas.

La TFD es un tratamiento selectivo, no invasivo, que permite el tratamiento de múltiples lesiones simultáneamente y la realización de varias lesiones si es necesario con muy buenos resultados cosméticos. Como efectos secundarios destaca el dolor en el área iluminada, eritema, edema, erosiones y costras (curación en 2-6 semanas) y las alteraciones locales de la pigmentación (que se resuelven en 6 meses).

1.1.3. Genodermatosis con riesgo de cáncer cutáneo: síndrome de Gorlin y Xeroderma pigmentoso

El síndrome de Gorlin (SG) y el Xeroderma pigmentoso (XP) son dos genodermatosis poco frecuentes de etiopatogenia distinta que tienen en común un elevado riesgo de desarrollar cáncer cutáneo no melanoma (CCNM) en edades precoces. En el caso del XP existe además un elevado riesgo de desarrollar melanoma. Ambas enfermedades requieren un abordaje en un hospital de tercer nivel, dado el elevado número de lesiones malignas que pueden desarrollar a lo largo de sus vidas, que hace fundamental un seguimiento especializado muy estrecho para minimizar la morbi-mortalidad. Estos pacientes suponen un reto tanto diagnóstico como terapéutico. Las nuevas técnicas de diagnóstico no invasivo como la dermatoscopia están demostrando su utilidad para el control de estas enfermedades[24-26]. Parece que los nuevos tratamientos inmunomoduladores tópicos (imiquimod)[27-30] así como la terapia fotodinámica

(TFD)[31-34] pueden ser de gran ayuda en estos pacientes con lesiones multifocales cuando se diagnostican en momentos iniciales.

La microscopía confocal de reflectancia *in vivo* (MCR) se nos presenta como una herramienta útil para confirmar el diagnóstico y evaluar la respuesta al tratamiento, pudiendo evitar la realización de biopsias repetidas.

Síndrome de Gorlin

El síndrome de Gorlin (SG) es un trastorno autosómico dominante caracterizado por la presencia de múltiples carcinomas basocelulares (CBC), quistes mandibulares odontogénicos, *pitting* palmo-plantar, calcificación de la hoz cerebral, espina bífida y neoplasias (meduloblastoma y fibroma ovario)[35-37]. EL SG está causado mayoritariamente por una mutación germinal en el gen supresor de tumores (PTCH) localizado en el cromosoma 9q22[38,39].

Los CBCs en el SG se caracterizan por un inicio temprano, su presencia en gran número y menos relacionado con la exposición solar que en la población general. Clínicamente las lesiones son perladas, de color de la piel o marrón que varían en número desde pocas lesiones a miles de ellas, de un tamaño que oscila de 1 a 10 mm. Las lesiones tienden a aparecer en lugares poco habituales como son los párpados y el labio superior. Con la dermatoscopia los CBC pueden detectarse en etapas iniciales antes de hacerse invasivos[24]. En esta fase las lesiones son tributarias de terapias no invasivas que permitan un tratamiento multifocal con mínima morbilidad, como imiquimod[27] y la TFD[32].

Xeroderma pigmentoso

El Xeroderma pigmentoso (XP) es un trastorno en la reparación del ADN del daño producido por la radiación ultravioleta[40,41]. Estos pacientes desarrollan gran número de lesiones tumorales en edades precoces (CBC, carcinomas escamosos, queratosis actínicas, nevus displásicos y melanoma) con un grave fotoenvejecimiento asociado[42]. El pronóstico está vinculado a la fotoprotección UV estricta, un seguimiento clínico estrecho y el diagnóstico precoz de las lesiones con instauración de un tratamiento adecuado[43]. El importante daño actínico de estos pacientes dificulta la discriminación entre benignidad y malignidad, por lo tanto el diagnóstico precoz. La dermatoscopia permite un diagnóstico más preciso de estas lesiones[25]. Con la TFD[31] y con imiquimod[28-30] se puede hacer un tratamiento simultáneo de varias lesiones en los estadios iniciales con mínima morbilidad.

1.2. Técnicas de diagnóstico no invasivo en dermatología

En los últimos 15 años han surgido distintas técnicas de diagnóstico por la imagen en diversos ámbitos de la medicina. En el campo de la dermatología, disponemos de una serie de dispositivos que permiten obtener de forma no invasiva y en tiempo real valiosa información de la piel. Estas técnicas ofrecen la posibilidad de realizar un análisis repetitivo del área afecta, ofreciendo al médico no sólo la capacidad de obtener un diagnóstico inmediato, sino también la posibilidad de monitorizar el efecto de los diferentes tratamientos a lo largo del tiempo sin causar daño alguno sobre la piel afecta[44].

En el área de la dermato-oncología, el objetivo último de muchas de estas técnicas es evitar biopsias innecesarias y garantizar un diagnóstico mejor y más temprano del melanoma maligno. Algunas de estas técnicas están aún en proceso de desarrollo y optimización, manteniéndose en el plano de la investigación. Su desarrollo va vinculado a los avances informáticos y de tecnología digital[45].

Distinguimos distintos grupos de técnicas de diagnóstico no invasivo:

1. Dermatoscopia y sistemas de microscopía de epiluminiscencia digitalizada.
2. Tecnología láser: Microscopía confocal de reflectancia, microscopía confocal de fluorescencia, tomografía óptica coherente.
3. Técnicas de imagen generales aplicadas a la dermatología: ecografía de alta frecuencia, resonancia magnética nuclear, PET-Scan.

Destacamos entre estas técnicas la microscopía de epiluminiscencia o dermatoscopia y la microscopía confocal de reflectancia que son objeto del presente proyecto y se desarrollarán en detalle en el apartados 1.2.1 y 1.2.2, respectivamente.
Otras técnicas destacadas por su difusión y aplicabilidad clínica y que describiremos brevemente son la ecografía de alta frecuencia y la tomografía óptica coherente.

Ecografía de alta frecuencia

La ecografía de alta frecuencia a 20 MHz permite la visualización *in vivo* de tejidos próximos a la superficie cutánea con una resolución axial de 50 µm y una resolución lateral de 350 µm . El principio fundamental de la ecografía es la emisión de un ultrasonido pulsado desde el transductor y el registro del sonido que retorna del tejido (el eco)[46]. La profundidad de penetración de los ultrasonidos en los tejidos es inversamente proporcional a su frecuencia, de manera que los ultrasonidos de alta frecuencia son adecuados para el estudio de estructuras cutáneas, y gracias a su localización superficial pueden ser exploradas consiguiendo mayor resolución y magnificación. Mientras los ecógrafos de 50 a 150 MHz serían útiles para el estudio de la epidermis, los de 20 mHz son ideales para el estudio de la epidermis y la dermis como es el caso de los tumores cutáneos. Las características de los distintos tumores cutáneos han sido objeto de estudio en diferentes trabajos. Sin embargo, dado que la mayor parte de ellos son hipoecogénicos, en el momento actual no es posible hacer un diagnóstico diferencial

sin los datos clínicos. La ecografía sí parece una técnica prometedora para determinar la profundidad de ciertos tumores, en especial para estimar el Breslow prequirúrgico del melanoma. Existen no obstante el riesgo de sobreestimación de Breslow en casos de presencia de infiltrado inflamatorio o nevus subyacente de manera que se ha propuesto como técnica complementaria a los datos clínicos y dermatoscópicos[47]. La determinación de la profundidad en caso del carcinoma basocelular podría permitir determinar qué tumores pueden tratarse con crioterapia u otros procedimientos no quirúrgicos como imiquimod y terapia fotodinámica. En un estudio reciente que evaluó queratosis actínicas y carcinomas basocelulares menores a 2 mm se observó una sobreestimación de la profundidad mediante esta técnica[48].

Finalmente, otras aplicaciones de la ecografía en dermatología consiste en calcular el área y volumen de la masa tumoral empleando métodos de reconstrucción tridimensional que puedan ofrecernos nuevos parámetros pronósticos[49,50].

Tomografía óptica coherente

La tomografía óptica coherente (TOC) en una técnica de imagen en desarrollo basada en la reflectancia de la luz al incidir sobre los tejidos. Ofrece imágenes de corte vertical en tiempo real con una penetración hasta 2 mm y una resolución de unas 10 micras, por lo que no permite visualizar los detalles de las células[51]. Mientras se aplica de forma rutinaria en oftalmología, su aplicación en dermatología está en proceso de investigación. Se han estudiado los anejos cutáneos así como diversas enfermedades. Tanto el cáncer de piel como diversos procesos inflamatorios cutáneos se han estudiado con buena correlación entre las imágenes tomográficas y la arquitectura histológica. En el cáncer de piel no melanoma puede ser de ayuda en el diagnóstico y medición de su profundidad. En un estudio reciente la TOC fue más precisa que la ecografía de alta frecuencia para medir el grosor de queratosis actínicas y carcinomas basocelulares menores a 2 mm, aunque se observó una tendencia a la sobreestimación de la profundidad[48].

Esta técnica podría permitir monitorizar de forma no invasiva los cambios morfológicos en respuesta al tratamiento no invasivo del cáncer cutáneo. Su precisión en el diagnóstico de procesos cutáneos tiene que ser todavía estudiada en profundidad a medida que esta nueva tecnología mejore sus prestaciones[48].

1.2.1. Microscopía de epiluminiscencia o dermatoscopia

De todas las técnicas complementarias a la exploración clínica para el diagnóstico y despistaje de melanoma la más extendida es la dermatoscopia.

Diversos estudios clínicos y metanálisis parecen demostrar que esta técnica, llevada a cabo por dermatólogos experimentados, podría mejorar la precisión diagnóstica del melanoma respecto

la exploración clínica convencional hasta en un 49%[52,53]. Según un metanálisis reciente[54] la *odds ratio* relativa para el diagnóstico de melanoma por dermatoscopia era de 15.6 (intérvalo de confianza 95% 2.9-83.7, P = 0.016) respecto al diagnóstico clínico. En este estudio los autores concluyen que la dermatoscopia es más precisa que el examen clínico convencional para el diagnóstico de melanoma ante una lesión cutánea sospechosa en un contexto clínico.

En Australia, el país con mayor incidencia de melanoma del mundo, desde el año 2009 la exploración mediante dermatoscopia está incluida y recomendada dentro de las guías nacionales para el control del cáncer cutáneo[55].

La dermatoscopia es un técnica sencilla, barata y no invasiva que permite la visualización de características morfológicas de las lesiones pigmentadas cutáneas que no son visibles en la exploración clínica convencional (Fig.2). El estudio sistemático de estas características en diversos estudios y trabajos de consenso ha permitido establecer algoritmos diagnósticos útiles para el diagnóstico de tumores cutáneos y en particular el melanoma[56].

En el mercado existen dispositivos de dermatoscopia de mano (Fig.3) y otros más complejos asociados a una cámara y a un sistema de imagen digital (microscopía de epiluminiscencia digitalizada). Los primeros son de fácil utilización en el día a día de cualquier visita dermatológica, los segundos son más aparatosos y costosos, pero nos van a permitir registrar las lesiones y hacer un seguimiento a lo largo del tiempo en pacientes de manejo clínico complejo, como son aquellos con gran número de lesiones, pacientes de alto riesgo para padecer melanoma o en casos de lesiones pigmentadas inestables.

Los instrumentos de dermatoscopia pueden utilizar luz polarizada o luz no polarizada. La primera modalidad no requiere de medio de inmersión para la visualización de las estructuras sub-macroscópicas, mientras en el caso de la luz no polarizada será necesario la utilización de aceite mineral, alcohol y en algunos casos agua para poder realizar la exploración de forma adecuada minimizando la dispersión de la luz. Mientras los dispositivos con luz polarizada serían mejores para darnos información de estructuras dérmicas, los de luz no polarizada serían más adecuados para el estudio de las estructuras intraepidérmicas[57].

Los diversos instrumentos disponibles en el mercado utilizan lentes cuya magnificación oscilan entre 10 y 40 aumentos, pero los instrumentos de mano utilizados de rutina ofrecen 10 aumentos.

Es innegable el avance que ha significado la dermatoscopia en el diagnóstico de tumores cutáneos, pero en la práctica clínica los dermatólogos se enfrentan a menudo con lesiones en las que no queda claro su origen melanocítico o no melanocítico (Fig. 4) y en caso de ser melanocíticas puede resultar muy difícil a pesar de utilizar la dermatoscopia si aquella lesión es benigna o por lo contrario se trata de un melanoma (Fig. 5). Si la lesión es única y fácilmente extirpable por el contexto del paciente y/o localización, el problema se resuelve de forma relativamente coste-eficaz con una extirpación y estudio histológico convencional. Pero a menudo nos encontramos con pacientes con múltiples lesiones de estas características, o simplemente en localizaciones donde la biopsia o extirpación puede tener importante

relevancia cosmética para el paciente. De ahí que sea necesario disponer de técnicas fiables que nos ofrezcan una información similar a la histología y sirvan de verdadero puente entre la información clínica y dermatoscópica y la biopsia convencional. Con esta intención surge la microscopía confocal de reflectancia *in vivo*.

Fig. 2. Ejemplo de lesión clínicamente no sospechosa en la espalda de un hombre de 55 años. La dermatoscopia ofrece información adicional: múltiples colores, estructuras de regresión azul-gris, glóbulos en periferia irregulares que hicieron sospechar el diagnóstico de melanoma, confirmado histológicamente (Clark II, Breslow 0,6).

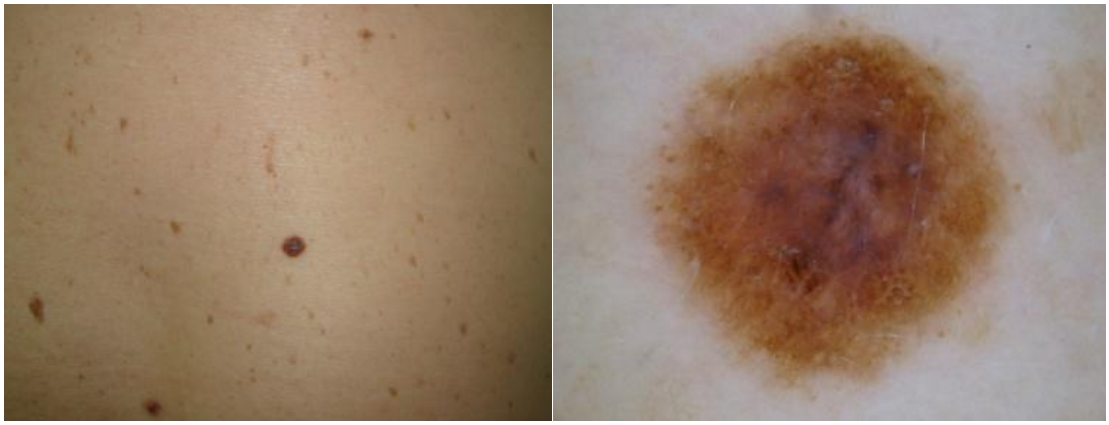

Fig. 3. Dermatoscopio de mano de luz polarizada. Esquema de su funcionamiento.

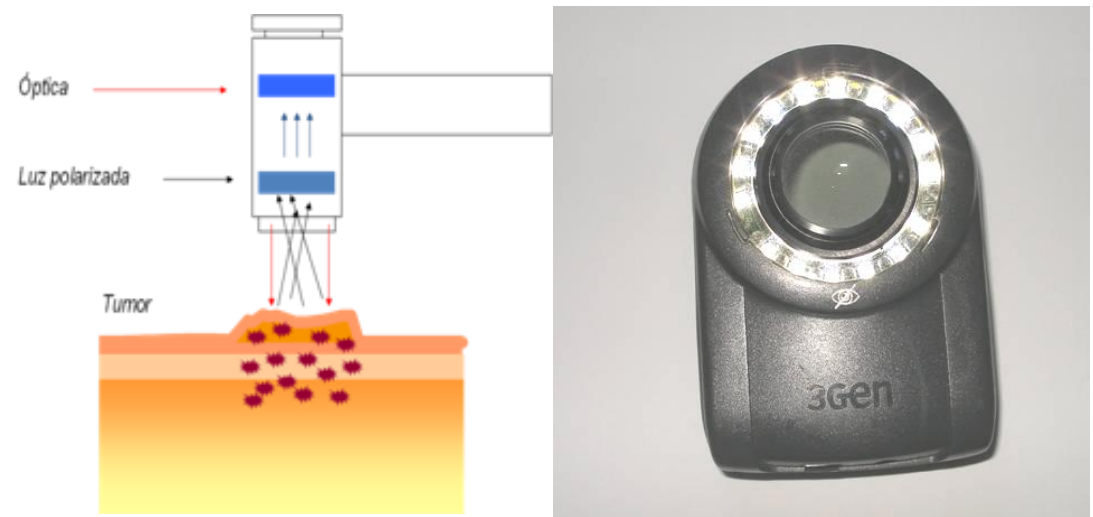

Fig. 4. Dos tumores que plantean el diagnóstico diferencial entre lesión no melanocítica (carcinoma basocelular) y melanoma tras la exploración clínica y dermatoscópica. **A)** Nódulo pigmentado facial en una mujer de 56 años. Por dermatoscopia, pigmentación homogénea con telangiectasias no enfocadas y crisálidas. Lesión sin criterios de lesión melanocítica pero tampoco criterios claros de una lesión no melanocítica. El estudio histológico demostró un carcinoma basocelular nodular. **B)** Mácula rosada focalmente pigmentada en el tórax de un hombre de 63 años. Por dermatoscopia, vascularización prominente (vasos finos lineales) con nido ovoide azul-gris y restos de pigmento melánico en el extremo derecho de la lesión, sin claros criterios de lesión melanocítica pero tampoco criterios claros de CBC. Se trataba de un melanoma hipopigmentado.

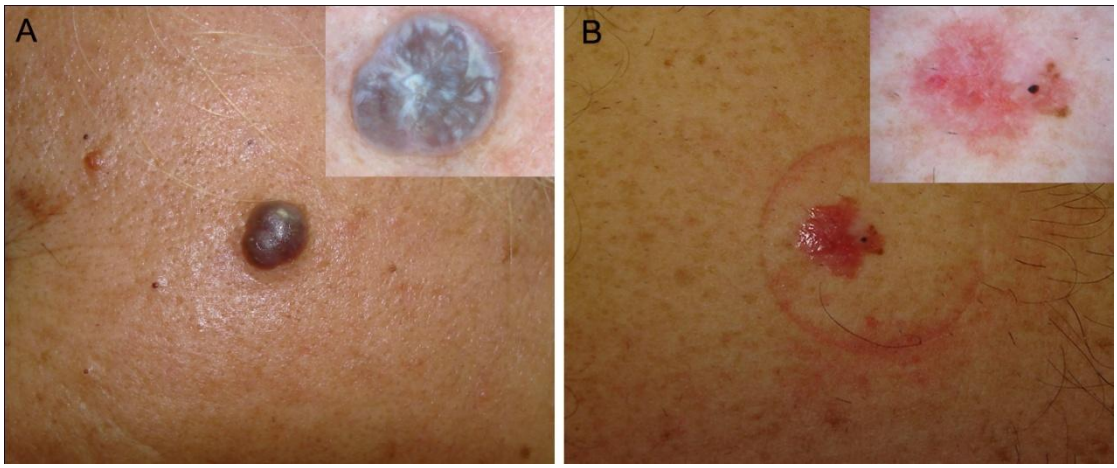

Fig. 5. Dos lesiones melanocíticas de difícil diagnóstico tras exploración clínica y dermatoscópica. Se trata de lesiones pigmentadas de menos de 6 mm en pacientes con síndrome del nevus con atipia clínica en seguimiento con dermatoscopia digital. En ambos casos se observa por dermatoscopia la presencia de estructuras de regresión en más del 50% de la lesión que sugiere la posibilidad de melanoma a pesar de la ausencia de otros criterios positivos para dicho tumor. El estudio histológico confirmó el diagnóstico de melanoma (Estadio IA).

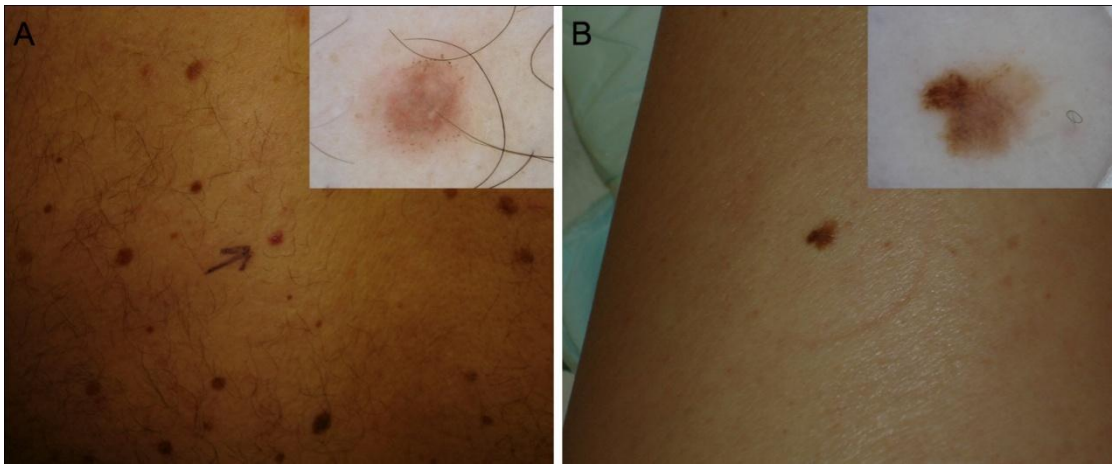

1.2.2. Microscopía confocal de reflectancia

a) Concepto e historia

La microscopía confocal de reflectancia (MCR) es una técnica de imagen no invasiva que utilitza una luz láser y el principo de *confocalidad* (ver más adelante) para el estudio *in vivo* (o *ex vivo*) de tejidos humanos. Se trata de un microscopio, por tanto de un instrumento con una resolución comparable a la obtenida por el microscopio óptico. Su principal limitación es la pofundidad que viene dada por la baja potencia del láser y varía de 200 a 250 µm según el tejido.

En los últimos 15 años la MCR se ha utilizado y extendido en diversos ámbitos de la medicina, en todas aquellas especialidades que estudian el recubrimiento externo o interno del cuerpo humano y por tanto tienen fácil acceso desde el exterior. Por ello la mayor repercusión la ha tenido en dermatología, pero existen también diversos trabajos en otras áreas y especialidades del conocimiento médico como son la ginecología[58], la oftalmología[59] y la endoscopia digestiva[60,61] (Fig.6). También se ha utilizando la microscopía de reflectancia *ex vivo* en el estudio de biopsias hepáticas[62] y más recientemente en cáncer de mama[63,64].

El microscopio confocal de escaneo (*Confocal Scanning Microscope*) fue inventado y patentado en 1957 por Marvin Minsky, becario postdoctoral en la Universidad de Harvard (Minsky M. Microscopy apparatus. US Patent Nº 3013467; 1957). Sin embargo, se necesitó del desarrollo de la tecnología láser y de la informática para poder tomar imágenes *in vivo*. Desde la década de los 80 se ha utilizado la MCR para estudiar tejido animal y humano *in vivo*. La primera publicación en la bibliografía en la que se consigue explorar la piel humana *in vivo* data de 1993 por un grupo francés[65] (Fig. 7). Dos años más tarde, un grupo de Harvard[66] reporta en el *Journal of Investigative Dermatology* la visualización de la piel humana con un prototipo del microscopio confocal que la empresa americana Lucid comercializará poco después con el nombre de Vivascope® (Fig. 8-10)[67]. Desde entonces y en especial en los últimos 5 años se han sucedido un número exponencial de publicaciones de distintos grupos de trabajo de todo el mundo para intentar establecer las bases del diagnóstico de lesiones cutáneas (tumorales sobre todo pero también inflamatorias e infecciosas) mediante microscopía confocal. Para ello ha sido clave la constitución en el año 2006 de un grupo internacional de trabajo en microscopía confocal (*International Confocal Working Group*). Este grupo se reúne dos veces al año desde el año 2008 coincidiendo respectivamente con las reuniones anuales de la Academia Americana de Dermatología y la Academia Europea de Dermatología y Venereología y tiene como finalidad la investigación y la docencia en microscopía confocal. Del trabajo de dicho grupo han surgido importantes publicaciones que constituyen la base para la futura aplicación de la microscopía confocal en la práctica clínica. Entre ellas destaca un trabajo que recoge la terminología de consenso en microscopía confocal[68]; el estudio multicéntrico de correlación de los parámetros de microscopía confocal

con la dermatoscopia y la histología, llevado a cabo por el grupo de Módena y el grupo de Barcelona[69] (Anexo III) y el reciente estudio de reproducibilidad de los parámetros de microscopía confocal[70].

Fig. 6. **Endomicroscopía confocal. A**, Equipo comercial de endomicroscopía confocal de fluorescencia. Se administra fluoresceína endovenosa para realzar el contraste de las células. **B**, Imagen mosaico de una mucosa de colon de aspecto normal. **C**, Aspecto por endomicroscopía confocal de un adenoarcinoma de colon.

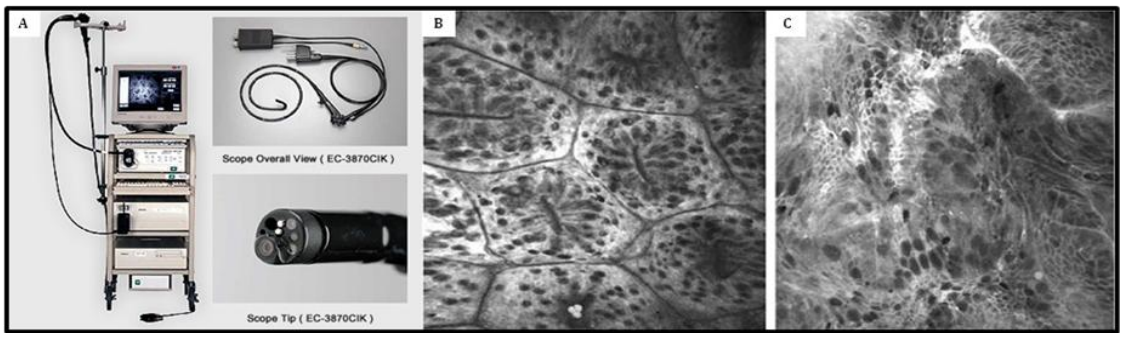

Fig. 7. Primera publicación literatura dermatológica de microscopia confocal reflectancia *in vivo*[65].

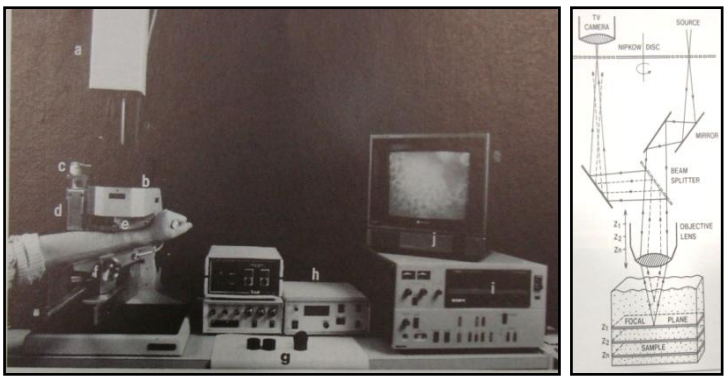

Fig. 8. Primer microscopio confocal comercializado por Lucid para el estudio *in vivo* de la piel (Vivascope® 1000).

Fig. 9. **Primera publicación de microscopía confocal utilizando la versión comercial del microscopio confocal (Vivascope®, Lucid, Henrietta, NY).** En este trabajo se expone la correlación de las estructuras histológicas de la piel normal (en cortes horizontales) con los cortes obtenidos por microscopía confocal[67].

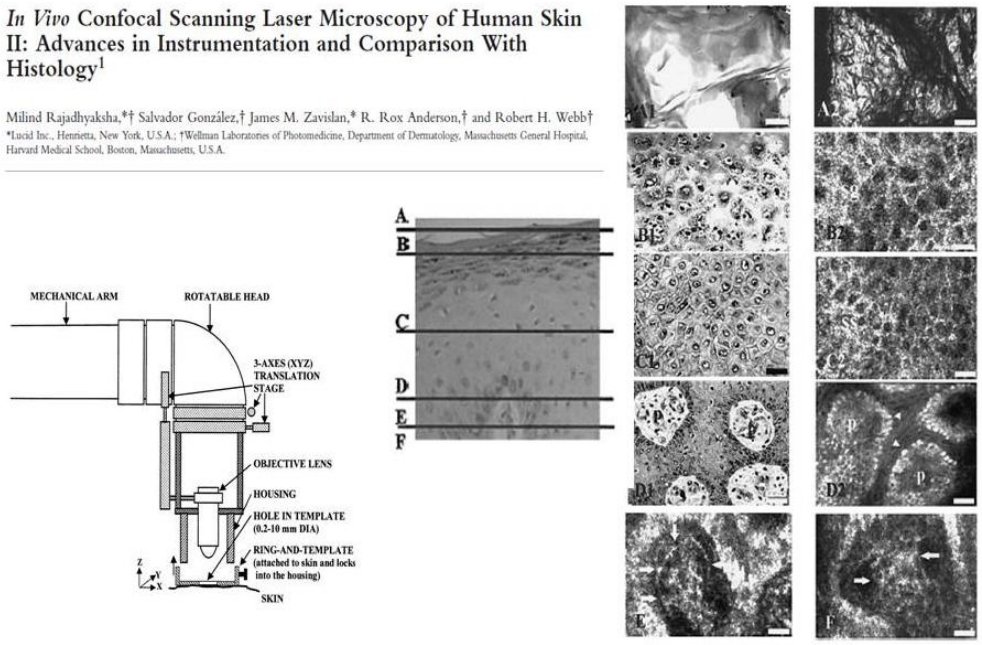

Fig. 10. Modelo comercial actual de microscopía confocal de reflectancia *in vivo*. **A,** Equipo completo con el cabezal, brazo articulado y sistema informático. **B,** Detalle del cabezal del equipo donde se sitúa el láser y el sistema óptico, con sistema de acoplamiento a la superficie cutánea.

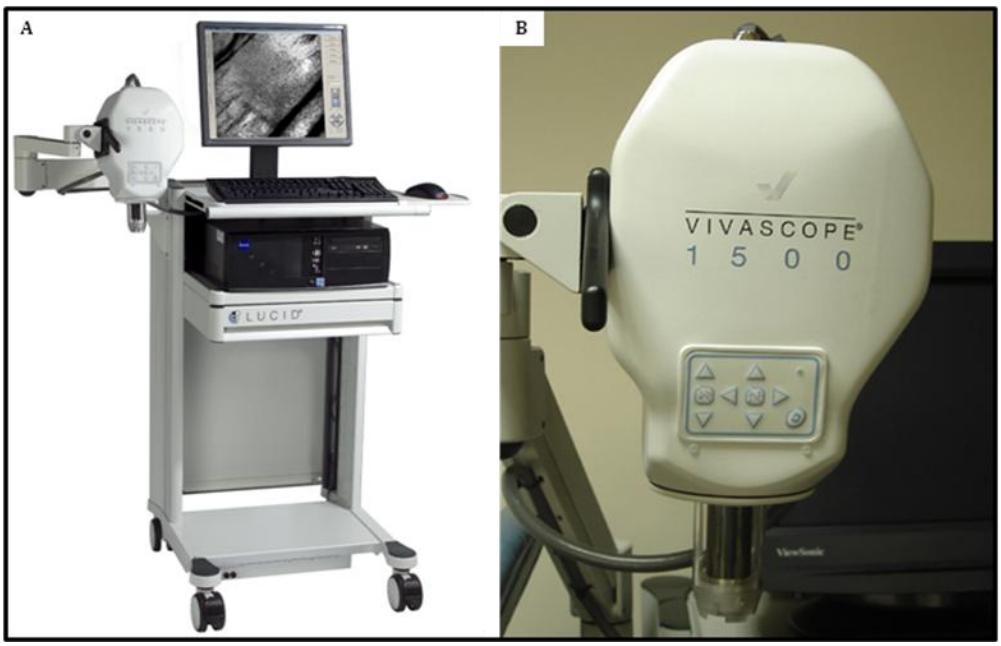

b) Bases físicas del funcionamiento y utillaje

Confocalidad

La microscopía confocal permite la visualización de estructuras microscópicas situadas bajo la superficie en muestras gruesas de tejido, gracias a un proceso óptico capaz de eliminar la información fuera de foco. Sólo aquella luz reflejada que procede del plano conjugado (confocal) pasará a través de un detector de orificio muy pequeño, aislando ópticamente el plano focal de las estructuras circundantes[71] (Fig. 11). De esta manera es posible que el plano focal esté situado debajo de la superficie del tejido, y se pueden obtener imágenes microscópicas de muestras más gruesas que el plano focal. Esta capacidad de realizar cortes ópticos sin necesidad de manipular y cortar el tejido permite que los tejidos puedan ser examinados en su estado original, sin los artefactos derivados del procesamiento de laboratorio, y permite estudiar *in vivo* y en tiempo real eventos tisulares dinámicos.

Fuente de luz

El microscopio confocal de reflectancia utiliza como fuente de luz un láser de potencia muy baja (menos de 30mW) con una longitud de onda cercana al infrarrojo (800-1064 nm) (Fig. 12). Los dispositivos comerciales disponibles en el mercado disponen de un láser de longitud de onda de 830 nm. La baja potencia del láser garantiza la total inocuidad para el tejido humano. La contrapartida es la limitada profundidad, que varía de 200 a 250 micras, pero es suficiente para llegar a la parte superior de la dermis reticular.

Principio de reflectancia

El láser incide sobre el tejido y el detector va a captar la luz retrodispersada una vez atravesado el tejido. Esta retrodispersión dependerá de dos factores:
1. Variaciones en el índice de refracción dentro del tejido.
2. El tamaño de la estructura que está siendo iluminada.

Cuando el tamaño de la estructura iluminada es similar a la longitud de onda de la luz, la retrodispersión es mayor. Esto es lo que ocurre con los melanosomas que producen una gran reflectancia, no sólo por el alto índice de refracción de la melanina sino también porque tienen un tamaño similar a la longitud de onda del láser.

Resolución

La resolución de un microscopio (o la capacidad del mismo de diferenciar dos puntos separados como distintos) depende de tres factores:

1. El tamaño del orificio del detector (*pinhole*).
2. La apertura numérica del objetivo.
3. La longitud de onda del láser.

Si bien las longitudes de onda mayores pueden penetrar más en el tejido tienen la contrapartida de tener menos resolución lateral. El microscopio comercial utilizado para el estudio de la piel utiliza un láser de 830nm y unas lentes de 30 aumentos con apertura numérica 0,9, lo que le confiere una resolución lateral de aproximadamente 1 µm y una resolución vertical (grosor del corte) de 3 a 5 µm. Esta resolución en equivalente a la obtenida por un microscopio óptico y permite el estudio de la arquitectura tisular pero también de las células.

Utillaje

El dispositivo de microscopía confocal de reflectancia comprende distintos elementos y aplicaciones además del microscopio láser en sí mismo. Estos componentes son:

Brazo articulado

Va a permitir aplicar el microscopio sobre distintas superficies para estudiar distintas áreas anatómicas con la máxima comodidad para el paciente y el explorador (Fig. 10).

Cámara de dermatoscopia

Esta herramienta está acoplada al microscopio y permite obtener imágenes de dermatoscopia con la misma orientación que las imágenes de microscopía confocal, permitiendo establecer correlaciones entre las estructuras dermatoscópicas y las imágenes de microscopía confocal, así como facilitando la orientación espacial dentro de la lesión (Fig. 13).

Medio de contacto

Las lentes utilizadas son de inmersión en agua pues el índice de refracción de ésta es 1.33 que es cercano al de la epidermis (1.44), lo cual minimiza las aberraciones esféricas causadas por el paso de la luz a través de la interfase tejido-aire. De este modo se utiliza agua o geles acuosos como medio de interfase (Fig. 14).

Sistema de fijación

El movimiento de la piel es una limitación importante para la toma de imágenes *in vivo*. Para evitar que las imágenes aparezcan borrosas y al mismo tiempo tener un receptáculo para contener el material de inmersión se utiliza un dispositivo de contacto. Éste consiste en un anillo de acero que se adhiere por un lado a la piel mediante un adhesivo desechable y al microscopio mediante imán (Fig.14).

Aplicativos para la obtención de imágenes secuenciales

La imagen obtenida representa 0,5x0,5 mm de tejido a una resolución de 1000x1000 píxeles, lo que equivale a la obtenida con un objetivo de 30x con un microscopio óptico (Fig. 15B).

El microscopio confocal dispone de unas aplicaciones que permiten obtener imágenes secuenciales en el plano horizontal (mosaicos) y el plano vertical.

La iluminación secuencial (escaneo*)* de múltiples píxeles en el plano focal, va a generar una imagen en mosaico en dos dimensiones (que puede ser de 1x1 hasta 8x8 mm), lo que permite la evaluación de la arquitectura tisular (Vivablock®) (Fig. 13D y 15A).

Por otro lado, la obtención de imágenes secuenciales en el plano vertical permite evaluar de forma rápida distintas profundidades del tejido en un punto determinado del plano horizontal (Vivastack®) (Fig. 15C).

Finalmente existe la posibilidad de obtener vídeos de las áreas de interés gracias a una aplicación que obtiene imágenes del mismo plano a lo largo del tiempo y permite estudiar eventos dinámicos como la circulación sanguínea.

Fig. 11. Esquema del funcionamiento del microscopio confocal. La pequeña apertura del detector (*pinhole*) permite que sólo la información situada en el plano focal pueda ser detectada, eliminando la derivada de las estructuras circundantes. Con permiso, González y cols[71].

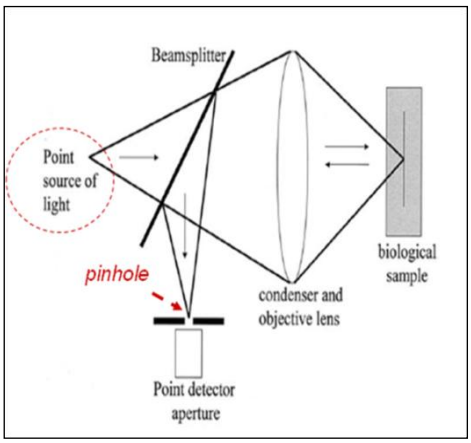

Fig. 12. Esquema del funcionamiento del microscopio confocal de reflectancia. Con permiso, Salvador González. An Atlas of Confocal Images of Human Skin In Vivo. 2nd Edition. Lucid, Inc. 2005.

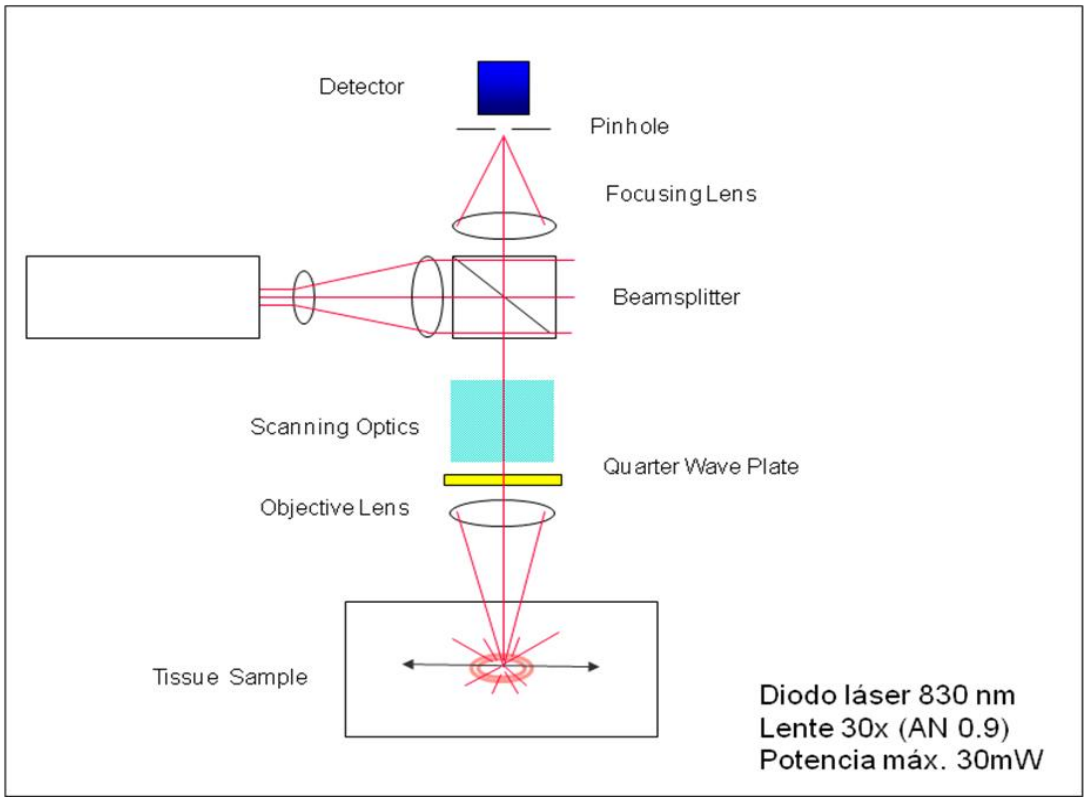

Fig. 13. **A,** Sistema de dermatosopia acoplado al microscopio confocal (Vivacam®). **B**, Imagen de dermatoscopia de un carcinoma basocelular tomada con Vivacam®. **C,** Esquema de la superficie explorada con el microscopio confocal, señalando las áreas de las que se han recogido imágenes. **D**, Obtención de un mosaico de la lesión de 4x4 mm mediante microscopía confocal.

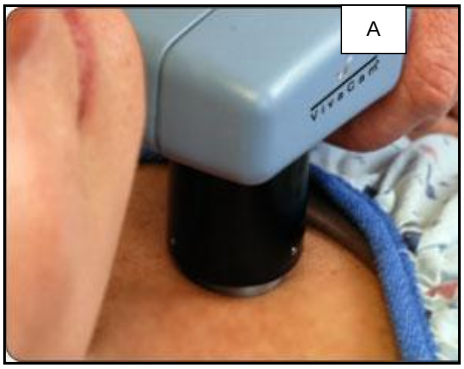

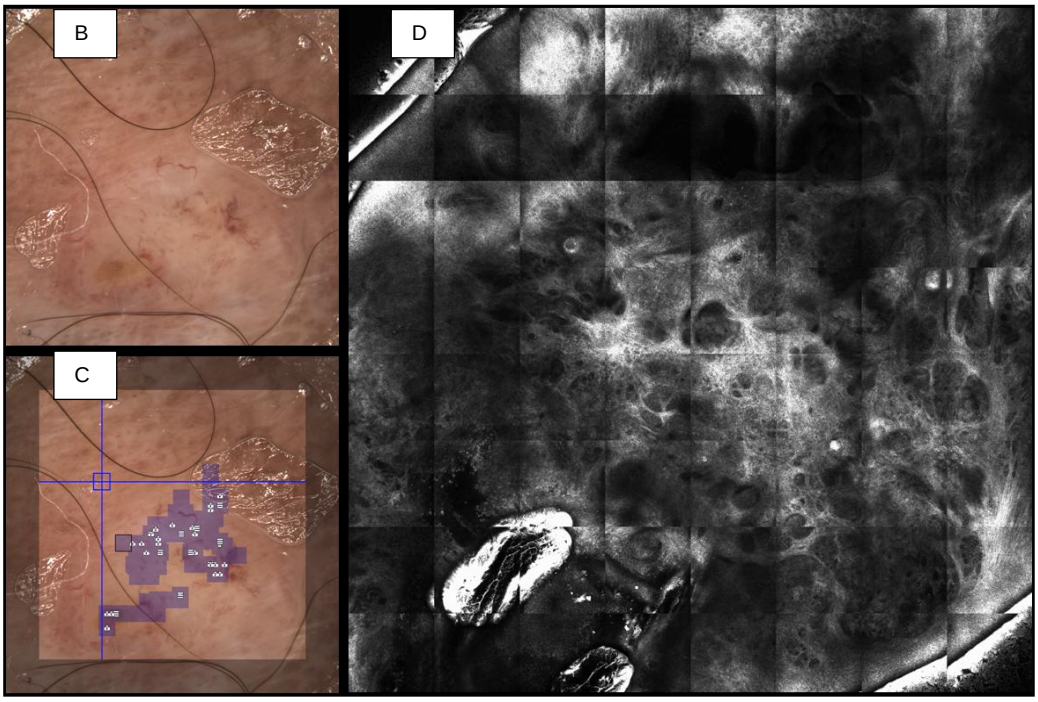

Fig. 14. Sistema de acoplamiento del microscopio confocal a la piel. Se realiza mediante un anillo de acero adherido a la piel por un adhesivo desechable y al microscopio por un imán. Gel acuoso utilizado como medio de contacto.

Fig. 15. Aplicativos para la obtención de imágenes secuenciales de microscopía confocal de reflectancia (MCR). A, Mosaico (Vivablock®) de 4x4 mm formado por 64 imágenes consecutivas en el mismo plano focal. Cada una de las imágenes representa 0,5x0,5mm en el plano horizontal. **B,** Imagen de MCR 0,5x0,5 mm a de la entrada de un folículo piloso a nivel de estrato córneo. **C,** Imágenes secuenciales en el plano vertical (Vivastack®) del mismo folículo piloso desde la capa granulosa a la dermis superficial.

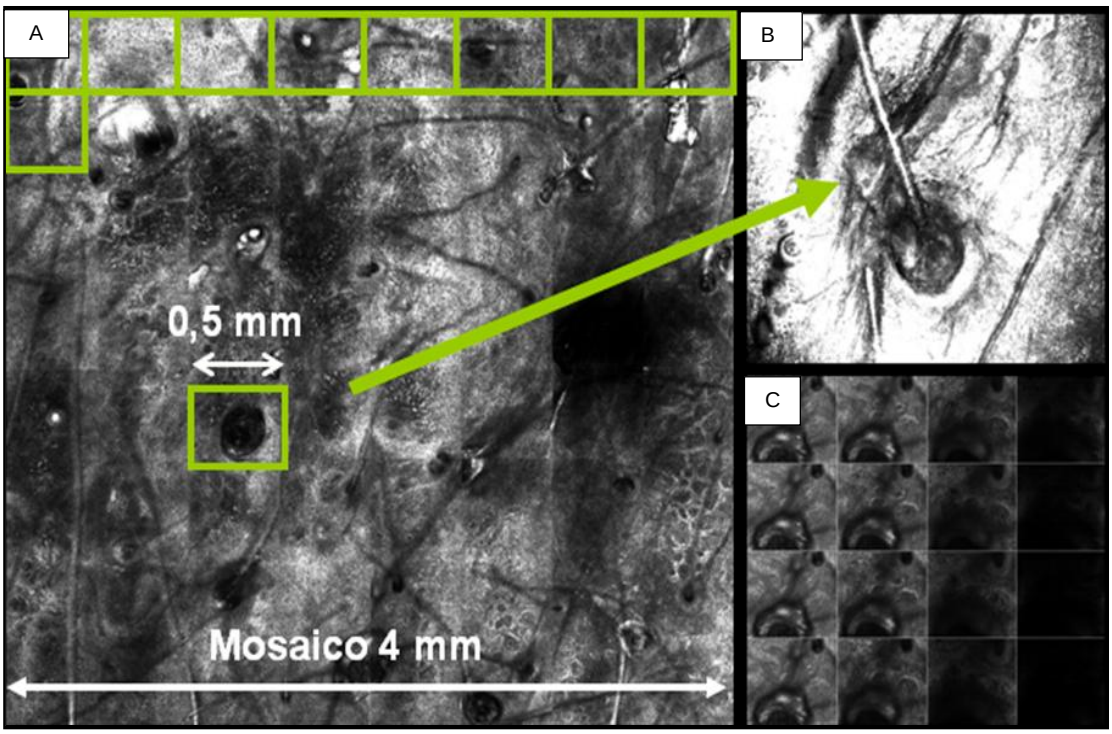

c) Aplicaciones en dermatología

La MCR se ofrece como una técnica complementaria a la dermatoscopia y a la histopatología convencional que puede establecer un puente entre ambas, una ventana abierta a la arquitectura tisular y a las mismas células para aumentar nuestra precisión diagnóstica de las lesiones cutáneas, y por tanto nuestra sensibilidad y especificidad para el diagnóstico de cáncer cutáneo. Con ello sería posible disminuir el número de biopsias que se realizan para mejorar el ratio entre biopsia realizada y diagnóstico de melanoma.

Si bien no puede sustituir a la histología convencional, la MCR ofrece ciertas ventajas respecto a aquélla, como el hecho de no requerir exéresis de tejido y por tanto ahorrar dolor y cicatrices a los pacientes; ausencia de daño tisular; y no se ve alterada por artefactos de laboratorio secundarios al procesamiento y tinción de la muestra. El hecho que la MCR trabaje en tiempo real acelera el tiempo de diagnóstico y permite evaluar cambios de la misma lesión así como respuestas a tratamientos [44].

En cirugía dermatológica puede servir de guía para la demarcación de márgenes en lesiones mal delimitadas o guiar el lugar más adecuado donde realizar una biopsia en casos de lesiones extensas [72,73]. En su versión *ex vivo* la MCR representa una valiosa promesa para el control de márgenes quirúrgicos en la cirugía de Mohs de forma más rápida que la histología convencional [74-76].

Por otro lado, como ya se ha comentado más arriba, puede ser útil para monitorizar la respuesta a tratamientos no invasivos con inmunomoduladores tópicos como el imiquimod[77,78] u otros procedimientos como la terapia fotodinámica en algunos tumores cutáneos.

La mayor difusión de la MCR se ha producido en el campo de la dermato-oncología, que es también el objeto de nuestro trabajo. Los trabajos iniciales hasta 2005 se centraron principalmente en el estudio del carcinoma basocelular [79-81] y las lesiones melanocíticas (nevus y melanoma)[72, 73, 82-90]. Más recientemente se ha extendido su aplicación en el estudio de queratosis actínicas y carcinoma espinocelular [91-94]. En los primeros años se utilizó de forma aislada en diversos tumores cutáneos benignos como las hiperplasias sebáceas[95], los angiomas seniles[96] o en el poroma ecrino[97]. Con los años la técnica se ha extendido al estudio de procesos inflamatorios como la psoriasis[98,99] dermatitis de contacto[100,101] esclerodermia[102], lupus eritematoso cutáneo[103] o xantogranuloma juvenil[104]. También ha demostrado ser útil para detectar procesos infecciosos *in vivo* y de forma inmediata, tales como foliculitis[105], onicomicosis[106,107], infecciones por herpes [108], escabiosis[109] o sífilis[110]. Recientemente se ha reportado su utilidad en el melasma[111] o en la ocronosis exógena[112] (Anexo II) para la evaluación de la respuesta al tratamiento. Finalmente, en un trabajo aislado, se ha estudiado la utilidad de la MCR en el diagnóstico de la micosis fungoides guiando el lugar más apropiado para realizar la biopsia[113].

Fig. 16. Microscopía confocal *ex vivo*. A, Modelo comercial de microscopia confocal *ex vivo.* **B**, Publicación sobre la aplicación de la microscopía confocal *ex vivo* en la detección de carcinoma basocelular durante la cirugía de Mohs[76].

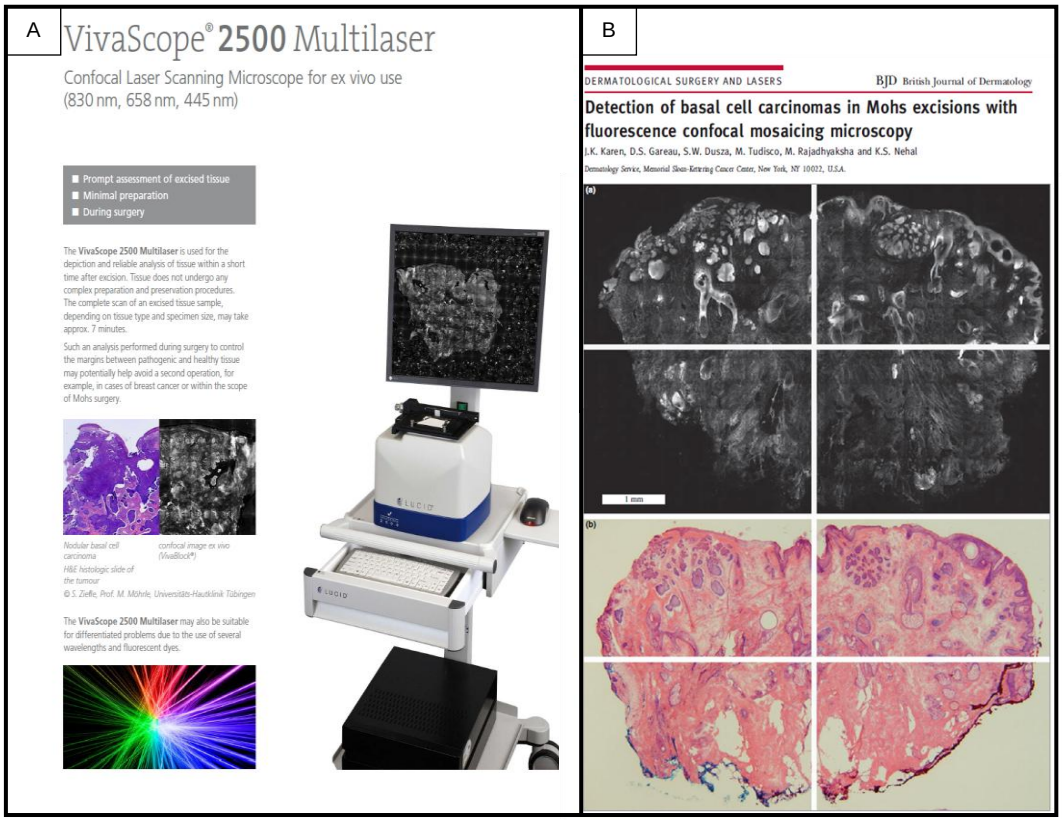

d) Dificultades y promesas

A pesar de que la microscopía confocal de reflectancia (MCR) es una técnica absolutamente prometedora en el campo de la dermatología y otras muchas especialidades, en el momento actual existen una serie de limitaciones técnicas que en el futuro deben optimizarse para poder establecer esta técnica como una herramienta útil en la práctica clínica habitual.

La principal limitación viene dada por la dificultad de evaluar las lesiones en profundidad, dada la pérdida de resolución de la herramienta por debajo de la dermis papilar. Este hecho impide estudiar el comportamiento profundo de lesiones tumorales infiltrativas, o evaluar lesiones en las cuales es esencial el estudio del componente dérmico profundo, como es el caso de algunos nevus de Spitz, para distinguirlos del melanoma. Otras lesiones como los nevus azules o los dermatofibromas ven dificultado su estudio mediante esta técnica por situarse predominantemente en la dermis. Las lesiones hiperqueratósicas o las superficies acrales también son de difícil exploración mediante MCR debido a la dificultad de penetración de la luz láser si la capa córnea está engrosada. Por otro lado, hay situaciones en las que las lesiones no tienen contraste suficiente para hacer un diagnóstico. El desarrollo en un futuro de sustancias exógenas inocuas que aumenten el contraste de las estructuras tisulares puede ofrecer una solución a esta limitación.

Además de las limitaciones inherentes a la técnica, existen otras de tipo logístico y económico. Por ello, a pesar de haberse optimizado el equipo comercial de MCR desde su primera versión, sigue siendo una herramienta voluminosa e incómoda en ciertas localizaciones, tales como en la región periocular, el pabellón auricular, la región interdigital o las mucosas. Por otro lado, la MCR es una herramienta coste económico elevado que dificulta su difusión y progresiva aplicación en los centros hospitalarios del sistema público de salud. A pesar de la optimización del *software* para su mayor funcionalidad y velocidad, en el momento actual el tiempo requerido para realizar una exploración mediante MCR es superior al necesario en un examen clínico y dermatoscópico.

El futuro de esta herramienta pasa además por el desarrollo de sistemas acoplados a una fibra óptica que permita el acceso a ciertas localizaciones imposibles de acceder en el momento actual; el desarrollo de modelos "de mano" más cómodos y menos voluminosos; y la mejoría de la calidad de la imagen, optimizando el contraste y la resolución en profundidad. Sería también de gran utilidad el desarrollo de un programa informático específico que permita la reconstrucción tridimensional de las imágenes.

La experiencia mundial en esta técnica es aún escasa, por ello son necesarios grupos de estudio para estandarizar la técnica y optimizar su aplicación en el diagnóstico de las lesiones cutáneas.

2. HIPÓTESIS DE ESTUDIO Y OBJETIVOS

2.1 Hipótesis de estudio

- La microscopía confocal de reflectancia *in vivo* (MCR) es una técnica no invasiva que permite obtener un diagnóstico de forma inmediata y en tiempo real de patología cutánea tumoral con una precisión diagnóstica que se acerca al diagnóstico histológico convencional.

- Los criterios diagnósticos de los tumores cutáneos mediante MCR son reproducibles y su aprendizaje factible con un curso de iniciación específico.

- La MCR puede permitir un seguimiento clínico de respuesta a tratamientos no invasivos de patología tumoral (terapia fotodinámica).

- Los pacientes con genodermatosis con alto riesgo de desarrollar cáncer cutáneo se pueden beneficiar del tratamiento con terapia fotodinámica dado la afectación multifocal y el difícil manejo clínico con tratamientos convencionales.

2.2. Objetivos

- Establecimiento de los parámetros de microscopía confocal de reflectancia *in vivo* (MCR) para el diagnóstico de la patología tumoral cutánea más frecuente.

- Cálculo de sensibilidad y especificidad de la MCR para el diagnóstico de melanoma frente nevus, carcinoma basocelular, carcinoma escamoso, queratosis actínica, queratosis seborreica, dermatofibroma y angioma.

- Estudio de la reproducibilidad inter-observador de los parámetros de MCR para el diagnóstico de patología tumoral cutánea.

- Correlacionar los parámetros de MCR con la dermatoscopia y la histología.

- Determinar la utilidad de la MCR para evaluar la respuesta al tratamiento con terapia fotodinámica de carcinomas basocelulares en pacientes afectos de síndrome de Gorlin y Xeroderma pigmentoso.

3. RESULTADOS

3.1. Trabajo I

Development of a two-step method for the diagnosis of melanoma by reflectance confocal microscopy
Sonia Segura, Susana Puig, Cristina Carrera, Josep Palou, Josep Malvehy
J Am Acad Dermatol 2009;61:216-29

Objetivos:
Desarrollar un algoritmo diagnóstico para la clasificación de tumores cutáneos mediante microscopía confocal de reflectancia (MCR).

Métodos:
Evaluación mediante MCR de 154 tumores cutáneos (100 lesiones melanocíticas [LM] y 54 lesiones no melanocíticas [LNM]) previa a su extirpación y estudio histopatológico. Análisis a ciegas de los criterios de MCR en imágenes almacenadas y estudio estadístico para determinar la asociación de cada característica de MCR con un tumor concreto. Estudio de la reproducibilidad de dichos parámetros y correlación de los mismos con la dermatoscopia y la histología.

Resultados:
Cuatro características observables mediante MCR permiten diferenciar las LM de las LNM: patrón epidérmico en empedrado, crecimiento pagetoide, presencia de nidos celulares en la dermis y presencia de papilas dérmicas bien definidas en toda la lesión. Dentro de las LM, la presencia de células redondas en estratos suprabasales y la presencia de células nucleadas atípicas en la dermis se asociaban a melanoma; mientras la presencia de papilas dérmicas con contorno reflectante (anillos basales) así como la presencia de células basales típicas, se asociaban a nevus. Basándonos en la reproducibilidad y correlación histológica y dermatoscópica de los criterios de MCR, se desarrolló un algoritmo en dos etapas para el diagnóstico de melanoma consiguiendo una sensibilidad del 86,1% y especificidad del 95.3%.

Development of a two-step method for the diagnosis of melanoma by reflectance confocal microscopy

Sonia Segura, MD,[a,b] Susana Puig, MD,[a,c] Cristina Carrera, MD,[a] Josep Palou, MD,[a] and Josep Malvehy, MD[a,c]
Barcelona, Spain

Background: Reflectance confocal microscopy (RCM) has been shown to improve accuracy in the differentiation of nevus from melanoma, but only a few studies have evaluated both melanocytic lesions (ML) and non-ML.

Objective: We sought to develop an algorithm for the in vivo diagnosis of skin tumors by RCM.

Methods: In 143 patients we evaluated 154 skin tumors (100 melanocytic, 54 nonmelanocytic) by RCM before their excision. We analyzed RCM features on stored images and performed univariate and multivariate analyses to determine the association of RCM features with tumor types.

Results: Four confocal features differentiated ML from non-ML: cobblestone pattern of epidermal layers, pagetoid spread, mesh appearance of the dermoepidermal junction, and the presence of dermal nests. Within ML, the presence of roundish suprabasal cells and atypical nucleated cells in the dermis was associated with melanoma, and the presence of edged papillae and typical basal cells was associated with nevi. Based on the correlation of RCM features with dermatoscopy and histology, we developed a two-step algorithm for the diagnosis of skin tumors by RCM.

Limitations: This is a preliminary study, and the results must be validated in further studies with a larger number of cases.

Conclusion: RCM appears to be helpful in improving the presurgical diagnosis of difficult skin tumors. (J Am Acad Dermatol 2009;61:216-29.)

Key words: basal cell carcinoma; dermatoscopy, melanoma, reflectance confocal microscopy, skin cancer.

New diagnostic techniques have been developed in recent years to improve accuracy in the diagnosis of skin cancer, especially early melanoma.[1] Dermatoscopy has been shown to improve sensitivity and specificity in the diagnosis of melanoma and is now widely accepted by dermatologists as an adjuvant technique in clinical practice.[2] However, physicians frequently deal with lesions that are difficult to diagnose, even with dermatoscopy, and differentiating between melanocytic and nonmelanocytic origin may be challenging. To improve diagnostic

Abbreviations used:

BCC:	basal cell carcinoma
CPN:	presence of cobblestone pattern, pagetoid spread, or dermal nests
DEJ:	dermoepidermal junction
DP:	dermal papilla
ML:	melanocytic lesions
NML:	nonmelanocytic lesions
RCM:	reflectance confocal microscopy
SK:	seborrheic keratosis

From the Department of Dermatology, Hospital Clinic[a]; Department of Dermatology, Hospital del Mar[b]; and Centro de Investigación Biomédica en Red (CIBER) de Enfermedades Raras.[c]

Supported in part by grants from Hospital Clinic, Barcelona, Spain, and from Novartis Pharmaceuticals, Barcelona, Spain. Work of Drs Malvehy and Puig is partially supported by grants 03/0019 and 06/0265 from Fondo de Investigaciones Sanitarias; grant RO-1 CA 83115 (fund 538226 from National Cancer Institute); and GenoMel consortium currently funded by CE, Net of Excellence.
Conflicts of interest: None declared.
Accepted for publication February 10, 2009.

Reprint requests: Sonia Segura, MD, Department of Dermatology, Hospital del Mar, Barcelona, Passeig Marítim 25-29, 08003 Barcelona, Spain. E-mail: ssegura@imas.imim.es.

Published online April 30, 2009.
0190-9622/$36.00
© 2009 by the American Academy of Dermatology, Inc.
doi:10.1016/j.jaad.2009.02.014

accuracy and at the same time satisfy the patient's desire for noninvasive, cosmetically acceptable clinical approaches, additional diagnostic tools are necessary.

Reflectance confocal microscopy (RCM) has been used for more than 10 years for the in vivo imaging[3,4] of melanocytic[5-8] and nonmelanocytic[9-11] skin tumors. In a few studies the correspondence of confocal features with dermatoscopy and histopathology has been evaluated.[12-16] Other studies suggest that RCM as an adjuvant technique to dermatoscopy may improve diagnostic accuracy in the differentiation of benign and malignant melanocytic lesions (ML)[17,18] Recently a standard RCM terminology was published with the aim of establishing a glossary of terms for RCM evaluation of ML[19]

A few reports describe systematic evaluation of nonmelanocytic tumors using RCM.[11,20,21] Nori et al[20] first included melanocytic and nonmelanocytic tumors to determine the sensitivity and specificity of RCM for the diagnosis of basal cell carcinoma (BCC). Gerger et al[21] developed an algorithm to differentiate ML and non-ML (NML), but only a selected number of images were evaluated.

We performed a systemic analysis of melanocytic and nonmelanocytic skin tumors, using dermatoscopy, RCM, and histopathology to develop a two-step method for melanoma diagnosis based on RCM features for use as an adjuvant to dermatoscopy.

CAPSULE SUMMARY

- Reflectance confocal microscopy (RCM) is a new technology for the in vivo study of skin tumors. RCM studies including melanocytic lesions and nonmelanocytic lesions are lacking. Studies demonstrating the use of this technique in clinical practice are necessary.
- We analyzed different skin tumors to determine which confocal features are characteristic of each lesion.
- We developed an easy two-step algorithm that may enhance the diagnosis of skin cancer in clinical practice and minimize the misdiagnosis of melanoma.

METHODS

Participants

All patients who attended the Dermatology Department and the Melanoma Unit of the Hospital Clinic, Barcelona, Spain, during the 8-month period from November 2005 to June 2006, with a lesion suggestive of malignancy, were invited to participate in the study and receive an RCM examination before excision of the lesion. Study participation did not affect the clinical decision or the excision schedule. Most of the patients with ML had dysplastic mole syndrome, which was managed by periodic dermatoscopic examinations. Thirteen patients had a personal and/or familial history of malignant melanoma, including 3 patients with a history of multiple melanoma. For most of the lesions examined in our study, dermatoscopic changes had been recorded during follow-up examinations.

We also recruited patients with lesions known to be clinically and dermatoscopically benign, who agreed to submit to an RCM examination as control subjects. All study participants gave informed consent for RCM examination of their lesions and for surgical excision of the lesions. The ethics committee of the hospital clinic approved the study, and institutional rules governing clinical investigation of human subjects were strictly followed.

Reflectance confocal microscopy

Confocal imaging was performed with commercially available, near-infrared reflectance confocal laser scanning microscope (Vivascope 1500, Lucid Inc, Henrietta, NY). To keep the skin laterally stable during image acquisition, a skin contact device, consisting of a housing for the objective lens and a ring-and-template, was positioned on the lesion and attached to the skin with medical-grade adhesive. The ring forms a well for holding the immersion medium (water or ultrasound gel). The immersion medium has a refraction index similar to that of the epidermis, thereby minimizing spherical aberrations caused by tissue-air interface when imaging is performed at deeper levels in the dermis.[4]

The instruments use a diode laser at 830 nm with a power of less than 16 mW at tissue level and ×30 water-immersion lenses, allowing a horizontal optical resolution of 2 μm and a vertical resolution of 5 μm. Each given image corresponds to a horizontal 500- × 500-μm section of the skin at a selected depth from epidermal surface to papillary dermis.

Representative images of the lesion were recorded at each skin level (captures). Horizontal montage images were acquired for each lesion to explore a 4- × 4-mm field of view (Vivablock, Lucid Inc, Henrietta, NY) at 3 skin levels: epidermis, dermoepidermal junction (DEJ), and papillary dermis. Vertical montage images (Vivastack, Lucid Inc, Henrietta, NY) from stratum corneum to papillary dermis were recorded at areas of interest. Videos at dermal level were acquired to evaluate vascularization. The stored confocal images were evaluated afterward, without regard to clinical or dermatoscopic data, based on

Table I. Frequency and reliability (kappa value) of confocal features to differentiate melanocytic from nonmelanocytic lesions and nevus from melanoma

RCM feature	Melanocytic lesion (%) (n = 100)	Nonmelanocytic lesion (%) (n = 54)	Nevus (%) (n = 64)	Melanoma (%) (n = 36)	Kappa value
Superficial layer					
Honeycombed pattern	62 (62)*	50 (92.6)	43 (67.2)	19 (52.8)	0.743
Cobblestone pattern	41 (41)†	1 (2)	33 (51.6)	8 (22.2)‡	0.757
Epidermal disarray	27 (27)*	0 (0)	0 (0.0)	12 (33.3)	0.105
Pagetoid cells	32 (32)†	3 (5)	6 (9.4)	25 (69.4)§	0.445
Dermoepidermal junction					
Visible dermal papilla	86 (86)†	17 (31.5)	59 (92.2)	27 (75)‡	0.601
Edged papilla	66 (66)*	13 (24.1)	55 (85.9)	11 (30.6)§	0.891
Nonedged papilla	45 (45)*	8 (14.8)	22 (34.4)	23 (63.9)‡	0.340
Typical basal cells	46 (46)*	9 (16.7)	44 (68.8)	2 (5.6)§	0.497
Marked atypia basal cells	21 (21)*	0 (0)	2 (3.1)	19 (52.8)‡	0.228
Cells in sheetlike structures	9 (9)*	0 (0)	2 (3.1)	7 (19.4)‡	0.465
Junctional clusters	29 (29)*	0 (0)	29 (45.3)	0 (0)‡	0.421
Papillary dermis					
Dermal nests	51 (51)†	2 (3.7)	31 (45.3)	18 (50)	0.500
Regular dense nests	26 (26)	3 (3.7)	21 (32.8)	5 (13.9)‡	0.525
Nonhomogeneous nests	15 (15)	0 (0)	5 (7.8)	10 (27.8)‡	0.324
Cerebriform nests	4 (4)	0 (0)	0 (0)	4 (11.1)‡	0.658
Nucleated dermal cells	51 (51)*	8 (15)	28 (43.8)	19 (52.8)	0.351
Atypical	21 (21)*	1 (1.9)	2 (3.1)	19 (52.8)§	0.351
Plump bright cells	50 (50)	29 (53.7)	33 (51.6)	17 (47.2)	0.361
Bright hyperreflecting spots	27 (27)	16 (29.6)	18 (28.1)	9 (25)	0.177
Enlarged dermal vessels	22 (22)	24 (44.4)	8 (12.5)	14 (38.9)‡	0.373

RCM, Reflectance confocal microscopy.
*Significant ($P < .05$) in univariate analysis to differentiate melanocytic from nonmelanocytic lesion.
†Significant ($P < .05$) in multivariate analysis to differentiate melanocytic from nonmelanocytic lesion.
‡Significant ($P < .05$) in univariate analysis to differentiate nevus from melanoma.
§Significant ($P < .05$) in multivariate analysis to differentiate nevus from melanoma.

melanocytic and nonmelanocytic confocal features as previously described (Tables I and II).[6,9,10,19]

Dermatoscopic study

The lesions were dermatoscopically evaluated and documented using a commercially available dermatoscope (DermliteFoto, 3 Gen, San Juan Capistrano, CA) in combination with a digital camera adapted for polarized dermatoscopic photographs. Spatial orientation of lesions for dermatoscopy and confocal correlation was performed using an external macro camera (VivaCam, Lucid Inc) adapted to the confocal microscope. Dermatoscopic criteria were evaluated according to published descriptions.[2]

Histopathological study

Lesions that were suggestive of malignancy were excised after RCM examination. The excised tissue was fixed in formalin and embedded in paraffin, and the slides were stained with hematoxylin-eosin after routine processing. Immunohistochemical stains were performed in selected cases to improve the correlation between confocal structures and histopathology. As dendritic melanocytes and Langerhans cells may be seen as refractive dendrites or dendritic cells under RCM, we used S-100, Melan-A, and HMB-45 to identify melanocytic pagetoid cells in melanoma and to identify melanocytes within BCC nodules. CD1a and S-100 were used to identify Langerhans cells.

Interobserver reproducibility of confocal features

A reproducibility study evaluated interobserver agreement of confocal features. Two investigators with some experience (S. P.) or no experience (C. C.) in evaluating RCM images of lesions were given a tutorial with written descriptions of the features and representative images demonstrating each of the features. The primary investigator (S. S.) selected 120 images that were considered representative of the confocal features that have been reported in skin tumors.[6,9] The images used in the tutorial were selected from a series of tumors not included in the current study. The participants evaluated the RCM

Table II. Description, reliability, and dermatoscopic and histopathological correspondence of confocal features in nonmelanocytic lesions

RCM feature	Description	Kappa value	Dermatoscopic correlation	Histopathological correlation
Basal cell carcinoma				
Tumor nodules	Dermal reflective tumor islands surrounded by a dark space and connected to the epidermis	0.375	Leaflike structures and ovoid nests	Nests of basaloid cells (clefting)
Polarization	Tumor cells with elongated nuclei orientated on the same axis	0.474	—	Polarization of basal cells
Dendritic structures	Bright thin or coarse dendritic-like structures within tumor islands frequently associated to a clearly visible nucleated cell	0.722	—	Dendritic melanocytes within tumor nests
Plump bright cells	Irregularly shaped bright cells with ill-defined borders and usually no visible nucleus distributed within and outside tumor islands	0.522	Blue-gray globules	Melanophages
Prominent vasculature	Enlarged, horizontal and sometimes tortuous vessels with rolling phenomena	0.299	Telangiectasia	Dermal neovessels
Seborrheic keratosis				
Corneal plugs/ corneal cysts	Bright laminar onionlike structures on epidermal surface/bright round homogeneous intraepidermal structures	0.559	Comedo-like openings/milia cysts	Keratin-filled invagination of epidermis
Crypts	Deep hyporeflective folds on the epidermal surface	NE	Fissures	Invaginations on SK surface
Cordlike structures	Monomorphic bright epidermal cords constituted by aggregated cells with ill-defined borders at dermoepidermal junction	0.597	Fingerprint-like structures	Epidermal lentiginous hyperplasia
Vascular tumor				
Vascular spaces	Widespread dermal dark spaces with circulating blood cells inside	0.388	Vascular lagoons	Dermal vascular proliferation
Dermatofibroma				
Edged papilla	Round, regular, edged papilla at the periphery of the lesion	NE	Peripheral thin reticulation	Elongation of rete ridges overlying epidermis
Broadened dermal fibers	Fibrillar bright dermal structures thicker than in normal dermis	NE	Central white patch	Densification of dermal collagen

NE, Not evaluated; *RCM*, in vivo reflectance confocal microscopy; *SK*, seborrheic keratosis.

images independently without clinical or dermatoscopic information of the tumors.

Statistics

Statistical evaluation was carried out using a statistical software package (SPSS for Windows, Version 15.0, SPSS Inc, Chicago, IL).

In the univariate analysis significant differences between ML and NML were evaluated by means of the χ^2 test of independence (Fischer exact test was applied if any expected cell value in the 2×2 table was <5). Within the NML group we assessed specific features to define BCC, seborrheic keratosis (SK), angioma, and dermatofibroma, and within the ML group we assessed differences between nevi and melanoma.

In the multivariate analysis we used binary logistic regression to differentiate ML from NML and nevi from melanoma, in the development of a two-step method for the diagnosis of melanoma by RCM. We

developed an algorithm in which we gave benign (protective) features a value of −1 and malignant (risk) features a value of 1. The value of each lesion was determined by adding the values of the benign and malignant features.

To evaluate interobserver agreement of confocal features Cohen kappa index was calculated for each descriptor. Kappa values range from 0 to 1, with a kappa value of 1.0 indicating full agreement beyond chance. Values greater than 0.70 indicate excellent agreement, values less than 0.7 but greater than 0.40 indicate moderate agreement, and values less than 0.40 indicate poor agreement.

RESULTS

In all, 124 patients with 134 suspicious lesions and 19 control subjects with 20 benign lesions agreed to participate in the study. We examined 100 ML and 54 NML, for a total of 154 skin tumors from 143 participants (86 women, mean age 49.45 years).

Among ML we observed 36 melanomas (19 superficial spreading melanoma, 8 in situ melanoma, 5 lentigo maligna, and 4 nodular melanomas) and 64 nevi (32 dysplastic, 20 common, 7 congenital, 2 blue, 2 Reed, and 1 Meyerson). A heterogeneous collection of tumors comprised the NML group: 27 BCC, 8 SK, 5 solar lentigines, 4 benign lichenoid keratoses, 4 vascular lesions, 3 actinic keratoses, 2 dermatofibromas, and 1 sebaceous hyperplasia. The majority of tumors were located on the trunk (82 lesions). Other sites were the head (34 lesions), lower limbs (22 lesions), upper limbs (14 lesions), and neck (2 lesions).

Fifteen lesions were not excised because they were banal lesions by clinical and dermatoscopic criteria. These lesions were used as controls (8 banal nevi, 2 solar lentigines, 2 SK, 2 angiomas, and 1 dermatofibroma).

We systematically evaluated the RCM images according to previously described RCM features.[6,9,10,19] Tables I and II show which confocal features were associated to each tumor and the interobserver agreement (reliability) for them in ML and NML, respectively. Correlation of the RCM features with dermatoscopic criteria and histopathology for NML is shown in Table II.

Dermatoscopic analysis

Within histologically confirmed benign ML (56 lesions), the most frequently observed dermatoscopic pattern was multicomponent pattern[22] (39 lesions). In all, 23 lesions were asymmetric and 10 exhibited 3 or more colors. The most frequent dermatoscopic structures were globules (43 lesions, 8 atypical) followed by network (38 lesions, 6 atypical) and blue- regression structures (peppering) (20 lesions). All lesions exhibited at least one criterion characteristic of ML.

All 36 melanomas were asymmetric in the distribution of dermatoscopic structures in at least one axis, and 26 exhibited 3 or more colors. A total of 28 melanomas had a multicomponent pattern. The most frequent dermatoscopic structures were dots (26 lesions), followed by structureless areas (20 lesions), atypical vessels (19 lesions), atypical globules (17 lesions), and atypical network (13 lesions). Notably, 8 melanomas did not exhibit any criteria for ML.[2,22]

Within 26 BCC, two lesions exhibited globular aggregates suggestive of ML. An additional lesion did not exhibit any BCC features of BCC. Nine lesions presented only a single dermatoscopic criterion for BCC. In 6 of these lesions, the criterion characteristic of BCC was the presence of telangiectasia, making amelanotic melanoma the differential diagnosis in these cases.

Of the 6 SK that were excised, one reticulated SK exhibited networklike structures that suggested a diagnosis of lentigo maligna. Three lesions were highly pigmented, with similarities to SK-like melanoma, and the appearance of two lesions raised the possibility of Bowen disease. None of the lesions exhibited dermatoscopic criteria for ML. The most frequent dermatoscopic feature was comedo-like openings (8 lesions) followed by fissures (4 lesions).

Because of the absence of clear cut-off criteria for vascular lesions, two of the 4 angiomas were excised.

Confocal study

Features to differentiate ML from NML. Some confocal features differentiated ML from NML (Table I). At epidermal layers the so-called cobblestone pattern was present in 41 ML (41%) compared with only one NML (2%; $P < .001$) (Fig 1, *A*). In 32 ML (32%) compared with only 3 NML (5%; $P < .001$) (Fig 1, *B*), we observed nucleated cells with a bright cytoplasm within suprabasal layers. These cells have been defined as pagetoid cells in RCM literature.[23] In some clinical and dermatoscopically difficult lesions this feature was the clue for the diagnosis of ML (Fig 2, *B*). At the DEJ ML exhibited a mesh appearance with widespread dark spaces (dermal papillae [DP]) surrounded by a refractive interpapillary process. This feature was significantly more common in ML than in NML (86% ML vs 31.5% NML; $P < .001$) (Fig 1, *C*). Junctional nests appeared under RCM as compact aggregates of refractive cells connected to the epidermis. Junctional nests were observed in 29 ML (29%) and in none of the NML ($P < .001$).

In the papillary dermis dense clusters of cells were observed in 51 ML (51%) compared with two NML

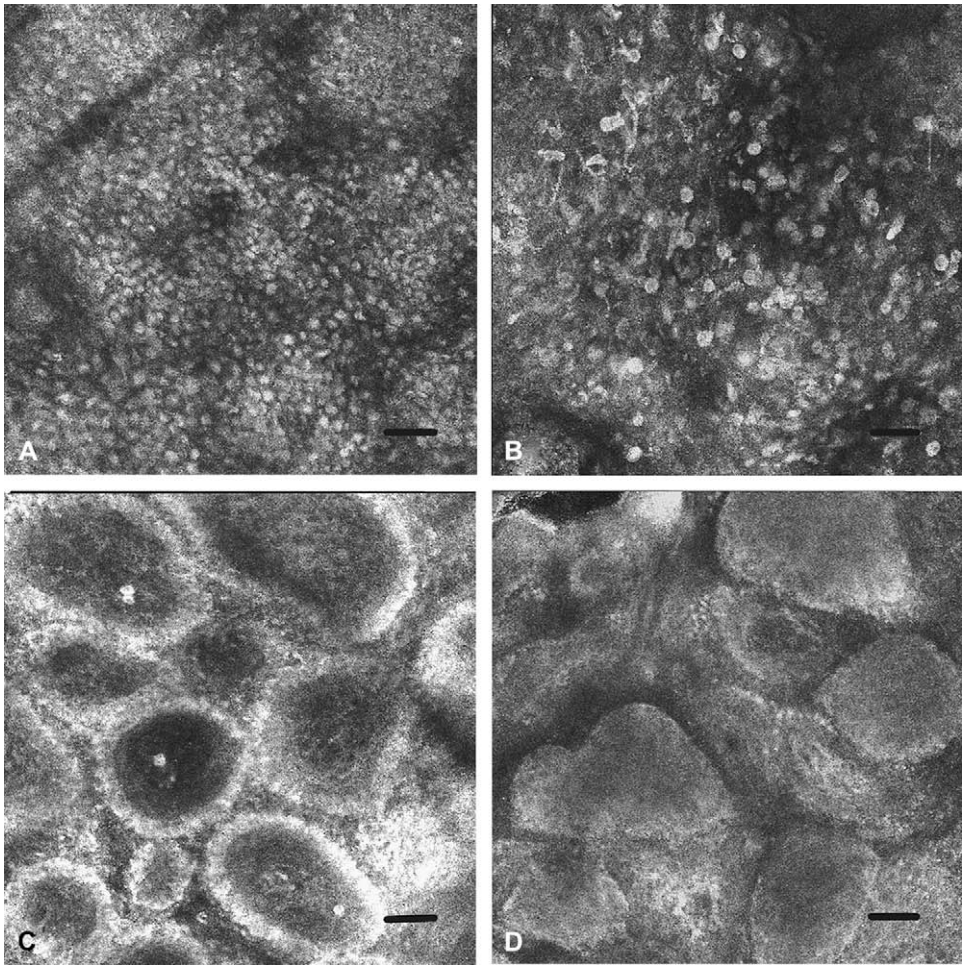

Fig 1. Confocal features to define melanocytic lesion (multivariate analysis). **A**, Cobblestone pattern. **B**, Pagetoid spread. **C**, Widespread dermal papillae (DP). **D**, Dermal nests filling DP. Bar = 50 μm.

(3.7%; $P < .001$) (Fig 1, *D*). Nucleated cells in the papillary dermis were more often found in ML than in NML (51 ML vs 15% NML; $P < .001$). Nonnucleated dermal cells (plump cells) and bright hyperreflecting spots could be observed in both ML and NML.

Features to differentiate nevi from melanoma. In corroboration with previous observations we noted several features within ML that may help to distinguish nevi from melanoma[5-8] (Table I).

In the epidermal layers, benign lesions were characterized by the presence of normal honeycombed pattern, cobblestone pattern, or both. In contrast, 12 melanomas (33.3%) showed disarrangement of the epidermal pattern ($P < .001$). The presence of pagetoid cells in the epidermal layers was observed in 25 (69.4%) melanomas compared with only 6 nevi (9.4%; $P < .001$) (Figs 3, *A*, and 4, *F*).

Malignant lesions tended to have moderate to high numbers of pagetoid cells compared with benign lesions, which had few pagetoid cells. In many of the malignant lesions the cells were large and displayed a roundish and dendritic morphology. By contrast, the cells were likely to be small and dendritic in benign lesions, and roundish cells were rarely observed. In the subgroup of lentigo maligna we observed a distinctive perifollicular distribution of pagetoid cells along with irregular perifollicular refractivity.

Compared with melanoma, nevi were more likely to have edged papillae at the DEJ (Figs 3, *D*, and 4, *B*) (55 nevi, 85.9% vs 11 melanomas, 30.6%; $P < .001$). In all, 23 melanomas (63.9%) had nonedged papillae (Fig 4, *G*), compared with 22 nevi (34.4%; $P = .006$). The diameter and shape of the DP were homogeneous in most of the common nevi but heterogeneous in melanoma and dysplastic nevi. Small typical cells within the basal layer were seen in 44 nevi (68.8%) compared with two melanomas (5.6%; $P < .001$) (Fig 3, *C*). Nearly a third of both nevi and melanomas showed mild atypia of basal cells, with a

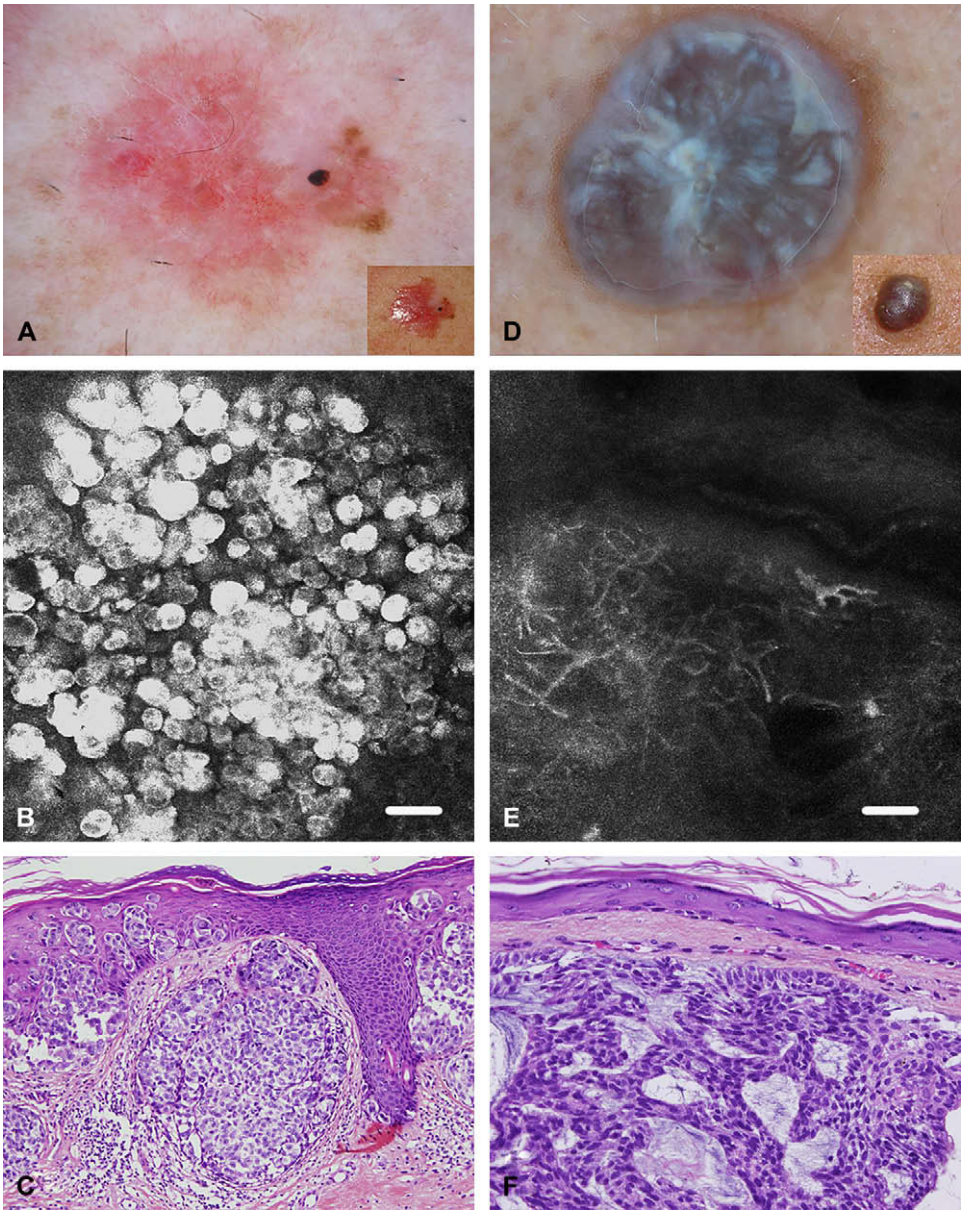

Fig 2. Two equivocal skin tumors with diagnostic confocal features. **A**, Clinical (*inset*) and dermatoscopic aspect of hypopigmented superficial spreading melanoma (SSM) on chest, exhibiting atypical vessels and ovoid nest. **B**, Confocal image of lesion over pigmented area at epidermal layers, showing intense roundish large nucleated pagetoid cells. **C**, SSM Clark level III, Breslow thickness 0.6 mm. Detail of pagetoid spread and dermal aggregates of atypical epithelioid cells. **D**, Clinical (*inset*) and dermatoscopic aspect of basal cell carcinoma (BCC) on cheek. Note absence of specific dermatoscopic criteria for melanocytic lesion or for BCC. **E**, Confocal image of lesion at dermoepidermal level. Hyporeflective nodule surrounded by dark area with presence of bright dendritic cells within. Enlarged vessel around nodule. **F**, Adenoid BCC. Nests of basaloid cells in dermis. Bar = 50 μm. (**C** and **F**, Hematoxylin-eosin stain; original magnifications: ×200.)

few large cells appearing in the basal layer. Marked atypia in the basal layer, with numerous large atypical cells and architectural disarray of the DEJ, was a characteristic of many of the melanomas (19; 52.8%) but not of the nevi (2; 3.1%; $P < .001$) (Fig 4, *G*). Dense, bright, regular clusters of cells connected to the basal layer (junctional nest) were observed in 29 (45.3%) of nevi but were not seen in melanomas ($P < .001$). A proliferation of atypical nonaggregated cells distributed in a sheetlike manner could be

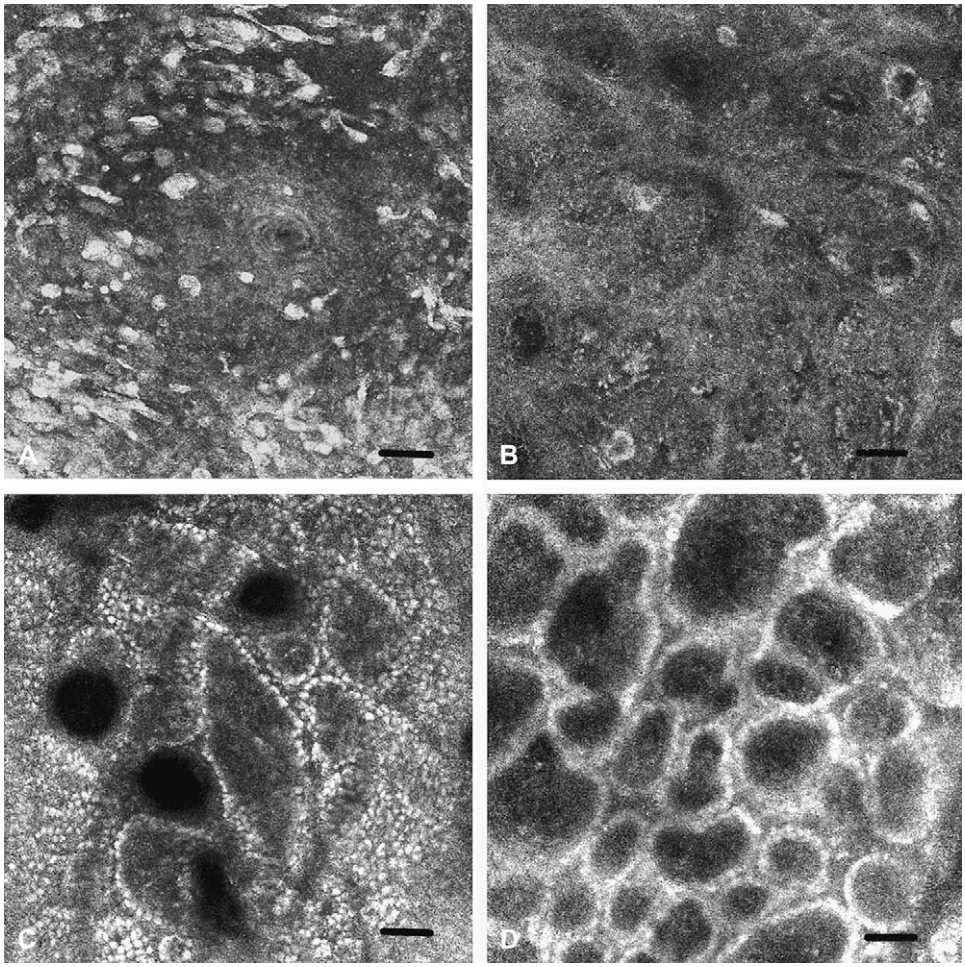

Fig 3. Confocal features to define melanoma and nevi (multivariate analysis). Features associated with malignancy (**A** and **B**) and with nevi (**C** and **D**). **A**, Roundish pagetoid cells. **B**, Atypical dermal nucleated cells. **C**, Typical basal cells. **D**, Edged papillae. Bar = 50 μm.

identified at the DEJ in 7 melanomas but only in two nevi ($P < .01$).

At the dermal level, nevi showed dense clusters that were mainly regular in contour, size, and refractivity (Fig 4, *C*). In contrast, cell aggregates in melanoma were frequently nonhomogeneous (Table I). In 4 thick melanomas, we also observed so-called cerebriform clusters, which were not seen in nevi.

Nucleated cells were observed within dermal nests in 51 ML. They were more likely to have an atypical morphology in malignant lesions compared with benign lesions (Fig 3, *B*): nucleated cells were large and pleomorphic in 19 melanomas (52.8%) compared with only two nevi (3.1%; $P < .001$). In both benign and malignant lesions we also observed nonnucleated dermal cells (plump cells) in the dermis.

Although vessels could be identified in both benign and malignant lesions (Table I), they tended to be larger in melanomas than in nevi. In addition, vessels in melanomas sometimes had a tortuous aspect that was not seen in nevi.

Nonmelanocytic lesions. Five criteria have been described[9] as characteristic of BCC under RCM: (1) presence of elongated monomorphic basaloid nuclei; (2) polarization of these nuclei along the same axis of orientation; (3) prominent inflammatory infiltrate; (4) increased vasculature; and (5) pleomorphism of the overlying epidermis, indicative of actinic damage. We observed all these features in our series. Two of them were significantly more frequent in BCC compared with non-BCC lesions (Table II): elongated monomorphic nuclei/polarized nuclei were observed in 4 of the 27 BCC (15.4%) compared with none of the non-BCC lesions ($P = .001$), and increased vasculature was seen in 80.8% of BCC compared with 19.5% of non-BCC lesions ($P < .001$). In the epidermis an atypical honeycombed pattern was observed in two BCC (7.7%). This pattern was also observed in other lesions, mainly malignant ML. Inflammatory cells were

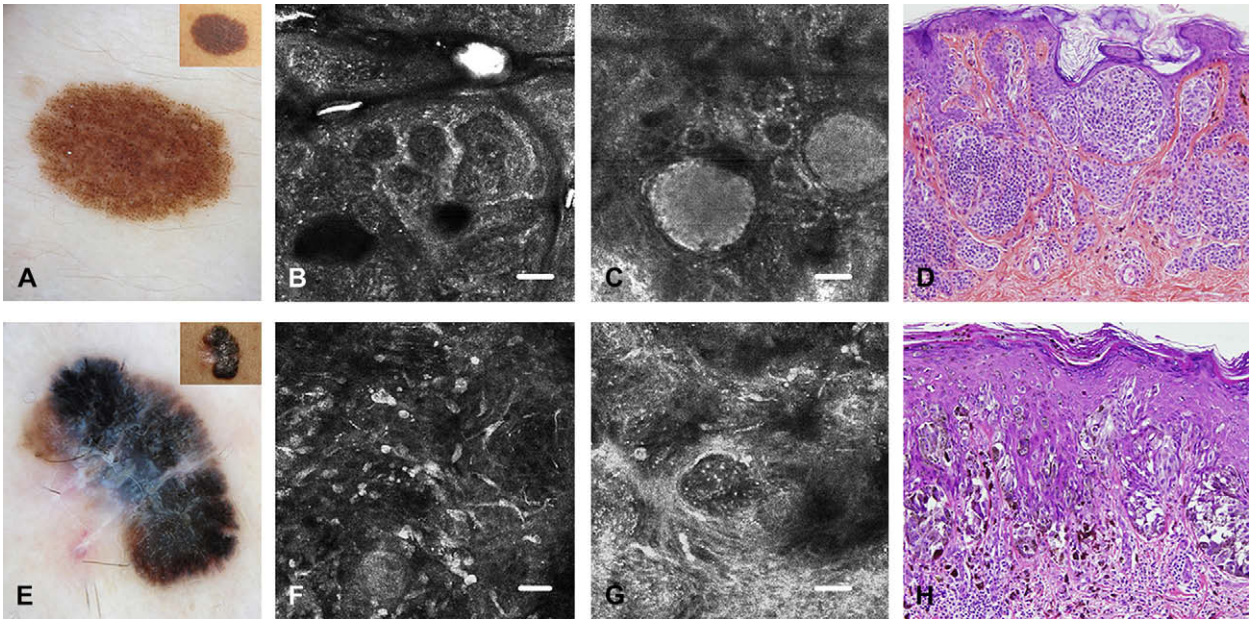

Fig 4. Dermatoscopic, confocal, and histopathological correlation of nevus and melanoma. **A**, Clinical (*inset*) and dermatoscopic appearance of growing nevus on abdomen, showing globular and reticular pattern. **B**, Confocal section at dermoepidermal junction (DEJ) shows typical small basal cells and edged papillae corresponding to network under dermatoscopy. **C**, Regular dense dermal nests corresponding to globules under dermatoscopy. **D**, Compound nevus, histologic section showing dermal and junctional aggregates of melanocytes and lentiginous hyperplasia of epidermis. **E**, Superficial spreading melanoma Clark level II, Breslow thickness 0.8 mm on leg. Dermatoscopy exhibiting multicomponent pattern. **F**, Confocal image at epidermal layers demonstrates widespread roundish and dendritic large pleomorphic pagetoid cells. **G**, Confocal image at dermoepidermal level shows disarray of structure with nonedged dermal papillae separated by large atypical basal cells. **H**, Histologic section of lesion shows marked pagetoid spread and disarray of DEJ with proliferation of atypical melanocytes that infiltrate dermis. Bar = 50 μm. (**D** and **H**, Hematoxylin-eosin stain; original magnifications: ×100.)

observed within the dermis in 10 BCC (38.5%) but could also be present in any other skin neoplasm (25.8%; $P = .231$).

We found some features previously described by others[10,24] and further corroborated by our studies[25] that may help to differentiate BCC from other lesions (Table II). In 22 of 26 BCC, nests of basaloid tumoral cells in the dermis appeared as well-defined nodules and tumor islands surrounded by a dark area (Fig 5, *A*). In these lesions, we observed bright irregular, nonnucleated structures, round to oval in shape, present both inside and outside the nodules. These bright structures were more obvious on pigmented areas. A third confocal feature characteristic of BCC in our series was the presence of bright, delicate, dendritic structures within the tumor nodules in 12 of the lesions, mostly pigmented BCC. To investigate these structures in more detail, we selected 5 cases for immunohistochemical studies with S-100, HMB-45, Melan-A, and CD1a antibodies, using formalin-fixed paraffin-embedded biopsy specimens. Results from 3 cases have been published elsewhere.[25] In all 5 cases we observed Melan-A$^+$ and HMB-45$^+$ dendritic cells, corresponding to melanocytes, within the tumoral nests. In 3 cases we also noted an increase in S-100$^+$ and CD1a$^+$ cells, corresponding to Langerhans cells, in the overlying epidermis. These bright, dendritic structures inside the dermal nodules were never observed in other tumors and their presence is a feature highly suggestive of BCC when observed in the examination of a pigmented skin tumor. In one case the lesion was clinically and dermatoscopically very difficult to diagnosis, and the observation of the bright, delicate, dendritic structures within the tumor nodules, in the absence of melanocytic features, helped in the diagnosis of the lesion (Fig 2, *E*).

The RCM features most characteristic of SK (Table II) were bright laminar onionlike structures on the epidermal surface and in the upper epidermal layers (100% SK vs 8% of other lesions; $P < .001$) and deep hyporeflective folds on the lesion surface that correlated dermatoscopically with fissures and crypts

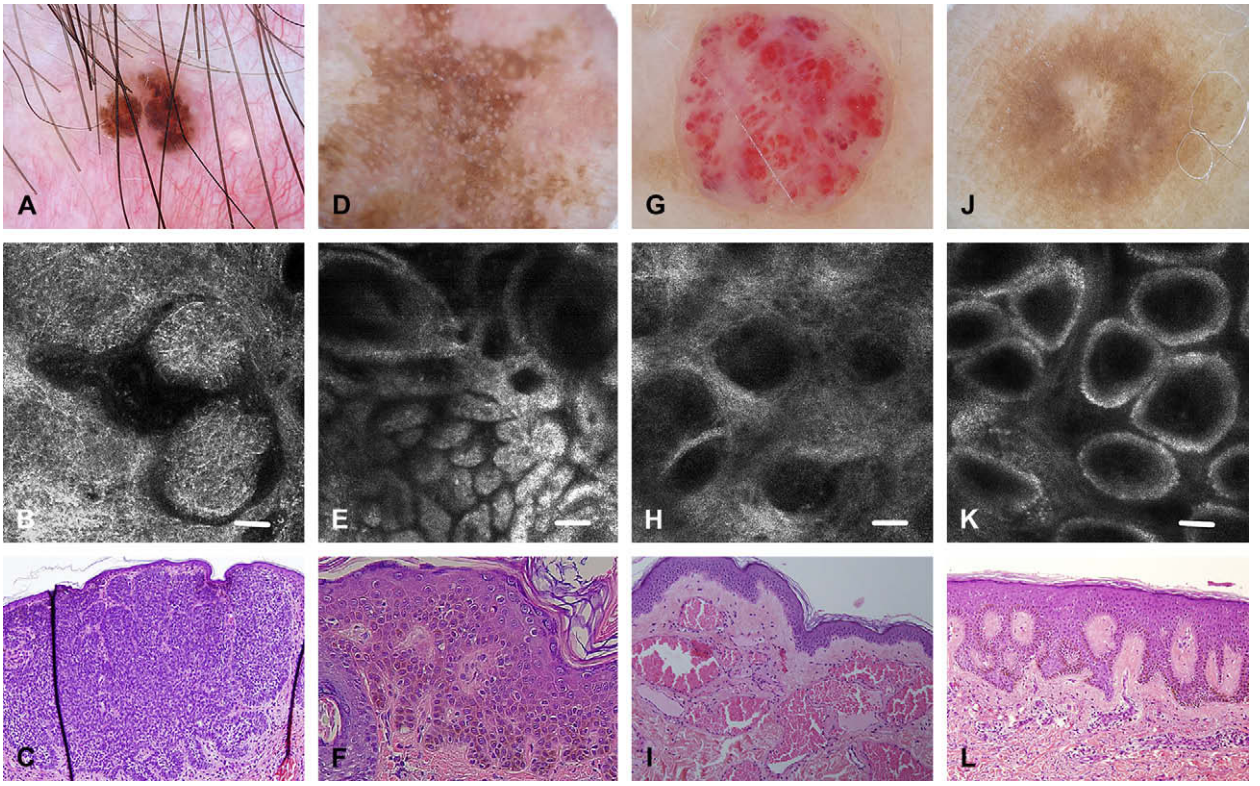

Fig 5. Dermatoscopic, confocal, and histopathological correlation of nonmelanocytic lesions. **A**, Small pigmented basal cell carcinoma on forehead. Dermatoscopy showing leaflike structures and ovoid nests. **B**, Confocal image at dermoepidermal level. Tumor nodule connected to epidermis surrounded by dark area and thin dendritic structures within. Enlarged tortuous vessel around nodule. **C**, Dermal nodule of basaloid cells. **D**, Reticulated seborrheic keratosis on nose. Dermatoscopy showing networklike structures. **E**, Confocal image at dermoepidermal junction demonstrates cordlike bright structures. **F**, Lentiginous epidermal hyperplasia, pigmentation of basal layer. **G**, Cherry angioma on back. Dermatoscopy showing vascular lagoons. **H**, Confocal image at dermal level demonstrates widespread dark spaces with circulating blood cells inside. **I**, Dermal proliferation of vessels. **J**, Dermatofibroma on thigh. Dermatoscopy showing peripheral delicate network and central whitish scar. **K**, Confocal image at periphery of lesion at dermoepidermal junction demonstrates regular edged papillae. **L**, Histologic section of periphery of lesion shows hyperplasia of epidermis with pigmentation of basal layer. Bar = 50 μm. (**C**, **F**, **I**, and **L**, Hematoxylin-eosin stain; original magnifications: **C**, **I**, and **L** ×100; **F**, ×200.)

(75% SK vs 12% of other lesions; $P < .001$). Typical milia cysts seen in dermatoscopy appeared under RCM as round bright intraepidermal structures with a regular contour. However, this feature was only observed in two cases (25%) and was also present in other lesions such as nevi, BCC, melanoma, and lentigo. Epidermal cordlike bright structures were observed in two SK (25%) and in 3 lentigo (60%) (Fig 5, *E*). Bright plump cells filling DP were observed in two cases. In 3 of the 8 SK enlarged vessels correlated dermatoscopically with hairpin vessels.

Angiomas exhibited widespread hyporeflective spaces separated by a bright border with circulating blood cells inside (Table II and Fig 5, *H*). These spaces can be easily identified in vivo but are less obvious in static images. For that reason this feature had a poor interobserver agreement in the reliability study.

By RCM dermatofibromas showed two characteristic features (Table II). At the periphery of the lesion, under an epidermis with a normal honeycombed pattern, the DEJ appeared as regular and round-edged DP (Fig 5, *K*). The center of the lesion lacked these structures and thick refractile fibers were observed in the papillary dermis layer.

Development of the two-step method for RCM diagnosis of melanoma

First step: Melanocytic versus nonmelanocytic. In the multivariate analysis, only 4 confocal features significantly differentiated ML from NML:

Table III. Features to differentiate melanocytic lesions from nonmelanocytic lesions

Confocal feature	Nonmelanocytic lesion (%)	Melanocytic lesion (%)	Total
CPN+ and DP−	4 (13.8)	25 (86.2)	29 (100%)
CPN+ and DP+	2 (3.3)	59 (96.7)	61 (100%)
CPN− and DP−	40 (95.2)	2 (4.8)	42 (100%)
CPN− and DP+	8 (33.3)	14 (58.3)	22 (100%)
Total	54 (35)	100 (65)	154 (100%)

CPN, Presence of cobblestone pattern, pagetoid cells, or dermal nests; *DP*, visualization of widespread dermal papilla forming a mesh at dermoepidermal junction.

cobblestone pattern, pagetoid spread, mesh appearance of the DEJ (visualization of widespread DP), and presence of dermal clusters of cells or dermal nests (Fig 1). As variables in the analysis, the features cobblestone pattern, pagetoid spread, and dermal nests all had a similar statistical behavior. We grouped these 3 features into a single variable (presence of cobblestone pattern, pagetoid cells, or dermal nests [CPN]) (Table III). Presence of at least one CPN feature together with widespread DP was highly suggestive of ML (96.7% ML vs 3.3% NML). Presence of at least one CPN feature in the absence of widespread visible DP was also highly suggestive of ML (86.2% ML vs 13.8% NML). Lesions with neither DP nor CPN features were rarely diagnosed as melanocytic (95.2% NML vs 4.8% ML). The fourth combination, in which widespread DP were seen in the absence of a CPN feature, was not predictive for either ML or NML: 58.3% of the lesions in this category were melanocytic and 33.3% were nonmelanocytic (Table III).

In the absence of other features, the presence of a mesh appearance of the DEJ is not diagnostic of ML. However, when accompanied by at least one CPN feature, a mesh appearance of the DEJ supports the diagnosis of ML.

Second step: Melanoma versus nevi. Within ML, only 4 confocal features discriminated between nevus and melanoma in the multivariable analysis. Two protective features were associated with benign lesions (typical basal cells and edged papillae) and two risk features were associated with melanoma (roundish pagetoid cells and atypical dermal nucleated cells) (Fig 3). According to the presence or absence of protective and risk factors, we assigned lesions a value from −2 to 2 (Fig 6). With a cutoff of −1 to distinguish benign from malignant lesions, the algorithm had a sensitivity of 86.1% and a specificity of 95.3%. However, with this threshold there were 5 false-negative results: 4 in situ melanomas and a superficial spreading melanoma. The latter lesion had a central crust with an extensive area of regression and was located on the leg. It was a difficult lesion to assess by RCM but it had distinct clinical and dermatoscopic signs of malignancy that would have prevented misclassification in a clinical setting.

If we consider only the 92 ML that were excised because of clinical and dermatoscopic signs of malignancy and we assign a cutoff of −2 to distinguish benign/melanoma, we reach a sensitivity of 100% and a specificity of 57.1%. Despite low specificity, with a cutoff of −2 we avoid more than 50% of the unnecessary biopsies without missing a melanoma.

DISCUSSION

RCM is an emerging imaging technique that is moving from research to clinical practice. The development of decision trees based on RCM results is needed to assist dermatologists who want to implement this technique in the diagnosis of skin tumors. Previous studies have described RCM features of ML and criteria for malignancy assessed,[5,6,18] and preliminary studies on NML have also been reported.[9-11] In clinical practice dermatologists deal with both ML and NML. To establish RCM as a useful tool for the in vivo diagnosis of skin tumors, algorithms that include both types of lesions are necessary. Only a single previous study analyzed together ML and NML to determine sensitivity and specificity of RCM for the diagnosis of malignant skin tumors.[21] Based on an analysis of 162 lesions, including nevi, melanoma, BCC, and SK, the authors found 3 highly diagnostic features and attempted to develop a simple 3-node classification tree with 4 terminal nodes for the diagnosis of each tumor. However, distinction between ML and NML is not considered in their classification. In this report, we describe the development of a two-step RCM algorithm that differentiates ML from NML in the first step and nevus from melanoma in the second step. CPN suggests the diagnosis of ML in the first step, particularly if these features occur together with a mesh appearance of the DEJ. The latter feature alone was not sufficient to warrant a diagnosis of ML in our series; application of the algorithm in larger series is needed to confirm or discount its relevance.

Misdiagnosis of ML carries the risk that melanoma might be overlooked. In our series, two ML were misclassified as NML in the first step of our two-step diagnostic algorithm because they lacked features characteristic of ML. Neither of the two lesions showed typical RCM features suggestive of ML. Histopathologic analysis showed one lesion to be a Meyerson nevus, with intraepidermal vesicles and an intense inflammatory reaction that may have obscured RCM features characteristic of ML. The other

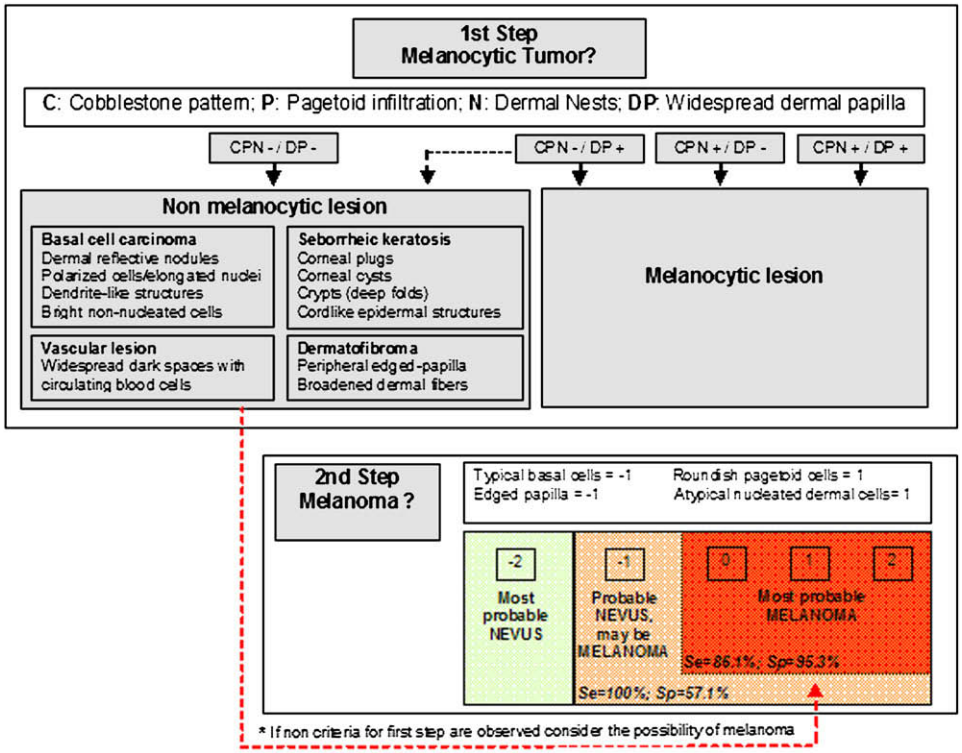

Fig 6. Algorithm for confocal diagnosis of skin tumors. In first step, decision is made if lesion is melanocytic or not according to presence or absence of DP and CPN criteria. Lesions that are nonmelanocytic must fulfill known confocal features for basal cell carcinoma, seborrheic keratosis, angioma, or dermatofibroma. If absent, they must be considered melanocytic and might represent melanoma (*). In second step, melanocytic lesions are assessed for presence of protective features (score −1) and/or risk features (score +1) for melanoma diagnosis. Final score gives probability of melanoma depending on established threshold. *CPN*, Presence of cobblestone pattern, pagetoid cells, or dermal nests; *DP*, widespread dermal papilla; *Se*, sensitivity; *Sp*, specificity.

lesion was a nodular melanoma. In that case, histologic analysis showed no epidermal involvement, which may explain the absence of characteristic RCM features. We recommend that cases that fail to show positive RCM features characteristic of either category of lesions should be regarded as possibly ML and, therefore, possibly melanoma.

Within NML we found some RCM features that may suggest the diagnosis of BCC, SK, dermatofibroma, and angioma, although we could not perform a multivariate analysis because of the small sample size. We found 5 features that may suggest the diagnosis of BCC when a diagnosis of ML has been excluded: polarized nuclei, tortuous vessels, nodules and tumor islands connected to the epidermis, bright thin dendritic structures within nodules, and irregular distributed aggregates of round to oval bright structures. Elongated nuclei and polarization were not common features of BCC in our series. It is likely that these features, which were initially reported by González and Tannus[9] and later validated by Nori et al,[20] refer to a BCC subtype different from that of our series. In our series most BCC were pigmented, nodular, or adenoid type. Disarray in epidermal layers was also not commonly seen in our series, possibly because most of the BCC in our series were from nonsun-exposed areas.

In the second step of our algorithm, distinguishing melanoma from nevi, we found that a benign/malignant cutoff of −2 in RCM score (ie, two protective RCM features and no risk features) allowed us to identify lesions as highly unlikely to be melanoma. With a cutoff of −2, we avoid 57% of unnecessary excisions. A benign/malignant cutoff of −1 (two protective features and one risk feature) diagnosed nevi with a sensitivity of 86.1%, and a negative predictive value of 92.42. However, increasing the cutoff to −1 resulted in 5 false-negative findings. Of these, 4 were in situ melanomas, a type of lesion that may be particularly difficult to evaluate by RCM because of the features shared with dysplastic nevus. The other false-negative finding was clearly a malignant melanoma by clinical and dermatoscopic evaluation. The lesion had a crust and extensive

regression that may have hampered RCM evaluation. Notably, of the lesions that appeared suggestive of melanoma by dermatoscopy, those with an RCM score of 0 or higher (one risk feature together with one protective feature; or at least two risk factors, regardless of protector features) were diagnosed as melanoma with a specificity of 95.3% and positive predictive value of 91.2%.

Pellacani et al[6] proposed a diagnostic semiquantitative algorithm for RCM evaluation of clinically and dermatoscopically equivocal ML. Confocal features associated with melanoma included two major features (presence of nonedged papillae and cytologic atypia) and 4 minor features (the presence of roundish cells in the superficial layers, pagetoid cells widespread throughout the lesion, cerebriform clusters, and nucleated cells within the DP). In our algorithm 4 features differentiated melanoma and nevi: two features of the DEJ were protective (edged papillae and absence of basal cell atypia) and two features of the epidermis and papillary dermis were risk factors (roundish pagetoid cells and atypical nucleated dermal cells). Our study also confirmed pagetoid spreading as a well-established indication of malignancy.[6,16,23]

In multivariate analysis we failed to demonstrate significant differences between nevi and melanoma in the morphology of dermal nests. For example, cerebriform nests are observed in some thick melanomas, but they were too rare in our series for comparisons to reach statistical significance.

Although the number of SK in our series was small, we observed some RCM features that appeared characteristic of these tumors. In the absence of other features, the presence of widespread corneal plugs, crypts, or corneal cysts may suggest a diagnosis of SK. Flat SK and some solar lentigo may be identified by the presence of characteristic epidermal cordlike structures at the DEJ, corresponding to fingerprint-like structures in dermatoscopy. This RCM feature was recently described by Langley et al[12] in solar lentigo to distinguish benign lentigines from lentigo maligna. Vascular lesions and dermatofibromas exhibit characteristic features with a correlation with dermatoscopy easy to identify. However, our results in these lesions are limited considering the small number of cases. Whereas confocal features of dermatofibroma have not been previously reported in the literature, RCM was used by Aghassi et al[26] in cherry angiomas as a noninvasive assessment before laser treatment.

Most of the features discriminative of ML and malignancy (melanoma and BCC) were reliable and reproducible in our study. However, one of the risk features for melanoma diagnosis (atypical nucleated dermal cells) showed a poor interobserver agreement. This result underscores the need to better define RCM features and illustrates the importance of performing further studies before definitive application of a new technique in clinical practice. Evaluation of the dermis is usually more difficult than evaluation of the epidermis and DEJ because of technical limitations of the laser in deep skin assessment. This difficulty may explain the lower reliability in the evaluation of dermal structures.

RCM is a promising technique for the in vivo discrimination of malignant tumors. Its use may prevent unnecessary biopsies of benign tumors and allow an immediate quasihistologic diagnosis of malignant lesions. The two-step diagnostic approach that we developed may reduce the number of overlooked melanomas in clinical practice; however, we recognize that ours is a preliminary study, and the results must be validated in further studies with a larger number of cases in a completely blinded setting. As with all imaging techniques, better definitions of diagnostic criteria and greater training and experience on the part of the practitioners may improve the diagnostic results.

We thank Barbara J. Rutledge, PhD, for editing assistance. We want to acknowledge Sergi Mojal Garcia from IMIM, Institut Municipal d'Investigació Mèdica (IMIM). Consorci Sanitari de Barcelona, Spain, for his assessment in statistical analysis of data.

REFERENCES

1. Brochez L, Verhaeghe E, Bleyen L, Naeyaert JM. Diagnostic ability of general practitioners and dermatologists in discriminating pigmented skin lesions. J Am Acad Dermatol 2001;44:979-86.
2. Argenziano G, Soyer HP, Chimenti S, Talamini R, Corona R, Sera F, et al. Dermoscopy of pigmented skin lesions: results of a consensus meeting via the Internet. J Am Acad Dermatol 2003;48:679-93.
3. Rajadhyasksha M, Grossman M, Esterowitz D, Webb RH, Anderson RR. In vivo confocal scanning laser microscopy of human skin: melanin provides strong contrast. J Invest Dermatol 1995;104:946-52.
4. Rajadhyasksha M, González S, Zavislan JM, Anderson RR, Webb RH. In vivo confocal scanning laser microscopy of human skin II: advances in instrumentation and comparison with histology. J Invest Dermatol 1999;113:293-303.
5. Langley RGB, Rajadhyasksha M, Dawyer PJ, Sober AJ, Flotte TJ, Anderson RR. Confocal scanning laser microscopy of benign and malignant melanocytic skin lesions in vivo. J Am Acad Dermatol 2001;45:365-76.
6. Pellacani G, Cesinaro AM, Seidenari S. Reflectance-mode confocal microscopy of pigmented skin lesions—improvement in melanoma diagnostic specificity. J Am Acad Dermatol 2005;53:979-85.
7. Gerger A, Koller S, Kern T, Massone C, Steiger K, Richtig E, et al. Applicability of in vivo confocal laser scanning microscopy in melanocytic skin tumors. J Invest Dermatol 2005;124:493-8.
8. Marghoob AA, Charles CA, Busam KJ, Rajadhyaksha M, Lee G, Clark-Loeser L, et al. In vivo confocal scanning laser

microscopy of a series of congenital melanocytic nevi suggestive of having developed malignant melanoma. Arch Dermatol 2005;141:1401-12.
9. González S, Tannus Z. Real-time in vivo confocal reflectance microscopy of basal cell carcinoma. J Am Acad Dermatol 2002; 47:869-74.
10. Agero AL, Busam KJ, Benvenuto-Andrade C, Scope A, Gill M, Marghoob AA, et al. Reflectance confocal microscopy of pigmented basal cell carcinoma. J Am Acad Dermatol 2006; 54:638-43.
11. Ulrich M, Maltusch A, Röwert-Huber J, González S, Sterry W, Stockfleth E, et al. Actinic keratoses: non-invasive diagnosis for field cancerization. Br J Dermatol 2007;156(Suppl):13-7.
12. Langley RG, Burton E, Walsh N, Propperova I, Murray SJ. In vivo confocal scanning laser microscopy of benign lentigines: comparison to conventional histology and in vivo characteristics of lentigo maligna. J Am Acad Dermatol 2006;55: 88-97.
13. Pellacani G, Cesinaro AM, Grana C, Seidenari S. In vivo confocal scanning laser microscopy of pigmented Spitz nevus: comparison of in vivo confocal images with dermoscopy and routine histopathology. J Am Acad Dermatol 2004; 51:372-6.
14. Scope A, Benvenuto-Andrade C, Agero AL, Halpern AC, Gonzalez S, Marghoob AA. Correlation of dermoscopic structures of melanocytic lesions to reflectance confocal microscopy. Arch Dermatol 2007;143:176-85.
15. Pellacani G, Bassoli S, Longo C, Cesinaro AM, Seidenari S. Diving into the blue: in vivo microscopic characterization of the dermoscopic blue hue. J Am Acad Dermatol 2007;57:96-104.
16. Pellacani G, Longo C, Malvehy J, Puig S, Carrera C, Segura S, et al. In vivo confocal microscopic and histopathologic correlations of dermoscopic features in 202 melanocytic lesions. Arch Dermatol 2008;144:1597-608.
17. Pellacani G, Guitera P, Longo C, Avramidis M, Seidenari S, Menzies S. The impact of in vivo reflectance confocal microscopy for the diagnostic accuracy of melanoma and equivocal melanocytic lesions. J Invest Dermatol 2007;127: 2759-65.
18. Gerger A, Hofmann-Wellenhof R, Langsenlehner U, Richtig E, Koller S, Weger W, et al. In vivo confocal laser scanning microscopy of melanocytic skin tumors: diagnostic applicability using unselected tumor images. Br J Dermatol 2008;158:329-33.
19. Scope A, Benvenuto-Andrade C, Agero AL, Malvehy J, Puig S, Rajadhyaksha M, et al. In vivo reflectance confocal microscopy imaging of melanocytic skin lesions: consensus terminology glossary and illustrative images. J Am Acad Dermatol 2007;57: 644-58.
20. Nori S, Rius-Díaz F, Cuevas J, Goldgeier M, Jaen P, Torres A, et al. Sensitivity and specificity of reflectance-mode confocal microscopy for in vivo diagnosis of basal cell carcinoma: a multicenter study. J Am Acad Dermatol 2004;51:923-30.
21. Gerger A, Koller S, Weger W, Richtig E, Kerl H, Samonigg H, et al. Sensitivity and specificity of confocal laser-scanning microscopy for in vivo diagnosis of malignant skin tumors. Cancer 2006;107:193-200.
22. Malvehy J, Puig S, Braun RP, Marghoob AA, Kopf AW, editors. Handbook of dermoscopy. London: Taylor and Francis; 2006.
23. Pellacani G, Cesinaro AM, Seidenari S. Reflectance-mode confocal microscopy for the in vivo characterization of pagetoid melanocytosis in melanomas and nevi. J Invest Dermatol 2005;125:532-7.
24. Sauermann K, Gambichler T, Wilmert M, Rotterdam S, Stücker M, Altmeyer P, et al. Investigation of basal cell carcinoma by confocal laser scanning microscopy in vivo. Skin Res Technol 2002;8:141-7.
25. Segura S, Puig S, Carrera C, Palou J, Malvehy J. Dendritic cells in pigmented basal cell carcinoma: a relevant finding by reflectance-mode confocal microscopy. Arch Dermatol 2007; 143:883-6.
26. Aghassi D, Anderson RR, González S. Time-sequence histologic imaging of laser-treated cherry angiomas with in vivo confocal microscopy. J Am Acad Dermatol 2000;43:37-41.

3.2. Trabajo II

In Vivo Microscopic Features of Nodular Melanomas
Dermoscopy, Confocal Microscopy, and Histopathologic Correlates
Sonia Segura, Giovanni Pellacani, Susana Puig, Caterina Longo, Sara Bassoli, Pascale Guitera, Josep Palou, Scott Menzies, Stefania Seidenari, Josep Malvehy
Arch Dermatol 2008;144:1311-20

Objetivos:
Caracterizar mediante dermatoscopia, microscopía confocal de reflectancia (MCR) e histología una serie de melanomas nodulares (MNs), comparándolos con melanomas de extensión superficial (MES) en fase de crecimiento vertical.

Métodos:
Se incluyeron de forma prospectiva 10 MN, 10 MES con área nodular y 10 MES con área palpable. Se realizó un análisis sistemático y estudio estadístico de las características dermatoscópicas, confocales e histológicas de los 3 grupos de lesiones.

Resultados:
Mientras los MNs muestran patrones de dermatoscopia inespecíficos, los MES exhiben patrones multicomponente y puntuaciones más altas en los algoritmos de dermatoscopia. Por MCR, los MNs tienen poco crecimiento pagetoide y presentan a menudo un patrón normal de la epidermis, a diferencia de los MES que se caracterizan por un patrón desestructurado de la epidermis y la presencia de abundantes células en estratos suprabasales (crecimiento pagetoide). Tanto en los MNs como en las áreas nodulares de los MES, en la unión dermo-epidérmica no se visualizan las papilas dérmicas, en su lugar se observan una proliferación de células reflectantes atípicas no agregadas. En la dermis, los MNs presentan unos agregados celulares característicos de aspecto cerebriforme, que pueden observarse también en las áreas nodulares de algunos MES.

STUDY

In Vivo Microscopic Features of Nodular Melanomas

Dermoscopy, Confocal Microscopy, and Histopathologic Correlates

Sonia Segura, MD; Giovanni Pellacani, MD; Susana Puig, PhD; Caterina Longo, MD; Sara Bassoli, MD; Pascale Guitera, MD; Josep Palou, MD; Scott Menzies, MB BS, PhD; Stefania Seidenari, MD; Josep Malvehy, MD

Objective: To characterize nodular melanoma (NM) using dermoscopy, in vivo reflectance-mode confocal microscopy, and histopathologic analysis.

Design: Consecutive pure NMs and superficial spreading melanomas (SSMs) with nodular or blue areas were studied using dermoscopy and confocal microscopy, and a correlation with histopathologic findings was performed.

Materials: Ten NMs, 10 SSMs with a nodular area, and 10 SSMs with a blue palpable but not yet nodular area.

Main Outcome Measure: Confocal differences within the nodular component between pure NMs and SSMs with a nodular area, hypothesizing different biological behaviors.

Results: Whereas NMs had predominantly nonspecific global dermoscopic patterns, SSMs exhibited a multicomponent pattern and higher dermoscopic scores. Globules, blue-white veil, atypical vessels, and structureless areas were frequent in NMs and in nodular areas from SSMs. At confocal microscopy, NMs exhibited few pagetoid cells within a typical epidermal architecture in the superficial layers in most cases, differing from SSMs frequently characterized by epidermal disarrangement and pagetoid infiltration. At the dermoepidermal junction, dermal papillae were rarely seen in nodular areas both from NMs and from SSMs, frequently substituted by nonaggregated atypical cells distributed in sheetlike structures. In the upper dermis, all groups exhibited plump bright cells, dense dishomogeneous cell clusters, and atypical nucleated cells, whereas cerebriform clusters were characteristic of NMs.

Conclusion: Distinctive dermoscopic and confocal features seen in NMs compared with SSMs are helpful in making the diagnosis and suggest different biological behavior.

Arch Dermatol. 2008;144(10):1311-1320

Author Affiliations:
Departments of Dermatology, Hospital Clinic, Barcelona, Spain (Drs Segura, Puig, Palou, and Malvehy), and University of Modena and Reggio Emilia, Modena and Reggio Emilia, Italy (Drs Pellacani, Longo, Bassoli, and Seidenari); and Sydney Melanoma Diagnostic Centre, Sydney Cancer Centre, and Dermatology Department, Royal Prince Alfred Hospital, University of Sydney, Sydney, Australia (Drs Guitera and Menzies).

NODULAR MELANOMA (NM) is responsible for approximately 9% to 15% of invasive melanomas[1,2] and as many as 50% of melanomas thicker than 2 mm. Nodular melanoma arises in healthy skin or in a precursor lesion but without the presence of a radial growth phase. Thus, even in its early stages, NM has the potential to metastasize.[3] The classification of melanoma by subtype is based on anatomical and epidemiological features and pattern of progression. However, recent research has shown molecular and genetic differences between melanoma subtypes.[4-7] These differences may explain the difference in the natural evolution of melanoma subtypes. In NM, classic clinical criteria for diagnosis of melanoma, with the exception of change, fail because these tumors are often small, round, and symmetric, with regular borders.[8-10]

For editorial comment see page 1375

The color is often homogeneous compared with that of superficial spreading melanoma (SSM) and may be pink or red rather than black, blue, or brown. In some cases, NM can be hypochromic or amelanotic. Because of these peculiarities, diagnosis of NM is challenging, and misdiagnosis at the first consultation leads to delay in treatment and worse prognosis.

Dermoscopy of NM is also difficult because the asymmetric pattern is less marked than in SSM.[11] Nevertheless, irregularity in color is usually present in pigmented NMs. In NM, many of the classic dermoscopic features of SSM are usually lacking, especially those dermoscopic structures that correspond to the flat parts of the SSM. Pigment network is often absent in NM, with the ex-

Downloaded from www.archdermatol.com on October 21, 2008
©2008 American Medical Association. All rights reserved.

Table 1. Demographic Data

Melanoma Group	Sex	Age, Mean (SD), y	Site, %	Breslow Tumor Thickness, Mean (SD), mm
NM	5 Male 5 Female	53 (14.4)	Head, 20; upper limbs, 30; trunk, 20; breast, 10; and lower limbs, 20	3.72 (2.16)
SSM_{Nod}	6 Male 4 Female	68.5 (10.6)[a]	Upper limbs, 30; back, 50; and lower limbs, 20	2.01 (0.87)[a]
SSM_{Blue}	3 Male 7 Female	49 (12.8)[b]	Upper limbs, 20; back, 10; abdomen, 10; and lower limbs, 60	1.21 (0.3)[b]

Abbreviations: NM, pure nodular melanoma; SSM_{Blue}, superficial spreading melanoma with blue palpable area not yet nodular; SSM_{Nod}, SSM with a nodular area.
[a] Significant ($P<.05$) compared with NM.
[b] Significant ($P<.05$) compared with SMM_{Nod}.

Table 2. Relevant Dermoscopic Findings

Melanoma Group	Global Dermoscopy Pattern	Structureless Areas	Globules/ Dots	Network	Blue Hue	Regression+	Atypical Vessels	Blue-White Veil	Total Dermoscopy Score, Mean (SD)	
									ABCD	7-Point Checklist
NM	Nonspecific, 8; and globular, 2	10	6	1	8	1	7	4	5.79 (0.81)	4.3 (1.64)
SSM_{Nod}	Multicomponent, 9; and nonspecific, 1	10	10	8[a]	10	7[a]	6	9[a]	7.29 (0.32)[a]	6.5 (1.96)[a]
SSM_{Blue}	Multicomponent, 7; and globular plus homogeneous, 3	10	10	6	10	7	2	2[b]	6.29 (1.22)[b]	5.1 (2.08)

Abbreviations: ABCD, asymmetry, borders sharpness, colors, and dermoscopic structures; NM, pure nodular melanoma; SSM_{Blue}, superficial spreading melanoma with a blue palpable area not yet nodular; SSM_{Nod}, SSM with a nodular area; +, blue (peppering) and/or white regression.
[a] Significant ($P<.05$) compared with NM.
[b] Significant ($P<.05$) compared with SMM_{Nod}.

ception of the presence of contiguous melanocytic nevus or melanocytic hyperplasia. However, NM often exhibits dermoscopic findings associated with deep tumors such as multiple colors, a blue-white veil, and atypical vessels caused by angiogenesis. In the case of amelanotic or hypopigmented NM, the visualization and remnants of pigment are the most important findings.[12]

Reflectance-mode confocal microscopy (RCM) is a new technique for the in vivo study of cutaneous tumors.[13,14] During the last 5 years, several studies of melanocytic tumors have attempted to describe features for RCM evaluation of these lesions.[15-29] Recent studies have demonstrated an improvement in melanoma diagnostic specificity, and several criteria for the diagnosis of melanoma have been established.[24,28,29]

To date, features of RCM for nodular melanoma have not been described, and studies of dermoscopic criteria for theses lesions are also lacking. To determine confocal, dermoscopic, and histologic features in NM, we examined 10 NMs and compared them with 10 SSMs with a nodular area (SSM_{Nod}) and 10 SSMs with a blue palpable area not yet nodular (SSM_{Blue}).

METHODS

PATIENTS

Thirty patients were recruited from the Departments of Dermatology of 3 medical centers: Hospital Clinic, Barcelona, Spain; University of Modena and Reggio Emilia, Modena and Reggio Emilia, Italy; and Royal Prince Alfred Hospital, University of Sydney, Sydney, Australia. Patients gave informed consent for RCM examination of lesions. The dermoscopic evaluation was performed by 2 clinicians (S. Segura and J.M.), as were the confocal evaluation (S. Segura and G.P., who were not blinded to the dermoscopic images) and the histologic evaluation (S. Segura and J.P.). The agreement between RCM and histopathologic findings was made by a single nonindependent observer (S. Segura).

REFLECTANCE-MODE CONFOCAL MICROSCOPY

Confocal imaging was performed with near-infrared reflectance-mode confocal laser scanning microscopes (Vivascope 1000 and Vivascope 1500; Lucid Inc, Rochester, New York). The instruments use a diode laser at 830 nm with a power of less than 16 mW at tissue level and ×30 water-immersion lenses enabling a horizontal optical resolution of 2 µm and a vertical resolution of 5 µm. Instruments and acquisition procedures have been described elsewhere.[13] Each image corresponded to a horizontal section at a selected depth with an effective field of view of 475×350 µm for the Vivascope 1000 and 500×500 µm for the Vivascope 1500. Block images were acquired for each lesion to explore a 4×4-mm field of view. Confocal sections and vertical montage images (stack images) from the stratum corneum to the papillary dermis were recorded at areas of interest. Already described confocal criteria for benign and malignant melanocytic lesions were systematically evaluated.[25]

DERMOSCOPIC STUDY

The lesions were evaluated and documented by epiluminescence microscopy using different devices in the 3 study sites: a commercially available videodermoscope (FotoFinder;

Downloaded from www.archdermatol.com on October 21, 2008
©2008 American Medical Association. All rights reserved.

TeachScreen Software GmbH, Bad Birnbach, Germany), a dermoscope (DermLite DL100; 3 Gen LLC, San Juan Capistrano, California) in combination with a digital camera for dermoscopic photographs (DermLite FOTO; 3 Gen LLC), and a high-resolution digital oil immersion dermoscopy camera (SolarScan Sentry; Polartechnics Ltd, Sydney, Australia). Spatial orientation of lesions for dermoscopy and confocal correlation was performed using an external macrocamera (VivaCam; Lucid Inc) adapted to the confocal microscope, which was available only in the centers equipped with the Vivascope 1500 scanning microscope.

HISTOPATHOLOGIC STUDY

After tumor excision, the tissue was fixed in 10% formalin and embedded in paraffin. After routine processing, the slides were stained with hematoxylin-eosin. For confocal, dermoscopic, and histopathologic correlations, sections passing through the nodule in NM and SSM_{Nod} were obtained from each lesion. In the SSM_{Blue} group, the study area was where the tumor was thicker because that is the part that corresponds to the clinically palpable area.

STATISTIC ANALYSIS

Statistical evaluation was carried out using the SPSS statistical software package for Windows (version 11.0; SPSS, Inc, Chicago, Illinois) and performed on data referring to all of the lesions for confocal, dermoscopic, and histopathologic features. Absolute and relative frequencies of each confocal, dermoscopic, and histopathologic criterion were evaluated in the NM, SSM_{Nod} and SSM_{Blue} groups. Significant differences between NM and SMM_{Nod} and between both SMM groups were evaluated using the χ^2 test of independence (the Fisher exact test was used if any expected cell value was <5 in the 2×2 table). For the confocal, dermoscopic, and histopathologic correlations, the Cohen κ index was calculated for each descriptor. κ Values ranged between 1 and 0. A κ value of 1.00 indicates full agreement beyond chance, values greater than 0.70 are generally considered excellent, values less than 0.40 are considered poor, and values between 0.40 and 0.70 are considered fair to good.

RESULTS

GENERAL OBSERVATIONS

Demographic data for the study population and Breslow thickness of the tumors are given in **Table 1**. Clinically, NM were small to medium, measuring 10 mm or less in most cases and less than 6 mm in 2 of these lesions. Four of 10 lesions were asymmetric, whereas borders were irregular in only 2 cases. Color was homogeneous in most lesions, being predominantly brown in 6 cases and blue and pink in 2 lesions each. In contrast, most melanomas in the other 2 groups fulfilled ABCD (asymmetry, borders irregular, color variegated, and diameter >6 mm) clinical criteria for suspect lesions. Clinical ulceration was present in 5 NM, 4 SSM_{Nod}, and 2 SSM_{Blue} lesions.

DERMOSCOPIC FINDINGS

Two pure NMs were hypomelanotic, and the remaining 28 lesions were pigmented. The most relevant dermoscopic findings are given in **Table 2**. Although NMs usually were clinically symmetric, an asymmetric color and pattern distribution was observed in all lesions at dermoscopy. All lesions exhibited at least 3 colors, but the numbers of colors and structures were significantly lower in the NM group than in the SSM groups. Total dermoscopic scores (ABCD and 7-point checklist) were lower for NMs than for the other 2 groups, and differences were statistically significant when comparing pure NMs with SSM_{Nod} lesions.

Table 3. Relevant Confocal Findings

Confocal Feature	NM (n=10)	SSM_{Nod} (n=10)	SSM_{Blue} (n=10)
Epidermal layers			
Epidermal pattern			
Honeycomb pattern	8	2[a]	1
Broadened	7	2[a]	0
Cobblestone pattern	0	0	1
Disarranged	2	8[a]	8
Pagetoid cells	6	8	10
Mild	5	2	2
Moderate to intense	1	6	8
Roundish	2	8[a]	10
Dendritic	6	7	7
Basal layer and dermoepidermal junction			
Visible papilla	1	5	10[b]
Edged papilla	0	0	4
Nonedged papilla	1	5	10
Diffuse atypical cells	7	9	2[b]
Marked cell atypia in basal layer	8	7	9
Superficial dermis			
Single nucleated cells	10	10	10
Plump cells	7	7	10
Clusters of cells	7	7	10
Dense regular nests	0	0	3
Dense irregular nests	6	7	7
Cerebriform nests	6	1[a]	0
Enlarged vessels	9	7	5
Bright fibrillar structures	9	2[a]	0

Abbreviations: NM, pure nodular melanoma; SSM_{Blue}, superficial spreading melanoma with a blue palpable area not yet nodular; SSM_{Nod}, SSM with a nodular area.
[a] Significant ($P<.05$) compared with NM.
[b] Significant ($P<.05$) compared with SMM_{Nod}.

RCM AND HISTOPATHOLOGIC CORRELATES

Confocal aspects observed in the epidermal layers, dermoepidermal junction, and superficial dermis are given in **Table 3**.

EPIDERMAL LAYERS

Eight NMs exhibited a honeycomb pattern in the epidermal layers, with only 2 lesions demonstrating a disarranged pattern, observed in 8 SMM_{Nod} ($P=.01$) and SMM_{Blue} lesions. Seven NMs (70%) had an atypical broadened honeycomb pattern that consisted of polygonal cells with black nuclei and a bright thick border (**Figure 1**B), observed also in 2 SSM_{Nod} lesions ($P=.04$). Pagetoid cells within the epidermis were more frequently observed in SSMs. In most NMs, pagetoid

Downloaded from www.archdermatol.com on October 21, 2008
©2008 American Medical Association. All rights reserved.

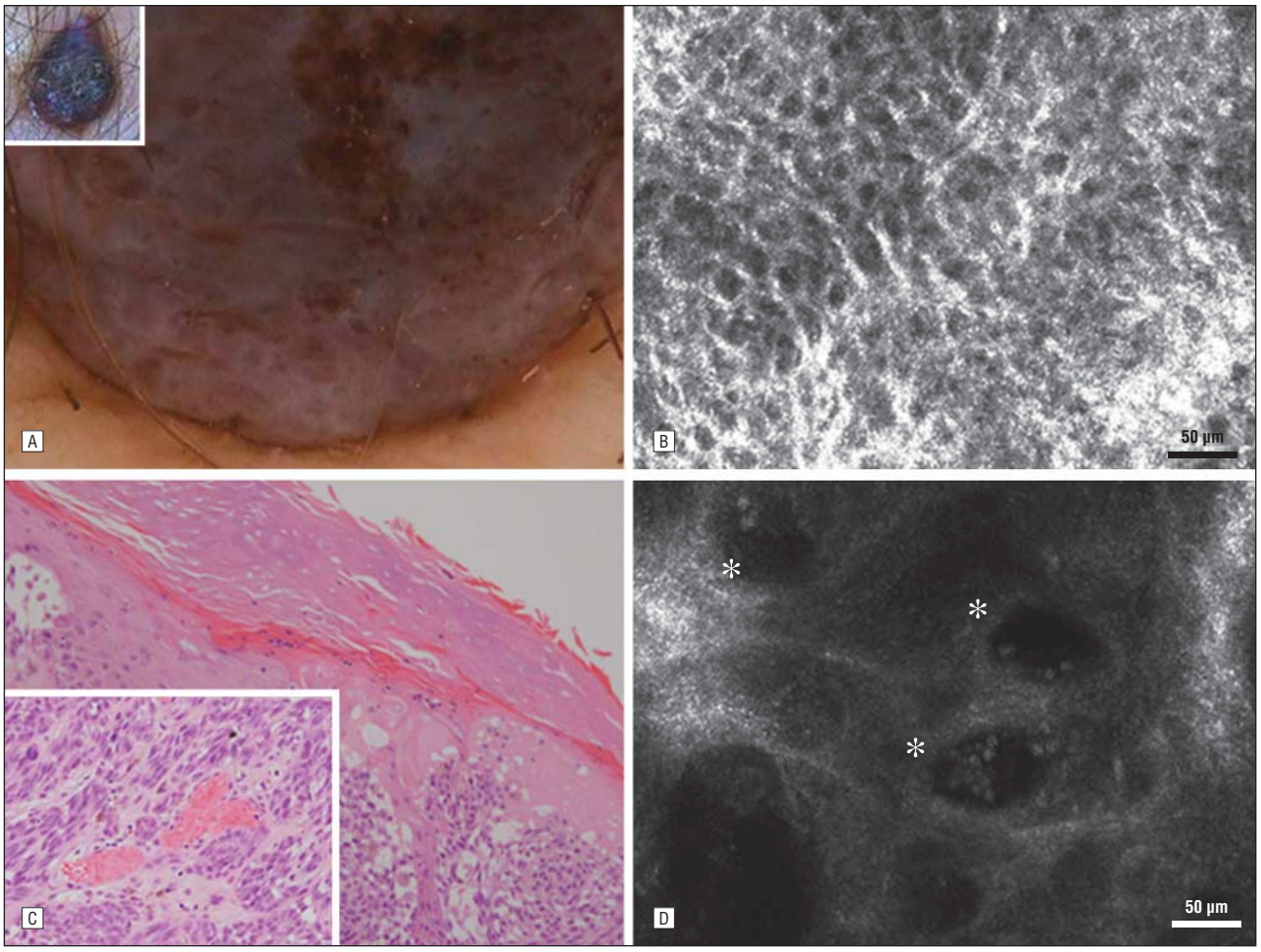

Figure 1. Nodular melanoma. A, Clinical (inset) and dermoscopic views show an atypical globular pattern, structureless areas, irregular dots, and a blue-white veil. B, Reflectance-mode confocal microscopic image of the epidermis (Vivascope 1000, 475×350 µm field of view; Lucid Inc, Rochester, New York) demonstrates a broadened honeycomb pattern characterized by polygonal cells with black nuclei and a bright thick border. C, Areas of hyperkeratosis without pagetoid spreading (hematoxylin-eosin, original magnification ×200). Inset, Detail of dermal aggregates of atypical melanocytes with dilated vessels (original magnification, ×200). D, Confocal microscopic image of the dermis shows dark spaces with small cells inside (asterisks) that corresponded in the in vivo study to the circulation of blood cells within dermal vessels.

melanocytosis was constituted by few focally distributed small dendritic cells, whereas 6 SSM_{Nod} lesions exhibited numerous round and dendritic pagetoid cells distributed throughout the entire lesion (**Figure 2**B and **Figure 3**B), showing statistical differences between both groups when round pagetoid cells were considered ($P=.01$). Pagetoid cells seen at RCM correlated with histologic pagetoid spreading in 22 lesions (73%), with good correlation in the evaluation of round cells ($\kappa=0.70$; $P<.001$). Dots observed at dermoscopy correlated with pagetoid cells seen at RCM in 24 lesions (80%) and with histologic pagetoid spreading ($\kappa=0.05$; $P=.004$). At confocal microscopy, intraepidermal bright granular particles between epidermal cells were present in 5 SSM_{Nod} lesions and were not found in the NM group ($P=.02$) They correlated with more pigmented lesions and may correspond to transepidermal melanin loss (free melanin). At RCM, comparison of SSM_{Nod} and SSM_{Blue} lesions demonstrated no significant differences in upper layers. The predominant epidermal pattern was disarranged, and pagetoid cells were present in all lesions.

DERMOEPIDERMAL JUNCTION

Dermal papilla were rarely visible in NMs and in only half of the SSM_{Nod} lesions ($P=.14$). The nonvisibility of dermal papillae resulted at confocal microscopy in the sudden transition between epidermal layers and dermal structures, corresponding at histologic analysis with a thin flattened epidermis overlying the tumor burden ($\kappa=0.05$; $P=.004$). When present, dermal papillae were irregular in shape and distribution, showing nonedged contours corresponding to marked architectural disarrangement of the rete ridge. In contrast, dermal papillae were visible in all SSM_{Blue} lesions, similarly showing a nonedged aspect in all cases (**Figure 4**B) but in combination with an edged aspect in 4 lesions. In SSM lesions, the observation of dermal papillae at the dermoepidermal junction at RCM correlated with the presence of a network at dermoscopy ($\kappa=0.04$; $P=.005$) and with the presence of elongated rete ridges ($\kappa=0.06$; $P=.004$) in histologic sections (Figure 4D).

Pleomorphic cells distributed in sheetlike structures were present at the dermoepidermal junction and in the

Downloaded from www.archdermatol.com on October 21, 2008
©2008 American Medical Association. All rights reserved.

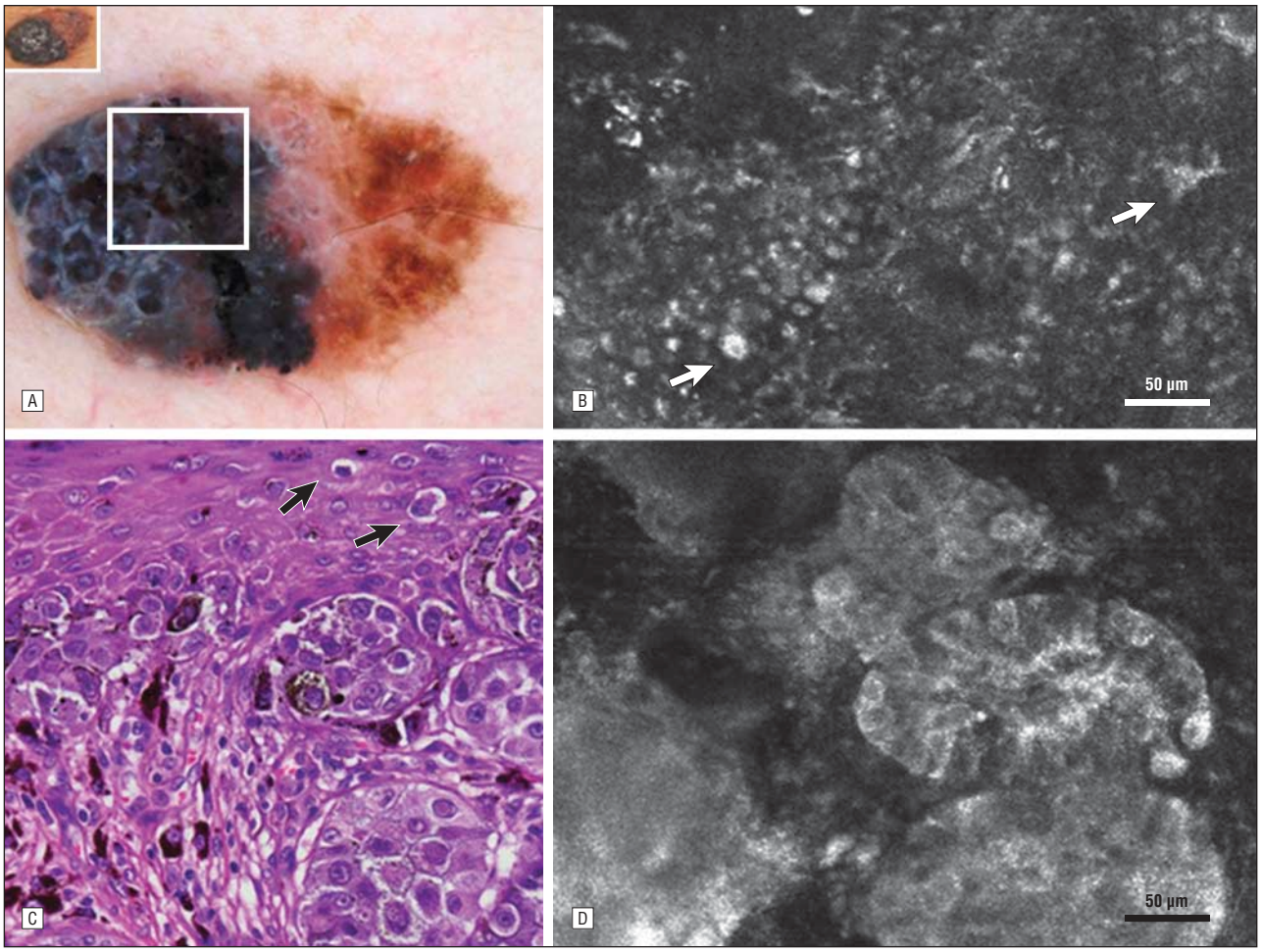

Figure 2. Superficial spreading melanoma with a nodular area. A, Clinical (inset) and dermoscopic views show an asymmetric lesion with a multicomponent pattern. Framed is the 4 × 4-mm area that was studied using confocal microscopy. B, Reflectance-mode confocal microscopic image of the epidermis (Vivascope 1500, 500 × 500 µm field of view; Lucid Inc, Rochester, New York) shows a disarranged pattern and mild presence of roundish and dendritic atypical cells (arrows). C, Acanthosis of the epidermis with mild pagetoid spreading (arrows) and nests of atypical melanocytes in the dermis (hematoxylin-eosin, original magnification ×200). D, Confocal microscopic images of the papillary dermis show dishomogeneous dense clusters of melanocytes.

superficial dermis in 7 NM and 9 SSM_{Nod} lesions (**Figure 5**C). Cells were large and markedly atypical in most cases (Table 3).

DERMIS

In both NM and SSM_{Nod} lesions, clusters of cells were visible in the dermis in 70% of cases. The NM group usually demonstrated both dense dishomogeneous clusters (6 lesions) (**Figure 6**A) and cerebriform clusters (6 lesions) (Figure 6C). In SSM_{Nod} and SSM_{Blue} lesions, nests were mostly dense and dishomogeneous (Figure 2C and Figure 4C), with a single SSM_{Nod} also exhibiting cerebriform clusters (Figure 3C). At dermoscopy, globules showed good correlation with histopathologic dermal nests ($\kappa = 0.05$; $P = .01$). In 22 lesions (73%), dense nests seen at RCM correlated with dermal aggregates of cells in papillary dermis. The observation of cerebriform clusters at RCM was associated with melanomas with a nodular pattern and deep tumoral infiltration ($\kappa = 0.05$; $P = .001$). Single nucleated cells were observed in all lesions, corresponding to atypical melanocytes infiltrating the dermis (Figure 4C). Plump, bright, irregularly shaped cells with ill-defined borders and nonvisible nuclei corresponding to melanophages were present in 7 NM lesions and in 7 SSM_{Nod} lesions, and in all SSM_{Blue} lesions. Refractive fibrillar structures gathered into large fasciae surrounding agreggates of cells were more frequently present in 9 NM compared with 2 SMM_{Nod} lesions and never seen in SSM_{Blue} lesions ($P = .003$). These structures corresponded to compact collagen bundles distributed around a tumoral mass ($\kappa = 0.04$; $P = .005$). Moreover, enlarged vessels were present in 9 NMs (90%) (Figure 5B and Figure 6C), 7 SSM_{Nod} (Figure 3C), and 5 SSM_{Blue} lesions (Table 3). Dermoscopic vessels correlated with the presence of vessels at RCM ($\kappa = 0.40$; $P = .01$) that corresponded to dilated vessels under the epidermis ($\kappa = 0.40$; $P = .01$). However, vessels visualized at dermoscopy and RCM were often more prominent than those observed in histopathologic sections.

COMMENT

In our study, dermoscopic evaluation revealed characteristic features in NM lesions and significant differ-

Downloaded from www.archdermatol.com on October 21, 2008
©2008 American Medical Association. All rights reserved.

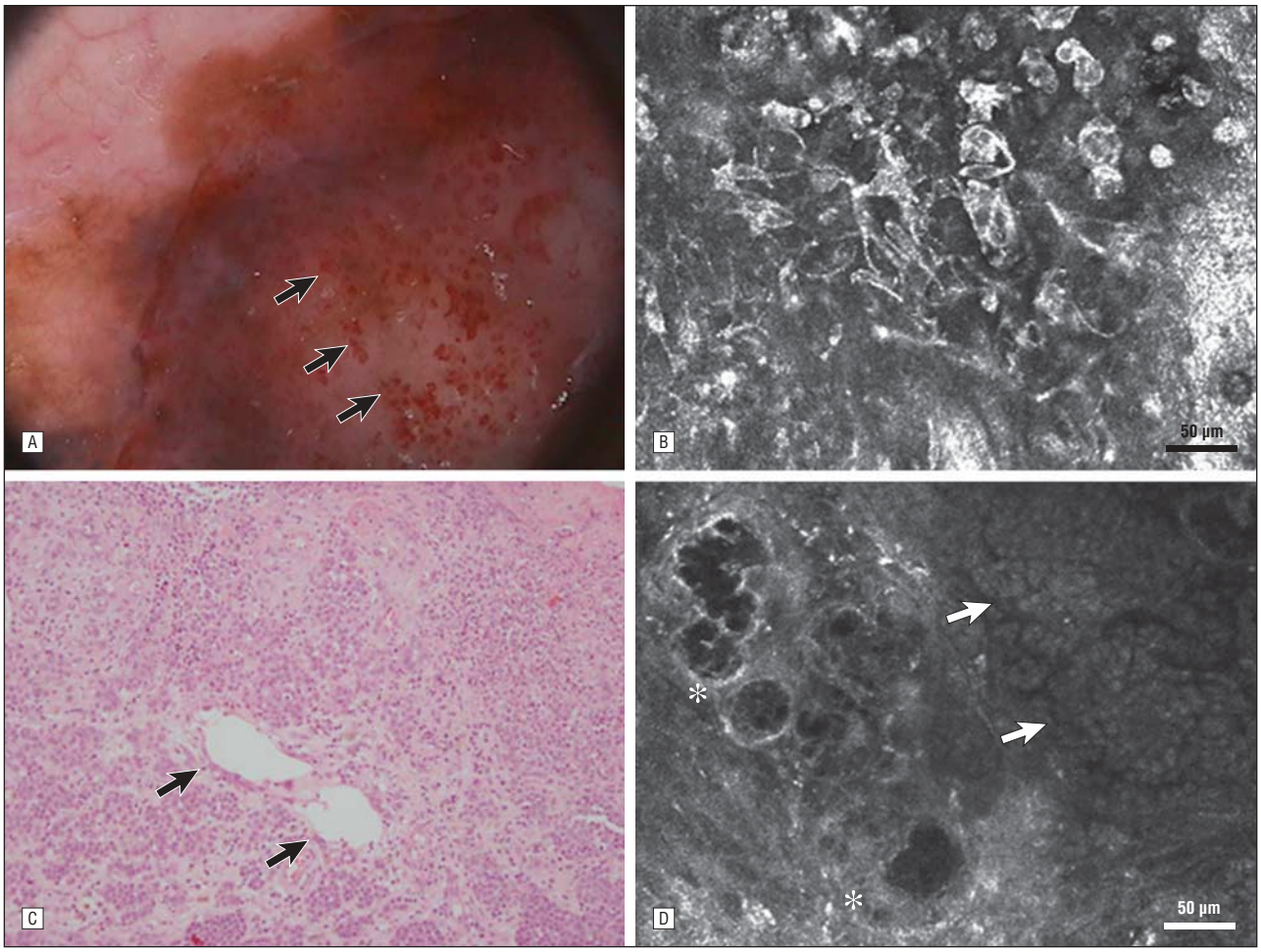

Figure 3. Superficial spreading melanoma. A, Dermoscopy of the nodular area shows prominent atypical vessels (arrows). B, Reflectance-mode confocal microscopic image of the epidermis (Vivascope 1000, 475 × 350 µm field of view; Lucid Inc, Rochester, New York) exhibits a disarranged pattern and abundant large dendritic atypical cells. C, Histologic sections of the dermis demonstrate a dense and deep proliferation of atypical epithelioid cells. Note the presence of dilated vessels (arrows) (hematoxylin-eosin, original magnification ×100). D, Confocal microscopic image of the dermis shows cerebriform nests (arrows) associated with enlarged vessels (asterisks).

ences compared with SSM groups. The dermoscopic pattern was nonspecific according to classic dermoscopic pattern analysis; however, the lesions exhibited at least 3 dermoscopic structures.[30] In contrast to clinical evaluation, dermoscopic analysis demonstrated enough criteria for malignancy in most NMs. The presence of a blue-white veil and vessels was more frequent in the nodular groups (NM and SSM_{Nod}) than in SSM_{Blue} lesions, demonstrating that NMs exhibit dermoscopic findings associated with deep tumoral extension.[12]

Like dermoscopy, RCM is a complementary imaging technique that enables the study of skin tumors in the horizontal plane.[13,14] Reflectance-mode confocal microscopy enables a quasi-histologic resolution and also a different architectural view of the tumor that can be better evaluated in combination with the dermoscopic images. In addition, dermoscopy enables localization of confocal images in the tumor and renders the area for exact pathologic correlation in the vertical plane.

Reflectance-mode confocal microscopy is useful in the diagnosis of skin tumors including melanocytic lesions[15-29] and basal cell carcinoma.[28,31,32] Several studies have attempted to describe confocal features for the characterization of melanocytic and nonmelanocytic skin tumors[15-29,31,32] and have performed dermoscopic[20-22,26,27] and histopathologic correlations.[15-27,31] A diagnostic semiquantitative algorithm for RCM evaluation of clinically and dermoscopically equivocal melanocytic lesions was recently proposed.[24] Two major confocal criteria (presence of nonedged papilla and cytologic atypia) and 4 minor confocal criteria (presence of roundish cells in the superficial layers, pagetoid cells widespread throughout the lesion, cerebriform clusters, and nucleated cells within the dermal papilla) were associated with malignancy.[24] The sensitivity and specificity of confocal features for the diagnosis of melanoma were later evaluated in a further study by 2 blinded expert observers.[29]

Previously, nodular melanoma was not investigated using RCM. In the present pilot study, pure NMs exhibited some differential features at RCM compared with SSMs. These differences often correlated with dermoscopic and histopathologic findings.

Within the epidermis, NMs lacked characteristic features of melanoma such as epidermal disarrangement and pagetoid spreading, usually showing a honeycomb pattern or a peculiar broadened pattern consisting of po-

Downloaded from www.archdermatol.com on October 21, 2008
©2008 American Medical Association. All rights reserved.

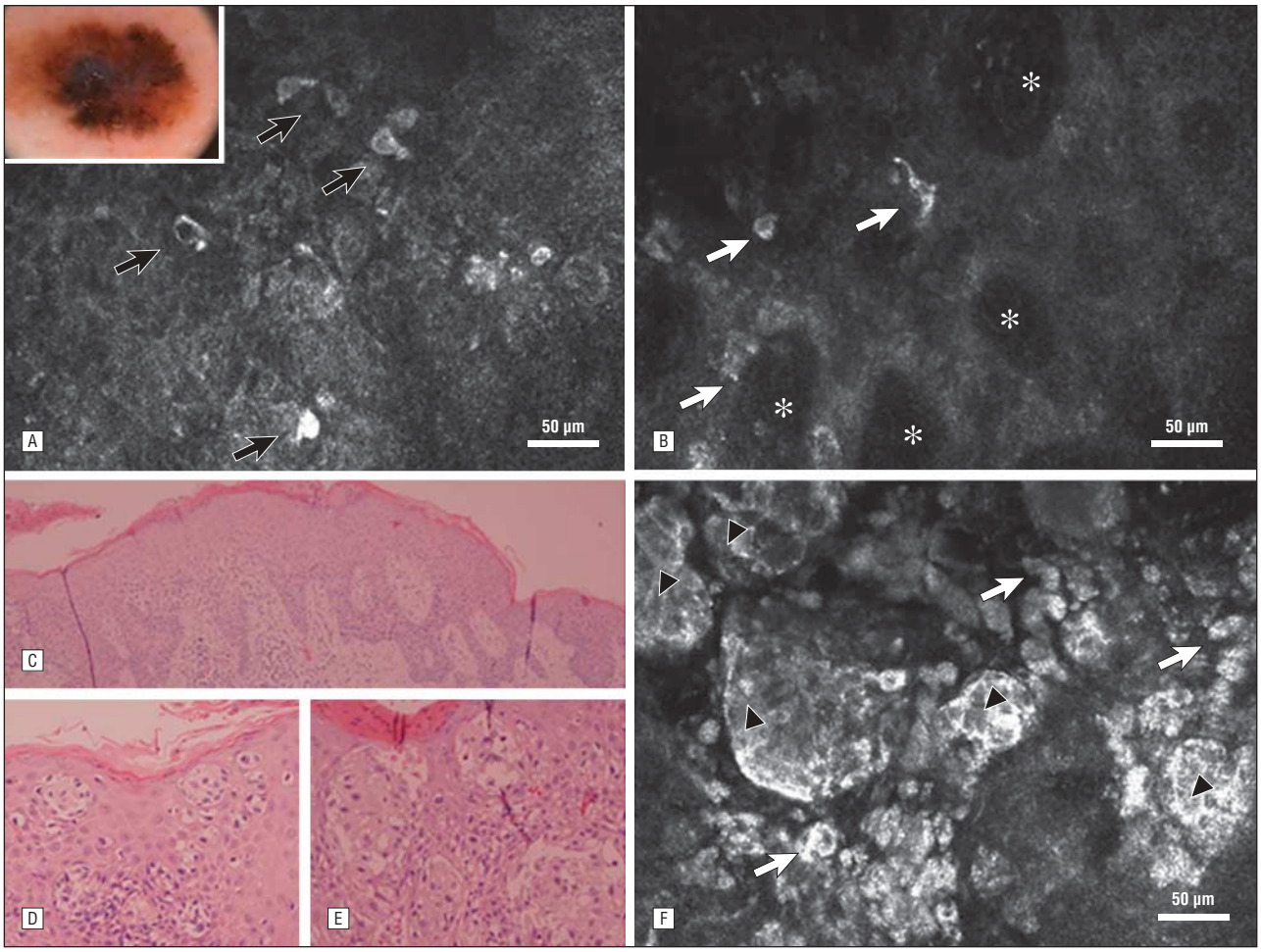

Figure 4. Superficial spreading melanoma with a blue area. A, Confocal image of epidermal layers (Vivascope 1000, 475×350 µm field of view; Lucid Inc, Rochester, New York) demonstrates pagetoid roundish cells on upper layers (arrows). Inset, Dermoscopic image shows multicomponent pattern and a central blue area. B, Confocal image of the dermoepidermal junction. Note the presence of nonedged papilla (asterisks) and atypical dendritic and roundish basal cells (arrows). C, Histologic section shows the epidermal aspect of the lesion over an area of regression. Note the elongation of rete ridges and its correspondence with nonedged papilla at reflectance-mode confocal microscopy (hematoxylin-eosin, original magnification ×40). D and E, Histologic sections show pagetoid spreading of melanocytes and tumoral nests of malignant melanocytes in the upper dermis (hematoxylin-eosin, original magnification ×200). F, Irregular dense clusters (arrowheads) and atypical nucleated cells in the upper dermis (arrows).

lygonal cells with black nuclei and bright thick borders. In contrast, at confocal microscopy, SSM groups showed similar epidermal patterns characterized by a mostly disarranged pattern and the presence of moderate to intense pagetoid cells.

At the dermoepidermal junction, the nodular component of both NMs and SSM_{Nod} lesions exhibited similar features. Immediately below the epidermal layers, the typical papillary architecture was not visible in the nodules, corresponding to the epidermal flattening caused by the massive proliferation of malignant cells in the dermis. Markedly pleomorphic cells with bright cytoplasm and dark nuclei were present both in the basal layer, sometimes distributed in sheetlike structures, and in the upper dermis, isolated or aggregated in dishomogeneous clusters, in both NM and SSM_{Nod} lesions, whereas deep, amorphous, hyporefractive nests, called "cerebriform nests," were more frequently observed in NMs, correlating with deep tumoral infiltration. In contrast, in SSM_{Blue} lesions, the rete ridge was markedly disarranged but grossly preserved, resulting in the frequent observation of irregularly sized and shaped nonedged papillae in combination with marked cytologic atypia. Nucleated cells corresponding to malignant melanocyte infiltration were also observable in SSM_{Blue} lesions, usually in combination with dishomogeneous aggregates of atypical cells.

As a new RCM feature of nodular melanomas, we found in the upper dermis some bright fibrillar structures bunched in large bundles and delimiting aggregates of atypical cells. Histopathologic correlation was difficult given the few lesions; however, they probably correspond to compacted collagen surrounding the tumoral mass. Plump cells were present in most lesions and correlated with dermal macrophages, usually associated with a moderate degree of inflammation. Moreover, NM and SSM_{Nod} lesions exhibited enlarged and tortuous vessels in most cases but were less frequent in SSM_{Blue} lesions, indicating the presence of prominent neovascularization in thicker and more advanced lesions.

Nodular melanomas and SSM_{Nod} showed similar confocal and histopathologic features in the dermal component, characterized by prominent cellularity and mod-

Downloaded from www.archdermatol.com on October 21, 2008
©2008 American Medical Association. All rights reserved.

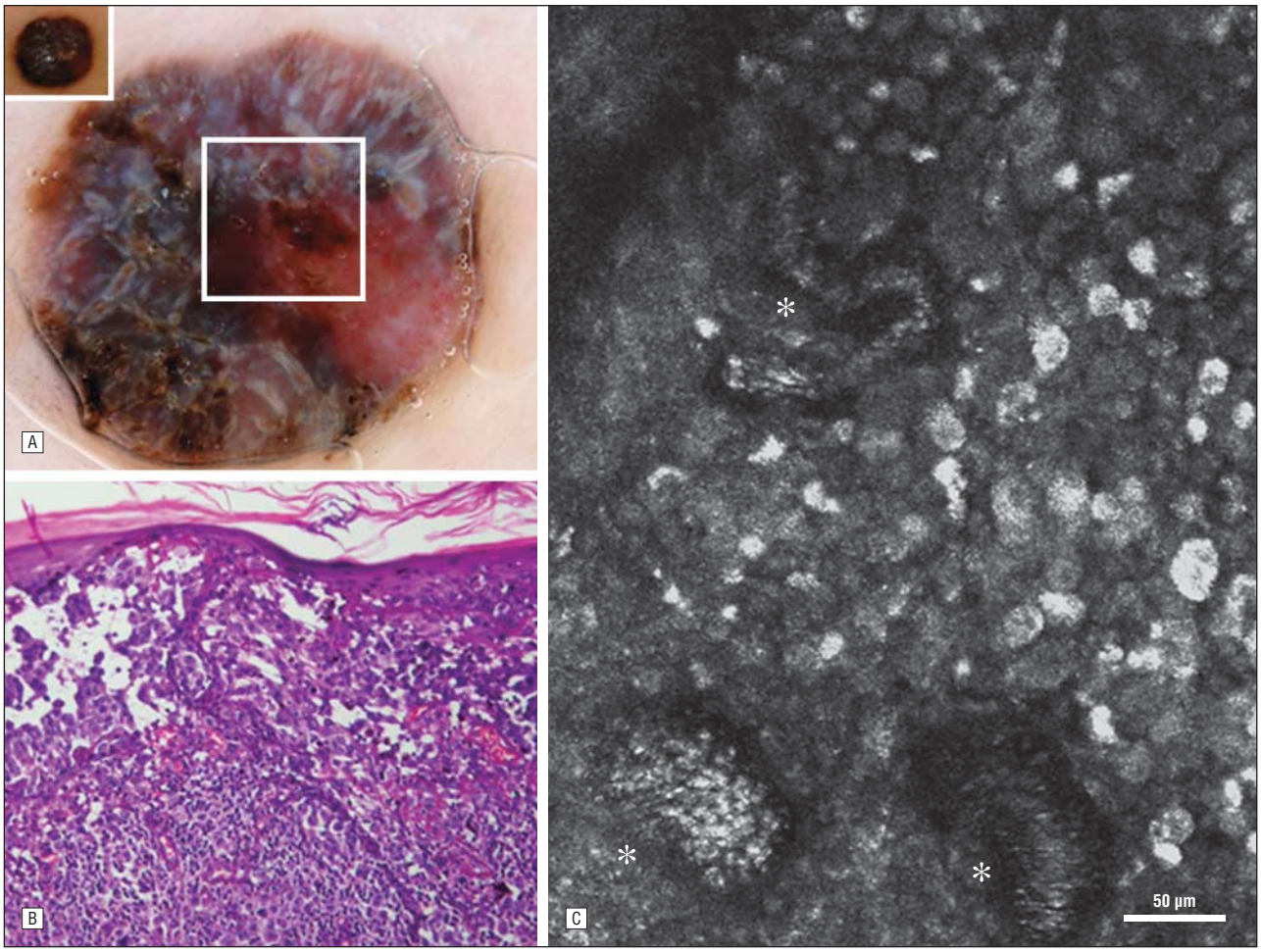

Figure 5. Nodular melanoma. A, Clinical (inset) and dermoscopic images exhibit a nonspecific dermoscopic pattern. Note the presence of a blue-white veil, structureless areas, multiple colors, and atypical vessels. Framed is the 4 × 4-mm area that was studied using confocal microscopy. B, Corresponding histologic section shows a flattened epidermis and a proliferation of noncoalescence atypical melanocytes in the papillary dermis (hematoxylin-eosin, original magnification ×100). C, Reflectance-mode confocal microscopic image of the papillary dermis (Vivascope 1500, 500 × 500 µm field of view; Lucid Inc, Rochester, New York) shows a diffuse sheetlike proliferation of atypical melanocytes related to dilated vessels with circulating blood cells (asterisks).

erate inflammatory infiltrate with the absence of regression. In contrast, within the epidermis, patterns of substantial intraepidermal growth such as marked pagetoid spread and epidermal disarrangement were present in lesions with a superficial spreading component (SSM_{Nod} and SSM_{Blue} lesions), but these were lacking, except for few sporadic pagetoid cells, in NMs. Thus, from these findings in SSMs, the vertical growth seemed to arise within a predominantly horizontal growing population that is still found in the epidermis overlying the nodule, in contrast to a vertical growth of pleomorphic cells from the beginning in pure NMs.

To our knowledge, histopathologic studies that systematically compared NMs and SSMs have not been reported in the recent literature. However, it is classically accepted that NMs demonstrate vertical growth without evidence of an associated radial growth phase beyond the width of 3 rete ridges beyond the invasive component in any section.[3] Intraepidermal spread in NMs is absent or limited to an area above the nodule, whereas SSMs characteristically exhibit prominent pagetoid spreading. In our pilot study, we were able to demonstrate these differences in vivo.

Confocal and histopathologic correlation enables in vivo visualization of some characteristic histologic features in the epidermis and superficial dermis, whereas aspects deeper than 300 µm were not visible owing to technical limitation. In this study, we confirmed some already described RCM criteria for SSM and their dermoscopic and histologic correlation. In addition, we characterized NMs using dermoscopy and RCM, demonstrating differential features between pure NMs and SSMs, with a subgroup of lesions in the middle of the spectrum (SSM_{Nod}).

Possible limitations of the present study are the few pure NMs and that clinicians who performed the confocal and histopathologic evaluations were not blinded to the dermoscopic images. Because the correlation of RCM, dermoscopy, and histopathologic analysis was performed by a single, nonblinded observer (S. Segura), the analysis of agreement between these methods was performed as a preliminary exploration, and further studies are required to confirm the findings.

Reflectance-mode confocal microscopy seems to be a promising technique for the study of melanocytic lesions and nodular-type malignant melanoma. However,

Downloaded from www.archdermatol.com on October 21, 2008
©2008 American Medical Association. All rights reserved.

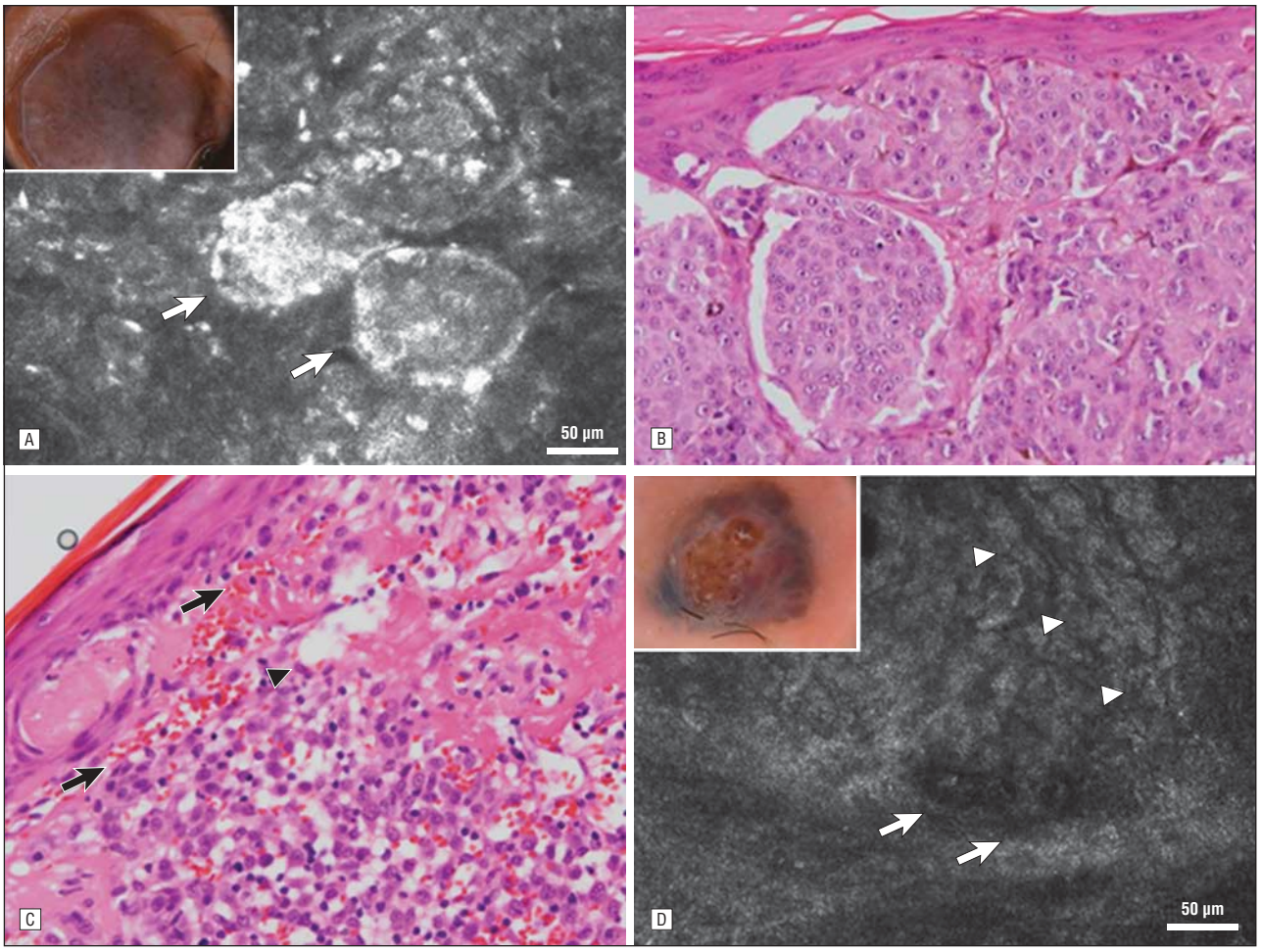

Figure 6. Nodular melanoma. A, Reflectance-mode confocal microscopic image of the dermis (Vivascope 1000, 475×350 µm field of view; Lucid Inc, Rochester, New York) demonstrates dishomogeneous dense clusters (arrows) that correlate with dermoscopic globules. Inset, Dermoscopic view shows an atypical globular pattern and a blue-white veil. B, Histologic section shows the corresponding dermal nests of atypical epithelioid cells (hematoxylin-eosin, original magnification ×200). C, Histologic section of the tumor shows a thin and flattened epidermis without pagetoid spreading. Note tumoral cells infiltrating the dermis, with the presence of purpura (arrows) and subepidermal telangiectatic vessels (arrowhead) (hematoxylin-eosin, original magnification ×200). D, Reflectance-mode confocal microscopic image of the dermis (Vivascope 1000, 475×350 µm; Lucid Inc, Rochester, New York) demonstrates cerebriform clusters (arrowheads) and enlarged vessels (arrows). Inset, Dermoscopic image of an ulcerated nodular melanoma shows the presence of red-blue lagoonlike structures mimicking a vascular lesion.

larger studies with pure NMs should be done to better characterize these lesions, and genetic studies should be performed to enable further understanding of the histogenic subtypes and biological behavior of malignant melanoma.

Accepted for Publication: December 28, 2007.
Correspondence: Sonia Segura, MD, Department of Dermatology, Hospital Clinic, Barcelona, 170 Villarroel, 08036 Barcelona, Spain (ssegura@imas.imim.es).
Author Contributions: Dr Segura had full access to the data in the study and takes responsibility for the integrity of the data and the accuracy of the data analysis. *Study concept and design*: Segura and Pellacani. *Acquisition of data:* Segura, Pellacani, Longo, Bassoli, Guitera, and Palou. *Analysis and interpretation of data*: Segura, Pellacani, Puig, and Malvehy. *Drafting of the manuscript*: Segura. *Critical revision of the manuscript*: Pellacani, Puig, Guitera, Menzies, Seidenari, and Malvehy.
Financial Disclosure: None reported.
Funding/Support: This study was supported in part by grants from Hospital Clinic, Barcelona; Novartis Pharmaceuticals; the Fondazione Cassa di Risparmio di Modena; and the Cancer Institute of New South Wales.

REFERENCES

1. Chang AE, Karnell LH, Menck HR; American College of Surgeons Commission on Cancer and the American Cancer Society. The National Cancer Data Base report on cutaneous and noncutaneous melanoma: a summary of 84,836 cases from the past decade. *Cancer.* 1998;83(8):1664-1678.
2. Demierre MF, Chung C, Miller DR, Geller AC. Early detection of thick melanomas in the United States: beware of the nodular subtype. *Arch Dermatol.* 2005; 141(6):745-750.
3. Clark WH Jr, From L, Bernardino EA, Mihm MC. The histogenesis and biologic behaviour of primary human malignant melanomas of the skin. *Cancer Res.* 1969; 29(3):705-727.
4. Poetsch M, Woenckhaus C, Dittberner T, Pambor M, Lorenz G, Herrmann FH. Differences in chromosomal aberrations between nodular and superficial spreading malignant melanoma detected by interphase cytogenetics. *Lab Invest.* 1998; 78(7):883-888.
5. Poetsch M, Dittberner T, Woenckhaus C. Can different genetic changes characterize histogenetic subtypes and biologic behaviour in sporadic malignant melanoma of the skin? *Cell Mol Life Sci.* 2003;60(9):1923-1932.
6. Treszl A, Adány R, Rákosy Z, et al. Extra copies of *c-myc* are more pronounced in nodular melanomas than in superficial spreading melanomas as revealed by fluorescence in situ hybridisation. *Cytometry B Clin Cytom.* 2004;60(1):37-46.

Downloaded from www.archdermatol.com on October 21, 2008
©2008 American Medical Association. All rights reserved.

7. Curtin JA, Fridlyand J, Kageshita T, et al. Distinct sets of genetic alterations in melanoma. *N Engl J Med*. 2005;353(20):2135-2147.
8. Richard MA, Grob JJ, Avril MF, et al. Delays in diagnosis and melanoma prognosis, II: the role of doctors. *Int J Cancer*. 2000;89(3):280-285.
9. Brochez L, Verhaeghe E, Bleyen L, Naeyaert JM. Diagnostic ability of general practitioners and dermatologists in discriminating pigmented skin lesions. *J Am Acad Dermatol*. 2001;44(6):979-986.
10. Chamberlain AJ, Fritschi L, Kelly JW. Nodular melanoma: patients' perceptions of presenting features and implications for earlier detection. *J Am Acad Dermatol*. 2003;48(5):694-701. doi:10.1067/mjd.2003.216.
11. Pizzichetta MA, Talamini R, Stanganelli I, et al. Amelanotic/hypomelanotic melanoma: clinical and dermoscopic features. *Br J Dermatol*. 2004;150(6):1117-1124.
12. Menzies SW. Nodular melanoma. In: Marghoob A, Braun PR, Kopf AW, eds. *Atlas of Dermoscopy*. London, England: Taylor & Francis; 2005.
13. Rajadhyaksha M, Grossman M, Esterowitz D, Webb RH, Anderson RR. In vivo confocal scanning laser microscopy of human skin: melanin provides strong contrast. *J Invest Dermatol*. 1995;104(6):946-952.
14. Rajadhyaksha M, González S, Zavislan JM, Anderson RR, Webb RH. In vivo confocal scanning laser microscopy of human skin, II: advances in instrumentation and comparison with histology. *J Invest Dermatol*. 1999;113(3):293-303.
15. Busam KJ, Hester K, Charles C, et al. Detection of clinically amelanotic malignant melanoma and assessment of its margins by in vivo confocal scanning laser microscopy. *Arch Dermatol*. 2001;137(7):923-929.
16. Langley RG, Rajadhyasksha M, Dawyer PJ, Sober AJ, Flotte TJ, Anderson RR. Confocal scanning laser microscopy of benign and malignant melanocytic skin lesions in vivo. *J Am Acad Dermatol*. 2001;45(3):365-376.
17. Busam KJ, Charles C, Lohmann CM, Marghoob A, Goldgeier M, Halpern AC. Detection of intraepidermal malignant melanoma in vivo by confocal scanning laser micoscopy. *Melanoma Res*. 2002;12(4):349-355.
18. Tannous ZS, Mihm MC, Flotte TJ, González S. In vivo examination of lentigo maligna and malignant melanoma in situ, lentigo maligna type by near-infrared reflectance confocal microscopy: comparison of in vivo confocal images with histologic sections. *J Am Acad Dermatol*. 2002;46(2):260-263.
19. Curiel-Lewandrowski C, Williams CM, Swidells KJ, et al. Use of in vivo confocal microscopy in malignant melanoma: an aid in diagnosis and assessment of surgical and nonsurgical therapeutic approaches. *Arch Dermatol*. 2004;140(9):1127-1132.
20. Pellacani G, Cesinaro AM, Grana C, Seidenari S. In vivo confocal scanning laser microscopy of pigmented Spitz nevus: comparison of in vivo confocal images with dermoscopy and routine histopathology. *J Am Acad Dermatol*. 2004;51:371-376.
21. Pellacani G, Cesinaro AM, Seidenari S. In vivo assessment of melanocytic nests in nevi and melanomas by reflectance confocal microscopy. *Mod Pathol*. 2005;18(4):469.
22. Pellacani G, Cesinaro AM, Longo C, Grana C, Seidenari S. Microscopic in vivo description of cellular architecture of dermoscopic pigmented network in nevi and melanomas. *Arch Dermatol*. 2005;141(2):147-154.
23. Pellacani G, Cesinaro AM, Seidenari S. Reflectance-mode confocal microscopy for the in vivo characterization of pagetoid melanocytosis in melanomas and nevi. *J Invest Dermatol*. 2005;125(3):532-537.
24. Pellacani G, Cesinaro AM, Seidenari S. Reflectance-mode confocal microscopy of pigmented skin lesions: improvement in melanoma diagnostic specificity. *J Am Acad Dermatol*. 2005;53(6):979-985.
25. Gerger A, Koller S, Kern T, et al. Applicability of in vivo confocal laser scanning microscopy in melanocytic skin tumors. *J Invest Dermatol*. 2005;124(3):493-498.
26. Marghoob AA, Charles CA, Busam KJ, et al. In vivo confocal scanning laser microscopy of a series of congenital melanocytic nevi suggestive of having developed malignant melanoma. *Arch Dermatol*. 2005;141(11):1401-1412.
27. Langley RG, Burton E, Walsh N, Propperova I, Murray SJ. In vivo confocal scanning laser microscopy of benign lentigines: comparison to conventional histology and in vivo characteristics of lentigo maligna. *J Am Acad Dermatol*. 2006;55(1):88-97.
28. Gerger A, Koller S, Weger W, et al. Sensitivity and specificity of confocal laser-scanning microscopy for in vivo diagnosis of malignant skin tumors. *Cancer*. 2006;107(1):193-200.
29. Pellacani G, Guitera P, Longo C, Avramidis M, Seidenari S, Menzies S. The impact of in vivo reflectance confocal microscopy for the diagnostic accuracy of melanoma and equivocal melanocytic lesions. *J Invest Dermatol*. 2007;127(12):2759-2765.
30. Malvehy J, Puig S, Braun RP, Marghoob AA, Kopf AW, eds. *Handbook of Dermoscopy*. London, England: Taylor & Francis; 2006.
31. González S, Tannous Z. Real-time in vivo confocal reflectance microscopy of basal cell carcinoma. *J Am Acad Dermatol*. 2002;47(6):869-874.
32. Nori S, Rius-Díaz F, Cuevas J, et al. Sensitivity and specificity of reflectance-mode confocal microscopy for in vivo diagnosis of basal cell carcinoma: a multicenter study. *J Am Acad Dermatol*. 2004;51(6):923-930.

Archives Web Quiz Winner

Congratulations to the winner of our July quiz, Khaled Ezzedine, MD, PhD, Department of Dermatology, Hôpital Saint André, Centre Hospitalier Universitaire, Bordeaux, France. The correct answer to our July challenge was tungiasis. For a complete discussion of this case, see the Off-Center Fold section in the August *Archives* (Zand S, Mumm CD, Fung MA, Eisen DB. Nodule on the toe after traveling to Africa. *Arch Dermatol*. 2008;144[8]:1051-1056).

Be sure to visit the *Archives of Dermatology* Web site (http://www.archdermatol.com) to try your hand at the interactive quiz. We invite visitors to make a diagnosis based on selected information from a case report or other feature scheduled to be published in the following month's print edition of the *Archives*. The first visitor to e-mail our Web editors with the correct answer will be recognized in the print journal and on our Web site and will also receive a free copy of *The Art of JAMA II*.

Downloaded from www.archdermatol.com on October 21, 2008
©2008 American Medical Association. All rights reserved.

3.3. Trabajo III

Dendritic Cells in Pigmented Basal Cell Carcinoma
A Relevant Finding by Reflectance-Mode Confocal Microscopy
Sonia Segura, Susana Puig, Cristina Carrera, Josep Palou, Josep Malvehy
Arch Dermatol 2007;143:883-86

Objetivos:
Caracterizar por microscopía confocal de reflectancia (MCR) los carcinomas basocelulares (CBCs) pigmentados.

Métodos:
Estudiamos mediante microscopía confocal, histología e inmunohistoquímica (S-100, MelanA, HMB-45 y CD1a) tres CBC pigmentados consecutivos, focalizando en el origen de las estructuras dendríticas observadas en estos tumores.

Resultados:
Mediante MCR demostramos la presencia de estructuras reflectantes de aspecto dendrítico dentro de los nidos tumorales situados en la dermis de los CBC estudiados, que correspondían por estudio inmunohistoquímico a melanocitos no neoplásicos que poblaban los nidos. En un caso se observaron células con proyecciones dendríticas en la epidermis que correspondían con células de Langerhans. Las estructuras en hoja de arce observadas en dermatoscopia se correlacionaban por MCR con islotes tumorales hiporeflectantes claramente conectados con la epidermis, mientras que los glóbulos azul-grises se correlacionaban con células reflectantes de bordes mal definidos situadas en el interior y fuera de los nidos tumorales y correspondían a melanófagos. Las telangiectasias arboriformes presentes en la dermatoscopia de estos tumores se correspondían con vasos de gran tamaño tortuosos en la dermis.

OBSERVATION

Dendritic Cells in Pigmented Basal Cell Carcinoma

A Relevant Finding by Reflectance-Mode Confocal Microscopy

Sonia Segura, MD; Susana Puig, MD; Cristina Carrera, MD; Josep Palou, MD; Josep Malvehy, MD

Background: Reflectance-mode confocal microscopy (RCM) is a new approach for the in vivo diagnosis of skin tumors. A few studies of RCM on basal cell carcinoma (BCC) have provided specific diagnostic criteria, but large studies on pigmented basal cell carcinoma are lacking. Proliferation of large dendritic-shaped cells within a melanocytic tumor has been associated with the diagnosis of melanoma by RCM. Benign melanocytes and Langerhans cells may populate BCC according to previous histological studies. We studied 3 consecutive pigmented BCC by means of RCM and performed a histological and immunohistochemical correlation focusing on the presence of dendritic structures.

Observations: Reflectance-mode confocal microscopy revealed highly refractive dendritic structures within tumor nests that correlated with the presence of melanocytes within the tumor by immunochemical analysis. In 1 case, dendritic structures on the overlying epidermis corresponding to Langerhans cells were also noted. Leaf-like areas observed on dermoscopy correlated with low-refractive cordlike structures and nodules by RCM and corresponded to nests of basaloid cells, whereas blue-gray globules presented as bright oval structures with ill-defined borders corresponding to melanophages.

Conclusions: Reflectance-mode confocal microscopy allows the study of pigmented BCC and the identification of specific criteria described previously. In these tumors, dendritic melanocytes can be easily identified with this technique.

Arch Dermatol. 2007;143(7):883-886

Author Affiliations:
Department of Dermatology, Hospital Clinic Barcelona, Barcelona, Spain.

DIFFERENTIAL DIAGNOSIS between pigmented basal cell carcinoma (BCC) and melanoma can be difficult. Reflectance-mode confocal microscopy (RCM) is useful in the recognition of BCC[1] and melanocytic lesions.[2] Three pigmented BCC were studied using RCM, dermoscopy, and histopathologic analysis. Emphasis was placed on the analyses of dendritic cells detected by RCM. Reflectance-mode confocal microscopy was performed with a commercially available, near-infrared reflectance confocal laser scanning microscope (Vivascope 1500; Lucid Inc, Henrietta, New York). Histological slides were stained with hematoxylin-eosin, and immunohistochemical studies were performed.

REPORT OF CASES

Patient 1 was a 78-year-old woman with a gray-brown papule on the back. Findings from dermoscopy showed leaflike structures and blue-gray globules suggestive of BCC (**Figure 1**A). Reflectance-mode confocal microscopy revealed focally elongated and polarized nuclei, multiple solid units of tumor cells forming cordlike structures and nodules surrounded by a dark area, and bright oval structures with ill-defined borders within tumor nests and surrounding them. Long, thin dendritic structures were observed all over the lesion and were located within tumor nests and on the overlying epidermis (Figure 1B). Dilated vessels with rolling phenomena were also noted. Histopathologic analysis confirmed the diagnosis of nodular BCC (Figure 1C). Immunohistochemical studies demonstrated S100 and $CD1a^+$ dendritic cells on the epidermis and S100, MelanA, and $HMB45^+$ within tumoral nests (Figure 1D), indicating the presence of melanocytes within tumoral nests and activated Langerhans cells on the epidermis.

Patients 2 and 3 exhibited similar dermoscopical, confocal, histological, and immunohistochemical findings (**Figure 2**).

COMMENT

Reflectance-mode confocal microscopy and dermoscopy are imaging techniques that allow the study of skin tumors in the

©2007 American Medical Association. All rights reserved.

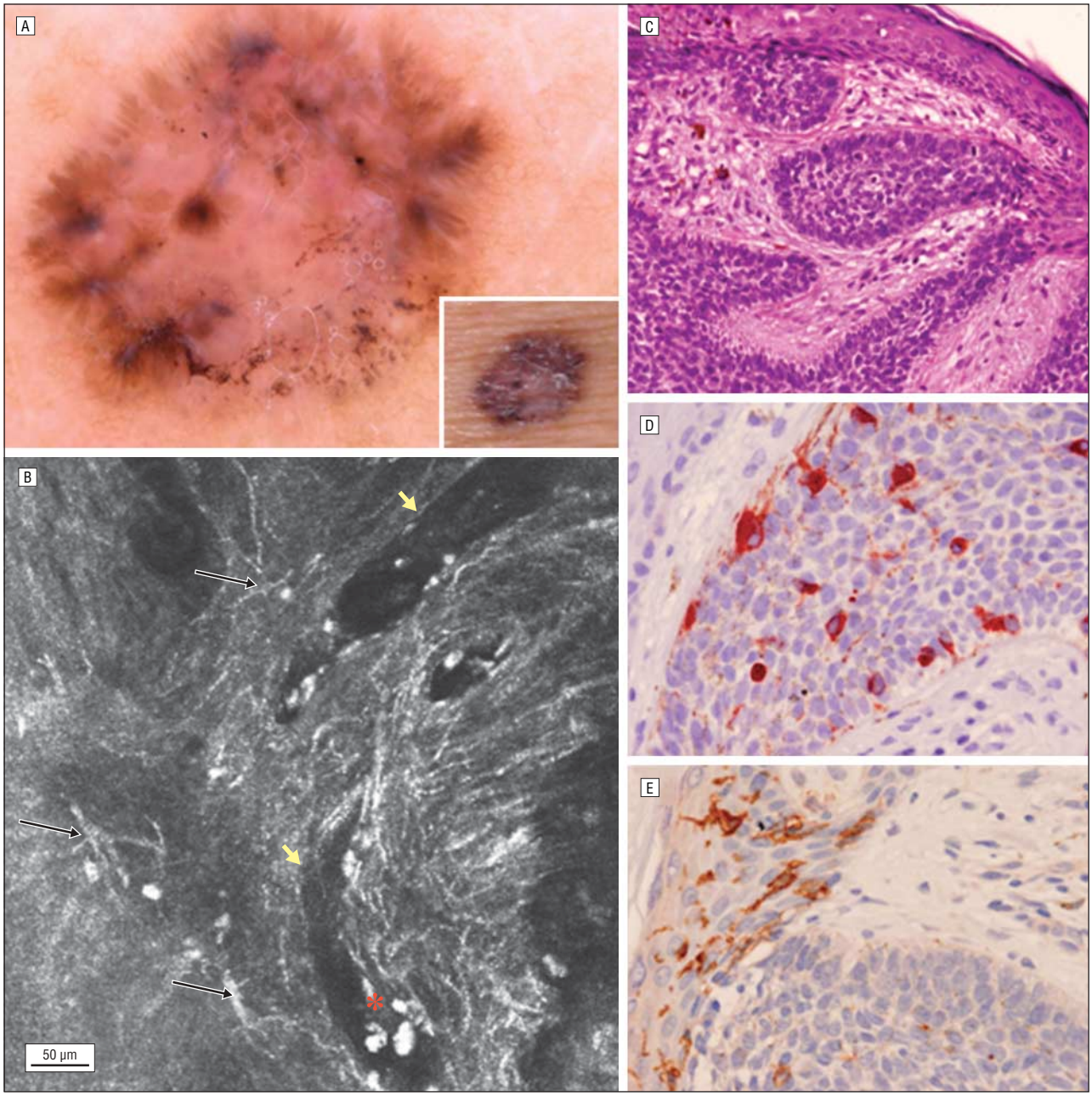

Figure 1. Nodular pigmented basal cell carcinoma on the back (patient 1). A, Dermoscopic image showing leaflike structures and blue-gray globules. B, Reflectance-mode confocal microscopy image showing solid units of tumor cells forming nodules surrounded by a dark area (yellow arrows). Note the hyperrefractile thin dendrites (black arrows) and bright oval structures within and around tumor islands (red asterisk). C, Tumor nests with basaloid palisading cells in the upper dermis (hematoxylin-eosin, original magnification ×200). D, Positive dendritic melanocytes within the tumor nests (MelanA, original magnification ×400). E, Langerhans cells on the overlying epidermis (CD1a, original magnification ×400).

horizontal plane. Reflectance-mode confocal microscopy allows a quasihistological resolution and an architectural view of the tumor that is better evaluated in combination with dermoscopy. As already been reported,[3] in patient 1, low-refractive cordlike structures and nodules correlated with dermoscopic leaflike areas. In all 3 cases, blue-gray granules correlated with confocal bright oval structures and corresponded to melanophages. Typical arborizing vessels correlated with enlarged horizontal vessels.

González et al[1] first described 5 criteria for the diagnosis of BCC by RCM,[1] which was later validated in a larger study. Another study with 12 lesions found additional criteria for the diagnosis of BCC by RCM[4] and described bright structures within tumor parenchyma that resembled dendritic cells. The same finding was recently reported by Agero et al[3] and correlated with intratumoral melanocytes or Langerhans cells.

Melanocytes can be assessed in melanocytic lesions by RCM as bright roundish or dendritic cells within the epidermis, at dermoepidermal junction or in dermal papilla.[2] Langerhans cells can be identified by RCM as dendritic cells within epidermal layers in inflamed nevi or scars of lesions recently removed.

©2007 American Medical Association. All rights reserved.

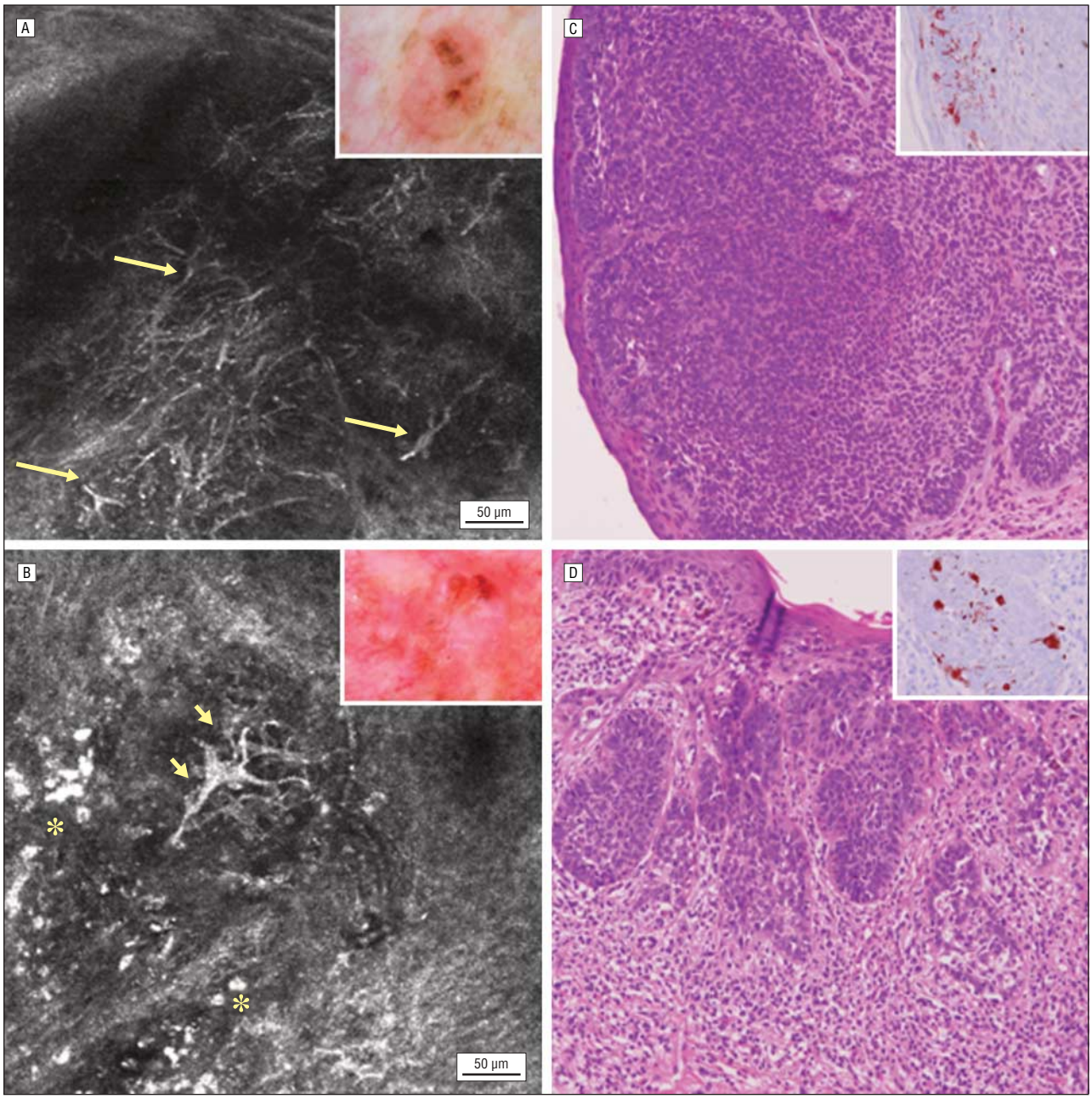

Figure 2. Adenoid basal cell carcinoma (BCC) on the arm and superficial BCC on the chest (patients 2 and 3). A, Dermoscopy and reflectance-mode confocal microscopy (RCM) images showing thin bright dendrites throughout the tumor nests (yellow arrows) (patient 2). B, Dermoscopy and RCM images showing large dendritic cells (yellow arrows) and bright oval structures within the tumor (yellow asterisks) (patient 3). C, Dendritic melanocytes distributed at the periphery of tumor nests (patient 2) (hematoxylin-eosin, original magnification ×200, and HMB45, original magnification ×400 [inset]). D, Large melanocytes within the tumor nests (patient 3) (hematoxylin-eosin, original magnification ×100, and HMB45, original magnification ×400 [inset]).

In our study, dendritic cells in BCC nests correlated with melanocytes, whereas dendritic cells in the epidermis corresponded to Langerhans cells. Our findings are supported by previous studies that demonstrated the presence of melanocytes and Langerhans cells in BCC.[5] The importance has to be stressed of being aware of the presence of dendritic cells in RCM of pigmented BCC to avoid the incorrect classification of a melanocytic tumor including melanoma. Larger studies are needed to elucidate the frequency, characteristics, and meaning of dendritic cells in pigmented skin tumors.

Accepted for Publication: November 17, 2006.
Correspondence: Josep Malvehy, MD, Department of Dermatology, Hospital Clinic Barcelona, Villarroel 170, 08036 Barcelona, Spain (jmalvehy@clinic.ub.es).
Author Contributions: *Study concept and design:* Segura, Puig, and Malvehy. *Acquisition of data:* Segura, Palou, and Malvehy. *Analysis and interpretation of data:* Segura, Puig, Carrera, Palou, and Malvehy. *Drafting of the manuscript:* Segura and Carrera. *Critical revision of the manuscript for important intellectual content:* Puig, Palou, and Malvehy. *Study supervision:* Malvehy.

©2007 American Medical Association. All rights reserved.

Financial Disclosure: None reported.
Funding/Support: Dr Segura received a personal grant from Hospital Clinic Barcelona. This work was supported in part by Novartis Pharmaceuticals.

REFERENCES

1. González S, Tannus Z. Real-time in vivo confocal reflectance microscopy of basal cell carcinoma. *J Am Acad Dermatol.* 2002;47(6):869-874.
2. Pellacani G, Cesinaro AM, Seidenari S. Reflectance-mode confocal microscopy of pigmented skin lesions-improvement in melanoma diagnostic specificity. *J Am Acad Dermatol.* 2005;53(6):979-985.
3. Agero AL, Busam KJ, Benvenuto-Andrade C, et al. Reflectance confocal microscopy of pigmented basal cell carcinoma. *J Am Acad Dermatol.* 2006;54(4):638-643.
4. Sauermann K, Gambichler T, Wilmert M, et al. Investigation of basal cell carcinoma by confocal scanning microscopy in vivo. *Skin Res Technol.* 2002;8(3):141-147.
5. Florell SR, Zone JJ, Gerwels JW. Basal cell carcinomas are populated by melanocytes and Langerhans' cells. *Am J Dermatopathol.* 2001;23(1):24-28.

Correction

Errors in Author Contributions. In the Study titled "Store-and-Forward Teledermatology in Skin Cancer Triage: Experience and Evaluation of 2009 Teleconsultations" by Moreno-Ramirez et al, published in the April issue of the *Archives* (2007;143[4]:479-484), several errors occurred in the "Author Contributions" section. The corrected author contributions are reproduced here.

Author Contributions: Drs Moreno-Ramirez, Ferrandiz, and Nieto-Garcia had full access to all the data in the study and take responsibility for the integrity of the data and the accuracy of the data analysis. *Study concept and design:* Moreno-Ramirez, Ferrandiz, Nieto-Garcia, Carrasco, Moreno-Alvarez, Galdeano, and Camacho. *Acquisition of data:* Moreno-Ramirez, Ferrandiz, Bidegain, Moreno-Alvarez, Galdeano, and Rios-Martin. *Analysis and interpretation of data:* Moreno-Ramirez, Ferrandiz, Nieto-Garcia, Galdeano, and Camacho. *Drafting of the manuscript:* Moreno-Ramirez and Ferrandiz. *Critical revision of the manuscript for important intellectual content:* Moreno-Ramirez, Ferrandiz, Carrasco, Moreno-Alvarez, Galdeano, Rios-Martin, and Camacho. *Statistical analysis:* Moreno-Ramirez, Ferrandiz, and Nieto-Garcia. *Obtained funding:* Moreno-Ramirez, Carrasco, Bidegain, and Camacho. *Administrative, technical, and material support:* Moreno-Ramirez, Carrasco, Moreno-Alvarez, Galdeano, and Camacho. *Study supervision:* Moreno-Ramirez, Rios-Martin, and Camacho.

©2007 American Medical Association. All rights reserved.

3.4. Trabajo IV

Non-invasive management of non-melanoma skin cancer in patients with cancer predisposition genodermatosis: A role for reflectance confocal microscopy and methyl-aminolevulinate photodynamic therapy

Sonia Segura, Susana Puig, Cristina Carrera, Mario Lecha, Valeria Borges, Josep Malvehy

JEADV 2010 Oct 15. doi: 10.1111/j.1468-3083.2010.03871.x.[Epub ahead of print]

Objetivos:

Evaluar la eficacia de la terapia fotodinámica con metil-aminolevulinato (TFD-MAL) en los carcinomas basocelulares (CBCs) de pacientes con síndrome de Gorlin (SG) y Xeroderma pigmentoso (XP) y determinar la utilidad de la microscopía confocal de reflectancia (MCR) en el diagnóstico y la evaluación de la respuesta terapéutica en estos pacientes.

Métodos:

Se incluyeron 4 pacientes con SG y 2 hermanos con XP. Se trataron lesiones únicas o múltiples en zonas localizadas con 1 a 3 ciclos de TFD-MAL. La exploración con MCR se realizó antes y 3 meses después del tratamiento en las lesiones diana en todos los pacientes. Los pacientes fueron seguidos durante 3 años.

Resultados:

A los pacientes con XP se les trató 13 CBCs pigmentados en la cara. Todas las lesiones respondieron al tratamiento y 6 lesiones mostraron remisión completa clínica. A los pacientes con SG, se les realizó tratamiento de múltiples lesiones en cara o tronco (hasta 200). Se obtuvo una remisión clínica completa en un 25- 67% de las lesiones. Algunas lesiones nodulares y pigmentadas no alcanzaron la remisión completa. El examen mediante MCR pudo identificar las características descritas en estudios previos para el CBC. La respuesta al tratamiento pudo ser evaluada por esta técnica**.**

ORIGINAL ARTICLE

Non-invasive management of non-melanoma skin cancer in patients with cancer predisposition genodermatosis: a role for confocal microscopy and photodynamic therapy

S Segura,[†,‡,*] S Puig,[†,§] C Carrera,[†] M Lecha,[†] V Borges,[†] J Malvehy[†,§]

[†]Melanoma Unit, Department of Dermatology, Hospital Clinic, IDIBAPS, [‡]Department of Dermatology, Hospital del Mar, Barcelona, and [§]CIBER de Enfermedades Raras, Barcelona, Spain

*Correspondence: S Segura. E-mail: ssegura@parcdesalutmar.cat

Abstract

Background Patients with genodermatosis such as Gorlin syndrome (GS) and Xeroderma pigmentosum (XP) require a close follow-up for early diagnosis and treatment of skin cancer. We aimed to evaluate the efficacy of methyl-aminolevulinate (MAL) photodynamic therapy (PDT) in basal cell carcinomas (BCCs) from patients with GS and XP, and to determine the utility of reflectance confocal microscopy (RCM) in the diagnosis and the evaluation of therapeutic response.

Patients and methods We included four patients with GS and two siblings with XP. Single or multiple lesions in localized areas were treated with 1–3 cycles of MAL PDT. RCM was performed before and 3 months after the treatment in target lesions in all the patients. Patients were followed up for 3 years.

Results In XP patients, we treated 13 pigmented BCCs on the face. All the lesions responded to the treatment and six lesions showed a complete clinical clearing. In GS patients, facial or trunk areas with multiple BCCs were treated (up to 200). Complete clinical remission was obtained in 25–67% of the lesions. Some nodular and pigmented lesions failed to achieve a complete remission. RCM could identify already described confocal features for BCC. Tumour remissions could be assessed by this technique.

Conclusions Methyl-aminolevulinate PDT may be useful for the treatment of superficial BCC in GS and XP. In some nodular lesions, PDT may complement surgery reducing tumour size. RCM may be regarded in the future as a complementary technique in BCC for the diagnosis and post-treatment assessment to non-invasive therapeutic modalities.

Received: 30 May 2010; Accepted: 9 September 2010

Keywords

Gorlin syndrome, photodynamic therapy, reflectance confocal microscopy, Xeroderma pigmentosum

Conflict of interest

None declared.

Funding sources

This study was partially supported by grants from Hospital Clinic, Barcelona (Spain) and from Novartis Pharmaceuticals (Spain). J Malvehy and Susana Puig work is partially supported by grants 03/0019 and 06/0265 from Fondo de Investigaciones Sanitarias; grant RO-1 CA 83115 (fund 538226 from National Cancer Institute); and GenoMel consortium actually funded by CE, Net of Excellence.

Introduction

Both Gorlin syndrome (GS) and xeroderma pigmentosum (XP) share an inheritance risk to develop early skin cancer. For these reason, these conditions require a close follow-up and patients are submitted to frequent biopsies.

Gorlin syndrome or nevoid basal cell carcinoma syndrome is an autosomal dominant hereditary condition characterized by multiple nevoid basal cell carcinomas (BCCs), jaw cysts and bifid ribs.[1] Other developmental defects and tumours can be found in this syndrome that include palmar and plantar pits, medulloblastoma, vertebral synostosis, ocular hypertelorism, brachymetacarpalism, calcification of the falx cerebri and ovarian fibroma.[2,3] GS is caused by a germline mutation of a tumour human suppressor gene (PTCH) on chromosome 9q22.3 that negatively regulates the hedgehog signalling pathway.[4,5] BCCs in GS are characterized by an early onset of appearance, their presence in an increased

© 2010 The Authors

number, and less related to sun exposure than BCCs in patients non-affected by GS. Clinically they appear as pearly, flesh coloured to brown papules varying in number from a few up to thousands and ranging in size from 1 to 10 mm.[2] The lesions tend to appear in unusual sites, like the eyelid or the upper lip.[2,3,6] Dermoscopy of cutaneous manifestations of GS have been described in a series of five patients.[7] This non-invasive technique may be useful in the follow-up of these patients, either in the differential diagnosis of BCC as well as in the early diagnosis of new arising tumours.

Xeroderma pigmentosum is a complex genetic disorder with a DNA repair defect of ultraviolet (UV)-induced damage.[8,9] Patients with XP usually develop a great number of skin tumours at an early age such as basal cell carcinoma (BCC) and squamous cell carcinoma, actinic keratosis (AK), atypical moles and malignant melanoma associated with severe photoageing.[10] The prognosis in these cases depends on strict UV photoprotection,[11] and the early diagnosis and surgical treatment of skin tumours. The clinical diagnosis of skin tumours at an early stage and the discrimination between malignant lesions and benign lesions is challenging in these patients because of the presence of severe UV-induced skin damage with the generalized presence of actinic lentigines, AKs and poikiloderma. Recently, dermoscopy has demonstrated to be useful in the clinical assessment and follow-up of these patients.[12,13]

Reflectance confocal microscopy (RCM) is a non-invasive diagnostic technique for the study of skin tumours through obtaining optical sections of the lesions at tissular level.[14] During the last 10 years, it has been used for the *in vivo* assessment of melanocytic and non-melanocytic lesions.[15–18] We have recently developed a two-step algorithm by RCM to characterize skin tumours previous to excision.[19] As demonstrated by Guitera *et al.* this technique may improve and complement dermoscopy in the assessment of ambiguous melanocytic lesions.[20] In patients with genodermatosis with high risk of developing skin cancer, RCM could be of help for the non-invasive diagnosis of difficult lesions. Photodynamic therapy (PDT) may be useful in the treatment of BCC in these patients because of the possibility to treat wide areas with low morbidity and favourable cosmetic results.

We aimed to evaluate the efficacy of methyl-aminolevulinate (MAL) PDT in the treatment of BCC from patients with GS and XP, and to determine the utility of RCM in the pretreatment and post-treatment assessment of these lesions.

Patients and methods

Patients

We prospectively included four patients with GS and two siblings with XP. All of them had biopsy confirmed superficial or nodular BCC. The lesions that persisted after PDT were surgically removed. All study participants gave informed consent for RCM examination of their lesions. The Ethics Committee of the Hospital Clinic approved the study, and institutional rules governing clinical investigation of human subjects were strictly followed.

Reflectance confocal microscopy

Target lesions were imaged by RCM in all patients before and 3 months after the treatment. Confocal imaging was performed with commercially available, near-infrared reflectance confocal laser scanning microscope (Vivascope 1500®; Lucid Inc, Henrietta, NY). The instruments use a diode laser at 830 nm with a power of <16 mW at tissue level and ×30 water-immersion lenses, allowing a horizontal optical resolution of 2 μm and a vertical resolution of 5 μm.[14] Each given image corresponds to a horizontal 500 × 500 μm section of the skin at a selected depth from epidermal surface to upper dermis. Representative images of the lesion and 4 × 4 mosaics were recorded at different skin levels.

Photodynamic therapy protocol

After a gentle debridement of the tumour surface with a curette, a 1 mm thick layer of 160 mg/g MAL cream (Metvix®; Penn Pharmaceutical Services Ltd, Tredegar, UK) was applied on the lesions and 5 mm around. The lesions were covered with an adhesive occlusive dressing for 3 hours. Thereafter, the cream was washed off with 0.9% saline solution immediately prior to illumination with non-coherent red light (Aktilite® lamp; PhotoCure-Galderma S.A., Lausanne, Switzerland) (wavelength 630 nm, light intensity 70–100 mW/cm^2, light dose 75 J/cm^2). The light source was placed around 50 mm from the skin lesion.

Single or multiple lesions in localized areas were treated with 1–3 cycles of MAL PDT following manufacturer recommendations. Every cycle comprised two sessions of PDT 7 days apart. Patients were evaluated after 3 months and followed thereafter every 6 months for 3 years.

Results

The main clinical features of the six patients included in the study as well as treatment response are shown in Table 1.

Patient 1 was a 23-year-old man with genetically confirmed GS diagnosed at the age of 14 because of the presence of odontogenic jaw cysts. PDT was indicated in multiple focally pigmented superficial BCCs located on fronto-temporal, peri-ocular and malar areas. A total of 29 lesions were treated in three areas. A clinical clearance of 19 lesions (66%) was obtained after two cycles of PDT. In the 3 years follow-up, the patient developed new small lesions in the same areas that were treated with imiquimod and with criotherapy without response. As the treatment with PDT was more successful and less painful, a new cycle of PDT was indicated, with similar results to previous ones.

Patient 2 was a 37-year-old man diagnosed with GS at the age of 23 because of the presence of multiple BCCs on the face and trunk, jaw cysts, vertebral alterations and palmar pits. The genetic study of the PTCH gen could not demonstrate any known mutation for GS. Recently, his son has been diagnosed of two

© 2010 The Authors

Table 1 Main clinical features of the patients and clinical response to PDT

Case	Age	Gender	Disease	Genetic alteration	Associated findings	Previous treatments	N. lesions treated	Location of treated lesions	N. cycles* per area	Global response rate (%)†
1	23	M	GS	c.283_284insA	Jaw cystsmacrocephaly, partial agenesia of corpus callosum, pectum excavatum, megaureter, cryptorchid, palmar pits	Surgery, cryotherapy, electrodissection, imiquimod	2	Fronto-temporal	1	66
							27	Periocular and malar area	2	
2	37	M	GS	Not found	Jaw cysts, vertebral alterations (transverse apofisiomegalia of L5 and biconcavus L2), palmar pits	Surgery, cryotherapy, electrodissection, imiquimod	>200	Back (six areas)	2	25
3	35	F	GS	Not found	None	Cryotherapy, electrodissection, imiquimod	20	Lumbar area	2	66
4	24	F	GS	c.2454delACTT	Jaw cysts, bifid ribs, palmar pits	Surgery, cryotherapy	1	Right flank	2	67
							11	Left axilla	2	
5	24	M	XP	Complementation group B	Desmoplastic melanoma	Surgery, imiquimod	2	Right and left cheek	1	50
6	25	F	XP	Complementation group B	Four malignant melanomas (3 *in situ*)	Surgery, imiquimod	1	Nose	3	50
							10	Forehead	2	

M, male; F, female; GS, Gorlin syndrome; XP, Xeroderma pigmentosum; N, number.

*Consisting in two sessions 1 week apart.

†Percentage of lesions completely cleared in each patient at 3 months after finishing treatment.

© 2010 The Authors

BCCs at the age of 10, thus supporting the diagnosis of GS in the father. Patient 2 presented multiple nevoid BCCs (more than 200) on the eyelids and on the back consisting in 2–3 mm skin-colour firm papules. After multiple treatments with fair results, PDT was proposed. As a result of the extension of the lesions the back was divided in six quadrants. Every area was treated with two cycles of PDT, with an overall clinical clearance of 25% of treated lesions. Partial and complete remissions could be demonstrated by RCM examination (Fig. 1). The patient was lost to follow-up for 3 years when he consulted again showing hundreds of small BCCs on the treated areas. We took close-up photographs of these areas and compared them with the previous ones. We could observe that most of the lesions were new BCCs rather than recurrences.

Patient 3 was a 35-year-old woman diagnosed with GS at the age of 30 because of multiple BCCs on the lower back. Genetic study of the PTCH gen did not detect any mutation between exon 2 and 22. The lesions consisted in multiple (up to twenty) 2–4 mm translucent papules on the lumbar area. Two cycles of PDT were administrated. The control 3 months after finalization of the treatment showed a clinical clearance of two-thirds of the lesions. This patient was lost to follow-up.

Patient 4 was a 24-year-old woman diagnosed with GS at the age of five after the diagnosis of a BCC on the back. The study of the mutation of the PTCH gene revealed a mutation in exon 15. Eleven 0.5–2 mm pigmented BCCs on the left axilla and a 4 mm BCC on the right flank were treated with two cycles of PDT. The flank lesion exhibited a clear involution in the evaluation 6 weeks after the treatment that could be assessed by RCM (Fig. 2). Eight of the lesions on the axilla cleared whereas the remaining three partially regressed (Fig. 3). In the 3-year follow-up, new lesions appeared and some of the previously treated relapsed, which was confirmed by RCM (Fig. 3c,d).

Patient 5 was a 24-year-old man affected by XP and history of multiple BCCs since infancy and a desmoplastic melanoma. One pigmented superficial BCC on the right cheek was successfully treated with one cycle of PDT. In a consecutive visit, we identified an ill-delimited slightly depressed focally pigmented lesion on the left cheek. Dermoscopy showed features suggestive of basal cell carcinoma (Fig. 4a). RCM examination could demonstrate the presence at upper dermis of reflective nodules and islands connected to the epidermis formed by polarized cells with elongated nuclei. Enlarged and tortuous vessels were also seen intermingled with plump bright cells (Fig. 4b) confirming the diagnosis of BCC. The RCM examination 1 week after one cycle of PDT demonstrated multiple cells with dendritic shape in epidermal layers that were not present at the previous examination and probably corresponded to Langerhans' cells secondary to inflammation (Fig. 4d). The evaluation 3 months after two cycles of PDT showed clinical remission of the lesion. However, a tiny blue globule could be noted by dermoscopy suggesting persistence of the

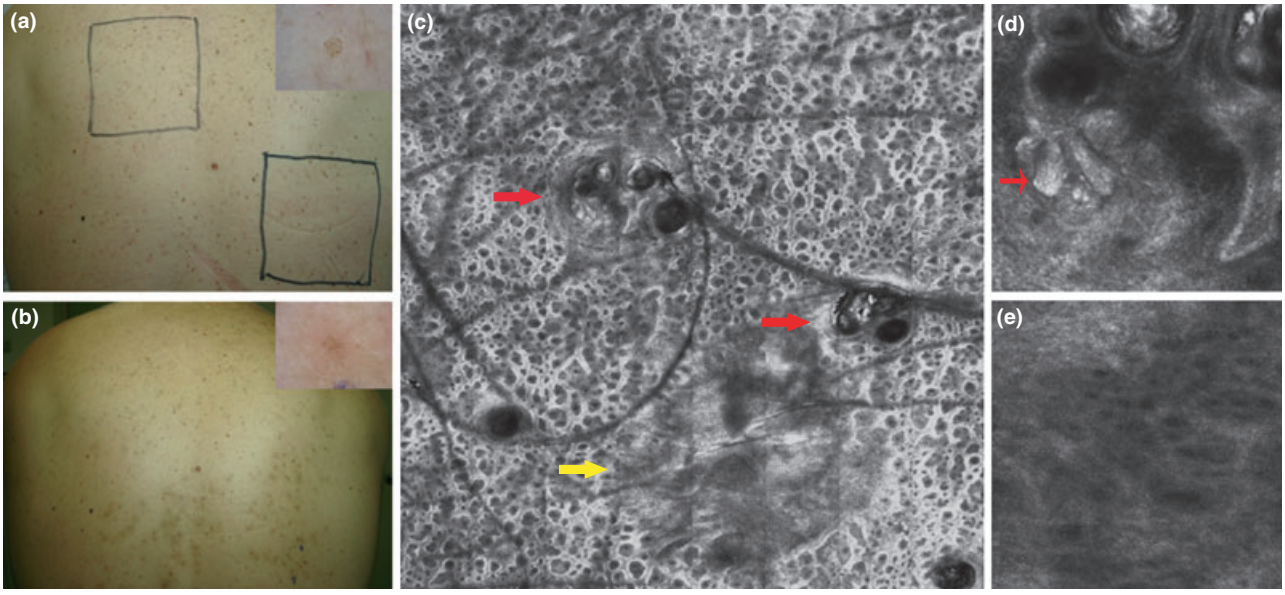

Figure 1 Case 2, 37-year-old man affected by Gorlin syndrome with multiple nevoid basal cell carcinomas (BCCs) on the back. (a) Clinical aspect of the back before treatment. Dermoscopy (inset) of one target lesion. (b) Clinical aspect and dermoscopy after two cycles of treatment on the lower back. (c–e) Confocal images after treatment: (c) Mosaic image (4 × 4 mm) showing partial remission of two lesions (red arrows) and complete remission of one lesion (yellow arrow). (d) Confocal capture at upper dermis level (0.5 × 0.5 mm) of a remaining BCC, note the presence of reflecting nodules (red arrowhead) corresponding to tumoural nests. (e) Confocal capture at upper dermis level (0.5 mm field of view) demonstrates the clearance of the tumour, with presence of reticulated collagen fibres.

© 2010 The Authors
Journal of the European Academy of Dermatology and Venereology © 2010 European Academy of Dermatology and Venereology

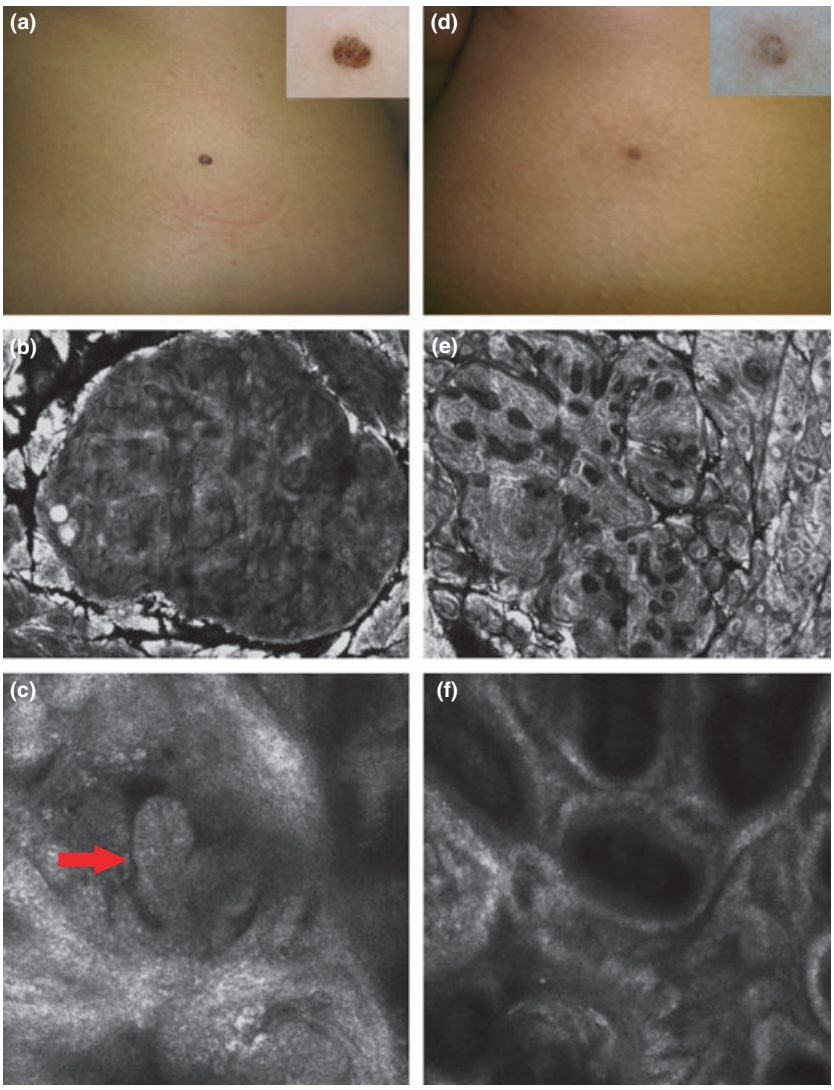

Figure 2 Case 4, 25-year-old woman with Gorlin syndrome with 4 mm pigmented basal cell carcinoma on the abdomen. (a) Clinical and dermoscopic (inset) aspect of the lesion before photodynamic therapy (PDT). (b) Reflectance confocal microscopy (RCM) mosaic (4 × 4 mm) of the lesion before treatment. (c) Confocal capture (0.5 × 0.5 mm) at dermal epidermal junction. Reflecting tumoural nodules surrounded by a dark area (red arrow). (d) Clinical and dermoscopic (inset) aspect of the lesion after two cycles of PDT. (e) RCM mosaic (4 × 4 mm) of the lesion after treatment shows the reduction in the tumour size. (f) Involution of the lesion with presence of normal dermal papilla and absence of tumour nests at dermal epidermal junction.

tumour (Fig. 4e) that was confirmed in the RCM examination (Fig. 4f). Subsequent application of imiquimod cream 7 days a week for 6 weeks resulted in complete clearance of the lesion with no relapse after 3 years.

Patient 6 was a 25-year-old woman affected by XP. She had a history of four malignant melanomas since the age of 19 that had been successfully treated with no evidence of recurrence. He presented with a 6 × 5 mm pigmented lesion on the nasal alar area (Fig. 5a). Dermoscopy revealed blue-grey globules and telangiectasia compatible with basal cell carcinoma (Fig. 5b). A treatment with PDT was proposed with the aim to reduce the tumour size before surgery. She received three cycles of PDT with significant reduction in tumour size (Fig. 5c–d). Three months after the end of the treatment, RCM examination confirmed the persistence of the lesion. She underwent surgical excision that confirmed the presence of residual BCC. In addition, she presented multiple pigmented tiny papules on the forehead suggestive of BCCs. Two cycles of PDT resulted in the clinical clearance of half of the lesions and half size reduction in the remaining ones (Fig. 6). We could observe a global blanching of lentigo and AK on the forehead of our patient.

The treatment was well-tolerated in all the patients. The most important secondary effect was pain, followed by crust formation and hyperpigmentation. The pain was more evident on the forehead and on the nose as well as in the patient treated for multiple papules on the back. All the patients referred to be satisfied with the treatment and admitted the willing to undergo the treatment again.

Discussion

Patients with GS and XP are prone to develop skin cancer since a very young age and frequently present with extensive and multiple

© 2010 The Authors

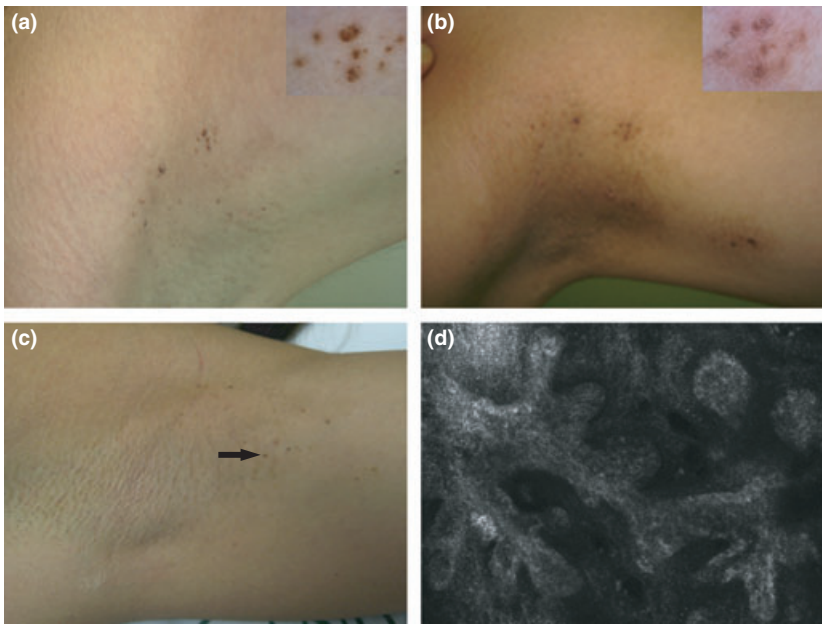

Figure 3 Case 4, 24-year-old woman affected by Gorlin syndrome. Multiple small pigmented basal cell carcinomas (BCCs) on the left axilla. (a) Clinical and dermoscopic (inset) aspect before photodynamic therapy (PDT). (b) Clinical and dermoscopic (inset) aspect 6 weeks after the treatment. (c) Clinical aspect 3 years after PDT. Note the global improvement but appearance of new BCCs (arrow). (d) Confocal image (original capture 0.5 × 0.5 mm) of one of the lesions at the papillary dermis showing nodular and cordlike structures surrounded by a dark space.

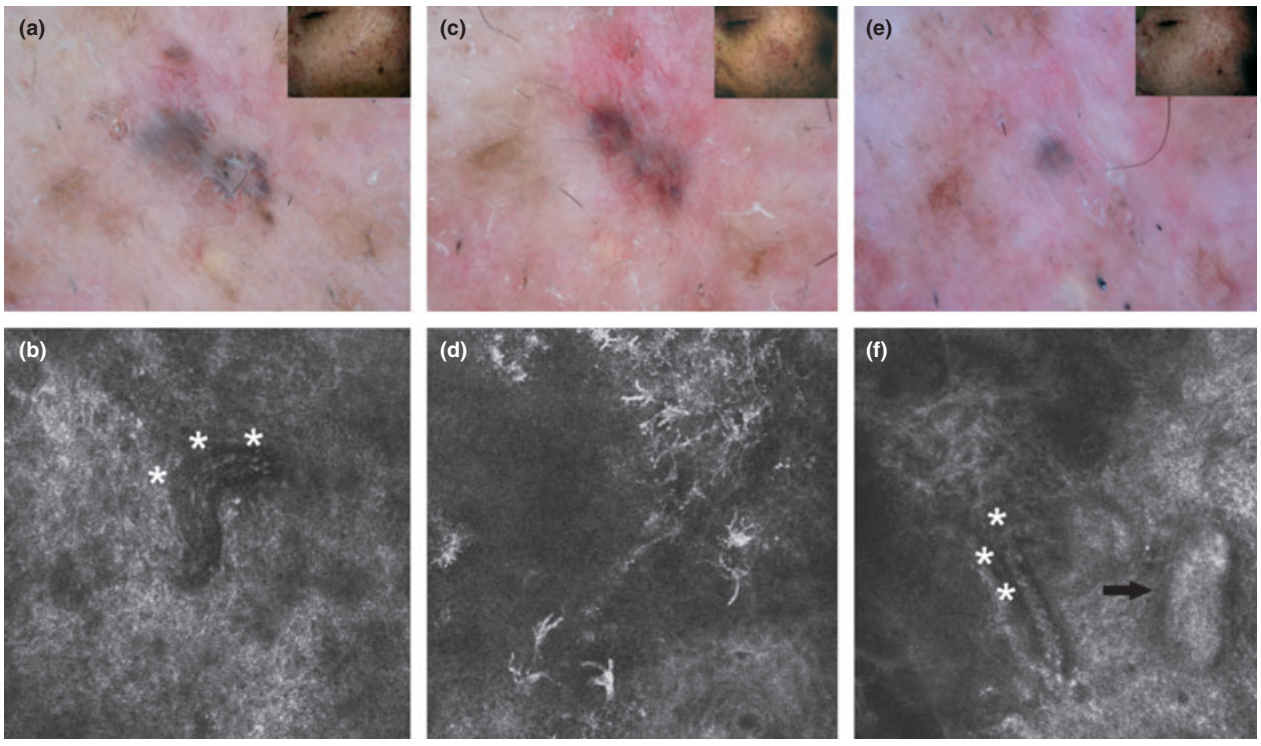

Figure 4 Case 5, 24-year-old man affected by xeroderma pigmentosum. (a) Ill-delimited focally pigmented lesion on the left cheek (inset). Dermoscopy showing blue ovoid nests and telangiectasia suggestive of basal cell carcinoma (BCC). (b) Reflectance confocal microscopy (RCM) examination (0.5 × 0.5 mm) at upper dermis showing enlarged and tortuous vessels confirming BCC*. (c) Clinical (inset) and dermoscopic aspect of the lesion 1 week after photodynamic therapy (PDT). (d) RCM image (0.5 × 0.5 mm) demonstrates multiple cells with dendritic shape at epidermal layers that were not present in the previous examination, corresponding to Langerhans' cells secondary to inflammation in relation to PDT. (e) Evaluation 3 months after PDT shows clinical remission of the lesion (inset) but presence of a blue globule under dermoscopy suggestive of persistence of the lesion. (f) RCM image (0.5 × 0.5 mm) demonstrates reduction in vessel size* but persistence of small reflecting tumoural nodule at upper dermis (arrow).

© 2010 The Authors

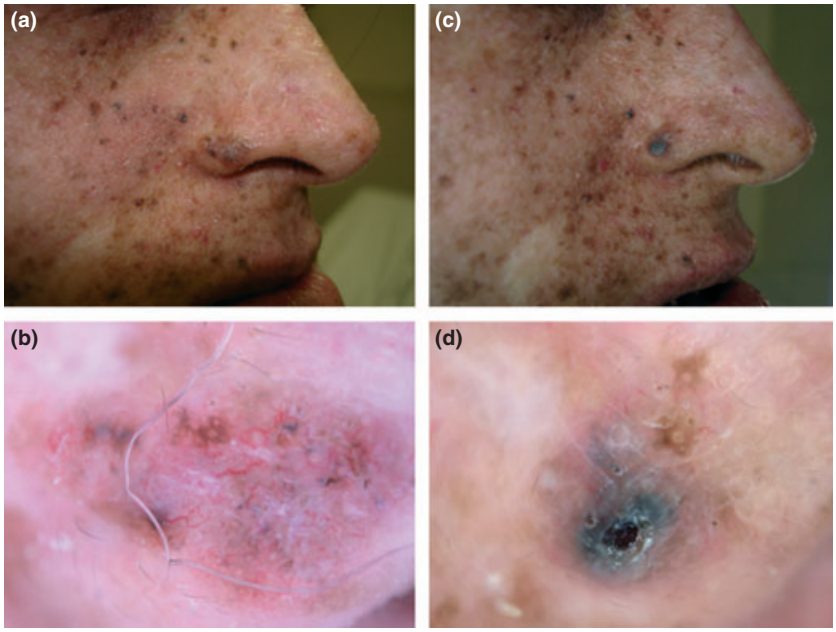

Figure 5 Case 6, 25-year-old woman affected by xeroderma pigmentosum. (a) Clinical aspect of a basal cell carcinoma (BCC) on the nasal alar area before photodynamic therapy (PDT). (b) Dermoscopy showing blue-grey globules and arborizing vessels. (c) Clinical result 3 months after three PDT cycles. Significant reduction in tumour size that enabled posterior surgical removal. Focal increase of pigmentation. (d) Dermoscopy of the BCC after the treatment showing reduction in size, clearance of telangiectasia but presence of blue ovoid structure suggestive of persistence of the tumour.

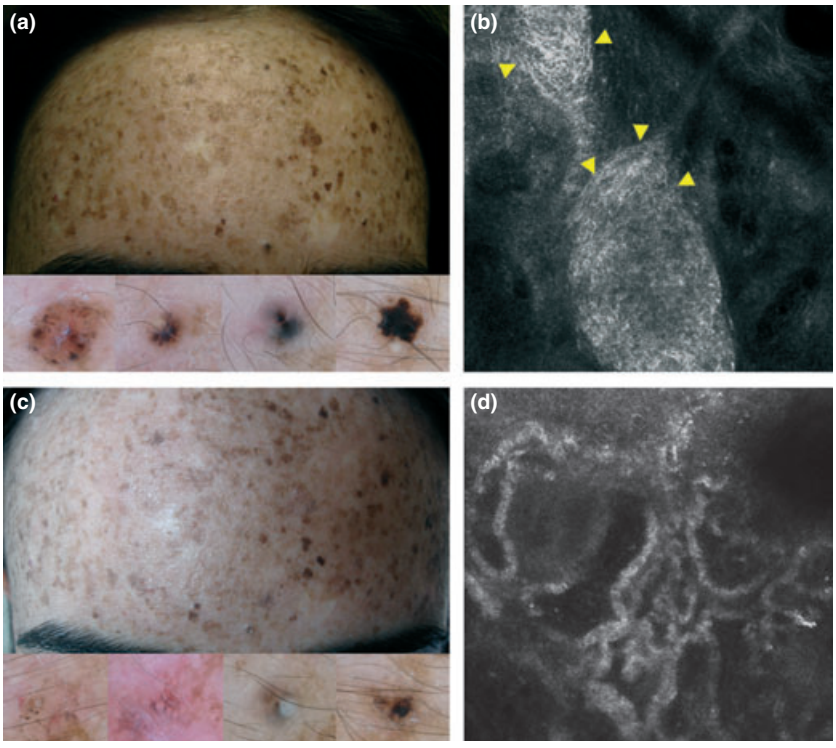

Figure 6 Case 6, multiple lentigines and small pigmented basal cell carcinomas on the front. (a) Basal clinical and dermoscopic aspect of four lesions. (b) Basal confocal image (0.5 × 0.5 mm) of a target lesion on the front showing reflecting tumoural nodules (arrowheads) (c) Clinical and dermoscopic aspect after two photodynamic therapy cycles. (d) Confocal image (0.5 × 0.5 mm) after the treatment showing the clearance of the reflecting tumoural nodule. Instead we observed irregularly shaped dermal papillae surrounded by a bright monomorphic layer of cells corresponding to overlying actinic lentigo.

lesions. For this reason, non-invasive procedures such as PDT[21–25] and other non-invasive drugs such as imiquimod[26,27] appear as a suitable therapeutic option in these patients.

We have reported our experience in the treatment of multiple BCCs using PDT in two genodermatosis. Our results are worse than those reported in the literature for basal cell carcinoma in clinical assays[21] but similar to other studies using PDT in patients affected with GS.[24,25] These may be attributed to the fact that most of the lesions treated were pigmented and/or nodular type small BCCs in which PDT is known to be less effective.[21] Unfortunately, specific

© 2010 The Authors

guidelines regarding patients with GS or XP are lacking. We considered PDT as an alternative therapy to the multiple treatments previously used in these high-risk patients.

As far as we know, there is only one article reported in the literature using PDT in XP, in which a 47-year-old woman with a superficial squamous cell carcinoma on the hand was successfully treated with ALA PDT.[22] A few articles have been published during the last years using PDT in patients with GS. The first article was reported in 2005 by Oseroff AR *et al.*[23] The authors used wide-area 5-ALA PDT to treat multiple BCCs and basaloid follicular hamartomas in three children with GS. The cream was applied to up to 22% of the body surface for 24 h under occlusion. Morbidity was minimal, with selective phototoxicity and rapid healing. After 4–7 sessions, with individual areas receiving 1–3 treatments, the patients had 85% to 98% overall clearance and excellent cosmetic outcomes without scarring. Responses were durable up to 6 years. More recently, two main series using MAL in GS have shown a benefit for this treatment. Mougel *et al.*[24] reviewed the evolution of 62 lesions from patients with multiple BCCs treated with PDT. They obtained a response rate of 85% and recurrence rate of 7.5%. The patients were followed up for 13 months. In a larger series reported by Loncaster *et al.*[25], 33 patients were treated with topical PDT in lesions with depth smaller than 2 mm and with systemic photosensitiser in lesions larger than 2 mm. The authors achieved local control rates of up to 60% at 12 months.

Non-invasive tools for the diagnosis and post-treatment assessment in this setting may be useful to improve quality of life of patients who are subjected to repeated biopsies. In this sense, dermoscopy has been reported to be useful for the detection of BCC in GS in early stages (<3 mm) by the presence of blue-grey globules. In larger lesions, arborizing telangiectasia may also be present. In these patients dermoscopy is also useful for the detection of acral pits that are often overlooked during physical examination.[7] In XP, dermoscopy allowed a more detailed preoperative evaluation of the tumours, aiding decisions regarding biopsy and excision in a study by Malvehy *et al.*[11]

In this sense, new technologies like reflectance confocal microscopy (RCM) allows resolution similar to histology and also a different architectural view of the tumour that can be better evaluated in combination with the dermoscopic images. To our knowledge, RCM has not been previously used in the management of either GS or XP. This technique has been used to evaluate the response of BCC to imiquimod.[28,29] Torres *et al.*[29] performed a confocal examination of 23 cases and obtained after surgical examination a negative predictive value of 70% and a positive predictive value of 84.6%. Unfortunately, these values could not be calculated in our series because we did not perform biopsies after treatment in those cases that appeared resolved. We followed up the patients for 3 years to be sure that the lesions that had been considered healed did not persist or recur. Most of the lesions that had a complete response remained cleared. However, many other lesions appeared during the follow-up.

The confocal features of basal cell carcinoma have been already reported. Gonzalez *et al.*[15] first described five criteria for confocal diagnosis of BCC: presence of elongated monomorphic basaloid nuclei; polarization of these nuclei along the same axis of orientation; prominent inflammatory infiltrate; increased vasculature; and pleomorphism of the overlying epidermis. Additional features to describe pigmented BCC have been later reported. Tumour cells are tightly packed in the papillary dermis with nodular and/or cordlike growth pattern surrounded by a cleft like space. Moreover, scattered bright oval, plump structures corresponding to melanophages are located between tumour nodules. Sometimes, dendritic-shape structures can be identified within the tumoral nodules.[30] We further characterized these structures demonstrating its melanocytic nature.[31]

In this study, we could demonstrate the presence of the above mentioned BCC confocal features in our patients, and what is most important, we could assess the response to therapy using RCM. In cases presenting clinical and dermoscopic complete remission, we could confirm the clearance of the lesion (Fig. 1) and in cases clinically and dermoscopically doubtful, RCM assessment could demonstrate persistent lesion (Fig. 4f).

It has been suggested that PDT may prevent skin cancer, and several studies in animal model have been conducted to demonstrate a roll in skin cancer prophylaxis.[32–35] The mechanism by which PDT could prevent skin cancer is unknown. It has been hypothesized that topical PDT may cause selective destruction of keratinocytes with mutated p53.[33] Another mechanism may be the induction by PDT of an immune response against neoplastic cells and acting thus as a biological response modifier.[35,36] However, evidence of a primary preventive effect of topical PDT in humans is lacking. In our experience, we obtained fair to good clinical responses in the clearance of BCC in patients with GS and XP, but we probably did not prevent the appearance of new lesions. To evaluate the real impact in BCC prevention, we should have compared treated and non-treated areas or treated patients and non-treated patients, but this was not the intention of the present study.

In our experience, the treatment was well tolerated, being pain the most frequent secondary effect, especially on the forehead and nose (Patient 6) and in the case we treated wide areas on the back (Patient 2). Pain is known to be the most common and troublesome acute effect during light exposure in PDT. The patients refer a burning or stinging pain that occurs during light exposure and appears more intense in large area lesions. As observed in our patients, after the treatment an acute inflammatory response is observed, sometimes followed by erosion and crust formation, but complete healing usually occurs within 2 weeks, and only occasionally take up to 6 weeks.[21] Any of the six patients treated herein experienced scarring, which is known to be a rare secondary effect of topical PDT.[21]

In conclusion, MAL PDT may be useful for the treatment of superficial BCC in GS and XP with minimal secondary effects.

© 2010 The Authors

Some nodular and pigmented lesions failed to achieve a complete remission in our series. In these lesions, PDT may complement surgery reducing tumour size. RCM may be regarded in the future as a complementary technique for the assessment at histological level previous to non-invasive therapeutic modalities and to evaluate the response to those treatments.

Acknowledgement

We thank Gerardo Moreno Arias, MD, from Centro Médico Teknon (Barcelona), who identified case 3.

References

1 Gorlin RJ, Goltz RW. Multiple nevoid basal-cell epithelioma, jaw cysts and bifid rips. *N Engl J Med* 1960; **262**: 909–912.
2 Gorlin RJ. Nevoid basal cell carcinoma syndrome. *Dermatol Clin* 1995; **13**: 113–125.
3 Manfredi M, Vescovi P, Bonanini M, Porter S. Nevoid basal cell carcinoma syndrome: a review of the literature. *Int J Oral Maxillofac Surg* 2003; **33**: 117–124.
4 Farndon PA, Del Mastro RG, Evans DG, Kilpatrick MW. Location of the gene for Gorlin syndrome. *Lancet* 1992; **339**: 581–582.
5 Unden AB, Holmberg E, Lundh-Rozell B *et al.* Mutations in the human homologue of Drosophila patched (PTCH) in basal cell carcinomas and the Gorlin syndrome: different *in vivo* mechanisms of PTCH inactivation. *Cancer Res* 1996; **56**: 4562–4565.
6 Honavar SG, Shields JA, Shields CL *et al.* Basal cell carcinoma of the eyelid associated with Gorlin-Goltz syndrome. *Ophthalmology* 2001; **108**: 1115–1123.
7 Kolm I, Puig S, Iranzo P, Malvehy J. Dermoscopy in Gorlin-Goltz syndrome. *Dermatol Surg* 2006; **32**: 847–851.
8 Bootsma D, Hoeijmakers JHJ. The genetic basis of xeroderma pigmentosum. *Ann Genet* 1991; **34**: 143–150.
9 Cleaver JE. Xeroderma pigmentosum: biochemical and genetic characteristics. *Ann Rev Genet* 1975; **9**: 19–38.
10 Robbins JH, Kraemer KH, Lutzner MA *et al.* Xeroderma pigmentosum: an inherited disease with sun sensitivity, multiple cutaneous neoplasm, and abnormal DNA repair. *Ann Intern Med* 1974; **80**: 221–248.
11 Davis BE, Koh HK, Rohrer TE *et al.* Sunlight avoidance and cancer prevention in xeroderma pigmentosum. *Arch Dermatol* 1994; **130**: 806–808.
12 Malvehy J, Puig S, Martí-Laborda RM. Dermoscopy of skin lesions in two patients with xeroderma pigmentosum. *Br J Dermatol* 2005; **152**: 271–278.
13 Green WH, Wang SQ, Cognetta AB Jr. Total-body cutaneous examination, total-body photography, and dermoscopy in the care of a patient with xeroderma pigmentosum and multiple melanomas. *Arch Dermatol* 2009; **145**: 910–915.
14 Rajadhyaksha M, González S, Zavislan JM *et al. In vivo* confocal scanning laser microscopy of human skin II: advances in instrumentation and comparison with histology. *J Invest Dermatol* 1999; **113**: 293–303.
15 González S, Tannus Z. Real-time *in vivo* confocal reflectance microscopy of basal cell carcinoma. *J Am Acad Dermatol* 2002; **47**: 869–874.
16 Pellacani G, Guitera P, Longo C *et al.* The impact of *in vivo* reflectance confocal microscopy for the diagnostic accuracy of melanoma and equivocal melanocytic lesions. *J Invest Dermatol* 2007; **127**: 2759–2765.
17 Scope A, Benvenuto-Andrade C, Agero AL *et al. In vivo* reflectance confocal microscopy imaging of melanocytic skin lesions: consensus terminology glossary and illustrative images. *J Am Acad Dermatol* 2007; **57**: 644–658.
18 Ulrich M, Maltusch A, Rius-Diaz F *et al.* Clinical applicability of *in vivo* reflectance confocal microscopy for the diagnosis of actinic keratoses. *Dermatol Surg* 2008; **34**: 610–619.
19 Segura S, Puig S, Carrera C *et al.* Development of a two-step method for the diagnosis of melanoma by reflectance confocal microscopy. *J Am Acad Dermatol* 2009; **61**: 216–229.
20 Guitera P, Pellacani G, Longo C *et al. In vivo* reflectance confocal microscopy enhances secondary evaluation of melanocytic lesions. *J Invest Dermatol* 2009; **129**: 131–138.
21 Morton CA, McKenna KE, Rhodes LE. British Association of Dermatologists Therapy Guidelines and Audit Subcommittee and the British Photodermatology Group Guidelines for topical photodynamic therapy: update. *Br J Dermatol* 2008; **159**: 1245–1266.
22 Wolf P, Kerl H. Photodynamic therapy in patient with xeroderma pigmentosum. *Lancet* 1991; **337**: 1613–1614.
23 Oseroff AR, Shieh S, Frawley NP *et al.* Treatment of diffuse basal cell carcinomas and basaloid follicular hamartomas in nevoid basal cell carcinoma syndrome by wide area 5- aminolevulinic acid photodynamic therapy. *Arch Dermatol* 2005; **141**: 60–67.
24 Mougel F, Debarbieux S, Ronger-Savlé S *et al.* Methylaminolaevulinate photodynamic therapy in patients with multiple basal cell carcinomas in the setting of Gorlin-Goltz syndrome or after radiotherapy. *Dermatology* 2009; **219**: 138–142.
25 Loncaster J, Swindell R, Slevin F *et al.* Efficacy of photodynamic therapy as a treatment for Gorlin syndrome-related basal cell carcinomas. *Clin Oncol (R Coll Radiol)* 2009; **21**: 502–508.
26 Stockfleth E, Ulrich C, Hauschild A *et al.* Successful treatment of basal cell carcinomas in a nevoid basal cell carcinoma syndrome with topical 5% imiquimod. *Eur J Dermatol* 2002; **12**: 569–572.
27 Nagore E, Sevila A, Sanmartín O *et al.* Excellent response of basal cell carcinomas and pigmentary changes in xeroderma pigmentosum to imiquimod 5% cream. *Br J Dermatol* 2003; **149**: 858–861.
28 Goldgeier M, Fox CA, Zavislan JM *et al.* Noninvasive imaging, treatment, and microscopic confirmation of clearance of basal cell carcinoma. *Dermatol Surg* 2003; **29**: 205–210.
29 Torres A, Niemeyer A, Berkes B *et al.* 5% imiquimod cream and reflectance-mode confocal microscopy as adjunct modalities to Mohs micrographic surgery for treatment of basal cell carcinoma. *Dermatol Surg* 2004; **30**(12 Pt 1): 1462–1469.
30 Agero AL, Busam KJ, Benvenuto-Andrade C *et al.* Reflectance confocal microscopy of pigmented basal cell carcinoma. *J Am Acad Dermatol* 2006; **54**: 638–643.
31 Segura S, Puig S, Carrera C *et al.* Dendritic cells in pigmented basal cell carcinoma: a relevant finding by reflectance-mode confocal microscopy. *Arch Dermatol* 2007; **143**: 883–886.
32 Stender IM, Bech-Thomsen N, Poulsen T, Wulf HC. Photodynamic therapy with topical delta-aminolevulinic acid delays UV photocarcinogenesis in hairless mice. *Photochem Photobiol* 1997; **66**: 493–496.
33 Sharfaei S, Juzenas P, Moan J, Bissonnette R. Weekly topical application of methyl aminolevulinate followed by light exposure delays the appearance of UV-induced skin tumours in mice. *Arch Dermatol Res* 2002; **294**: 237–242.
34 Caty V, Liu Y, Viau G, Bissonnette R. Multiple large surface photodynamic therapy sessions with topical methyl aminolaevulinate in PTCH heterozygous mice. *Br J Dermatol* 2006; **154**: 740–742.
35 Korbelik M, Dougherty GJ. Photodynamic therapy-mediated immune response against subcutaneous mouse tumours. *Cancer Res* 1999; **59**: 1941–1946.
36 Oseroff A. PDT as a cytotoxic agent and biological response modifier: implications for cancer prevention and treatment in immunosuppressed and immunocompetent patients. *J Invest Dermatol* 2006; **126**: 542–544.

© 2010 The Authors

4. DISCUSIÓN

4.1. Utilidad de la MCR en la clasificación de los tumores cutáneos

El objetivo principal de la presente tesis doctoral es demostrar la utilidad clínica de la microscopía confocal de reflectancia (MCR) en el diagnóstico de tumores cutáneos, por tanto la capacidad de esta tecnología para distinguir un tumor de otro a través del estudio de las características observables en cada grupo de tumores. La aplicación de la MCR en la práctica clínica está supeditada a dos factores fundamentales: los criterios que permitan distinguir los distintos tumores tienen que tener una buena correlación histológica (aquello que podemos visualizar por MCR tiene que tener un sustrato histológico); y los criterios tienen que ser reproducibles entre distintos observadores (distintas personas tienen que ser capaces de distinguir del mismo modo los criterios definitorios de cada tumor). Estos distintos puntos han podido ser estudiados y publicados por nuestro grupo en los distintos artículos que constituyen la tesis doctoral, en especial en los trabajos I y II, como a se desarrollará en los siguientes apartados.

4.1.1. Distinguir una lesión melanocítica de una lesión no melanocítica

La MCR es una tecnología en desarrollo que de forma progresiva está pasando de la investigación a la práctica clínica. La elaboración de árboles de decisión es necesaria para poder aplicar esta herramienta en la práctica habitual. En los últimos 10 años y especialmente en el último quinquenio se han descrito las características observables mediante MCR de los principales tumores cutáneos. El mayor número de trabajos giran en torno de las lesiones melanocíticas[82-90]. También ha habido trabajos intentando describir las características de tumores no melanocíticos con MCR, especialmente el carcinoma basocelular (CBC)[79-81] y las queratosis actínicas[91-94] . En la práctica clínica el dermatólogo se enfrenta a lesiones de diferente estirpe, por lo que tiene interés realizar estudios que incluyan diversos tipos de tumores y planteen algoritmos diagnósticos de utilidad clínica.

Según los resultados de nuestros trabajos, en particular el trabajo I, la MCR permitiría obtener datos adicionales y complementarios a la exploración clínica y a la dermatoscopia en tumores cutáneos, que nos ayudarían a clasificar de forma más precisa su origen melanocítico o no melanocítico, así como su malignidad o benignidad. En el trabajo I, se han incluido tanto lesiones melanocíticas (LM) como lesiones no melanocíticas (LNM) para desarrollar un algoritmo diagnóstico en dos etapas de aplicabilidad clínica que minimice el número de melanomas infra-diagnosticados así como el número de biopsias. En una primera etapa distinguimos los tumores de origen melanocítico de los de origen no melanocítico y en una segunda etapa se decide la benignidad o malignidad de la lesión, de forma análoga al algoritmo empleado en dermatoscopia[114].

La gran mayoría de los parámetros analizados en el trabajo I habían sido previamente descritos en la bibliografía[68,72-75,77-91]. El significado y descripción de los distintos parámetros están detallados en el Anexo V .

Previo a nuestro trabajo, un único estudio analizó de forma conjunta LM y LNM para determinar la sensibilidad y especificidad de esta técnica en el diagnóstico de cáncer cutáneo[115]. En este estudio se analizaron 162 lesiones incluyendo nevus, melanoma, CBC, y queratosis seborreicas. Los autores encontraron 3 características de gran valor diagnóstico con lo que desarrollaron un algoritmo sencillo con tres nudos para clasificar estos tumores. En esta clasificación no se tenían en cuenta las diferencias entre LM y LNM. Consideramos esta distinción de gran valor en la práctica clínica por el riesgo de clasificar incorrectamente un melanoma como LNM banal, por el parecido de algunos melanomas con tumores benignos como queratosis seborreicas o angiomas.

En nuestro trabajo, tras el estudio estadístico de regresión logística de todos los parámetros analizados, obtuvimos 4 características que permitían diferenciar en una primera etapa las LM de las LNM (Fig. 17). Estos criterios comprendían dos características epidérmicas (aspecto en empedrado de la epidermis o *cobblestone pattern* y crecimiento pagetoide), una característica de la unión dermo-epidérmica (presencia de papilas bien definidas en toda la lesión) y una característica de la dermis papilar (nidos de melanocitos en la dermis). Tres de los criterios (patrón epidérmico en empedrado, crecimiento pagetoide y nidos en la dermis) tenían un comportamiento estadístico similar y se pudieron agrupar de manera que la presencia de uno de ellos ya era muy sugestivo de LM. La presencia de papilas bien definidas en toda la lesión reforzaba la sospecha de lesión melanocítica pero no era un criterio suficiente de forma aislada, pues tanto los dermatofibromas como las queratosis seborreicas reticuladas lo pueden presentar. Este último criterio ha evolucionado en la bibliografía posterior en el patrón reticulado (*meshwork*) y en el patrón en anillos basales *(ringed)*, ambos característicos de las lesiones melanocíticas. A pesar de poder clasificar la mayoría de lesiones obtuvimos 3 falsos positivos (LNM clasificadas como LM), se trataba de una queratosis seborreica muy pigmentada con aspecto en empedrado en la epidermis y dos carcinoma basocelulares nodulares cuyos nidos tumorales se confundieron con los de un nevus. Mayor importancia tienen a nuestro entender las dos LM que se clasificaron incorrectamente como LNM. Una de las lesiones correspondía histológicamente a un nevus de Meyerson, con vesículas intraepidérmicas e intensa reacción inflamatoria que podría haber obscurecido las características de LM por MCR. La segunda lesión se trataba de un melanoma dérmico sin afectación por tanto ni de la unión dermo-epidérmica ni de la epidermis, que explicarían la ausencia de semiología propia de las LM por MCR. Por este motivo, del mismo modo que procedemos en dermatoscopia, recomendamos que cuando una lesión no cumple criterios de LM por MCR pero tampoco cumple criterios conocidos de los tumores no melanocíticos, tenemos que plantearnos que pueda tratarse de un melanoma, y proceder en consecuencia.

Reconocemos las limitaciones de esta primera clasificación. El criterio histológico "crecimiento pagetoide" no es exclusivo de algunas lesiones melanocíticas (melanoma, nevus de Spitz, nevus recurrente, algunos nevus congénitos y algunos nevus acrales). Como el nombre indica, el crecimiento pagetoide es característico de la enfermedad de Paget (de la

mama o extramamaria), pero también de las histiocitosis de Langerhans y de algunos linfomas con epidermotropismo. En una publicación reciente se describe un caso de enfermedad de Paget de la mama mediante MCR[116], donde efectivamente se pueden visualizar células reflectantes redondas en la epidermis como se han descrito repetidamente en el melanoma, correspondientes en este caso a la infiltración del epitelio por células de un carcinoma intraductal de mama. En cuanto al criterio "patrón en empedrado" consistente en la visualización de queratinocitos suprabasales intensamente reflectantes, aunque es típico de los nevus melanocíticos no es exclusivo de estos, pues algunos tumores no melanocíticos muy pigmentados, como algunas queratosis seborreicas, pueden presentar dicho patrón. El criterio "nidos de melanocitos en la dermis" es un criterio constante en las LM. Consiste en agregados celulares reflectantes compactos o discohesivos, de medida y reflectividad variable. Cuando se trata de nidos compactos, la imagen evaluada de forma aislada podría en algunas ocasiones confundirse con los nidos tumorales observados el CBC. Para distinguir unos de otros es preciso ver la estructura global de la lesión y la relación de estos nidos con la capa basal, así como la presencia de una característica área oscura alrededor de los islotes tumorales, que nos orientará a que se trata de un CBC.

Fig. 17. Primera etapa del algoritmo: distinguir una lesión melanocítica de una lesión no melanocítica. Cuatro criterios que sugieren lesión melanocítica (imágenes de microscopía confocal de reflectancia 0,5x0,5 mm): **A,** Aspecto en empedrado en la epidermis (*cobblestone pattern*); **B**, Presencia de células reflectantes dendríticas o redondas en estratos epidérmicos (crecimiento pagetoide); **C**, Presencia de agregados celulares en la dermis (nidos dérmicos); **D,** Presencia de papilas dérmicas bien definidas en la unión dermo-epidérmica en toda la lesión.

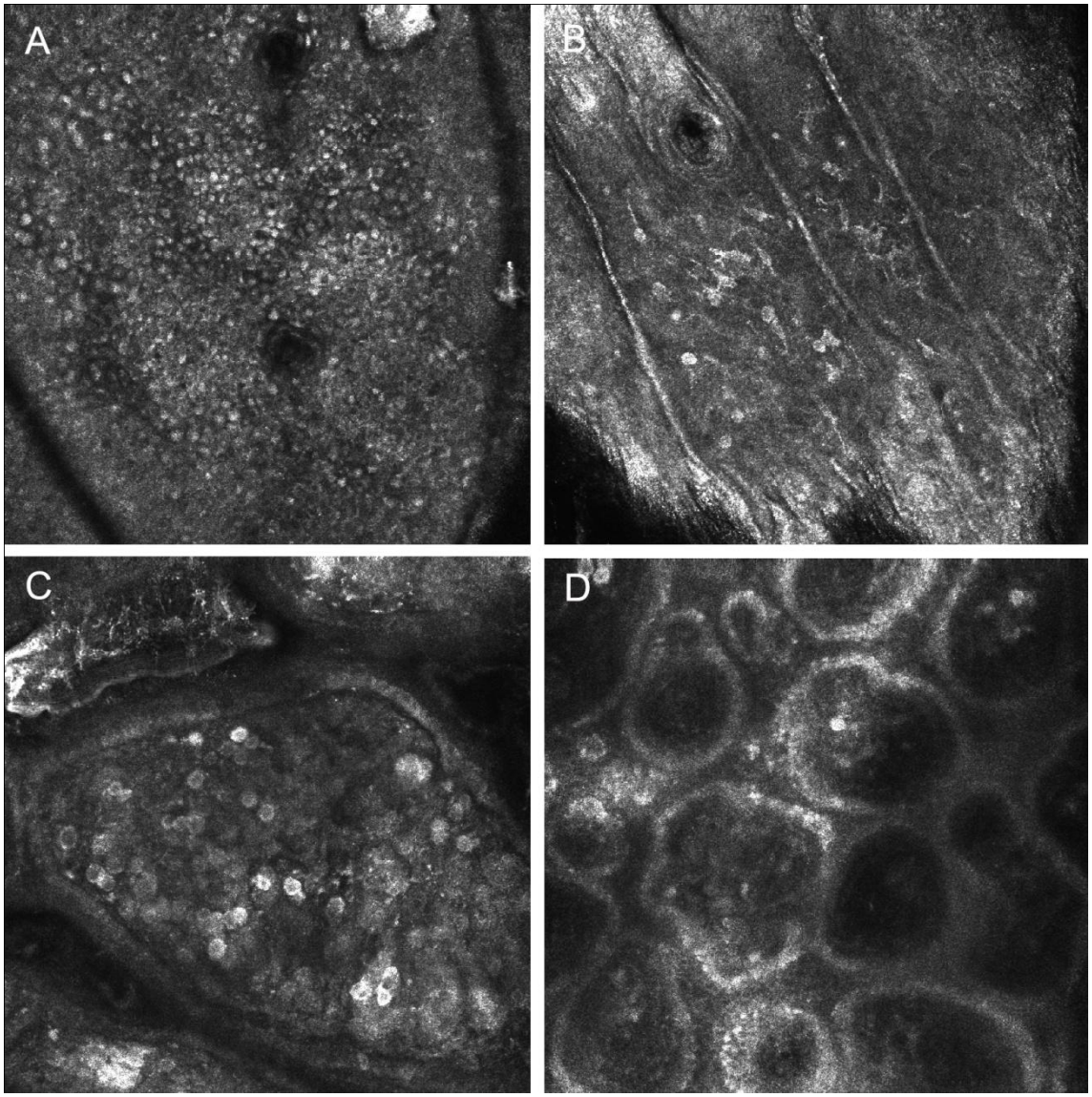

4.1.2. Diagnóstico de los tumores no melanocíticos

a) Criterios de carcinoma basocelular

Las LNM presentan por MCR características que les son propias. El mejor estudiado dentro de este grupo es el CBC, el tumor maligno más frecuente del cuerpo humano. Si bien en un gran número de casos el diagnóstico clínico es fácil, en algunos casos, especialmente en algunas formas pigmentadas, puede plantearse el diagnóstico diferencial con melanoma. En lesiones incipientes en gente joven con importante daño solar que sean susceptibles de tratamientos no quirúrgicos, la dermatoscopia y la MCR pueden ofrecernos un diagnóstico no invasivo fidedigno.

En el trabajo I, después de analizar 27 CBC encontramos 5 características que no estaban presentes en el resto de lesiones y que favorecen el diagnóstico en caso que se hayan excluido los criterios de LM descritos más arriba: 1) Islotes tumorales hiporeflectantes rodeados de espacio oscuro, denominados en artículos posteriores *dark silouhettes*[117], observables principalmente en CBCs nodulares y adenoides; 2) Núcleos polarizados y elongados, las células que forman los islotes parecen orientarse en un mismo axis y en ocasiones puede distinguirse un núcleo elongado; 3) Vasos tortuosos en la dermis, con la visualización de células sanguíneas en el interior adheridas a la pared y presentando fenómeno de tráfico leucocitario, *rolling* o desplazamiento a lo largo de la pared del vaso; 4) Estructuras dendríticas reflectantes dentro de los islotes tumorales, de grosor y longitud variable, que en la correlación histopatológica resultan positivas para S-100, HMB-45, Melan A y en general negativas para CD1a y corresponden a melanocitos; 5) Estructuras reflectantes irregulares, sin núcleo visible, redondeadas u ovaladas, de bordes mal definidos, dentro y alrededor de los nidos tumorales, denominadas *plump cells* por algunos autores. Corresponden histológicamente a melanófagos, por lo que pueden observarse con otra distribución en distintos tumores cutáneos y procesos liquenoides.

Nuestros resultados concuerdan con estudios previos. González y Tannus[79] definieron por primera vez 5 criterios de MCR para el diagnóstico de CBC: 1) Presencia de células de núcleos elongados monomorfos; 2) Polarización de los mismos en el mismo axis; 3) Vascularización prominente; 4) Presencia de células inflamatorias en la dermis y 5) Pleomorfismo en la epidermis suprayacente, sugestiva de daño solar. En su descripción original no se hace referencia a los nidos e islotes celulares descritos por otros autores[80,118] y en nuestros trabajos I y III. Un estudio multicéntrico posterior con 89 CBCs[81] determinó la sensibilidad y especificidad de los criterios descritos por González y Tannus[79]. Las diferencias en los parámetros encontrados en nuestros trabajos radican en que en nuestro caso la mayoría de tumores eran CBC nodulares pigmentados o adenoides y se encontraban en zonas no fotoexpuestas. Los primeros autores que hablan del parénquima del CBC como áreas oscuras en la dermis con células con ligera reflectancia fueron Sauermann y cols.[80] en su estudio de 12 lesiones. En este artículo se describen unas estructuras reflectantes de aspecto dendrítico en el interior del tumor, pero no hablan del origen de estas estructuras. Agero y cols. reportaron posteriormente la misma observación, y atribuyeron estas estructuras dendríticas brillantes a

la presencia de melanocitos o células de Langerhans intratumorales[118]. Hemos tenido la oportunidad de estudiar mediante inmunohistoquímica 5 casos de CBC que presentaban abundantes estructuras dendríticas en su interior (tres de ellos publicados en el trabajo III de la presente tesis). En todas las lesiones se observaban células con largas proyecciones dendríticas positivas para S-100, HMB-45 y MelanA y negativas para CD1a en el interior del parénquima tumoral, correspondientes por tanto a melanocitos intratumorales (Fig. 18) Algunos tumores presentaban un aumento de células CD1a intraepidérmicas correspondientes a células de Langerhans.

La presencia de melanocitos en los CBCs concuerda con estudios histopatológicos y ultraestructurales previos que han demostrado la presencia de melanocitos benignos en este tumor[119-121]. Florell y cols.[120] encontraron melanocitos dendríticos en los 10 CBC evaluados, distribuidos en la periferia o en el interior de los nidos tumorales. Los melanocitos se disponían por separado o en dos o más células, pero nunca en grupos como se observaría en CBCs infiltrados por melanocitos malignos en las lesiones de colisión entre CBC y melanoma maligno. Nueve de cada 10 casos también presentaban células dendríticas de Langerhans en el interior del tumor. Otro estudio demostró la presencia de numerosos melanocitos distribuidos de forma difusa entre las células del tumor en 12 de 15 CBCs[119]. En estos casos el número y la distribución de los melanocitos no se correlacionaba con la cantidad de pigmentación visible en el examen clínico. En un estudio ultraestructural con 12 CBCs parcialmente pigmentados, se demostró que los melanocitos de las áreas pigmentadas del tumor presentaban dendritas más largas y anchas, con melanosomas maduros, en comparación con las áreas no pigmentadas del mismo tumor[121]. La presencia de melanocitos en CBC no es un hallazgo sorprendente, considerando que estos tumores se desarrollan a partir de la capa basal de la epidermis, donde residen habitualmente los melanocitos.

Fig. 18. Carcinoma basocelular pigmentado. Correlación entre dermatoscopia, microscopía confocal de reflectancia e histología. **A,** Dermatoscopia mostrando una lesión pigmentada sin criterios de lesión melanocítica con presencia de hojas de arce, glóbulos y puntos azul-grises, que sugieren el diagnóstico de carcinoma basocelular. **B-D**, Nidos tumorales formando islotes hiporeflectantes con estructuras dendríticas en el interior y células reflectantes redondas (*plump cells*) en el interior y exterior de los mismos. **E-G**, Correlación histológica. **E**, H-E 100x. Nidos de células basaloides conectados con la epidermis. **F,** Presencia de células dendríticas intratumorales HMB-45 y MelanA positivas que corresponden a melanocitos. **G**, Células de Langerhans (CD1a positivas) en la epidermis suprayacente. Escala: 50 µm.

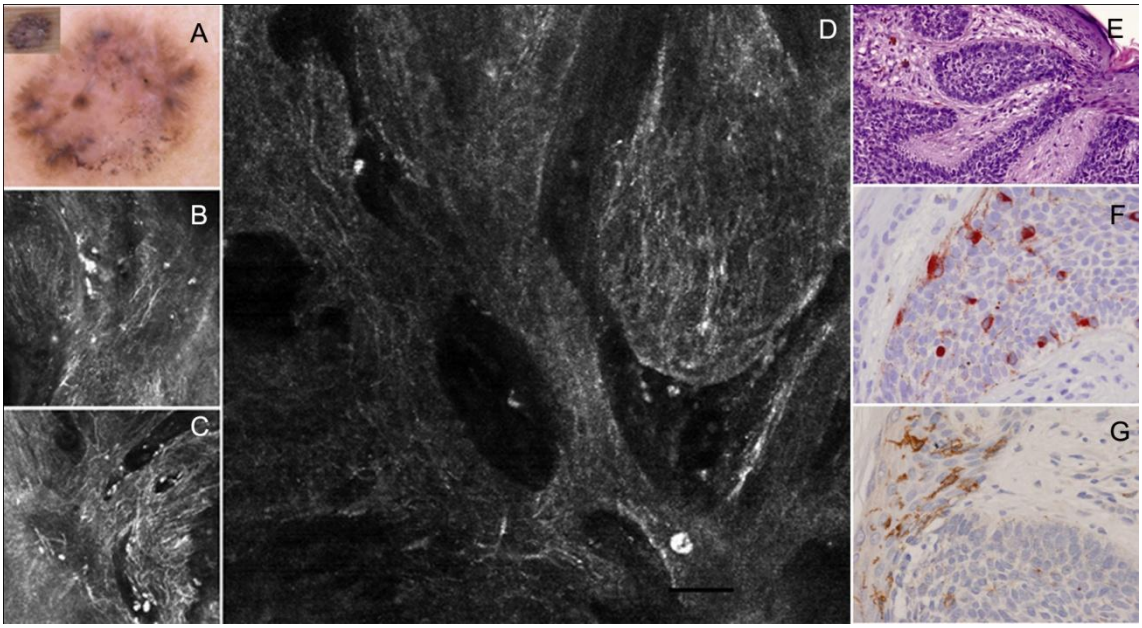

b) El valor de la presencia de células dendríticas en el estudio de lesiones pigmentadas cutáneas

Es importante conocer que algunos CBC presentan células de morfología dendrítica en su interior, pues de lo contrario, la observación de las mismas en la exploración mediante MCR de una lesión pigmentada de diagnóstico clínico y dermatoscópico ambiguo, nos puede conducir a error y hacernos creer que nos encontramos ante una lesión melanocítica y con la posibilidad de melanoma.

En las lesiones melanocíticas, los melanocitos se pueden visualizar mediante MCR como células reflectantes redondeadas o dendríticas en la epidermis, en la unión dermo-epidérmica o en las papilas dérmicas. Cuando se encuentran en la epidermis superior en el contexto de una lesión melanocítica son indicativos de crecimiento pagetoide y se asocia con el diagnóstico de melanoma[82-84,89,90] o nevus de Spitz[85]. Según las descripciones originales, en el melanoma maligno las dendritas se describen como grandes y ramificadas, mientras que en lesiones pigmentadas benignas son pequeñas y delgadas[82]. La refracción de los melanocitos se debe a la presencia de melanina y melanosomas[122], por tanto podrán visualizarse también en los melanomas amelanóticos[72].

Las células de Langerhans, por su lado, pueden ser identificadas por MCR como células dendríticas dentro de la epidermis y pueden dificultar la evaluación de los nevus inflamados, o el nevus eccematoso de Meyerson[123] (Anexo II), así como cicatrices de lesiones recientemente extirpadas, lesiones tratadas con láser, terapia fotodinámica (TFD) o incluso en queratosis liquenoides benignas. Ejemplos de estas situaciones se detallan en las Figs. 19-22.

Se necesitan estudios con mayor número de casos para dilucidar la frecuencia, características y significado de las células dendríticas (melanocitos, células de Langerhans) en los tumores cutáneos, incluyendo tumores melanocíticos, CBCs pigmentados y cualquier tumor inflamado o sometido a cirugía, terapia fotodinámica, láser, etc.

Fig. 19. Nevus eccematoso de Meyerson (Anexo I). Lesión pigmentada de 10x8mm, marrón claro, de pigmentación homogénea, en la espalda en una mujer de 35 años. La paciente refería crecimiento en las últimas semanas y discreto prurito. **a,** Imagen dermatoscópica 30x, muestra pigmentación difusa marrón claro con áreas blancas de aspecto cicatricial y algunos puntos de pigmento. Ausencia de criterios de lesión melanocítica pero tampoco de lesión no melanocítica, por lo que se decidió extirpación para descartar melanoma. **b,** Imagen de microscopía confocal de reflectancia (MCR) a nivel del estrato espinoso/granuloso muestra dos células dendríticas aisladas. **c,** Imagen de MCR a nivel del estrato espinoso/granuloso donde se observan espacios hiporeflectantes redondeados que contienen partículas brillantes en el interior (asterisco), que corresponden a vesículas intraepidérmicas con células inflamatorias. **d,** Imagen de MCR a nivel de dermis superficial muestra agregados densos de células reflectantes sugestivos de nidos dérmicos de células névicas (cabeza de flecha). **e,** H-E 100x , hiperplasia psoriasiforme con espongiosis e infiltrado inflamatorio difuso en la dermis. Pequeños nidos de células névicas en unión dermo-epidérmica y dermis superficial entremezclados con el infiltrado. **f,** CD1a 100x, Abundantes células positivas de morfología dendrítica en la epidermis, que corresponden a células de Langerhans.

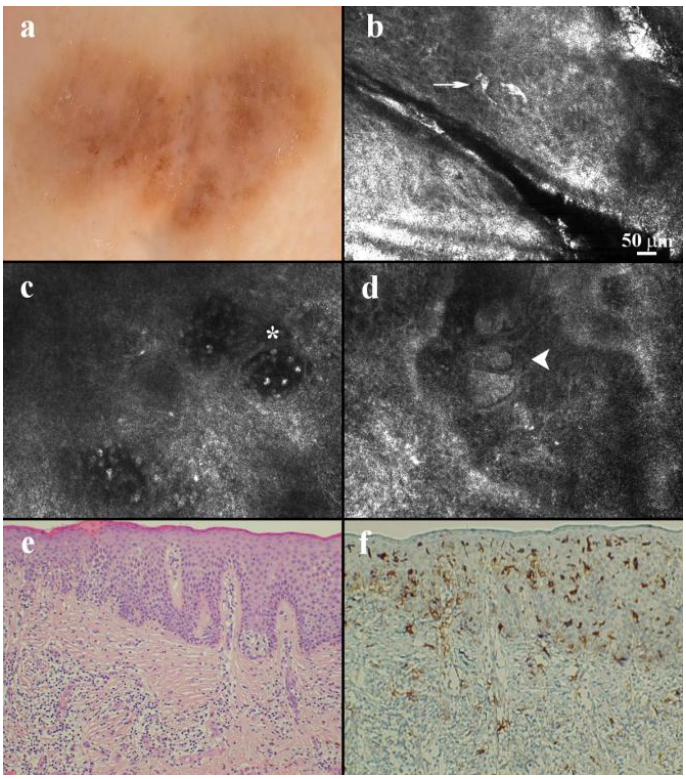

Fig. 20. Oronosis exógena tratada con láser (Anexo II). Mujer de 63 años, fototipo V, afecta de acronosis exógena por aplicación de despigmentantes con hidroquinona en melasma facial de larga evolución. **A,** Aspecto clínico de la lesión, máculas de color grisáceo con piqueteado característico "en caviar". **B,** Dermatoscopia, estructuras globulares marrón-gris alrededor de las aperturas foliculares. **C,** Imagen de microscopía confocal de reflectancia (0,5x0,5 mm) a nivel de la epidermis a los 3 días de tratamiento con luz pulsada intensa. Se observa un patrón en panal de abejas típico del estrato espinoso con abundantes células reflectantes de morfología dendrítica, ausentes en exploraciones previas al tratamiento y en el seguimiento posterior. La evolución sugiere que estas células dendríticas tan prominentes corresponden a células de Langerhans en relación con el tratamiento. **D y E**, Aspecto histológico típico de la lesión antes del tratamiento (H-E 40x y 400x) donde se observa el depósito ocronótico en dermis superficial.

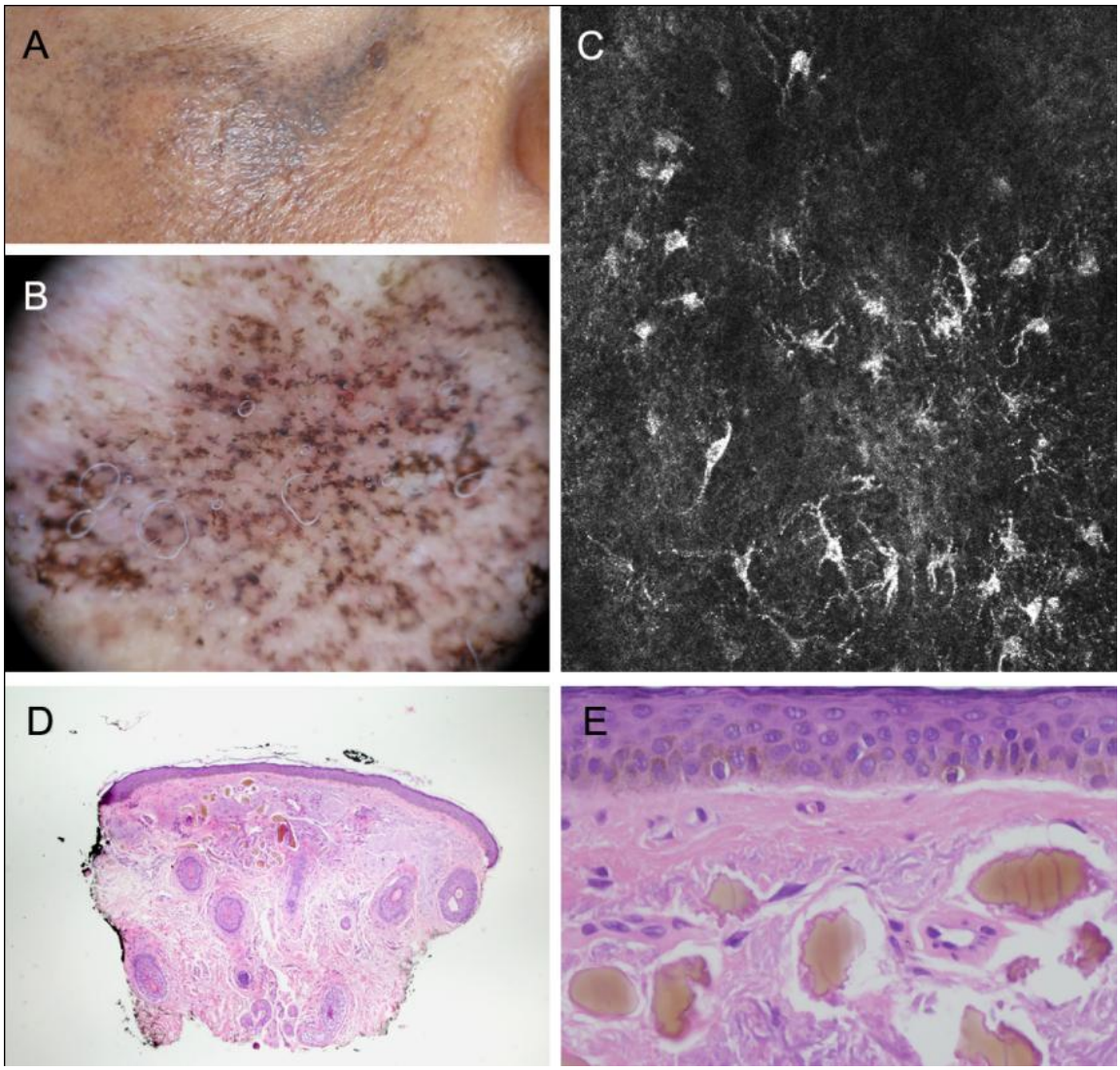

Fig. 21. Pigmentación focal en la cicatriz de extirpación de un lentigo maligno melanoma (LMM) estudiado mediante microscopía confocal de reflectancia (MCR) tras un mes de la cirugía. **A**, Aspecto clínico (recuadro) y dermatoscopia de la pigmentación, sin criterios específicos de recidiva de LMM. **B,** Imagen de MCR (0,5x0,5mm) donde se observan abundantes células de morfología dendrítica en los estratos suprabasales que hicieron sospechar recidiva de melanoma. **C-E,** Correlación histológica de las células visualizadas que demuestra que corresponden a células de Langerhans. Escala: 50 µm.

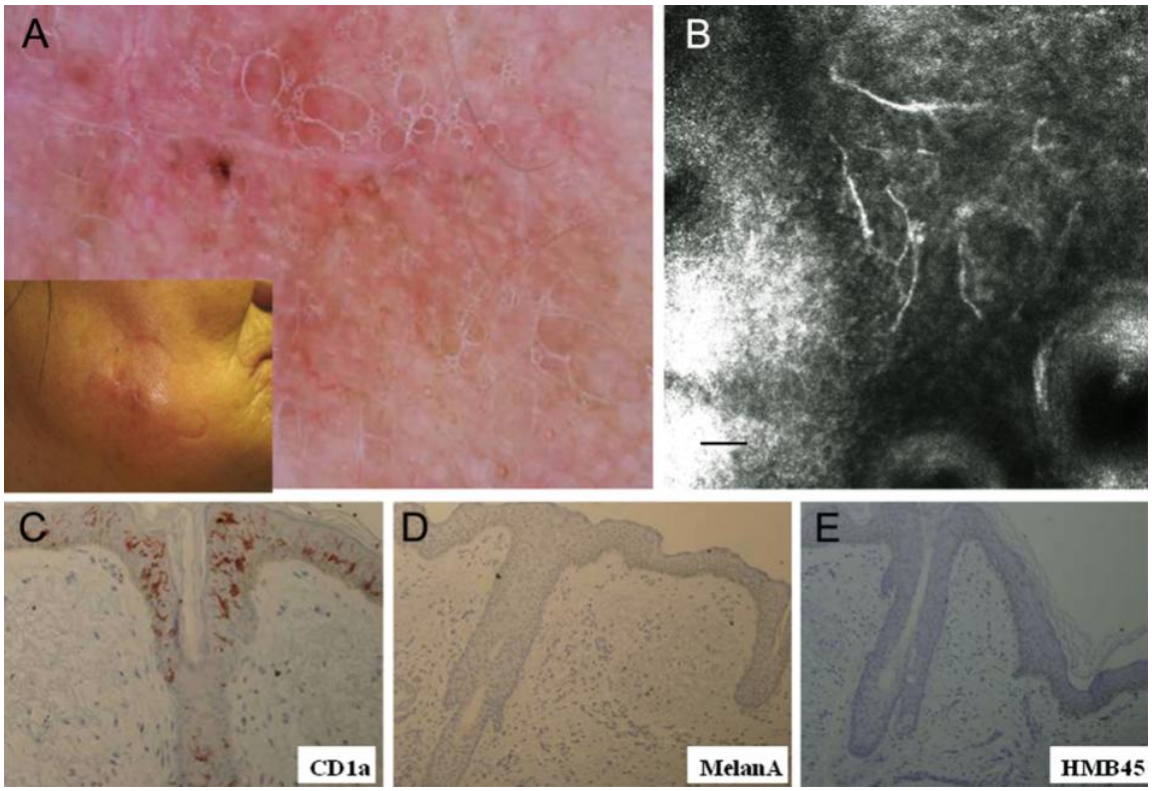

Fig. 22. Paciente con carcinoma basocelular (CBC) afecto de Xeroderma pigmentoso (XP) tratado con terapia fotodinámica (TFD) (Trabajo IV). A1, Dermatoscopia de la lesión 2 semanas tras el tratamiento, muestra nidos ovoides y signos de inflamación. **A2,** Imagen de microscopía confocal de reflectancia (MCR) **(**0,5x0,5 mm) en el mismo momento donde se aprecian múltiples células reflectantes de morfología dendrítica en estratos epidérmicos**. B,** Control de la lesión a los 3 meses del tratamiento**. B1,** Clara reducción de la lesión, pigmentación azul-gris focal mediante dermatoscopia. **B2**, Imagen de MCR (0,5x0,5mm) donde se aprecia persistencia de lesión (nido tumoral y vasos agrandados) pero ausencia de las células dendríticas presentes en el control anterior, que sugiere que correspondan a células de Langerhans en relación con el proceso inflamatorio post-TFD. Escala: 50 µm.

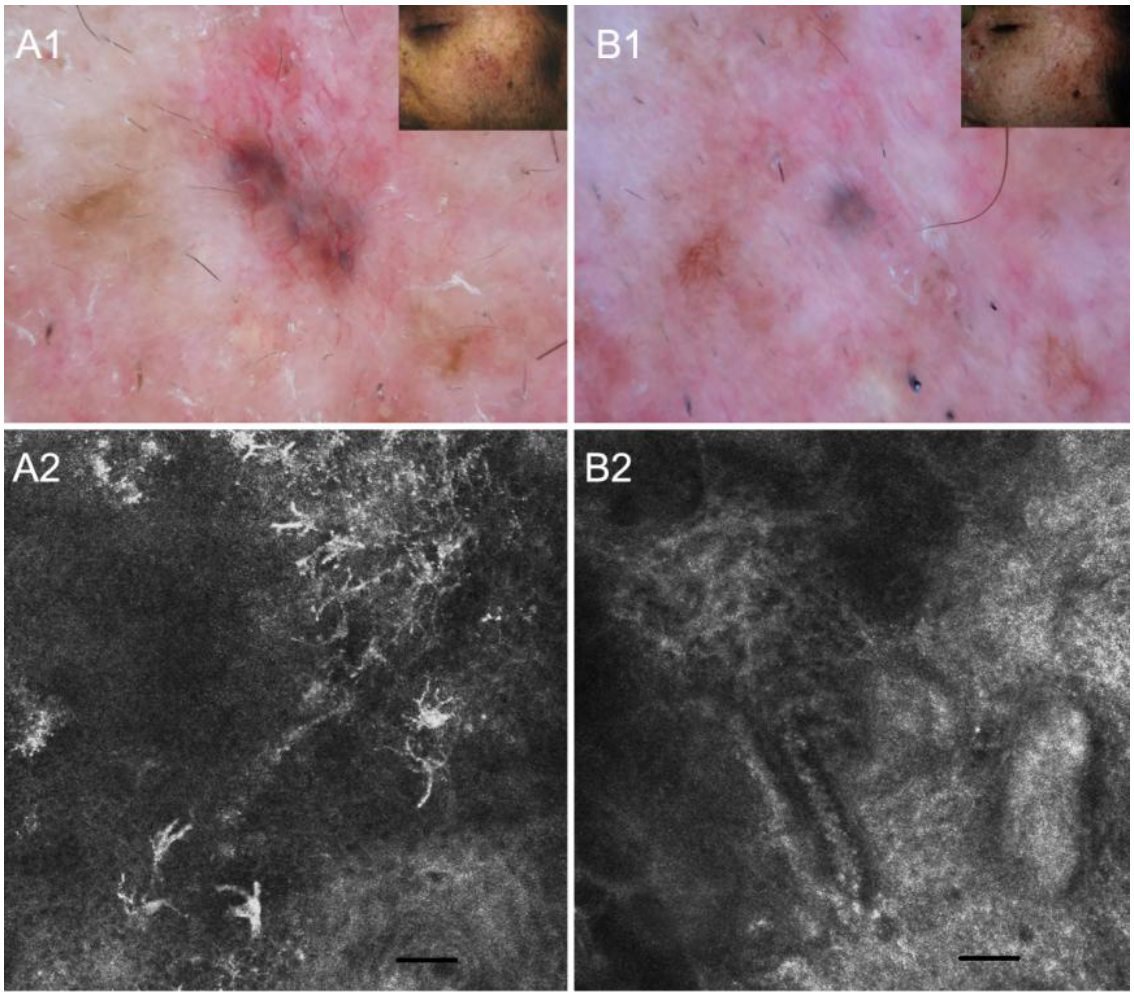

c) Queratosis seborreicas, angioma y dermatofibroma

Las queratosis seborreicas (QS) se caracterizan según nuestro estudio por la ausencia de criterios de lesión melanocítica. Hay que mencionar la excepción de aquellas lesiones muy pigmentadas que pueden presentar un patrón en empedrado (queratinocitos reflectantes) en estratos suprabasales. De forma interesante y para distinguirlas del resto de tumores presentan de forma invariable características propias. De este modo, en ausencia de otros hallazgos, la presencia de tapones córneos (estructuras brillantes en capas de cebolla en la superficie de la lesión), quistes de queratina (estructuras intraepiteliales redondeadas hiperreflectantes y de contorno liso) o criptas (repliegues hiporeflectantes en la superficie de la lesión), puede sugerir el diagnóstico de QS (Fig. 23). Hay que tener en cuenta que en ocasiones algunos nevus pueden presentar focalmente presencia de tapones córneos y quistes de queratina, especialmente en aquellos verrugosos. Por otro lado, las queratosis seborreicas reticuladas y los lentigos solares se pueden identificar por la presencia de unas estructuras reflectantes en forma de cordones en la epidermis y unión dermo-epidérmica. Este aspecto fue descrito por Langley y cols. en el lentigo solar para distinguir los lentigos solares del lentigo maligno[124]. Los lentigos malignos presentaran además células dendríticas atípicas en estratos suprabasales, frecuentemente de distribución perifolicular[125,126] (Fig. 24).

Las lesiones vasculares y los dermatofibromas presentan parámetros mediante MCR que se correlacionan bien con la dermatoscopia y la histología. Sin embargo nuestros resultados en estas lesiones son limitados teniendo en cuenta el pequeño número de casos. Las lesiones vasculares pueden distinguirse por MCR por la presencia de espacios hiporeflectantes en la dermis por los que se puede ver circular células sanguíneas (Fig. 25).

Los dermatofibromas por su lado, se distinguen por la presencia de anillos reflectantes homogéneos en la periferia de la lesión que corresponden a la hiperplasia epidérmica, elongación de los procesos interpapilares e hiperpigmentación de la capa basal. En la parte central de la lesión hay un ausencia de anillos reflectantes y puede apreciarse un engrosamiento del colágeno dérmico de aspecto fibrilar (Fig. 26).

Fig. 23. Queratosis seborreica convencional. A, Imagen clínica de la lesión**. B,** Dermatoscopia que muestra pseudoaperturas foliculares en toda la lesión, quistes córneos y "borde cortado a pico"**. C,** Imagen de microscopía confocal de reflectancia (MCR) (0,5x0,5mm) en estrato granuloso con presencia de tapón córneo. **D,** Imagen MCR (0,5x0,5mm) a nivel del estrato espinoso donde se observa un quiste de queratina.

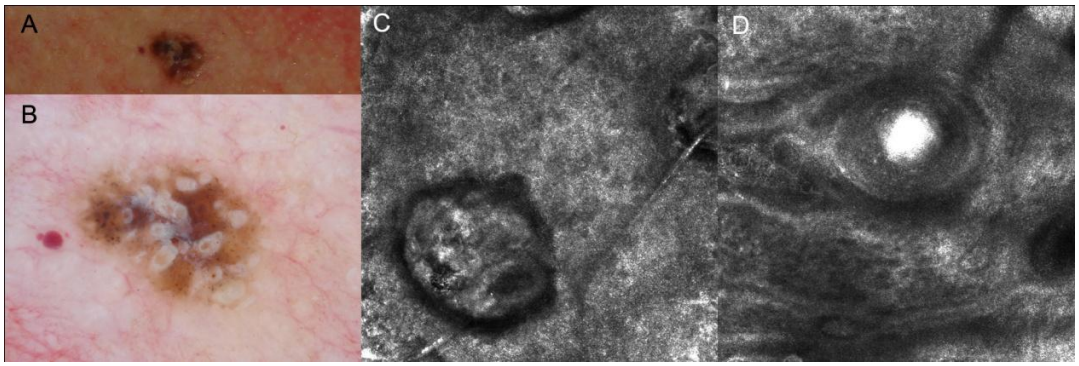

Fig. 24. Dos lesiones pigmentadas faciales de aspecto clínico similar. A1, Imagen clínica y dermatoscópica de una queratosis seborreica reticulada en dorso nasal. **B1**, Imagen de microscopía confocal de reflectancia (MCR) (0,5x0,5mm) que demuestra la presencia de cordones epiteliales hiperreflectantes a nivel de la unión dermo-epidérmica. **C1**, Correlación histológica H-E 200x donde se observa una hiperplasia epitelial lentiginosa con pigmentación de la capa basal. **A2,** Imagen clínica y dermatoscópica de un lentigo maligno interciliar. Pigmentación y puntos grises perifoliculares. **B2**, MCR (0,5x0,5mm) a nivel de la capa espinosa con abundantes células reflectantes dendríticas y algunas redondas. **B3**, Correlación histológica H-E 200x que aplanamiento de la epidermis y proliferación de melanocíticos basales atípicos.

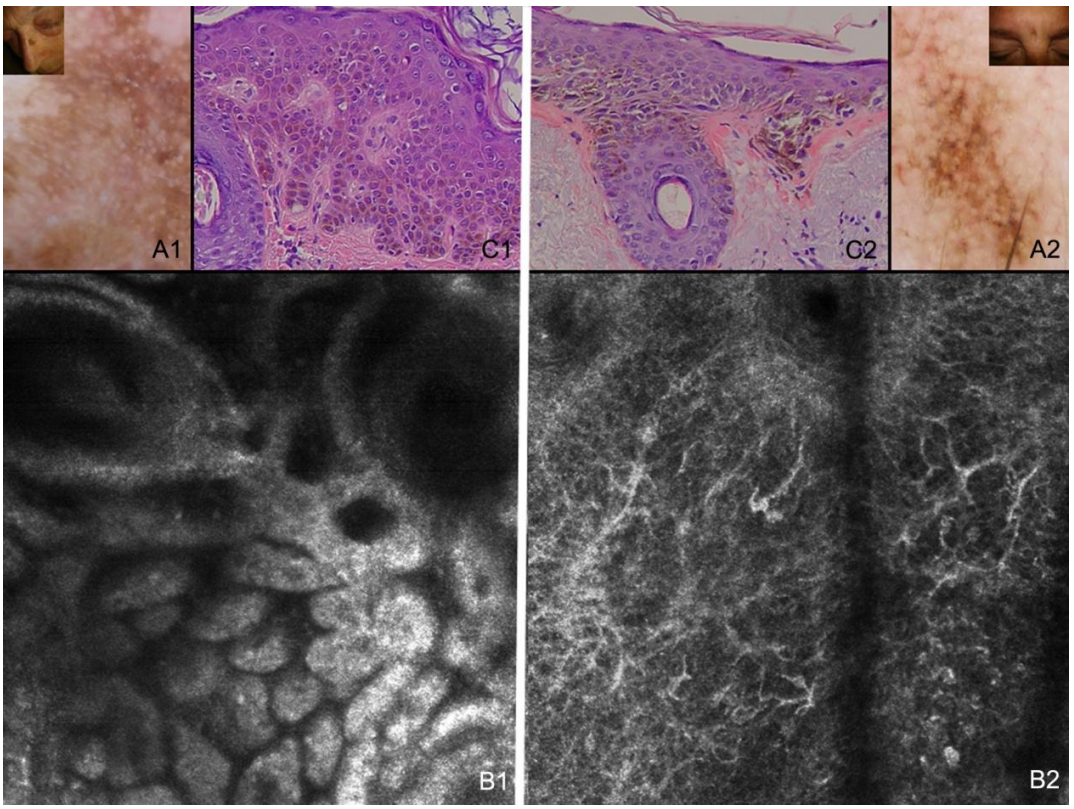

Fig. 25. Lesión vascular adquirida. Correlación de las lagunas vasculares observadas por dermatoscopia (**A**) con espacios hiporeflectantes rodeados de contorno reflectante visibles mediante microscopía confocal de reflectancia (MCR) (mosaico 4x4mm) (**B1**). Detalle MCR 0,5x0,5 mm (**B2**) de las lagunas vasculares con células sanguíneas circulantes (asterisco). Correlación histológica, H-E 100x **(C).**

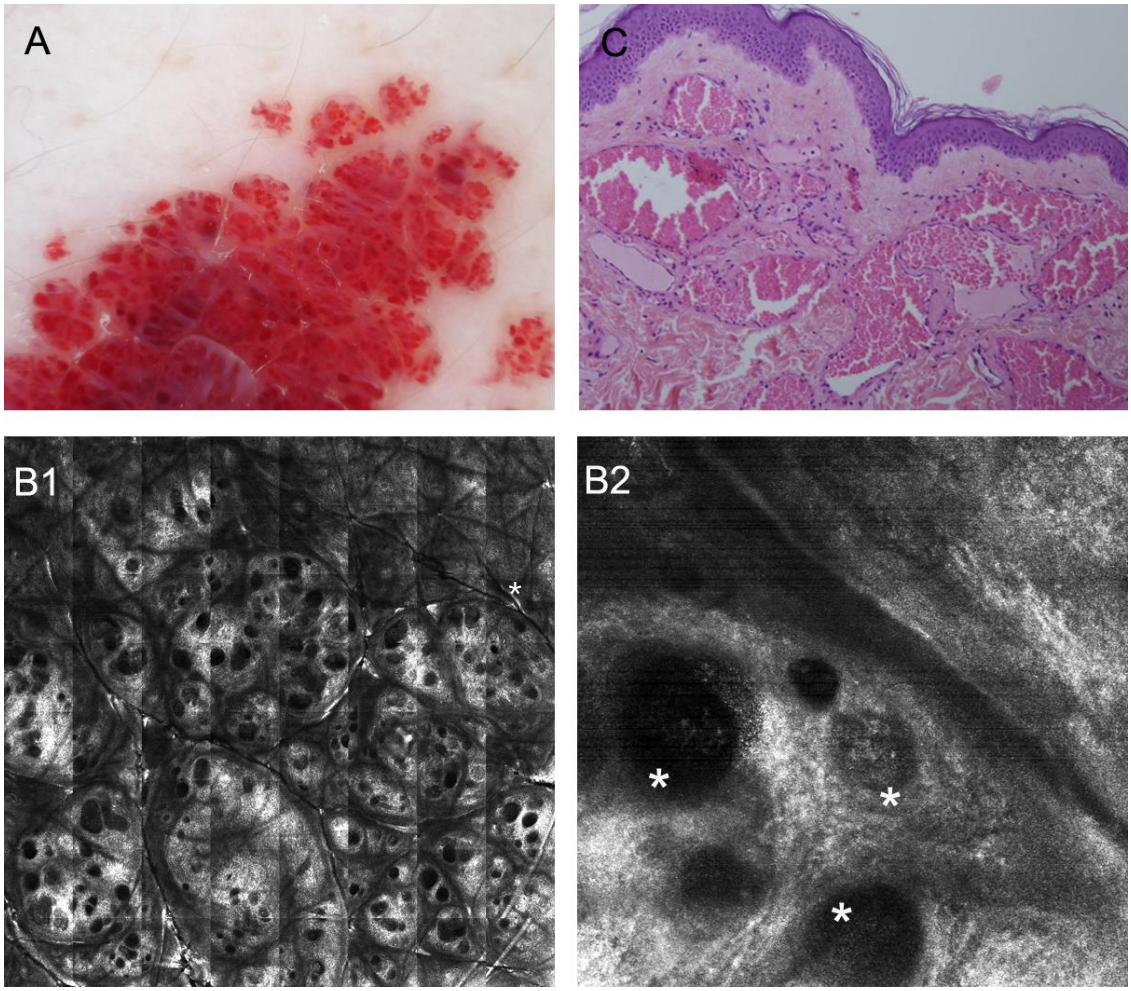

Fig. 26. Dermatofibroma. **A,** Imagen clínica y dermatoscópica característica. **B1**, Mosaico de microscopía confocal de reflectancia (MCR) (4x4mm) mostrando área hiperreflectante central y anillos reflectantes regulares en la periferia. **B2 y B3,** Imágenes de MCR (0,5x0,5mm) de la periferia y el centro de la lesión respectivamente. **C1,** H-E 40x, aspecto histológico típico de un dermatofibroma. **C2,** H-E 200x, detalle de unión dermo-epidérmica en la periferia de la lesión. Correlación del retículo pigmentado delicado observable por dermatoscopia con los anillos reflectantes regulares visibles mediante MCR, que corresponden histológicamente a la hiperplasia epidérmica con pigmentación de la capa basal. **C3,** H-E 200x, detalle de unión dermo-epidérmica en la parte central de la lesión. Obsérvese la correlación entre la cicatriz blanca central por dermatoscopia y el aumento de reflectividad de aspecto fibrilar visible por MCR, correspondiente a la densificación del colágeno dérmico.

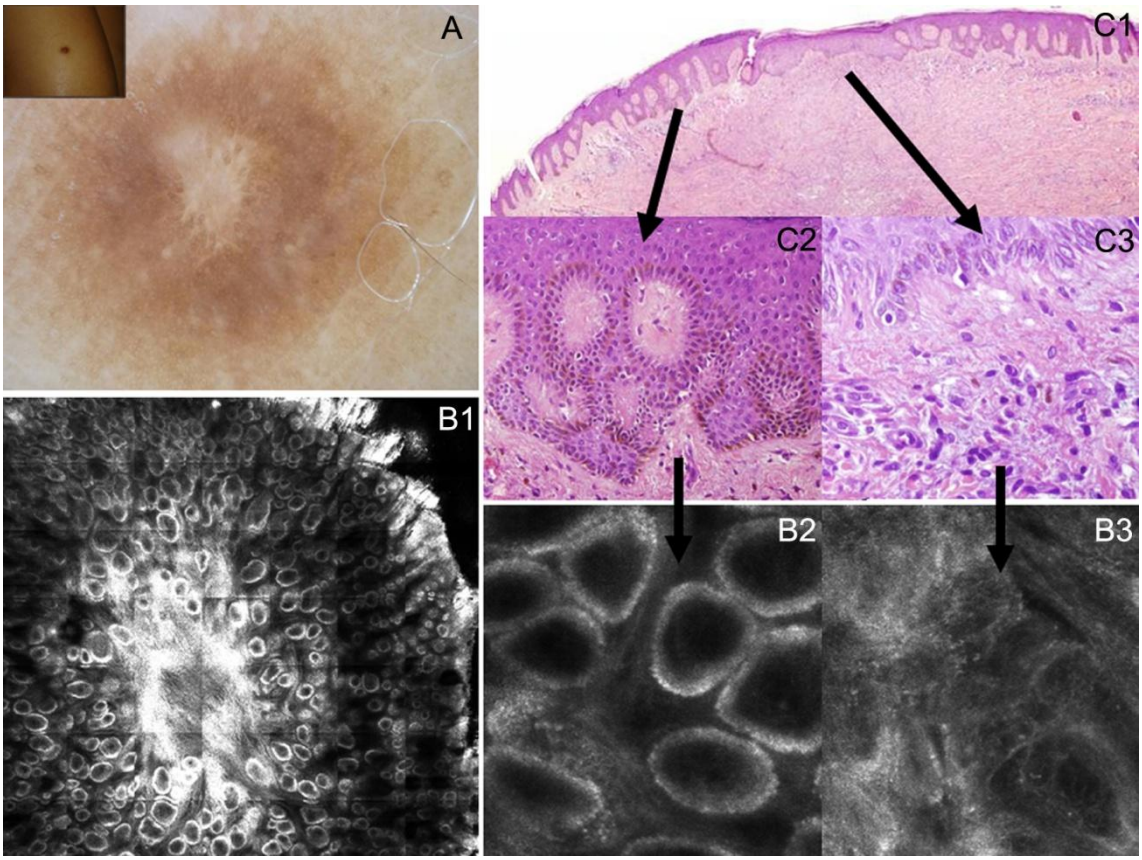

4.1.3. La distinción entre nevus y melanoma

En nuestro árbol de decisión para el diagnóstico de melanoma, una vez hemos decidido que nos hallamos ante una lesión melanocítica debemos decidir si nos encontramos ante un nevus o ante un melanoma. En el trabajo I, después del estudio sistemático de diversos parámetros de microscopía confocal en base a estudios previos[82,90,127,128], el análisis estadístico multivariable obtuvo dos criterios de riesgo que se asociaban a malignidad y por tanto a melanoma y dos criterios protectores asociados a benignidad y por tanto a nevus. Los criterios de melanoma incluían la presencia de células redondas infiltrando los estratos epidérmicos (crecimiento pagetoide) y la presencia de células nucleadas atípicas en la dermis, y se les adjudicó una puntuación de 1. Los criterios de nevus incluían la visualización de unas papilas

dérmicas regulares con contorno reflectante en la unión dermo-epidérmica y presencia de células típicas en la capa basal, y se les adjudicó una puntuación de -1 (Fig. 27). En función del punto de corte en la puntuación final (suma de los distintos criterios) se obtenían distintos valores de sensibilidad y especificidad (Fig. 28). Con un punto de corte -2 (ningún criterio de malignidad y 2 criterios de benignidad) obteníamos una sensibilidad de un 100%, y una especificidad del 57%. Teniendo en cuenta que las lesiones eran clínica y dermatoscópicamente dudosas, estábamos ahorrando la mitad de las biopsias. Con un punto de corte en -1 (dos criterios protectores y uno de riesgo) obtuvimos una sensibilidad de 85%, y un valor predictivo negativo de 92.42. Sin embargo, obtuvimos cinco falsos negativos. De estos, 4 fueron melanomas *in situ*, un tipo de lesión que puede ser particularmente difícil de evaluar por la MCR debido la presencia de características que se solapan con los nevus displásicos. El melanoma restante era una lesión ulcerada en la pierna con áreas de regresión que fue difícil de evaluar por MCR. Con este punto de corte ganábamos especificidad que se situaba en el 95,3%, con valor predictivo positivo del 91,2%.

Pellacani y cols.[90] propusieron un algoritmo diagnóstico semi-cuantitativo para la evaluación mediante MCR de lesiones clínica y dermatoscópicamente equívocas. Según estos autores las características asociadas con el diagnóstico de melanoma incluyen dos criterios mayores (presencia de papilas dérmicas sin contorno y presencia de atipia citológica) y cuatro criterios menores (presencia de células redondeadas en las capas superficiales, presencia de crecimiento pagetoide en toda la lesión, nidos cerebriformes y visualización células nucleadas en la dermis papilar). Este algoritmo se asemeja al nuestro en la mayoría de criterios, especialmente en el valor de la presencia de crecimiento pagetoide (Fig. 29). Este criterio se ha asociado a malignidad en diversos estudios de MCR[89,90,127]. En nuestro estudio como en el de Pellacani y cols. tiene también importancia la morfología de la unión dermo-epidérmica y la celularidad de la dermis superficial. Sin embargo, en nuestro estudio multivariable no encontramos diferencias en la morfología de los nidos. El criterio "nidos cerebriformes" que se observa en algunos melanomas gruesos, dado que eran poco frecuentes en nuestra serie no alcanzaron significación estadística.

En un estudio reciente publicado por nuestro grupo, el algoritmo diagnóstico en dos etapas de MCR permitió clasificar correctamente melanomas incipientes de las extremidades sin criterios clínicos de melanoma y criterios sutiles de malignidad mediante dermatoscopia[129] (Anexo IV).

Fig. 27. Segunda etapa del algoritmo: distinguir nevus melanocítico de melanoma. Cuatro imágenes de microscopía confocal de reflectancia (MCR) 0,5x0,5 mm: dos criterios de malignidad (A y B) y dos criterios de benignidad (C y D). **A,** Células reflectantes atípicas redondas en estratos suprabasales (crecimiento pagetoide). **B**, Células nucleadas atípicas en las papilas dérmicas. Papilas sin contorno con desestructuración de la arquitectura de la unión dermo-epidérmica. **C,** Células típicas en la capa basal. **D,** Papilas dérmicas regulares con contorno reflectante.

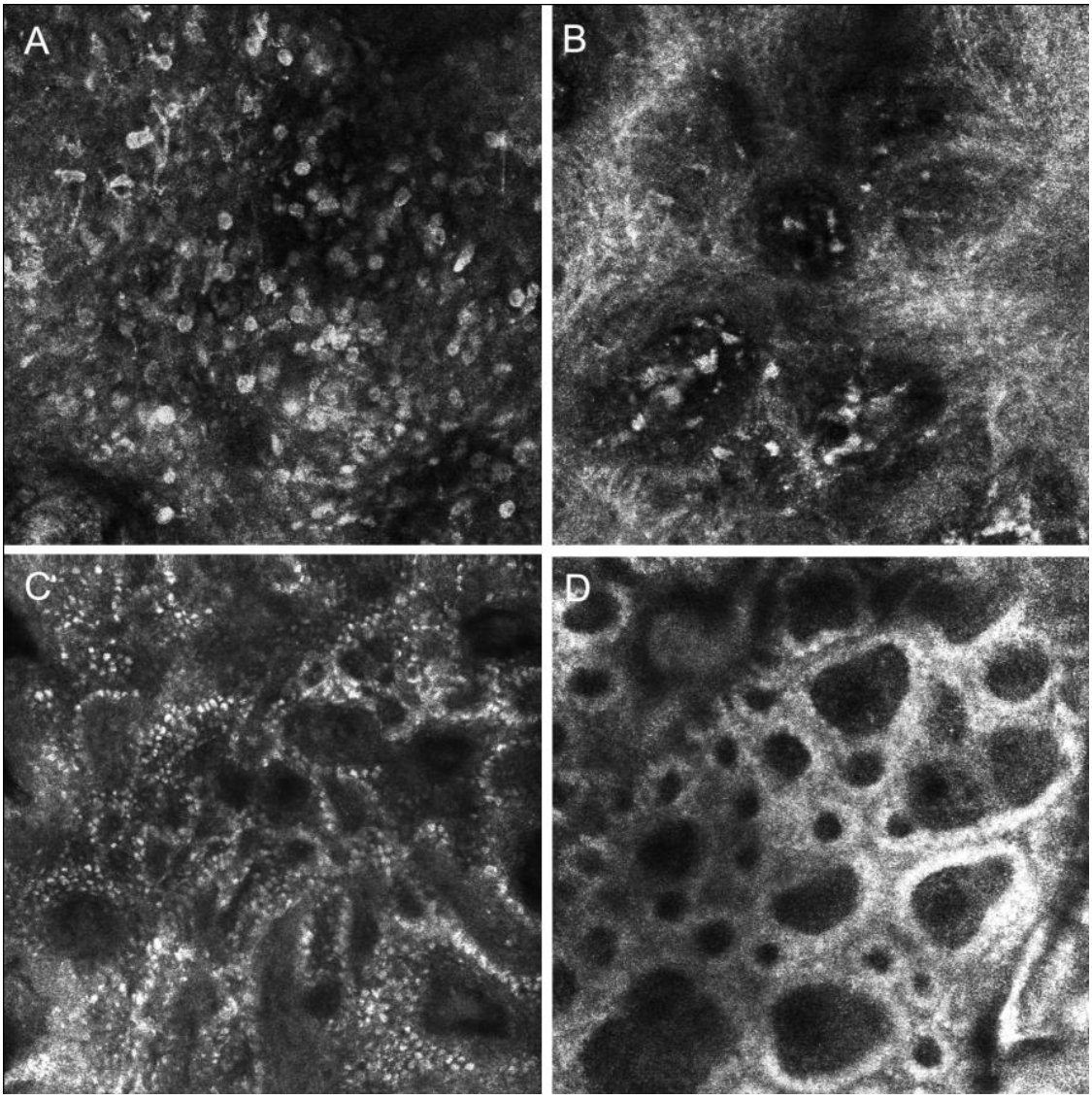

Fig. 28. Algoritmo diagnóstico de melanoma en dos etapas mediante microscopía confocal de reflectancia.

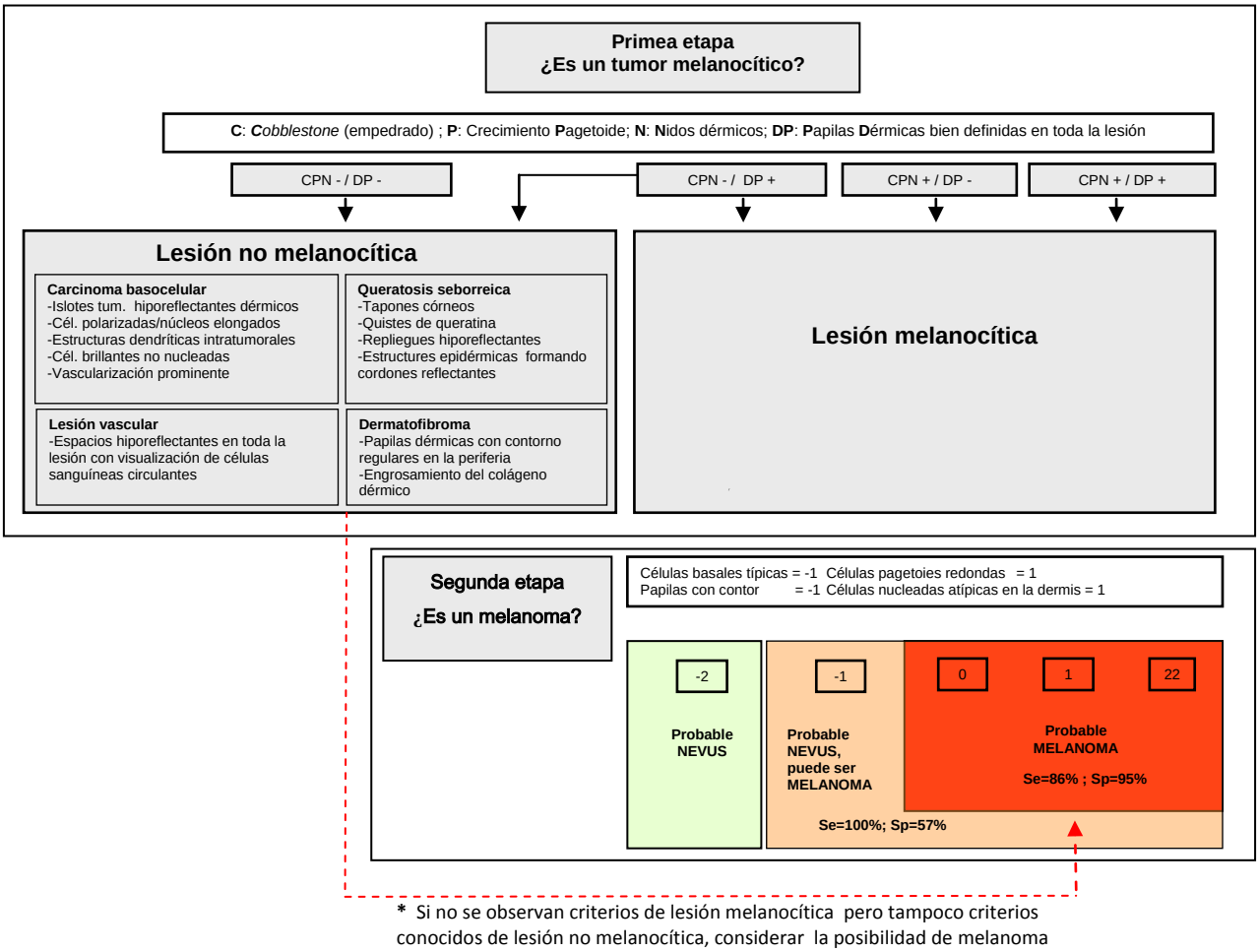

* Si no se observan criterios de lesión melanocítica pero tampoco criterios conocidos de lesión no melanocítica, considerar la posibilidad de melanoma

Fig. 29. Melanoma de extensión superficial con marcado crecimiento pagetoide. A, Imagen clínica y dermatoscópica de un melanoma en el brazo de una mujer de 46 años. Lesión clínicamente policroma con patrón multicomponente por dermatoscopia. Glóbulos atípicos, presencia de velo azul-gris y vascularización atípica. B, Imágenes de microscopía confocal de reflectancia (MCR) (0,5x0,5mm). B1, Corte a nivel del estrato espinoso que pone de manifiesto crecimiento pagetoide de células redondas. B2, Corte a nivel de dermis superficial con nidos reflectantes irregulares. C, H-E 200x. Correlación histológica de la lesión. Crecimiento pagetoide y nidos irregulares de melanocitos atípicos en la dermis superficial.

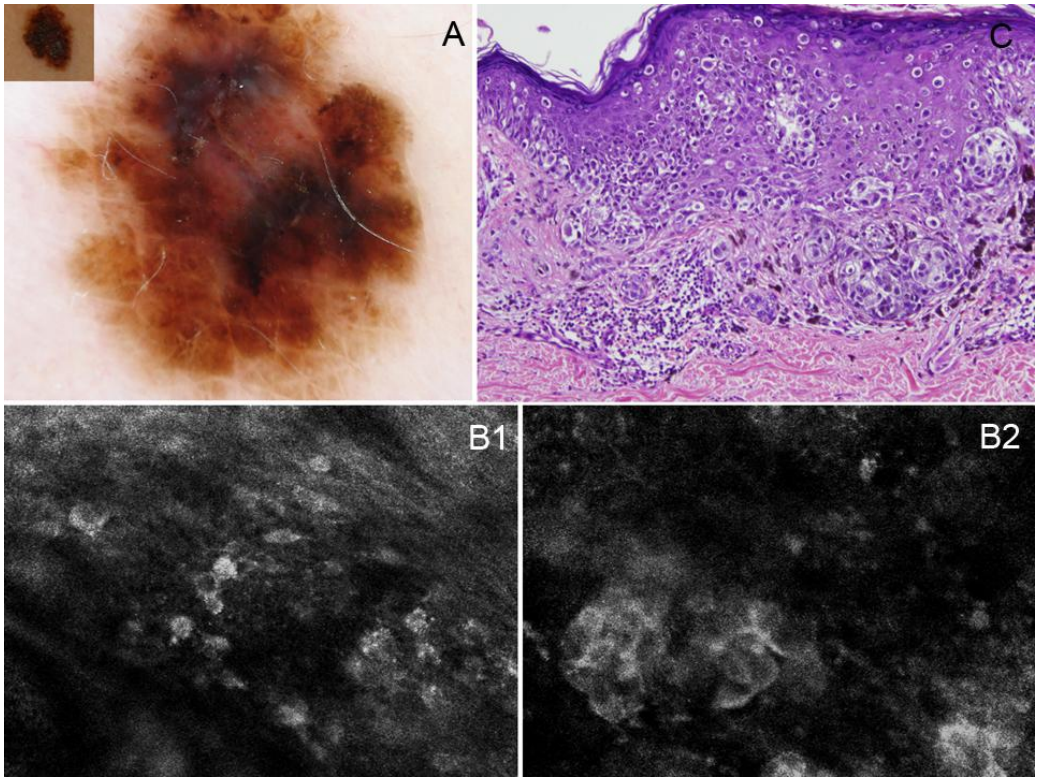

4.1.4. Correlación entre dermatoscopia, confocal e histología

Una de las ventajas de la MCR es la correlación con la imagen dermatoscópica, de manera que representa un puente o nexo de unión entre la dermatoscopia y la histología. El hecho que se realicen cortes horizontales y que el dispositivo sea capaz de hacer mosaicos de varios milímetros en el plano horizontal, facilita la correlación con la dermatoscopia y la posibilidad de orientarnos encima de la lesión. Esta correlación la hemos podido documentar en nuestros trabajos y se resume en las Tablas 1 y 2; Figs. 18, 23-26, 29, 30.

Además de la correlación con la dermatoscopia, es fundamental la correspondencia de los parámetros de MCR con la hallazgos histológicos, que permita validar esta técnica para su aplicabilidad clínica. Esta correlación se resume en las Tablas 1 y 2; Figs. 18, 24-26, 29, 30.

Los hallazgos de nuestra serie se hallan respaldados por un estudio más amplio de correlación entre dermatoscopia, microscopía confocal e histología en 202 lesiones melanocíticas, liderado por el departamento de dermatología de la Universidad de Módena y Reggio Emilia, Italia, con quien colaboró nuestro grupo de trabajo [69] (Anexo III).

Fig. 30. Correlación básica entre la dermatoscopia, la MCR y la histología de una lesión melanocítica benigna con patrón lentiginoso.

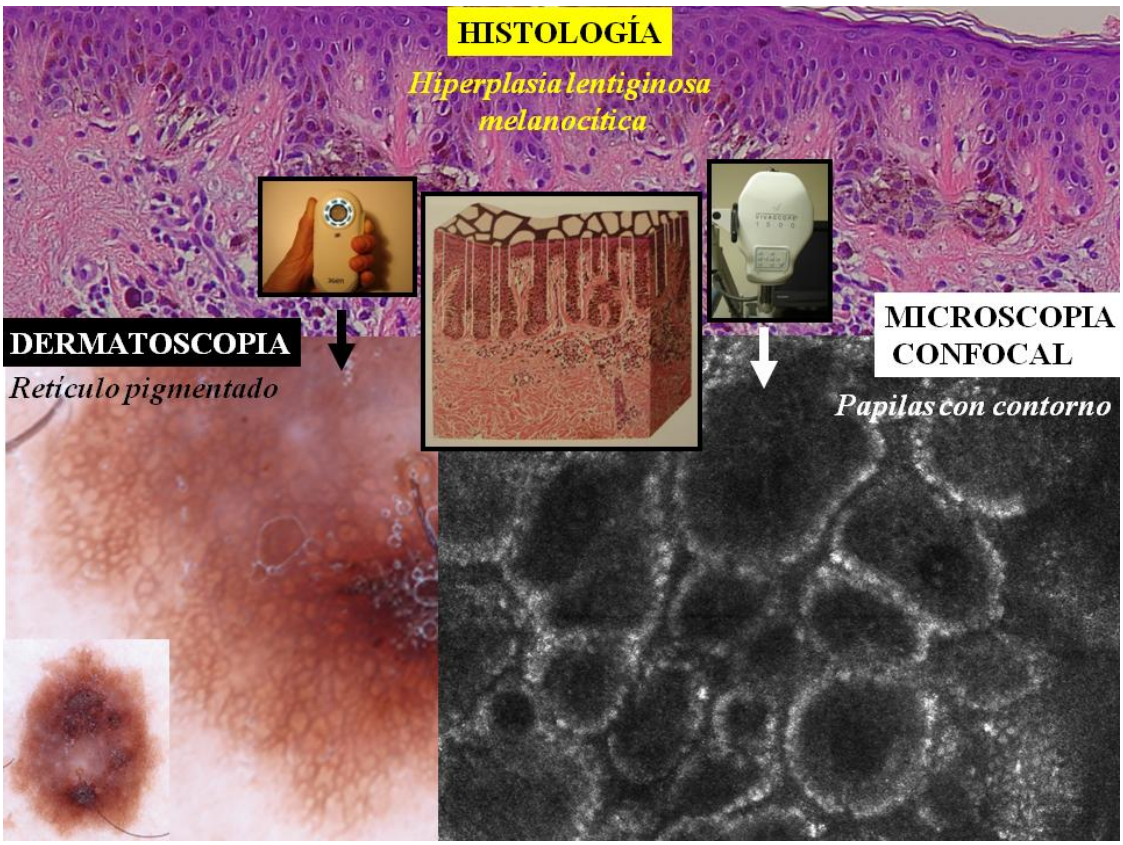

Tabla 1. Correlación dermatoscópica e histológica de los principales parámetros de MCR en lesiones melanocíticas. Valores de reproducibilidad interobservador (*kappa*).

Criterio MCR	Valor kappa	Dermatoscopia	Histología
Estratos superficiales			
Patrón en panal de abejas	0.743	-	Aspecto de la epidermis de la piel normal
Patrón en empedrado	0.757	-	Pigmentación de los queratinocitos basales y suprabasales
Desestructuración epidérmica	0.105	-	Pérdida del aspecto normal de la epidermis debido a la presencia de crecimiento pagetoide
Crecimiento pagetoide	0.445	Puntos marrones	Presencia de melanocitos intraepidérmicos
Unión dermo-epidérmica			
Papilas con contorno	0.891	Retículo típico	Elongación lentiginosa de los procesos interpapilares
Papilas sin contorno	0.340	Retículo atípico	Hiperplasia lentiginosa de melanocitos con atipia variable
Atipia en la capa basal	0.497	-	Grado de proliferación y atipia de los melanocitos basales
Células en sábana	0.465	Áreas sin estructuras	Proliferación de melanocitos en la unión dermo-epidérmica
Agregados juncionales	0.421	Glóbulos	Nidos juncionales
Dermis superficial			
Nidos densos regulares	0.525	Glóbulos típicos	Agregados de melanocitos dérmicos
Nidos densos dishomogéneos	0.324	Glóbulos atípicos	Agregados de melanocitos dérmicos
Nidos cerebriformes	0.658	Áreas sin estructura	Infiltración en dermis profunda de los nidos de melanoma
Células dérmicas nucleadas	0.351	-	Melanocitos infiltrando la dermis papilar
Células “rellenas” brillantes	0.361	Puntos azul-grises	Melanófagos
Vasos dérmicos agrandados	0.373	Vasos en coma o vasos atípicos	Aumento de la vascularización dérmica

Tabla 2. Correlación dermatoscópica e histológica de los principales parámetros de MCR en lesiones no melanocíticas. Valores de reproducibilidad interobservador (*kappa*).

Criterio MCR	**Valor Kappa**	**Correlación dermatoscópica**	**Correlación histológica**
Carcinoma basocelular			
Nódulos tumorales	0.375	Hojas de arce y nidos ovoides	Nidos de células basaloides
Polarización	0.474	-	Polarización de las células tumorales basaloides
Estructuras dendríticas	0.722	-	Melanocíticos dendríticos en los nidos tumorales
Células anucleadas brillantes	0.522	Puntos azul-grises	Melanófagos
Vascularización prominente*	0.299	Telangiectasias arboriformes	Neovascularización dérmica
Queratosis seborreica			
Tapones y quistes de queratina	0.559	Aperturas pseudofoliculares/quistes millium	Invaginaciones de la epidermis rellenas de queratina
Criptas (repliegues hiporeflectantes)	NE	Fisuras	Invaginaciones en la superficie de la QS
Cordones epiteliales reflectantes**	0.597	Estructuras en huella digital	Hiperplasia epitelial lentiginosa
Tumor vascular			
Espacios vasculares*	0.388	Lagunas vasculares	Proliferación en la dermis de vasos sanguíneos
Dermatofibroma			
Papilas con contorno	NE	Reticulado delicado periférico	Elongación de los procesos interpapilares
Colágeno dérmico engrosado	NE	Parche blanquecino central	Densificación del colágeno dérmico

MCR, microscopía confocal de reflectancia; QS: queratosis seborreica; NE, no evaluado;
*la evaluación se realizó con imágenes fijas;**en QS reticuladas y lentigos solares

4.1.5. Reproducibilidad de los criterios de microscopía confocal

La mayoría de las características discriminatorias de las lesiones pigmentadas y los tumores cutáneos malignos (melanoma y CBC) son fiables y reproducibles en nuestro estudio (Tablas 1 y 2). Sin embargo, una de las características de riesgo para el diagnóstico de melanoma (células atípicas nucleadas en la dermis) mostró una baja concordancia entre distintos observadores. Este resultado pone de relieve la necesidad de definir mejor las características de MCR e ilustra la importancia de realizar más estudios antes de la aplicación definitiva de una nueva técnica en la práctica clínica. La evaluación de la dermis es generalmente más difícil que la evaluación de la epidermis y la unión dermo-epidérmica debido a las limitaciones técnicas del láser en la evaluación profunda de la piel. Esta dificultad puede explicar la menor fiabilidad en la evaluación de estructuras dérmicas. Recientemente se ha publicado un artículo multicéntrico de reproducibilidad de los parámetros de MCR para el diagnóstico de lesiones melanocíticas[70]. De forma similar a nuestro estudio, en este trabajo se concluye que la mayoría de parámetros utilizados en el diagnóstico de melanoma son reproducibles excepto la presencia de células nucleadas en la dermis. Según el mismo trabajo, éste y otros parámetros como son los gránulos reflectantes en la epidermis, el grado de atipia de la basal, la presencia de células "rellenas" (*plump cells*) y las fibras reticuladas en la dermis, deben ser mejor definidos para alcanzar niveles óptimos de reproducibilidad[70].

4.2. Utilidad de la MCR para la caracterización de los subtipos de melanoma. Valor de la dermatoscopia y la MCR en el diagnóstico del melanoma nodular

Según la clasificación actual de la Organización Mundial de la Salud[130], se reconocen cuatro subtipos principales de melanoma: melanoma de extensión superficial (MES), melanoma nodular (MN), lentigo maligno melanoma (LMM) y melanoma lentiginoso acral (MLA). Este sistema de clasificación es utilizado por la mayoría dermatopatólogos y responde al concepto clásico de clasificación histológica de los melanomas[131]. Más recientemente se han categorizado los melanomas de acuerdo con el patrón de exposición solar del área afecta, que según algunos estudios parece tener mejor concordancia con vías oncogénicas específicas[132]. Por ejemplo, los melanomas en piel con daño solar crónico presentan con más frecuencia ganancias en el gen que codifica para ciclina D1 ubicado en 11q13. Esta alteración es relativamente menos común en melanomas en el tronco o en las zonas con exposición solar intermitente donde son más frecuentes la mutaciones en el oncogén B-RAF[132].

Otros autores, basándose en estudios recientes que han identificado *stem cells* de estirpe melanocítica en el folículo piloso, en la epidermis y en la dermis[133-135], así como en la evidencia de que algunos cánceres se originen de células *stem cells* transformadas[133,134] sugieren que los tres principales tipos de melanoma (MES, MN y LMM) se originan respectivamente de células *stem cells* de melanoma localizadas en la capa basal de la epidermis, en la vaina radicular externa del folículo piloso y en la dermis[136]. Esta teoría podría explicar porque la exposición solar se asocia a MES y LMM pero no parece estar tan implicada en el origen del MN, pues la radiación UV llega con menos intensidad a la dermis. También explicaría porque los melanomas que se originan de nevus congénitos gigantes (cuyos nidos se extienden en profundidad en la dermis) son fundamentalmente nodulares y subepidérmicos en origen.

Con la hipótesis que el MN puede tener un origen distinto al MES nos propusimos en el trabajo II caracterizar mediante microscopía confocal una serie de 10 melanomas nodulares, comparándolos con 20 MES (10 melanomas en fase de crecimiento horizontal y 10 melanomas en fase de crecimiento vertical). Quisimos asimismo establecer la correlación de los criterios de microscopía confocal con la dermatoscopia y la histología, con ello fundamentar la utilidad de la MCR en el diagnóstico de unas lesiones que suponen frecuentemente un desafío en la práctica clínica.

Los MNs carecen frecuentemente de criterios clínicos de malignidad (son a menudo tumores pequeños, redondos, simétricos, de bordes regulares y color homogéneo, a veces hipomelanóticos o amelanóticos)[137-139]. Estas peculiaridades hacen del MN un tumor de diagnóstico difícil que en ocasiones lleva a retrasos diagnósticos y al consecuente pronóstico infausto. La dermatoscopia nos ofrece algún dato más que la clínica pero en muchas ocasiones es también difícil pues la asimetría estructural es en general menos acusada que en el MES y los criterios clásicos de dermatoscopia del MES suelen estar ausentes. Sin embargo a menudo presentan hallazgos de dermatoscopia asociados a tumores profundos, como son la presencia de múltiples colores, velo azul-blanco y vasos atípicos debido a la angiogénesis[140].

El análisis de dermatoscopia de nuestros 30 casos reveló rasgos característicos en el grupo de MN y diferencias significativas en comparación con los grupos de MES. De acuerdo con el análisis clásico de patrones de dermatoscopia, el patrón era en la mayoría de casos "inespecífico", pero las lesiones mostraban 3 o más estructuras dermatoscópicas[141]. Por ello, a diferencia del examen clínico, la exploración mediante dermatoscopia ofrecía datos de sospecha de malignidad en la mayoría de casos. La presencia de un velo blanco-azulado y vascularización prominente eran más frecuentes en los MNs (y en las áreas nodulares de los MES) que en los MES en fase de crecimiento horizontal, lo que demuestra que los NMs exhiben características dermatoscópicas asociadas a tumores profundos[140]. Estos hallazgos concuerdan con publicaciones posteriores de melanoma nodular y dermatoscopia [142].

En cuanto al estudio mediante MCR, pudimos demostrar que los MNs exhibían características propias mediante MCR respecto a los MES. La mayoría de dichas características tenían buena correlación con la dermatoscopia y la histología. En la epidermis, los MNs carecían de las características descritas en los MES, como son el patrón desestructurado y la presencia de abundantes células nucleadas atípicas (redondas o dendríticas, crecimiento pagetoide)[89,90,127]. Los MN presentaban un patón en panal de abejas conservado, a menudo de "aspecto engrosado" *(broadened honeycomb*) (aumento de la reflectividad citoplasmática de los queratinocitos) con ocasionales células pagetoides suprabasales (Fig. 31C2, 32C2). En la unión dermo-epidérmica, los MNs y el área nodular de los MES presentaban características similares. No se observaban las papilas dérmicas debido al aplanamiento del epitelio. En la dermis superficial, inmediatamente debajo del epitelio, llamaba la atención la presencia de células reflectantes pleomórficas distribuidas "en sábana" (*sheets of cells*) (Fig. 31C3, 33C3), así como en nidos irregulares (Fig. 31C4, 33C4). En dermis más profunda y de forma característica en los MN, se observaban nidos celulares hiporeflectantes de aspecto amorfo denominados previamente por otros autores "nidos cerebriformes" que se correlacionaban con nidos profundos de células de melanoma (Fig. 32C4). Cabe destacar que en dermis, los MNs presentaban unas estructuras fibrilares reflectantes formando "bandas" que rodeaban los agregados celulares. Estas estructuras parecían correlacionarse con colágeno dérmico compactado alrededor de la masa tumoral. Por último, una constante de los MNs así como del componente nodular de los MES fue la presencia de estructuras vasculares prominentes y tortuosas, que tenían muy buena correlación con la dermatoscopia y se asociaban a tumores más profundos.

Las principales limitaciones del estudio son: el reducido número de casos, la ausencia de ciego en la evaluación de los casos y la limitación de la técnica en el estudio en profundidad de las lesiones. Son necesarios estudios más amplios con los distintos subtipos de melanoma para establecer diferencias estructurales y citológicas y correlacionarlas con estudios genéticos para poder así comprender mejor los subtipos histogénicos y el comportamiento biológico del melanoma maligno.

En cuanto al LMM, a pesar de que no hemos estudiado específicamente este subtipo de tumores, en el trabajo I pudimos observar que aquellos melanomas tipo LMM presentaban en general un prominente crecimiento pagetoide, así como reflectividad perifolicular irregular que se correlacionaba con las imágenes de dermatoscopia (Fig. 34C1). Algunas células con

crecimiento pagetoide se situaban alrededor del folículo y eran frecuentemente de morfología dendrítica presentando en algunos casos largas proyecciones. Guitera y cols.[126] estudiaron mediante MCR una serie de máculas faciales clínicamente equívocas (81 lentigos malignos y 203 máculas faciales benignas). Se analizaron a ciegas 64 parámetros de MCR y se elaboró un algoritmo diagnóstico que alcanzó una sensibilidad de 93% y una especificidad de 83% para el diagnóstico de lentigo maligno. En este algoritmo se tienen en cuenta dos criterios mayores: papilas sin contorno y células pagetoides redondas y grandes; y cuatro criterios menores (tres de riesgo [3 o más células atípicas en la unión dermo-epidérmica en un campo de 0,5x0,5 mm; localización perifolicular de las células atípicas y células nucleadas en las papilas dérmicas] y un criterio protector [patrón epidérmico en panal de abejas de "aspecto engrosado" *(broadened honeycomb*)]). La mayoría de criterios son similares a los utilizados en nuestro algoritmo (trabajo I) y otros estudios[90,127]. De forma adicional, en el trabajo de Guitera y cols.[126] se tiene en cuenta el número de células atípicas en la unión dermo-epidérmica y la localización perifolicular de las mismas.

Fig. 31. **Melanoma nodular en el muslo de una mujer**. **A,** Imagen clínica: lesión pápulo-nodular marrón oscuro con discreta descamación en superficie. **B,** Dermatoscopia: lesión policroma, estructuralmente asimétrica sin patrón de dermatoscopia específico. Áreas sin estructura con pigmentación irregular, puntos y glóbulos irregulares, crisálidas y vascularización prominente. **C1,** Mosaico de microscopía confocal de reflectancia (MCR) 4x4 mm del centro de la lesión en un corte oblicuo a nivel de estrato espinoso-unión dermo-epidérmica. Se aprecia una superficie irregular y múltiples estructuras reflectantes que corresponde a melanocitos. **C2**, Imagen MCR 0,5x0,5 mm en la unión dermo-epidérmica. Proliferación de células reflectantes atípicas *en sábana* com pérdida de las estructura normal de la unión dermo-epidérmica. **C3 y C4,** Imágenes de MCR 0,5x0,5 a nivel de dermis. Nidos irregulares de melanocitos asociados a vasos sanguíneos agrandados. **D1-D3,** H-E 40x, 100x, 200x. Correlación histológica. Aplanamiento epidérmico, proliferación de células atípicas epitelioides en la unión dermo-epidérmica con formación de nidos discohesivos. Proliferación densa y difusa de las mismas células en dermis media y profunda.

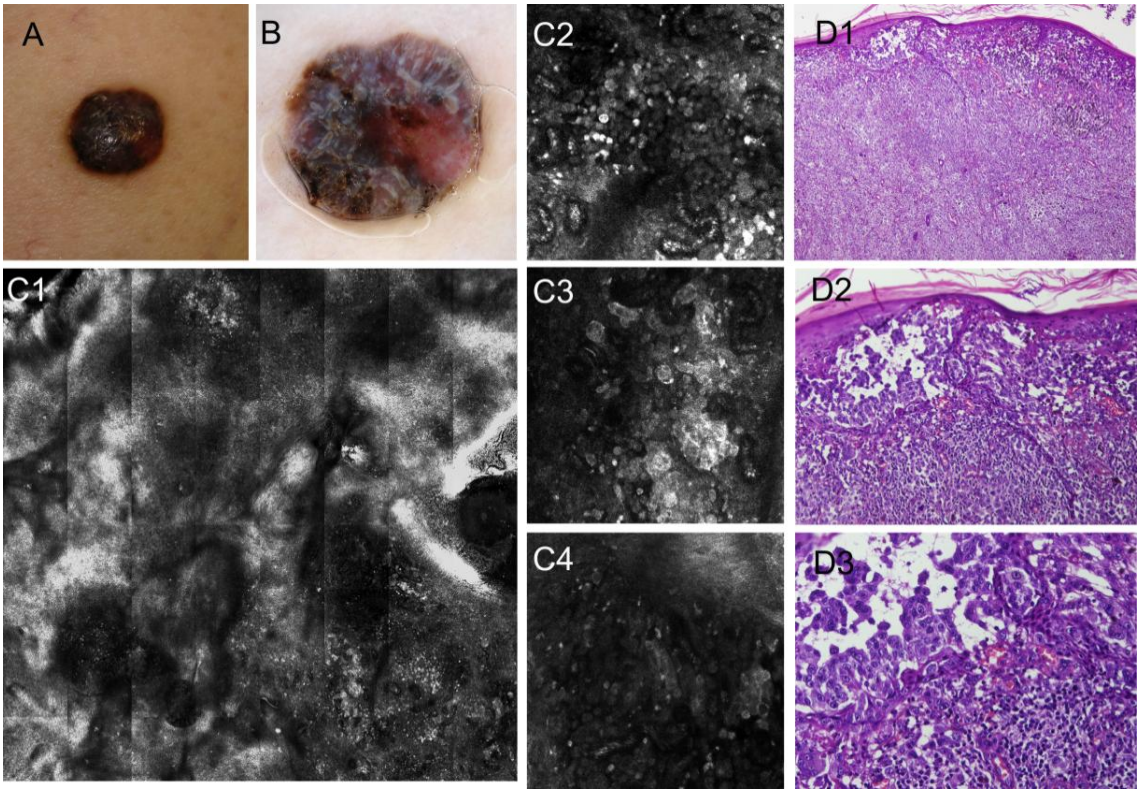

Fig. 32. **Melanoma nodular en región peri-areolar de difícil diagnóstico clínico y por dermatoscopia**. **A,** Aspecto clínico de la lesión, nódulo azulado ulcerado. **B,** Dermatoscopia, lagunas vasculares irregulares con ulceración central. **C1,** Mosaico de microscopía confocal de reflectancia (MCR) 4x4 mm de la mitad de la lesión. Se observan espacios hiporeflectantes con contorno reflectante que parecen corresponder a espacios vasculares. **C2,** Imagen de MCR 0,5x0,5 mm a nivel de estrato espinoso. Patrón en panal de abejas engrosado *(broadened honeycomb)*. Ausencia de crecimiento pagetoide. **C3,** Imagen de MCR 0,5x0,5 mm a nivel de unión dermo-epidérmica. Células basales atípicas. Vasos sanguíneos agrandados y tortuosos. **C4,** Imagen de MCR 0,5x0,5 mm a nivel de dermis media. Nidos cerebriformes. **D1-D3**, H-E 40x,100x, 200x. Correlación histológica. Lesión nodular con collarete periférico y pigmento en profundidad. Aplanamiento de la epidermis, proliferación de células epitelioides en toda la dermis, con abundante púrpura.

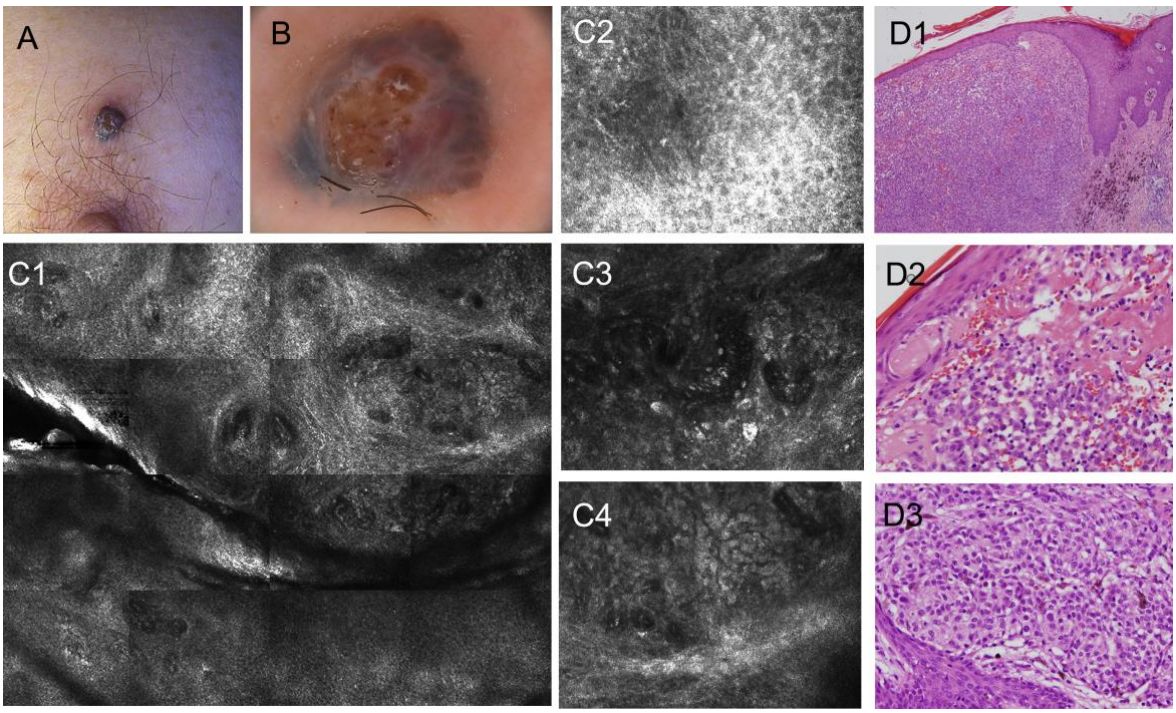

Fig. 33. **Melanoma de extensión superficial en fase de crecimiento vertical**. **A,** Aspecto clínico de la lesión. Lesión policroma, asimétrica, con componente nodular un la mitad de la lesión. **B,** Dermatoscopia, clara asimetría estructural con patrón multicomponente (glóbulos atípicos, retículo pigmentado, estructuras de regresión). **C1,** Mosaico de microscopía confocal de reflectancia (MCR) 4x4 mm sobre la parte nodular de la lesión a nivel de la unión dermo-epidérmica. Se observan agregados celulares reflectantes de tamaño y distribución irregular y múltiples estructuras celulares reflectantes dispersas. **C2,** Imagen de MCR 0,5x0,5 mm a nivel de estrato espinoso. Crecimiento pagetoide de células reflectantes redondas. **C3,** Imagen de MCR 0,5x0,5 mm a nivel de unión dermo-epidérmica. Proliferación de células reflectantes atípicas *en sábana*. **C4,** Imagen de MCR 0,5x0,5 mm a nivel de dermis. Nidos densos de tamaño y reflectividad irregular. **D1,D2**, H-E 200x, 400x. Correlación hstológica. Cortes de la parte nodular de la lesión. Proliferación de células epitelioides atípicas con abundante pigmento en la unión dermo-epidérmica, formando agregados que se extienden en profundidad.

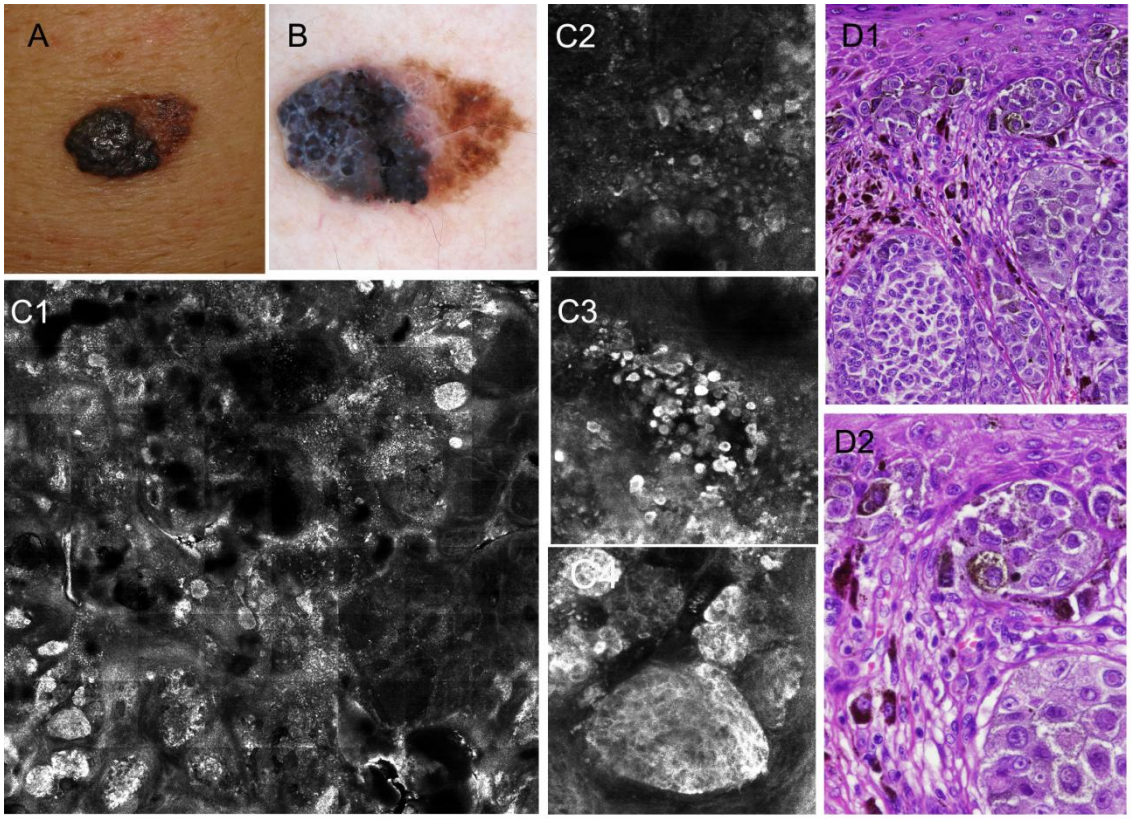

Fig 34. Lentigo maligno en la mejilla de un varón de 70 años. A, Imagen clínica, mácula pigmentada marrón oscuro con área cicatricial central de biopsia previa. **B,** Dermatoscopia. Pigmentación perifolicular irregular, con formación de algunas estructuras romboidales. **C1,** Imagen de microscopía confocal de reflectancia (MCR) 0,5x0,5 mm a nivel de unión dermo-epidérmica. Cordones epiteliales reflectantes irregulares. **C2**, Imagen de MCR 0,5x0,5 mm a nivel de estrato espinoso. Crecimiento pagetoide, abundantes células reflectantes de morfología dendrítica.

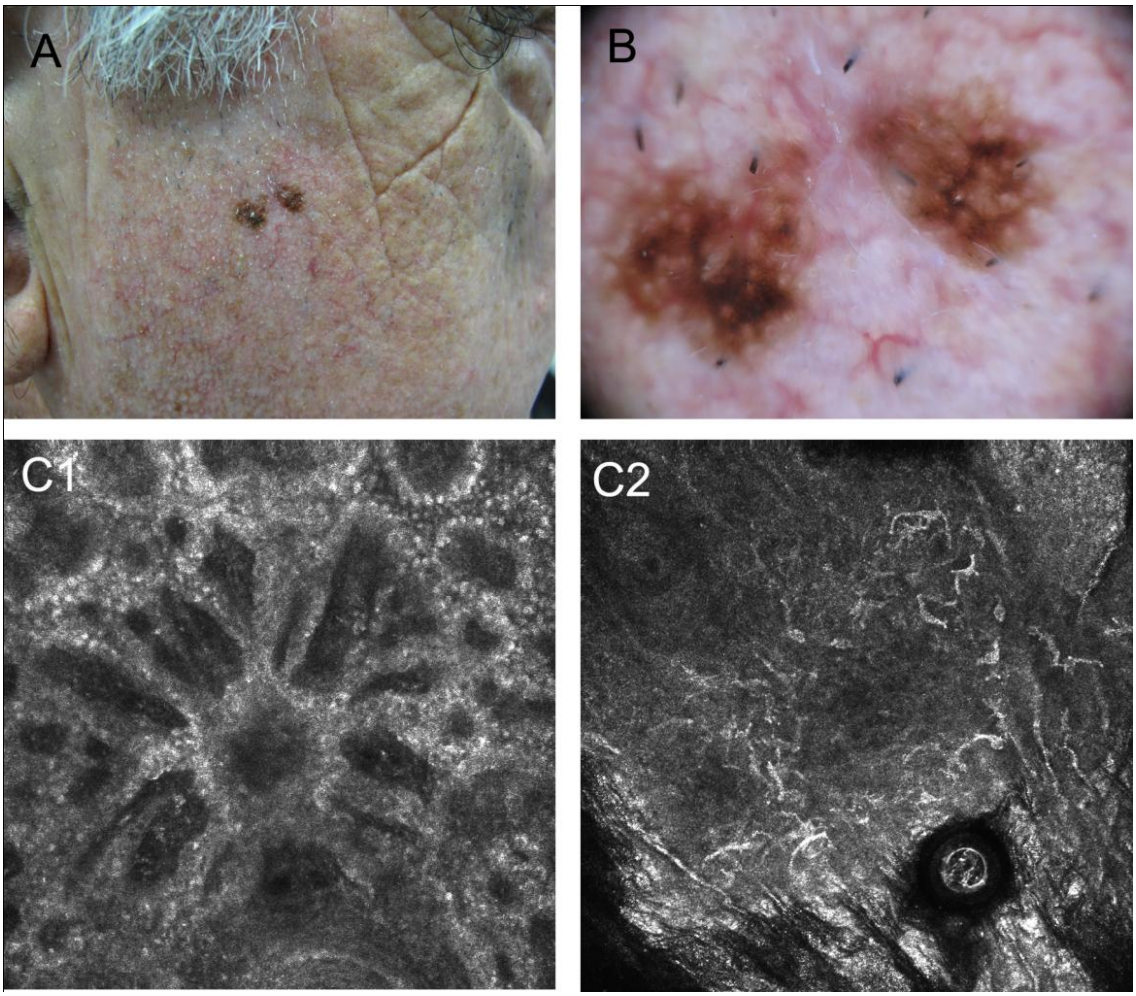

4.3. Utilidad de la MCR en el seguimiento de tratamientos no invasivos en el cáncer cutáneo no melanoma. Abordaje no invasivo en pacientes con síndrome de Gorlin y Xeroderma pigmentoso tratados con terapia fotodinámica

Una de las ventajas de la técnica de microscopía confocal de reflectancia (MCR) es que nos permite explorar una lesión a lo largo del tiempo, viendo la respuesta y evolución tras aplicar un tratamiento determinado. En el caso de los nuevos tratamientos no invasivos para algunos subtipos de cáncer cutáneo no melanoma esta aplicación adquiere un especial interés. Nos referimos a los ya bien conocidos y ampliamente utilizados imiquimod y terapia fotodinámica, pero también a los más novedosos AINEs tópicos en el caso de las queratosis actínicas[143] y a los aún en fase de ensayo clínico inhibidores de la vía de hedgehog para en tratamiento de algunos casos de carcinoma basocelular[23].

En los pacientes con predisposición a cáncer cutáneo esta modalidad de tratamientos, así como aquellas técnicas de imagen que nos den un diagnóstico fiable minimizando la necesidad de realizar biopsias, adquieren un máximo interés. Son diversas las patologías que pueden incluirse en este grupo, destacando quizás en frecuencia y de forma creciente, los pacientes sometidos a trasplantes de órgano sólido y su predisposición bien conocida al cáncer cutáneo en relación con la terapia inmunosupresora.

Otro subgrupo interesante es el de pacientes con genodermatosis con predisposición al cáncer cutáneo. Entre ellos destacamos el síndrome de Gorlin (SG) y aunque de lejos más infrecuente el Xeroderma pigmentoso (XP).

Los pacientes afectos de SG y XP son propensos a desarrollar cáncer de piel desde una edad muy temprana y con frecuencia se presentan con lesiones extensas y múltiples. Por esta razón, los procedimientos no invasivos como la terapia fotodinámica (TFD)[31-34] aparecen como una opción terapéutica adecuada en este contexto clínico.

En el trabajo IV se presenta nuestra experiencia en el tratamiento de carcinomas basocelulares (CBCs) múltiples usando TFD con aminolevulinato (MAL) en 4 pacientes con SG y 2 pacientes con XP y se evalúa la utilidad de la MCR para monitorizar la respuesta a dicho tratamiento.

Nuestras tasas de respuesta a TFD (entre 25-67%, según los pacientes) son inferiores a las reportados en la literatura para el CBC en ensayos clínicos[16] pero similares a otros estudios con TFD en pacientes con de SG[32-34]. Estos resultados pueden deberse al hecho de que la mayoría de las lesiones tratadas eran pigmentadas y / o nodulares en las que se conoce que la TFD es menos efectiva[16].

Hay un solo artículo del uso de la TFD con ácido 5-aminolevulínico (5-ALA) en XP, en el que se trató con éxito un carcinoma escamoso superficial en el dorso de la mano de una mujer de 47 años[31]. En cuanto a SG, el primer trabajo fue publicado en 2005 por Oseroff y cols.[32]. Estos autores utilizaron TFD con 5-ALA para tratar área amplias corporales con múltiples CBCs y hamartomas foliculares basaloides en 3 niños afectos de SG. La crema se aplicaba en extensas

áreas corporales durante 24 horas bajo oclusión y posteriormente se irradiaba la piel hasta 50 min bajo anestesia general, obteniéndose un aclaramiento del 85% al 98% de las lesiones. Los resultados de estos autores en tasa de respuesta son superiores a los nuestros probablemente debido a los largos tiempos de oclusión e irradiación, pero en contrapartida en dicho estudio se requería anestesiar a los pacientes.

Más recientemente se han publicado dos trabajos utilizando metilaminolevulinato (MAL). Mougel y cols.[33] revisaron retrospectivamente la evolución de 62 lesiones en 5 pacientes con CBCs múltiples tratados con TFD. Se obtuvo una tasa de respuesta del 85% y una tasa de recurrencia del 7,5%. La mayoría de los casos eran CBCs superficiales con un seguimiento medio de 13 meses. En una serie más grande con 33 pacientes afectos de SG, Loncaster y cols.[34] lograron tasas de control local de hasta 60% a los 12 meses, utilizando TFD tópica con MAL en lesiones de menos de 2 mm, y un fotosensibilizador sistémico en aquellas de más de 2 mm.

En cuanto al uso de herramientas no invasivas en pacientes con SG y XP, nuestro grupo de trabajo tiene experiencia en el uso de la dermatoscopia en este contexto clínico y que se traduce en dos publicaciones recientes[24,25]. En el caso del SG, la dermatoscopia es útil para la detección de CBC incipientes (menos de 3 mm) i detectar los característicos *pitts* acrales que a menudo pueden pasar por alto durante el examen físico[24].

La MCR se nos aparece como una técnica complementaria a la dermatoscopia que puede ofrecernos por un lado datos diagnósticos de los tumores que afectan estos pacientes y por otro servirnos de herramienta para evaluar la respuesta y seguimiento a largo plazo tras un tratamiento no invasivo del cáncer cutáneo como la TFD.

No nos consta la utilización de la MCR en pacientes con SG o XP previo a nuestro trabajo, pero sí se ha utilizado para evaluar la respuesta del CBC a imiquimod[77,78]. Torres y cols.[78] realizaron una exploración mediante MCR en 23 CBC tratados con imiquimod que fueron posteriormente extirpados, obteniendo un valor predictivo negativo del 70% y un valor predictivo positivo del 84,6%. Estos valores no se pudieron calcular en nuestra serie pues no se realizó biopsias sistemáticas después del tratamiento. De todas formas realizamos un seguimiento a los pacientes durante tres años para estar seguros de que las lesiones que se habían considerado curadas no persistían o no habían vuelto a aparecer.

En este cuarto trabajo pudimos confirmar los parámetros diagnósticos de CBC mediante MCR descritos en trabajos previos, tanto propios (trabajo I, trabajo III) como ajenos[79-81, 117,118]. La presencia de dichos parámetro nos permitía establecer un diagnóstico previo al tratamiento con TFD, así como evaluar la respuesta a dicho tratamiento. En un caso dudoso clínica y dermatoscópicamente, la exploración mediante MCR permitió de forma inequívoca demostrar la persistencia de tumor (Fig. 22B2).

El tratamiento fue bien tolerado por la mayoría de los pacientes, siendo el dolor el efecto secundario más frecuente. En el seguimiento a tres años la mayoría de lesiones que habían respondido al tratamiento no presentaron recidiva, pero la mayoría de los pacientes

presentaban lesiones nuevas. Por ello, a pesar de que el estudio no se diseñó para este fin, nuestros resultados sugieren que el tratamiento con TFD no parece prevenir la aparición de nuevas lesiones en pacientes con SG y XP. En contra de lo que podían sugerir los estudios experimentales en modelo animal[144-147], nuestros resultados ponen en duda la utilización de la TFD como tratamiento preventivo del cáncer cutáneo no melanoma en pacientes con factores de riesgo para desarrollar dichos tumores (al menos si se realiza el tratamiento siguiendo las indicaciones de ficha técnica, en cuanto a tiempo de aplicación de la crema e irradiación). Creemos que este tratamiento puede ser de utilidad en este grupo de pacientes para tratar CBC superficiales y algunos casos de CBC nodulares en localizaciones difíciles para reducir el tamaño de la lesión previo a la cirugía.

5. CONCLUSIONES

- La microscopía confocal de reflectancia (MCR) permite obtener criterios morfológicos distintivos de los principales tumores cutáneos (nevus, melanoma, carcinoma basocelular, queratosis seborreica, dermatofibroma, angioma).

- El uso de la MCR puede evitar biopsias innecesarias de los tumores benignos y permite un diagnóstico inmediato a nivel tisular de las lesiones malignas.

- El algoritmo de diagnóstico en dos etapas que hemos desarrollado puede mejorar la precisión diagnóstica de los tumores cutáneos, minimizando el número de melanomas mal diagnosticados.

- La mayoría de los criterios discriminatorios de cáncer cutáneo mediante MCR son reproducibles entre observadores independientes y presentan buena correlación con la histología y la dermatoscopia.

- La MCR puede detectar diferencias estructurales en los distintos tipos de melanoma, por lo que se nos ofrece como herramienta complementaria para caracterizar mejor los distintos tipos histogénicos de este tumor.

- La terapia fotodinámica (TFD) con aminolevulinato puede ser útil para el tratamiento de carcinomas basocelulares (CBCs) superficiales en síndrome de Gorlin y XP, con mínimos efectos secundarios.

- Algunos CBCs nodulares y pigmentados no logran una remisión completa tras TFD. En estas lesiones, la TFD puede complementar la cirugía mediante la reducción de tamaño del tumor.

- La MCR puede resultar útil en la evaluación antes y después del tratamiento con TFD de CBCs en pacientes con genodermatosis de alto riesgo de cáncer cutáneo, disminuyendo el número de biopsias necesarias.

BIBLIOGRAFÍA

1. Marcos-Gragera r, Vilar-Coromina N, Galceran J, Borràs J, Clèries R, Ribes J, Gispert R, Izquierdo A, Borràs JM. Rising trends in incidence of cutaneous malignant melanoma and their future projections in Catalonia, Spain: increasing impact or future epidemic? J Eur Acad Derm Vererol. 2010; 24: 1083–8.

2. Rogers, MD , Weinstock MA, Harris AR, Hinckley MR, Feldman SR, Fleischer AB, Coldiron BM. Incidence Estimate of Nonmelanoma Skin Cance

in the United States, 2006. Arch Dermatol. 2010 ;146:283-7.

3. JF Abarca , CC Casiccia. Cáncer de piel y la radiación ultravioleta-B en el agujero de ozono antártico: el sur de Chile, 1987-2000. Photoimmunol Photodermatol Photomed. 2002; 18 :294-302.

4. Jemal A, Tiwari RC, Murray T, Ghafoor A, Samuels A, Ward E, et al. Cancer statistics, 2004. CA Cancer J Clin 2004;54:8-29.

5. Albert LS, Rhodes AR, Sober AJ. Dysplastic melanocytic nevi and cutaneous melanoma:markers of increased melanoma risk for affected persons and blood relatives. J Am Acad Dermatol 1990;22:69-75.

6. Berwick M, Weinstock MA. Epidemiology: current trends. In: Balch C, Houghton. A, Sober A, Soong S, eds. Cutaneous melanoma. 4th ed. St. Louis: Quality Medical Publishing, 2003:15-23.

7. Jemal A, Siegel R, Ward E, Hao Y, Xu J, Thun MJ. Cancer statistics, 2009. CA Cancer J Clin. 2009;59:225-49.

8. Garbe C, Leiter U. Melanoma epidemiology and trends. Clin Dermatol. 2009; 27:3-9.

9. Balch CM, Gershenwald JE, Soong SJ, Thompson JF, Atkins MB, Byrd DR, Buzaid AC, Cochran AJ, Coit DG, Ding S, Eggermont AM, Flaherty KT, Gimotty PA, Kirkwood JM, McMasters KM, Mihm MC Jr, Morton DL, Ross MI, Sober AJ, Sondak VK. Final version of 2009 AJCC melanoma staging and classification. J Clin Oncol. 2009;27:6199-206.

10. Grin CM, Kopf AW, Welkovich B, Bart RS, Levenstein MJ. Accuracy in the clinical diagnosis of malignant melanoma. Arch Dermatol.1990; 126:763-6.

11. Miller M, Ackerman B. How accurate are dermatologists in the diagnosis of melanoma? Degree of accurancy and implications. Arch Dermatol 1992; 128: 559-60.

12. Wolf IH, Smolle J, Soyer HP, Kerl H. Sensitivity in the clinical diagnosis of malignant melanoma. Melanoma Res. 1998;8:425-9.

13. Bielsa I, Soria X, Esteve M, Ferrándiz C; Skin Cancer Study Group of Barcelonès Nord. Population-based incidence of basal cell carcinoma in a Spanish Mediterranean area.Br J Dermatol. 2009;161:1341-6.

14. Greenway HT. Interferon. West J Med. 1994; 160: 363.

15. Beutner KR, Geisse JK, Helman D, Fox TL, Ginkel A, Owens ML. Therapeutic response of basal cell carcinoma to the immune response modifier imiquimod 5% cream. L Am Acad Dermatol. 1999; 41: 1002-7.

16. Morton CA, Brown SB, Collins, S, Ibbotson S, Jenkinson H, Kurwa H, et al. Guidelines for topical photodynamic therapy: report of a workshop of the British Photodermatology Group. Br J Dermatol 2002; 146: 552-67.

17. Pariser DM, Lowe NJ, Stewart DM, Jarratt MT, Lucky AW, Pariser RJ, et al. Photodynamic therapy with topical methyl aminolevulinate for actinic Keratosis: Results of a prospective randimozed multicenter trial. J Am Acad Dermatol 2003; 48: 227-32.

18. Horn M, Wolf P, Wulf HC, Warloe T, Fritsch C, Rhodes LE, et al. Topical methyl aminolevulinate photodynamic therapy in patients with basal cell carcinoma prone to complications and poor cosmetic outcome with conventional treatment. Br J Dermatol 2003; 149: 1242-9.

19. Morton CA, McKenna KE, Rhodes LE; British Association of Dermatologists Therapy Guidelines and Audit Subcommittee and the British Photodermatology Group. Guidelines for topical photodynamic therapy: update. Br J Dermatol 2008;159:1245-66.

20. Ling G, Ahmadian A, Persson A, Undén AB, Afink G, Williams C, et al. PATCHED and p53 gene alterations in sporadic and hereditary basal cell carcinoma. Oncogene 2001; 20: 7770-8.

21. Quinn AG, Epstein E Jr. Patched, hedgehog, and skin cancer. Methods Mol Biol 2003; 222: 85-95.

22. Rubin L, de Sauvage FJ. Targeting the Hedgehog pathway in cancer. Nat Rev Drug Disc. 2006; 5: 1026-33.

23. Von Hoff DD, LoRusso PM, Rudin CM, Reddy JC, Yauch RL, Tibes R, et al. Inhbition of the Hedgehog pathway in advanced basal-cell carcinoma. N Engl J Med 2009; 361: 1164-72.

24. Kolm I, Puig S, Iranzo P, Malvehy J. Dermoscopy in Gorlin-Goltz syndrome. Dermatol Surg 2006; 32:847-51.

25. Malvehy J, Puig S, Martí-Laborda RM. Dermoscopy of skin lesions in two patients with xeroderma pigmentosum. Br J Dermatol 2005;152:271-8.

26. Green WH, Wang SQ, Cognetta AB Jr. Total-body cutaneous examination, total-body photography, and dermoscopy in the care of a patient with xeroderma pigmentosum and multiple melanomas. Arch Dermatol 2009; 145: 910–15.

27. Stockfleth E, Ulrich C, Hauschild A, Lischner S, Meyer T, Christophers E. Successful treatment of basal cell carcinomas in a nevoid basal cell carcinoma syndrome with topical 5% imiquimod. Eur J Dermatol 2002; 12: 569-72.

28. Nagore E, Sevila A, Sanmartín O, Botella-Estrada R, Requena C, Serra-Guillen C, et al. Excellent response of basal cell carcinomas and pigmentary changes in xeroderma pigmentosum to imiquimod 5% cream. Br J Dermatol 2003; 149: 858-61.

29. Giannotti B, Vanzi L, Difonzo EM, Pimpinelli N. The treatment of basal cell carcinomas in a patient with xeroderma pigmentosum with a combination of imiquimod 5% cream and oral acitretin. Clin Exp Dermatol 2003; 28 (suppl 1): 33-5.

30. Roseeuw D. The treatment of basal skin carcinomas in two sisters with xeroderma pigmentosum. Clin Exp Dermatol 2003; 28 (suppl 1): 30-32.

31. Wolf P, Kerl H. Photodynamic therapy in patient with xeroderma pigmentosum. Lancet 1991; 337: 1613-14.

32. Oseroff AR, Shieh S, Frawley NP, Cheney R, Blumenson LE, Pivnick EK, Bellnier DA. Treatment of diffuse basal cell carcinomas and basaloid follicular hamartomas in nevoid basal cell carcinoma syndrome by wide area 5- aminolevulinic acid photodynamic therapy. Arch Dermatol 2005; 141: 60-7.

33. Mougel F, Debarbieux S, Ronger-Savlé S, Dalle S, Thomas L. Methylaminolaevulinate Photodynamic Therapy in Patients with Multiple Basal Cell Carcinomas in the Setting of Gorlin-Goltz Syndrome or after Radiotherapy. Dermatology 2009; 219:138-42.

34. Loncaster J, Swindell R, Slevin F, Sheridan L, Allan D, Allan E. Efficacy of Photodynamic Therapy as a Treatment for Gorlin Syndrome-related Basal Cell Carcinomas. Clin Oncol (R Coll Radiol) 2009;21:502-8.

35. Gorlin RJ, Goltz RW. Multiple nevoid basal-cell epithelioma, jaw cysts and bifid rips. N Engl J Med 1960; 262: 909–12.

36. Gorlin RJ. Nevoid basal cell carcinoma syndrome. Dermatol Clin 1995; 13: 113–25.

37. Manfredi M, Vescovi P, Bonanini M, Porter S. Nevoid basal cell carcinoma syndrome: a review of the literature. Int J Oral Maxillofac Surg. 2003; 33: 117–24.

38. Farndon PA, Del Mastro RG, Evans DG, Kilpatrick MW. Location of the gene for Gorlin syndrome. Lancet 1992; 339: 581–2.

39. Unden AB, Holmberg E, Lundh-Rozell B, Stähle-Bäckdahl M, Zaphiropoulos PG, Toftgård R, Vorechovsky I. Mutations in the human homologue of Drosophila patched (PTCH) in basal cell carcinomas and the Gorlin syndrome: different in vivo mechanisms of PTCH inactivation. Cancer Res 1996; 56: 4562–65..

40. Bootsma D, Hoeijmakers JHJ. The genetic basis of xeroderma pigmentosum. Ann Genet 1991; 34: 143–50.

41. Cleaver JE. Xeroderma pigmentosum: biochemical and genetic characteristics. Ann Rev Genet 1975; 9: 19–38.

42. Robbins JH, Kraemer KH, Lutzner MA, Festoff BW, Coon HG. Xeroderma pigmentosum:an inherited disease with sun sensitivity, multiple cutaneous neoplasm, and abnormal DNA repair. Ann Intern Med 1974; 80: 221–48.

43. Davis BE, Koh HK, Rohrer TE, Gonzalez E, Cleaver JE. Sunlight avoidance and cancer prevention in xeroderma pigmentosum. Arch Dermatol 1994; 130: 806–8.

44. González S. Confocal reflectance microscopy in dermatology: promise and reality of non-invasive diagnosis and monitoring. Actas Dermosifiliogr. 2009;100 Suppl 2:59-69.

45. Patel JK, Konda S, Perez OA, Amini S, Elgart G, Berman B. Newer technologies/techniques and tools in the diagnosis of melanoma. Eur J Dermatol. 2008;18:617-31.

46. Altmeyer P, el-Gammal S, Hoffmann K, eds. Ultrasound in Dermatology. Berlin Heidelberg: Springer-Verlag, 1992.

47. Pellacani G, Seidenari S. Preoperative melanoma thickness determination by 20-MHz sonography and digital videomicroscopy in combination. Arch Dermatol. 2003;139:293-8.

48. Mogensen M, Nürnberg BM, Forman JL, Thomsen JB, Thrane L, Jemec GB. In vivo thickness measurement of basal cell carcinoma and actinic keratosis with optical coherence tomography and 20-MHz ultrasound. Br J Dermatol. 2009;160:1026-33.

49. Hoffmann K, Rochling A, Stucker M, et al. High frequency sonography of skin diseases. In: Serup J, Jemec GB, eds. Handbook on non-invasive methods of the skin. Boca Raton/Ann Arbor/London/Tokyo: CRC Press, 1995: 69-78.

50. Stücker M, Wilmert M, Hoffmann K, el-Gammal S, Dirting K, Altmeyer P.Objectivity, reproducibility and validity of 3D ultrasound in dermatology. Bildgebung 1995; 62: 179-88.

51. Mogensen M, Thrane L, Joergensen TM, Andersen PE, Jemec GB. Optical coherence tomography for imaging of skin and skin diseases. Semin Cutan Med Surg. 2009;28:196-202.

52. Argenziano G, Soyer HP. Dermoscopy of pigmented skin lesions--a valuable tool for early diagnosis of melanoma. Lancet Oncol. 2001;2:443-9.

53. Kittler H, Pehamberger H, Wolff K, Binder M. Diagnostic accuracy of dermoscopy.Lancet Oncol. 2002;3:159-65.

54. Vestergaard ME, Macaskill P, Holt PE, Menzies SW. Dermoscopy compared with naked eye examination for the diagnosis of primary melanoma: a meta-analysis of studies performed in a clinical setting. Br J Dermatol. 2008;159:669-76.

55. Clinical Practice Guidelines for the Management of Melanoma in Australia and New Zealand. Australia: ISBN 978-0-9775060-7-1; New Zealand: ISBN (Print) 978-1-877509-04-9; ISBN (Electronic) 978-1-877509-05-6.

56. Argenziano G, Soyer HP, Chimenti S, Talamini R, Corona R, Sera F, et al. Dermoscopy of pigmented skin lesions: results of a consensus meeting via the Internet. J Am Acad Dermatol 2003; 48:679-93.

57. Wang SQ, Dusza SW, Scope A, Braun RP, Kopf AW, Marghoob AA. Differences in dermoscopic images from nonpolarized dermoscope and polarized dermoscope influence the diagnostic accuracy and confidence level: a pilot study. Dermatol Surg. 2008;34:1389-95.

58. Carlson K, Pavlova I, Collier T, Descour M, Follen M, Richards-Kortum R. Confocal microscopy: imaging cervical precancerous lesions.Gynecol Oncol. 2005;99(3 Suppl 1):S84-8.

59. Mantopoulos D, Cruzat A, Hamrah P. In vivo imaging of corneal inflammation: new tools for clinical practice and research. Semin Ophthalmol. 2010;25:178-85.

60. Gheonea DI, Saftoiu A, Ciurea T, Popescu C, Georgescu CV, Malos A. Confocal laser endomicroscopy of the colon.J Gastrointestin Liver Dis. 2010;19:207-11.

61. Banno K, Niwa Y, Miyahara R, Nakamura M, Nagaya T, Nagasaka T, et al. Confocal endomicroscopy for phenotypic diagnosis of gastric cancer. J Gastroenterol Hepatol. 2010;25:712-8.

62. Campo-Ruiz V, Ochoa ER, Lauwers GY, González S. Evaluation of hepatic histology by near-infrared confocal microscopy: a pilot study. Hum Pathol. 2002;33:975-82.

63. Schiffhauer LM, Boger JN, Bonfiglio TA, Zavislan JM, Zuley M, Fox CA.Confocal microscopy of unfixed breast needle core biopsies: a comparison to fixed and stained sections. BMC Cancer. 2009;9:265.

64. Kumar K, Avritscher R, Wang Y, Lane N, Madoff DC, Yu TK, Uhr JW, Zhang X. Handheld histology-equivalent sectioning laser-scanning confocal optical microscope for interventional imaging. Biomed Microdevices. 2010;12:223-33.

65. Corcuff P, Lévêque JL.In vivo vision of the human skin with the tandem scanning microscope. Dermatology. 1993;186:50-4

66. Rajadhyaksha M, Grossman M, Esterowitz D, Webb RH, Anderson RR.In vivo confocal scanning laser microscopy of human skin: melanin provides strong contrast. J Invest Dermatol. 1995;104:946-52.

67 Rajadhyaksha M, González S, Zavislan JM, Anderson RR, Webb RH.In vivo confocal scanning laser microscopy of human skin II: advances in instrumentation and comparison with histology. J Invest Dermatol. 1999;113:293-303.

68. Scope A, Benvenuto-Andrade C, Agero AL, Malvehy J, Puig S, Rajadhyaksha M, et al. In vivo reflectance confocal microscopy imaging of melanocytic skin lesions: consensus terminology glossary and illustrative images. J Am Acad Dermatol. 2007;57:644-58.

69. Pellacani G, Longo C, Malvehy J, Puig S, Carrera C, Segura S, et al. In vivo confocal microscopic and histopathologic correlations of dermoscopic features in 202 melanocytic lesions. Arch Dermatol. 2008;144:1597-608.

70. Pellacani G, Vinceti M, Bassoli S, Braun R, Gonzalez S, Guitera P, et al. Reflectance confocal microscopy and features of melanocytic lesions: an internet-based study of the reproducibility of terminology. Arch Dermatol. 2009;145:1137-43.

71. González S, Swindells K, Rajadhyaksha M, Torres A. Changing paradigms in dermatology: confocal microscopy in clinical and surgical dermatology. Clin Dermatol. 2003;21:359-69.

72. Busam KJ, Hester K, Charles C, Sachs DL, Antonescu CR, González S, Halpern AC. Detection of clinically amelanotic malignant melanoma and assessment of its margins by in vivo confocal scanning laser micoscopy. Arch Dermatol 2001; 137: 923-29.

73. Curiel-Lewandrowsky C, Williams CM, Swidells KJ, Tahan SR, Astner S, Frankenthaler RA, González S. Use of in vivo confocal microscopy in malignant melanoma: an aid in diagnosis and assessment of surgical and nonsurgical therapeutic approaches. Arch Dermatol 2004; 140: 1127-32.

74.Rajadhyaksha M, Menaker G, Flotte T, Dawyer PJ, González S. Confocal examination of nonmelanoma cancers in thick skin excissions to potencially guide Mohs micrographic surgery without frozen histopathology. J Invest Dermatol 2001; 117: 1137-43.

75. Tannous Z, Torres A, González S. In vivo real-time confocal reflectance microscopy: a noninvasive guide for Mohs micrographic surgery facilitated by aluminium chloride, an excellent contrast enhancer. Dermatol Surg 2003; 29: 839-46.

76. Karen JK, Gareau DS, Dusza SW, Tudisco M, Rajadhyaksha M, Nehal KS. Detection of basal cell carcinomas in Mohs excisions with fluorescence confocal mosaicing microscopy. Br J Dermatol. 2009;160:1242-50.

77. Goldgeier M, Fox CA, Zavislan JM, Harris D, González S. Noninvasive imaging, treatment and microscopic confirmation of clearance of basal cell carcinoma. Dermatol Surg 2003; 29: 205-10.

78. Torres A, Niemeyer A, Berkes B, Marra D, Schanbacher C, González S, et al. 5% imiquimod cream and reflectance-mode confocal microscopy as adjunct modalities to Mohs micrographic surgery for treatment of basal cell carcinoma. Dermatol Surg 2004; 30: 1462-69.

79. González S, Tannus Z. Real-time in vivo confocal reflectance microscopy of basal cell carcinoma. J Am Acad Dermatol. 2002; 47: 869-74.

80. Sauermann K, Gambichler T, Wilmert M, Rotterdam S, Stücer M, Altmeyer P, Hoffmann K. Investigation of basal cell carcinoma by confocal scanning microscopy in vivo. Skin Res Technol 2002; 8: 141-47.

81. Nori A, Rius-Díaz F, Cuevas J, et al. Sensitivity and specificity of reflectance-mode confocal microscopy for in vivo diagnosis of basal cell carcinoma: a multicenter study. J Am Acad Dermatol. 2004; 51: 923-30.

82. Langley RGB, Rajadhyaksha M, Dawyer PJ, Sober AJ, Flotte TJ, Anderson RR. Confocal scanning laser micoscopy of benign and malignant melanocytic skin lesions in vivo. J Am Acad Dermatol 2001; 45: 365-76.

83. Busam KJ, Charles C, Lohmann CM, Marghoob A, Goldgeier M, Halpern AC. Detection of intraepidermal malignant melanoma in vivo by confocal scanning laser micoscopy. Melanom Res 2002; 12: 349-55.

84.Tannous ZS, Mihm MC, Flotte TJ, González S. In vivo examination of lentigo maligna and malignant melanoma in situ, lentigo maligna type by near-infrared reflectance confocal microscopy: comparison of in vivo confocal images with histologic sections. J Am Acad Dermatol 2002; 46: 260-63.

85. Pellacani G, Cesinaro AM, Grana C, Seidenari S. In vivo confocal scanning laser microscopy of pigmented Spitz nevus: comparison of in vivo confocal images with dermoscopy and rutine histopathology. J Am Acad Dermatol 2004; 51: 372-76.

86. Pellacani G, Cesinaro AM, Seidenari S. In vivo assessment of melanocytic nests in nevi and melanomas by reflectance confocal microscopy. Mod Pathol 2004; Oct 29: 1-6.

87. YamashitaT, Kuwahara T, Gonzalez S, Takahashi M. Non-invasive visualization of melanin and melanocytes by reflectance-mode confocal microscopy. J Invest Dermatol 2005: 124: 235-40.

88. Pellacani G, Cesinaro AM, Longo C, Grana C, Seidenari S. Microscopic in vivo description of cellular architecture of dermoscopic pigmented network in nevi and melanomas. Arch Dermatol 2005; 141: 147-54.

89. Pellacani G, Cesinaro AM, Seidenari S. Reflectance-mode confocal microscopy for the in vivo characterization of pagetoid melanocytosis in melanomas and nevi.J Invest Dermatol. 2005;125:532-7.

90. Pellacani G, Cesinaro AM, Seidenari S. Reflectance-mode confocal microscopy of pigmented skin lesions--improvement in melanoma diagnostic specificity.J Am Acad Dermatol. 2005;53:979-85.

91. Aghassi D, Anderson RR, González S. Confocal laser microscopic imaging of actinic keratoses in vivo: a preliminary report. J Am Acad Dermatol 2000; 43: 42-48

92. Ulrich M, Maltusch A, Röwert-Huber J, González S, Sterry W, Stockfleth E, Astner S. Actinic keratoses: non-invasive diagnosis for field cancerisation.Br J Dermatol. 2007;156 Suppl 3:13-7.

93. Ulrich M, Krueger-Corcoran D, Roewert-Huber J, Sterry W, Stockfleth E, Astner S. Reflectance confocal microscopy for noninvasive monitoring of therapy and detection of subclinical actinic keratoses. Dermatology. 2010;220:15-24.

94. Rishpon A, Kim N, Scope A, Porges L, Oliviero MC, Braun RP, et al. Reflectance confocal microscopy criteria for squamous cell carcinomas and actinic keratoses. Arch Dermatol. 2009; 145:766-72.

95. Agasshi D, González E, Anderson RR, Rajadhyaksha M, González S. Elucidating the pulse-dye laser treatment of sebaceous hyperplasia in vivo with real-time confocal scanning laser microscopy. J Am Acad Dermatol 2000; 43: 49-53.

96. Aghassi D, Anderson RR, González S.Time-sequence histologic imaging of laser-treated cherry angiomas with in vivo confocal microscopy. J Am Acad Dermatol 2000; 43: 37-41.

97. Tachihara R, Choi C, Langley RGB, Anderson RR, González S. In vivo confocal imaging of pigmented ecrine poroma. Dermatology 2002; 204: 185-89.

98. González S, Rajadhyaksha M, Rubinstein G, Anderson RR. Characterization of psoriasis in vivo by reflectance confocal microscopy. J Med 1999; 30: 337-56.

99. Ardigo M, Cota C, Berardesca E, González S.Concordance between in vivo reflectance confocal microscopy and histology in the evaluation of plaque psoriasis. J Eur Acad Dermatol Venereol. 2009;23: 660-7.

100. Swindells K, Burnett N, Rius-Diaz F, González E, Mihm MC, González S. Reflectance confocal microscopy may differentiate acute allergic and irritant contact dermatitis in vivo. J Am Acad Dermatology 2004: 50: 220-28.

101. Astner S, González E, Cheung AC, Rius-Díaz F, Doukas AG, William F, González S. Non-invasive evaluation of the kinetics of allergic and irritant contact dermatitis. J Invest Dermatol 2005; 124: 351-359

102. Sauermann K, Gambichler T, Jaspers S, Radenhausen M, Rapp S, Reich S, et al. Histometric data obtained by in vivo confocal laser sacanning microscopy in patients with systemic sclerosis. BCM Dermatology. 2002; 2: 8.

103. Ardigo M, Maliszewski I, Cota C, Scope A, Sacerdoti G, Gonzalez S, Berardesca E. Preliminary evaluation of in vivo reflectance confocal microscopy features of Discoid lupus erythematosus. Br J Dermatol. 2007;156:1196-203.

104. Lovato L, Salerni G, Puig S, Carrera C, Palou J, Malvehy J. Adult xanthogranuloma mimicking basal cell carcinoma: dermoscopy, reflectance confocal microscopy and pathological correlation. Dermatology. 2010;220:66-70.

105. González S, Rajadhyaksha M, González-Serva A, White WM, Anderson RR. Confocal reflectance imaging of folliculitis in vivo: correlation with routine histology. J Cutan Pathol 1999; 26: 201-5.

106. Hongcharu W, Dawyer P, González S, Anderson RR. Confirmation of onicomycosis by in vivo confocal microscopy. J Am Acad Dermatol 2000; 42: 214-16.

107. Markus R, Huzaira M, Anderson RR, González S. A better potassium hydroxide preparation?. J Am Acad Dermatol 2001; 137: 1076-1078.

108. Goldgeier M, Fox A, Muhlbauer JE. Immediate non-invasive diagnosis of herpes virus by confocal sacanning laser microscopy. J Am Acad Dermatol 2002; 46: 783-85.

109. Longo C, Bassoli S, Monari P, Seidenari S, Pellacani G.Reflectance-mode confocal microscopy for the in vivo detection of Sarcoptes scabiei. Arch Dermatol. 2005;141:1336.

110. Venturini M, Sala R, Semenza D, Santoro A, Facchetti F, Calzavara-Pinton P.Reflectance confocal microscopy for the in vivo detection of Treponema pallidum in skin lesions of secondary syphilis. J Am Acad Dermatol. 2009; 60:639-42.

111. Ardigo M, Cameli N, Berardesca E, Gonzalez S. Characterization and evaluation of pigment distribution and response to therapy in melasma using in vivo reflectance confocal microscopy: a preliminary study.J Eur Acad Dermatol Venereol. 2010;24:1296-303.

112. Gil I, Segura S, Martínez-Escala E, Lloreta J, Puig S, Vélez M, et al. Dermoscopic and reflectance confocal microscopic features of exogenous ochronosis. Arch Dermatol. 2010;146:1021-5.

113. Agero AL, Gill M, Ardigo M, Myskowski P, Halpern AC, González S. In vivo reflectance confocal microscopy of mycosis fungoides: A preliminary study. J Am Acad Dermatol. 2007; 57:435-41.

114. Malvehy J, Puig S. Follow-up of melanocytic skin lesions with digital total-body photography and digital dermoscopy: a two-step method. Clin Dermatol. 2002;20:297-304.

115. Gerger A, Koller S, Weger W, Richtig E, Kerl H, Samonigg H, et al. Sensitivity and specificity of confocal laser-scanning microscopy for in vivo diagnosis of malignant skin tumors. Cancer 2006; 107:193-200.

116. Longo C, Fantini F, Cesinaro AM, Bassoli S, Seidenari S, Pellacani G. Pigmented mammary Paget disease: dermoscopic, in vivo reflectance-mode confocal microscopic, and immunohistochemical study of a case. Arch Dermatol. 2007;143:752-4.

117. Ahlgrimm-Siess V, Horn M, Koller S, Ludwig R, Gerger A, Hofmann-Wellenhof R. Monitoring efficacy of cryotherapy for superficial basal cell carcinomas with in vivo reflectance confocal microscopy: a preliminary study. J Dermatol Sci. 2009;53:60-4.

118. Agero AL, Busam KJ, Benvenuto-Andrade C, Scope A, Gill M, Marghoob AA, et al. Reflectance confocal microscopy of pigmented basal cell carcinoma. J Am Acad Dermatol. 2006; 54:638-43.

119. Florell SR, Zone JJ, Gerwels JW. Basal cell carcinomas are populated by melanocytes and langerhan's cell. Am J Dermatopathol. 2001; 23: 24-28.

120. Schubert B, Rudolph O. Basal cell carcinoma: a natural milieu for melanocytes?. Am J Dermatopathol. 2001; 23: 558-60.

121. Lao LM, Kumakiri M, Kiyohara T, Kuwahara H, Ueda K. Sub-populations of melanocytes in pigmented basal cell carcinoma: a quantative, ultraestructural investigation. J Cutan Pathol. 2001; 28: 34-43.

122. Rajadhyaksha M, Grossman M, Esterowitz D, Webb RH, Anderson RR. In vivo confocal scanning laser microscopy of human skin: melanin provides strong contrast. J Invest Dermatol.1995; 104: 946-52.

123. Longo C, Segura S, Cesinaro AM, Bassoli S, Seidenari S, Pellacani G. An atypical Meyerson's naevus: a dermoscopic, confocal microscopic and immunohistochemical description of one case. J Eur Acad Dermatol Venereol. 2007;21:414-6.

124. Langley RG, Burton E, Walsh N, Propperova I, Murray SJ. In vivo confocal scanning laser microscopy of benign lentigines: comparison to conventional histology and in vivo characteristics of lentigo maligna. J Am Acad Dermatol. 2006; 55: 88-97.

125. Ahlgrimm-Siess V, Massone C, Scope A, Fink-Puches R, Richtig E, Wolf IH, et al. Reflectance confocal microscopy of facial lentigo maligna and lentigo maligna melanoma: a preliminary study. Br J Dermatol. 2009; 161: 1307–16.

126. Guitera P, Pellacani G, Crotty KA, Scolyer RA, Li LXL, Bassoli S, et al. The Impact of In Vivo Reflectance Confocal. Microscopy on the diagnostic accuracy of lentigo maligna and equivocal pigmented and non pigmented macules of the face. J Invest Dermatol. 2010;130:2080-91.

127. Pellacani G, Guitera P, Longo C, Avramidis M, Seidenari S, Menzies S. The impact of in vivo reflectance confocal microscopy for the diagnostic accuracy of melanoma and equivocal melanocytic lesions. J Invest Dermatol 2007;127: 2759-65.

128. Guitera, Pellacani G, Longo C, Seidenari S, Avramidis M, Menzies SW: In vivo reflectance confocal microscopy enhances secondary evaluation of melanocytic lesions. J Invest Dermatol. 2009;129:131-8.

129. Carrera C, Palou J, Malvehy J, Segura S, Aguilera P, Salerni G, et al. Early stages of melanoma on the limbs of high-risk patients: clinical, dermoscopic, reflectance confocal microscopy and histopathological characterization for improved recognition. Acta Derm Venereol. 2011;91:137-46.

130. LeBoit PE, Burg G, Weedon D, Sarasin A, eds. World Health Organization classification of tumours. Pathology and genetics. Skin tumours. Lyon, France: IARCPress; 2006.

131. Clark WH Jr, From L, Bernardino EA, Mihm MC. The histogenesis and biologic behaviour of primary human malignant melanomas of the skin. Cancer Res. 1969; 29: 705-27.

132. Curtin JA, Fridlyand J, Kageshita T, Patel HN, Busam KJ, Kutzner H, et al. Distinct sets of genetic alterations in melanoma. N Engl J Med. 2005;353: 2135-47.

133. Wong CE, Paratore C, Dours-Zimmermann MT, Rochat A, Pietri T, Suter U, et al. Neural crest derived cells with stem cell features can be traced back to multiple lineages in the adult skin. J Cell Biol. 2006;175:1005-15.

134.Yu H, Fang D, Kumar SM, Li L, Nguyen TK, Acs G, et al. Isolation of a novel population of multipotent adult stem cells from human hair follicles. Am J Pathol. 2006;168:1879-88.

135. Buac K, Pavan WJ. Stem cells of the melanocyte lineage. Cancer Biomark. 2007;3:203-9.

136. Zalaudek I, Marghoob AA, Scope A, Leinweber B, Ferrara G, Hofmann-Wellenhof R, et al. Three roots of melanoma. Arch Dermatol. 2008;144:1375-9.

137. Richard MA, Grob JJ, Avril MF, Delaunay M, Gouvernet J, Wolkenstein P, et al. Delays in diagnosis and melanoma prognosis,II: the role of doctors. Int J Cancer. 2000;89:280-85.

138. Brochez L, Verhaeghe E, Bleyen L, Naeyaert JM. Diagnostic ability of general practitioners and dermatologists in discriminating pigmented skin lesions. J Am Acad Dermatol. 2001;44:979-86.

139. Chamberlain AJ, Fritschi L, Kelly JW. Nodular melanoma: patients' perceptions of presenting features and implications for earlier detection. J Am Acad Dermatol.2003;48:694-701.

140. Menzies SW. Nodular melanoma. In: Marghoob A, Braun PR, Kopf AW, eds. Atlas of Dermoscopy. London, England: Taylor & Francis; 2005.

141. Malvehy J, Puig S, Braun RP, Marghoob AA, Kopf AW, eds. Handbook of Dermoscopy. London, UK: Taylor & Francis; 2006.

142. Kalkhoran S, Milne O, Zalaudek I, Puig S, Malvehy J, Kelly JW, Marghoob AA. Historical, Clinical, and Dermoscopic Characteristics of Thin Nodular Melanoma. Arch Dermatol. 2010;146:311-18.

143. Dirschka T, Bierhoff E, Pflugfelder A, Garbe C. Topical 3.0% diclofenac in 2.5% hyaluronic acid gel induces regression of cancerous transformation in actinic keratoses. J Eur Acad Dermatol Venereol. 2010;24:258-63.

144. Stender IM, Bech-Thomsen N, Poulsen T, Wulf HC. Photodynamic therapy with topical delta-aminolevulinic acid delays UV photocarcinogenesis in hairless mice. Photochem Photobiol 1997;66:493–6.

145. Sharfaei S, Juzenas P, Moan J, Bissonnette R. Weekly topical application of methyl aminolevulinate followed by light exposure delays the appearance of UV-induced skin tumours in mice. Arch Dermatol Res 2002; 294:237–42.

146. Caty V, Liu Y, Viau G, Bissonnette R. Multiple large surface photodynamic therapy sessions with topical methyl aminolaevulinate in PTCH heterozygous mice. Br J Dermatol 2006; 154:740–2.

147. Korbelik M, Dougherty GJ. Photodynamic therapy-mediated immune response against subcutaneous mouse tumours. Cancer Res 1999; 59:1941–6.

7. ANEXOS

Anexo I: Longo C, Segura S, Cesinaro AM, Bassoli S, Seidenari S, Pellacani G. An atypical Meyerson's naevus: a dermoscopic, confocal microscopic and immunohistochemical description of one case. J Eur Acad Dermatol Venereol. 2007;21:414-6.

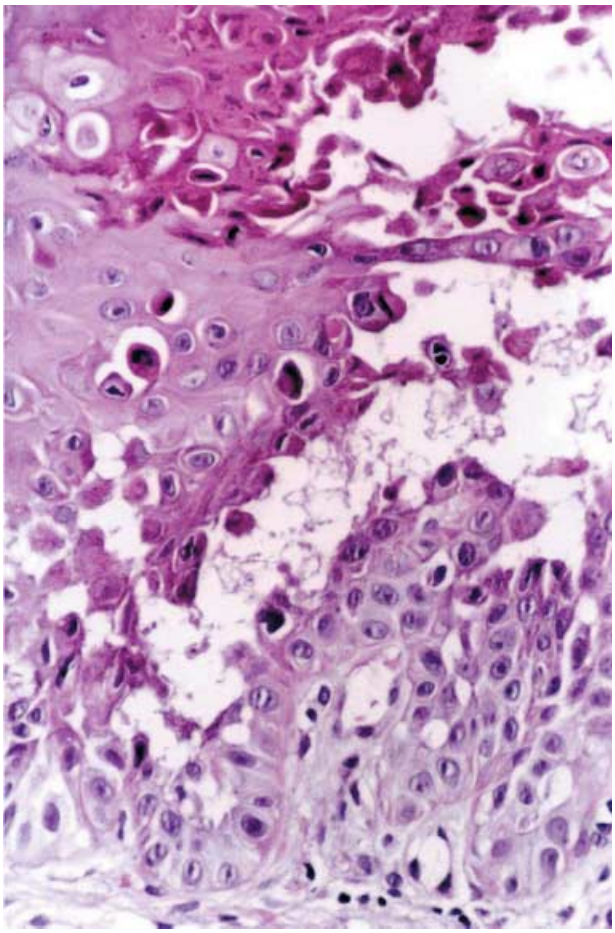

fig. 2 Light microscopy with suprabasilar cleft, acantholysis and dyskeratosis.

keratotic papules were extremely pruritic and more numerous. A new light microscopy confirmed the diagnosis of PAD, in which a suprabasilar cleft with acantholytic and dyskeratotic cells was found (fig. 2). She was treated with oral isotretinoin, 20 mg/day for 8 weeks with remission of her condition (fig. 1b).

In 1972 Ackerman introduced the term focal acantholytic dyskeratosis[5] to describe a peculiar histological pattern, characterized by suprabasal cleft, hyperkeratosis, parakeratosis, acantholytic and dyskeratotic cells, including *corps ronds*. This pattern is classical of DD, but is also found in other genetic diseases such as benign familial pemphigus, and in acquired dermatosis such as Groover (also named transient acantholytic dermatosis),[2] warty dyskeratoma and PAD. The latter was first described in the genital region.

There is little information regarding PAD therapy. Successful treatment with cryotherapy[4] and topical steroids[1] has been reported. Some other diseases of this group can be treated with oral retinoids or steroids.[6–8] A systemic therapy was preferable in the relapse of this patient, as over 300 lesions were seen on the lower legs, and a complete remission could be achieved. Oral isotretinoin should be considered a therapeutic option in cases of extensive PAD.

H Larangeira de Almeida Jr,* RP Duquia
*Departments of Dermatology, Federal and Catholic University of Pelotas, Federal University of Rio Grande do Sul, Brazil, *Corresponding author, Faculdade de Medicina – Dermatologia, Av. Duque de Caxias 250, 96.030-002 Pelotas, RS, Brazil, tel. +55 53 99836010; fax +55 53 32787582; E-mail: hiramalmeidajr@hotmail.com*

References

1 Bell HK, Farrar CW, Curley RK. Papular acantholytic dyskeratosis of the vulva. *Clin Exp Dermatol* 2001; **26**: 386–388.
2 Saenz AM, Cirocco A, Avendano M, Gonzalez F, Sardi JR. Papular acantholytic dyskeratosis of the vulva. *Pediatr Dermatol* 2005; **22**: 237–239.
3 Pestereli HE, Karaveli S, Oztekin S, Zorlu G. Benign persistent papular acantholytic and dyskeratotic eruption of the vulva: a case report. *Int J Gynecol Pathol* 2000; **19**: 374–376.
4 de Almeida Junior HL, Wolter M, Castro LA, Rocha NE. [Papular acantholytic dyskeratosis]. *Hautarzt* 2001; **52**: 1101–1103.
5 Ackerman AB. Focal acantholytic dyskeratosis. *Arch Dermatol* 1972; **106**: 702–706.
6 Eros N, Kovacs A, Karolyi Z. Successful treatment of transient acantholytic dermatosis with systemic steroids. *J Dermatol* 1998; **25**: 469–475.
7 Sehgal VN, Srivastava G. Darier's (Darier-White) disease/keratosis follicularis. *Int J Dermatol* 2005; **44**: 184–192.
8 Happle R, van de Kerkhof PC, Traupe H. Retinoids in disorders of keratinization: their use in adults. *Dermatologica* 1987; **175**: 107–124.

DOI: 10.1111/j.1468-3083.2006.01896.x

An atypical Meyerson's naevus: a dermoscopic, confocal microscopic and immunohistochemical description of one case

Editor

An eczematous halo around a melanocytic naevus is an uncommon clinical and histological variation of the melanocytic naevus first described by Meyerson[1] and later reported by other authors,[2] which clears spontaneously or resolves under topical steroids.

© 2006 The Authors

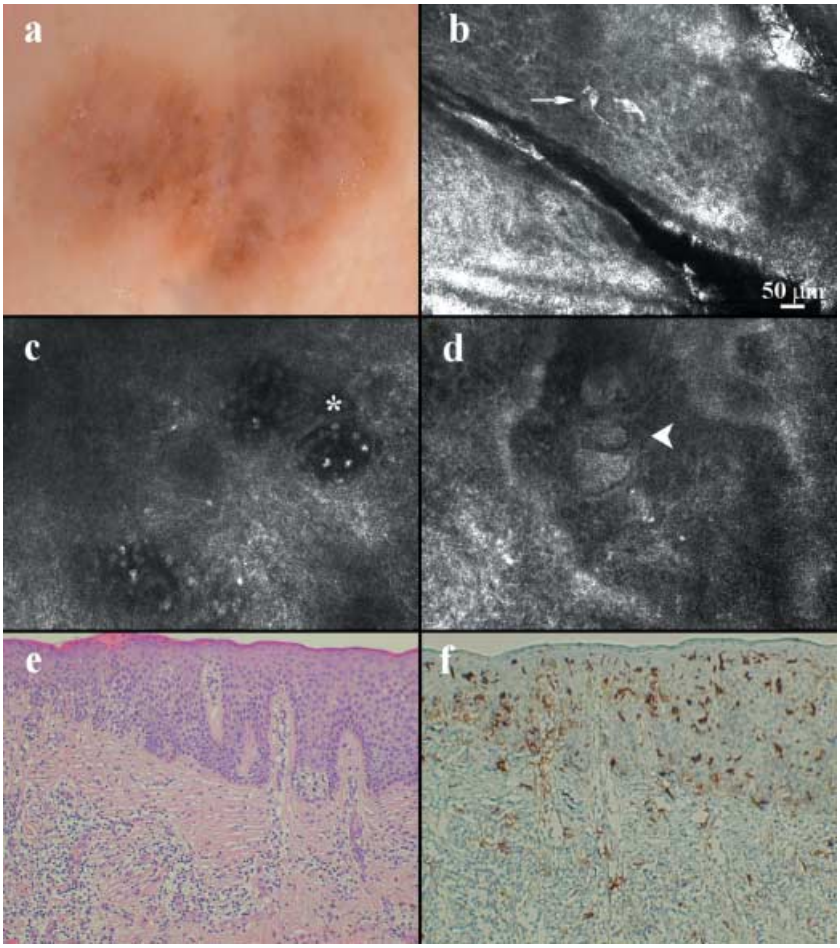

fig. 1 (a) Diffuse light brown region with multifocal scar-like hypopigmented areas and sparse pigmented dots (dermoscopic image, ×30 magnification). (b) Isolated large dendritic cells at the stratum corneum/granulosum (RCM image). (c) Dark spaces containing bright particles within the stratum granulosum/spinosum corresponding to intraepidermal vesicle formation containing inflammatory cells (asterisk) (RCM image). (d) Dense clusters in the upper dermis corresponding to melanocytic nests (arrowhead) (RCM image). (e) Psoriasiform hyperplasia, diffuse spongiosis and inflammatory infiltrate. Small typical nests at the dermal–epidermal junction and upper dermis (haematoxylin–eosin stain, ×100). (f) Positive stain for dendritic cells in the epidermis corresponding to Langerhans' cells (CD1a, ×100).

We report the case of an atypical Meyerson's naevus in which, despite mild itching, both a clear eczematous reaction and dermoscopic patterns referable to a melanocytic lesion were lacking.

In February 2005, during a routine skin examination, a 35-year-old woman presented with a slightly pigmented lesion on the lower back, and reported experiencing mild itching over the past few weeks. On clinical examination, a homogeneous, light brown palpable lesion, 10 × 8 mm in size, was observed. Neither eczema nor other dermatological diseases were present or had occurred in the past.

According to our standardized evaluation protocol, a clinical picture of the naevus and a series of dermoscopic and confocal images were recorded. Digital dermoscopy imaging was performed with a digital video-dermoscope (FotoFinder, TechScreen software GmbH, Bad Birnbach, Germany) using 20-, 30- and 50-fold magnification.[3] The lesion was characterized by an aspecific pattern consisting of a diffuse, light brown, structureless pigmentation predominantly located at the periphery and multifocal hypopigmented and scar-like areas with a few sparse brown dots (fig. 1a). According to the two-step procedure for dermoscopic evaluation,[4] the absence of a distinct pattern directed us towards the diagnosis of an equivocal lesion and excision was planned.

Subsequently, *in vivo* reflectance-mode confocal microscopy (RCM) was performed to obtain further diagnostic information by means of a commercially available device (Vivascope 1000, Lucid Inc., Henrietta, NY, USA).[5] In the superficial epidermal layers, some signs of inflammatory infiltration were observable, including the presence of intercellular brightness corresponding to spongiosis, widespread bright particles referable to exocytosis, and isolated large cells with long dendritic-like branches corresponding to Langerhans' cells (fig. 1b).[6–8] Within the stratum granulosum/spinosum we also observed dark spaces, containing bright round or oval particles, interspersed between keratinocytes, that seemed to be intraepidermal vesicle formations containing inflammatory cells and dyskeratotic keratinocytes[6–8] (fig. 1c). At the dermal–epidermal junction and within the papillary dermis, the presence of compact clusters with the aspect of small dense nests suggested the melanocytic nature of the lesion[9] (fig. 1d).

© 2006 The Authors

JEADV 2007, **21**, 392–435 Journal compilation © 2006 European Academy of Dermatology and Venereology

The histological examination revealed parakeratosis, irregular psoriasiform hyperplasia of the epidermis associated with diffuse spongiosis and exocytosis. The upper dermis was characterized by a dense inflammatory infiltrate composed of lymphocytes and eosinophils, and by marked signs of fibrosis. At the dermal–epidermal junction and upper dermis, small typical melanocytic nests were noted, revealing the presence of a compound melanocytic naevus (fig. 1e). To investigate the nature of the dendritic cells observed within the superficial layers by RCM, immunohistochemical investigation was performed, revealing CD1a stained dendritic cells in the epidermis, corresponding to Langerhans' cells (fig. 1f). Melan-A enhanced the melanocytic nests, whereas S-100 protein stained both Langerhans' cells and melanocytes.

This case confirmed the potential of RCM for the evaluation of inflammatory and neoplastic skin diseases at a quasi-histological resolution,[10] enabling in the present Meyerson's naevus the *in vivo* visualization of aspects referable both to the melanocytic nature of the lesion and to a subclinical eczema, closely correlated with the histopathology.

C Longo,† S Segura,‡ AM Cesinaro,§ S Bassoli,†
S Seidenari,† G Pellacani*†
Departments of †Dermatology and §Pathology, University of Modena and Reggio Emilia, via del Pozzo 71, 41100 Modena, Italy and ‡Department of Dermatology, Hospital Clinic, 170 Villareal, 08036 Barcelona, Spain,
**Corresponding author, tel. +39 59 422246; fax +39 59 4224271; E-mail: pellacani.giovanni@unimo.it*

References

1 Meyerson LB. A peculiar papulosquamous eruption involving pigmented nevi. *Arch Dermatol* 1971; **103**: 510–512.
2 Weedon D, Farnsworth J. Spongiotic changes in melanocytic nevi. *Am J Dermatopathol* 1984; **6**: 257–259.
3 Grana C, Pellacani G, Seidenari S. Practical color calibration for dermoscopy, applied to a digital epiluminescence microscope. *Skin Res Technol* 2005; **11**: 242–247.
4 Argenziano G, Soyer HP, Chimenti S *et al.* Dermoscopy of pigmented skin lesions: results of a consensus meeting via the Internet. *J Am Acad Dermatol* 2003; **48**: 679–683.
5 Pellacani G, Cesinaro AM, Seidenari S. Reflectance-mode confocal microscopy of pigmented skin lesions – improvement in melanoma diagnostic specificity. *J Am Acad Dermatol* 2005; **53**: 979–985.
6 Gonzalez S, Gonzalez E, White M *et al.* Allergic contact dermatitis: correlation of in vivo confocal imaging to routine histology. *J Am Acad Dermatol* 1999; **40**: 708–713.
7 Swindells K, Burnett N, Rius-Diaz F *et al.* Reflectance confocal microscopy may differentiate acute allergic and irritant contact dermatitis in vivo. *J Am Acad Dermatol* 2004; **50**: 220–228.
8 Astner S, Gonzalez E, Cheung A *et al.* Pilot study on the sensitivity and specificity of in vivo reflectance confocal microscopy in the diagnosis of allergic contact dermatitis. *J Am Acad Dermatol* 2005; **53**: 986–992.
9 Pellacani G, Cesinaro AM, Seidenari S. In vivo assessment of melanocytic nests in nevi and melanomas by reflectance confocal microscopy. *Mod Pathol* 2005; **18**: 469–474.
10 Gonzalez S, Gilaberte-Calzada Y, Gonzalez-Rodriguez A *et al.* In vivo reflectance-mode confocal scanning laser microscopy in dermatology. *Adv Dermatol* 2004; **20**: 371–387.

DOI: 10.1111/j.1468-3083.2006.01901.x

Acquired progressive lymphangioma

Editor

Acquired progressive lymphangioma (APL) is a rare disorder characterized by benign lymphatic proliferation. Children and young adults are most commonly affected, and in most cases lesions present as erythematous patches/plaques.[1–5] Herein we present a case of APL with unusual clinical features.

A 7-year-old girl presented with a slightly tender, flesh-coloured mass on the left little toe which had been present since birth (fig. 1). There was no trauma history and the lesion had shown gradual growth. Histopathologically, many irregular, dilated vascular spaces were observed in the dermis (fig. 2). The interlacing vascular channels were lined by a single layer of bland, flat endothelial cells with no cellular atypia. Erythrocytes were not seen in these channels. We diagnosed the case as APL and performed complete excision with advancement flap for closure. Two months has passed since the operation and currently there is no sign of local recurrence.

fig. 1 Slightly tender, solitary flesh-coloured nodular mass with gradual growth on the left little toe since birth.

Anexo II: Gil I, Segura S, Martínez-Escala E, Lloreta J, Puig S, Vélez M, Pujol RM, Herrero-González JE. Dermoscopic and reflectance confocal microscopic features of exogenous ochronosis. Arch Dermatol. 2010;146:1021-5.

OBSERVATION

Dermoscopic and Reflectance Confocal Microscopic Features of Exogenous Ochronosis

Inmaculada Gil, MD; Sonia Segura, MD; Estela Martínez-Escala, MD; Josep Lloreta, MD; Susana Puig, MD; Mariano Vélez, MD; Ramón M. Pujol, MD; Josep E. Herrero-González, MD

Background: Exogenous ochronosis presents as an acquired asymptomatic hyperpigmentation on photoexposed areas, predominantly over bony prominences, and is caused by the topical application of several skin-lightening agents.

Observations: We describe a 63-year-old Hispanic woman who developed exogenous ochronosis lesions on her face after using topical bleaching creams containing hydroquinone, 2% to 3%, and oxybenzone, 2%, for several years. Dermoscopy revealed irregular brown-gray globular, annular, and arciform structures that corresponded to focal deposition of ochronotic pigment on the dermis. These deposits correlated with multiple banana-shaped nonrefractile structures seen using reflectance confocal microscopy. Histopathologic sections revealed the deposition of a banana-shaped, yellow to brown material in the papillary and middle dermis. Ultrastructural examination revealed an amorphous electron-dense material mostly located in the core of elastic fibers and also in smaller amounts in the interstitium with prominent degenerative changes in the elastic fibers. A good correlation was observed between the results of both noninvasive techniques and the diagnostic histologic features of this condition.

Conclusions: We characterized by means of dermoscopy, reflectance confocal microscopy, and electronic microscopy a case of exogenous ochronosis. To our knowledge, this is the first description of reflectance confocal microscopic findings in this condition. Dermoscopy and reflectance confocal microscopy are proved to be useful noninvasive techniques for the diagnosis of this pigmentary disorder.

Arch Dermatol. 2010;146(9):1021-1025

Author Affiliations: Departments of Dermatology (Drs Gil, Segura, Martínez-Escala, Vélez, Pujol, and Herrero-González) and Pathology (Dr Lloreta), Hospital del Mar-Universitat Autònoma de Barcelona; and Department of Dermatology, Hospital Clínic, IDIBAPS (Institut d'Investigacións Biomèdiques August Pi i Sunyer), CIBER (Centros de Investigación Biomedica en Red) Enfermedades Raras (Dr Puig), Barcelona, Spain.

EXOGENOUS OCHRONOSIS IS AN uncommon disorder characterized by the deposition of microscopic, ochre-colored pigment in the dermis, giving rise to a blue-black hue in the skin. It is usually manifested by asymptomatic blue-black macules on photoexposed areas, predominantly on bony prominences (malar areas, temples, lower cheeks, and neck), and it is often associated with the prolonged application of various topical chemical substances, such as hydroquinone, phenol, resorcinol, mercurials, and picric acid, as well as with quinine injections and oral antimalarial agents. Hyperpigmentation occurs strictly on the topically treated areas.

Exogenous ochronosis can be clinically mistaken for other disorders manifested by acquired localized hyperpigmented facial macules and, specifically, for melasma. In some patients, histopathologic study is required to reach a definite diagnosis. Dermoscopy and in vivo skin reflectance confocal microscopy (RCM) are noninvasive in vivo diagnostic tools that may permit us to define morphologic patterns of skin disorders and to avoid the practice of unnecessary skin biopsies. We herein describe a patient with hydroquinone-induced exogenous ochronosis with some peculiar dermoscopic features. The morphologic features of deposition of ochronotic pigment using in vivo skin RCM were also defined. A correlation of RCM findings with dermoscopic and histopathologic findings was performed.

REPORT OF A CASE

A 63-year-old Hispanic woman with phototype V skin, a history of hypertension treated with enalapril maleate and hydrochlorothiazide, and primary hypothyroidism presented with a history of long-term localized symmetrical facial hyperpigmented macules on both cheeks, the superciliary arches, and the nasal dorsum (**Figure 1** A). She denied having any joint, genitourinary, or cardiac symptoms.

Downloaded from www.archdermatol.com at Universitat Pompeu Fabra, on September 28, 2010
©2010 American Medical Association. All rights reserved.

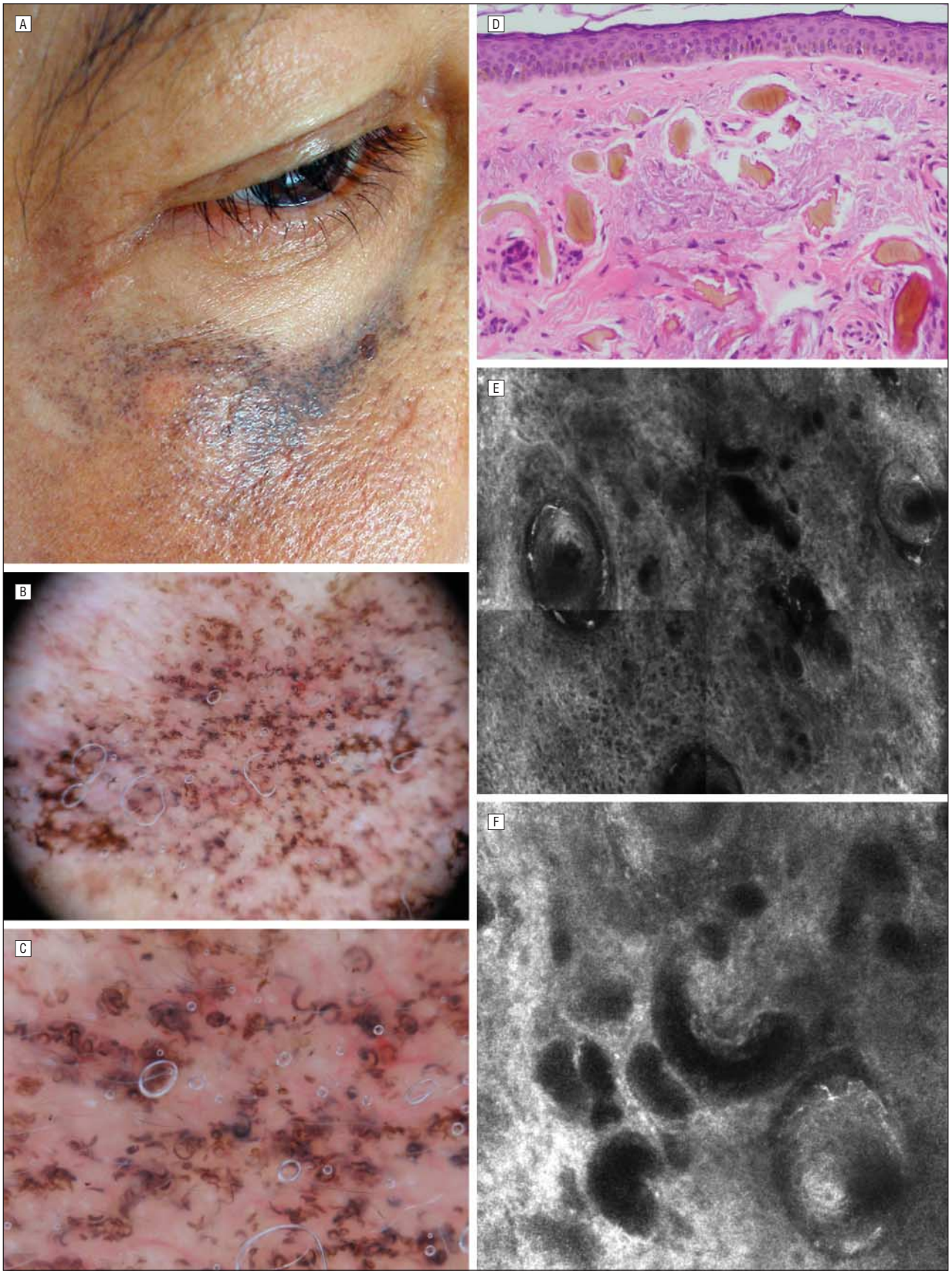

Figure 1. A, Clinical examination. Ill-defined gray macules on the cheeks. B, Dermoscopy. Irregular brown-gray globularlike structures throughout the lesion. C, Arciform to annular structures around the follicular openings. D, Punch biopsy specimen. Exogenous yellow to brown material (banana-shaped bodies) in the papillary and middle dermis (hematoxylin-eosin, original magnification ×400). E, Reflectance confocal microscopy 1 × 1-mm block image at the upper dermis. Multiple dark round to oval spaces located next to the follicles. F, Reflectance confocal microscopy 0.5 x 0.5-mm image at the upper dermis. Banana-shaped amorphous dark structures in the papillary dermis correlate with the histologic findings.

Downloaded from www.archdermatol.com at Universitat Pompeu Fabra, on September 28, 2010
©2010 American Medical Association. All rights reserved.

Her family history was noncontributory. The patient stated that she had been treated for melasma in her country of origin, Colombia, with bleaching creams and lotions containing hydroquinone, 2% to 3%, and oxybenzone, 2%, for several years. She noted worsening of the hyperpigmentation in the involved areas despite good adherence to those topical products. On physical examination, there were bilateral ill-defined speckled gray macules over both malar areas. A light brown regular oval macule 1 cm in diameter clinically consistent with solar lentigo was also noted above her left eyebrow. The remainder of the skin examination findings were unremarkable. Dermoscopic examination of the malar areas revealed irregular brown-gray globular, annular, and arciform structures and granules distributed throughout the lesion (Figure 1B). In some areas, these striking short arciform and annular structures were located around the follicular openings (Figure 1C).

A 4-mm punch biopsy sample was collected from the malar area. Deposition of a banana-shaped yellow to brown material was found in the papillary and middle dermis (Figure 1D). A sparse lymphocytic infiltrate was present, and a focal foreign body reaction surrounding this material was also detected. No remarkable epidermal changes were found. An additional biopsy performed on the left eyebrow macule showed characteristic histopathologic features of solar lentigo along with focal deposition of the same banana-shaped material in the dermis.

Ultrastructural examination of the skin dermal tissue revealed an amorphous electron-dense material mostly located in the core of elastic fibers and also in smaller amounts in the interstitium. In addition, elastic fibers showed several degenerative changes, including elastolysis (clearing), elastorrhexis (fragmentation into minute fiber fragments), and motheaten defects in the external outline (**Figure 2**). An RCM examination of the malar area (VivaScope 1500; Lucid Inc, Rochester, New York) was also performed. These instruments use a diode laser at 830 nm with a power of less than 16 mW at tissue level and ×30 water-immersion lenses, allowing a horizontal optical resolution of 2 µm and a vertical resolution of 5 µm. Each given image corresponds to a horizontal 500 × 500-µm section of the skin at a selected depth from the epidermal surface to the upper dermis at a maximum depth of 250 to 350 µm.[1] Using confocal examination, the epidermis exhibited a normal honeycombed pattern. At the dermoepidermal junction, we noted typical refractile basal cells corresponding to physiologic hyperpigmentation of the basal layer. At the dermal level, we observed widespread hyporefractile oval to banana-shaped spaces that corresponded to the banana-shaped bodies observed on histologic sections. These structures were located next to the inferior portion of hair follicles (Figure 1E and F). Complete blood and urinary biochemical surveys and chest radiographs disclosed no abnormalities. The diagnosis of exogenous ochronosis was established.

The patient underwent intense pulsed light (IPL) treatment (645 nm, 6 milliseconds, 20-22 J/cm^2) (Vasculight; Lumenis Ltd, Yokneam, Israel). Sunscreen and nonhydroquinone depigmentating cream containing kojic acid, 4%, and salicylic acid, 0.2%, were also prescribed. After 2 months of treatment and 6 IPL sessions, the patient exhibited mild clearing of the lesions (malar and supraciliary). Using dermoscopy, we observed a slight blanching of the brown background of the involved areas coexisting with a deep brown stellate network corresponding to transepidermal melanin loss. The brown-gray globules and arciform to annular structures persisted after treatment and were even more evident using dermoscopy. An RCM examination before and after IPL treatment did not show any significant differences, suggesting that the exogenous material persisted after IPL treatment.

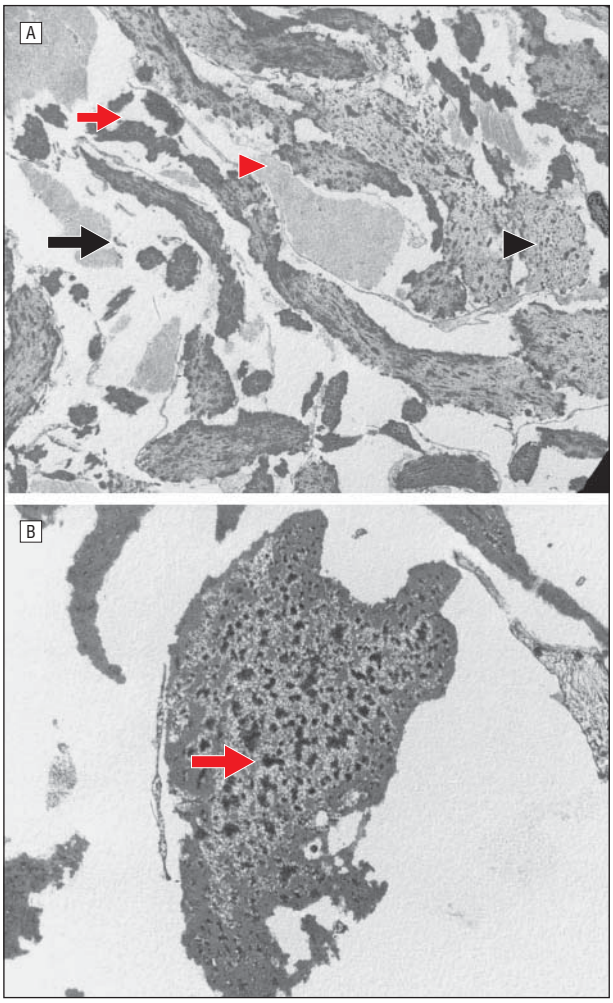

Figure 2. Electron microscopic image of exogenous ochronosis. A, Amorphous electron-dense structures deposited in the interstitium (black arrow). Elastolysis (black arrowhead), elastorrhexis (red arrow), and motheaten defects (red arrowhead) in the external outline of elastic fibers are noted. B, Deposition of the same electron-dense structures in the core of elastic fibers (red arrow).

COMMENT

Exogenous ochronosis presents as acquired asymptomatic hyperpigmented macules on photoexposed areas. Clinically it is manifested by asymptomatic bilateral symmetrical speckled blue-black macules and several gray-brown macules, previously described as "caviarlike" bodies, typically affecting the malar areas, temples, lower cheeks, and

Downloaded from www.archdermatol.com at Universitat Pompeu Fabra, on September 28, 2010
©2010 American Medical Association. All rights reserved.

neck. Some researchers have defined 3 different stages in exogenous ochronosis: initial erythema and mild pigmentary changes; followed by hyperpigmentation, black colloid milia, and atrophy; and, finally, papulonodules.[2] Exogenous ochronosis most commonly results from the use of topical hydroquinones (usually used as bleaching creams) but has also been associated with the use of phenol, quinine injection, resorcinol, and oral antimalarials. Initially, only the continual use of a high concentration of hydroquinone (6%-8%) for at least 6 months was thought to result in exogenous ochronosis,[3] but at least 1 study[4] has shown development of the disorder with the topical application of hydroquinone, 2%, for as little as 3 months. Clinically, the differential diagnosis of exogenous ochronosis should be established with a heterogeneous group of disorders causing facial hyperpigmented macules, such as melasma, bilateral nevus of Ota, drug-induced hyperpigmentation (amiodarone, minocycline, and methotrexate), postinflammatory hyperpigmentation, and dermatosis papulosa nigra. Melasma is, after postinflammatory hyperpigmentation, the most common cause of acquired facial hyperpigmentation. It is characterized by brown, gray, or even blue macules that coalesce in patches with irregular outlines. Darkly pigmented races are prone to this disorder, which is exacerbated by UV exposure. Considering that some patients with hydroquinone-induced exogenous ochronosis may have melasma, a combination of clinical, histopathologic, and dermoscopic features of both entities is often present.

Histologic examination of exogenous ochronosis reveals short, curvilinear, yellow to brown banana-shaped fibers of varying thickness in the upper dermis. Homogenization, swelling, and degeneration of collagen bundles can be noted, as can a moderate inflammatory infiltrate that may be rich in histiocytes and plasma cells. Sarcoid-like granulomas and multinucleated giant cells with phagocytized ochronotic fibers have also been described. Transfollicular elimination of the abnormal fibers can also be found.[5] Pigment incontinence and solar elastosis are often present. Ultrastructural findings have been reported in exogenous ochronosis and are described as homogenous electron-dense irregular structures nested in an amorphous granular material that permeates the collagen bundles.[6] Dermoscopic features of exogenous ochronosis have received little attention in the literature. The color of the ochronotic pigment observed clinically and using dermoscopy is blue-gray because of the depth at which the pigment is located. Some researchers initially pointed out the observation of blue-gray, granular, and annular structures around the follicles. Charlín et al[7] reported the dermoscopic features of 2 patients with hydroquinone-induced exogenous ochronosis with associated melasma. They observed blue-gray amorphous areas obliterating (but not surrounding) some follicular openings and characteristic dermoscopic features of melasma (accentuation of the normal pseudo-rete of the facial skin).[7] Berman et al[8] studied 5 patients with exogenous ochronosis secondary to the long-term application of hydroquinone cream and 3 patients with melasma with no history of hydroquinone use. In patients with exogenous ochronosis, dark brown globules and globularlike structures on a diffuse brown background were observed. In contrast, in patients with melasma, a fine brown reticular pattern on a background of a faint light brown, structureless area was noted. The authors stressed the usefulness of dermoscopy in differentiating these 2 entities.[8]

In the present patient, in addition to the previously reported brown-gray globules, short, thin arciform and annular structures were often distributed around the follicular openings. To our knowledge, these peculiar dermoscopic features have not been previously reported in exogenous ochronosis.

Dermoscopic differential diagnosis in the present patient includes several lesions with perifollicular hyperpigmentation, such as melasma and Ota nevus. However, these lesions show a homogenous pigmentation that spares follicular openings, and brown-gray globules and arciform to annular structures are not observed. The presence of brown-gray granules also raises the differential diagnosis of a benign lichenoid keratosis. In such lesions, granules are more blue-gray than brown-gray and correspond to aggregates of melanophages in the dermis. Moreover, these structures are regular and smaller than those seen in exogenous ochronosis. In addition, lichenoid keratoses are clinically localized and do not present as symmetrical bilateral patches. Other tumors that show blue-gray dots and globules are basal cell carcinoma and lentigo maligna, but they usually exhibit other additional dermoscopic features that allow us to establish the diagnosis. The striking dermoscopic features observed in the present patient are not previously described, to our knowledge; are characteristic of exogenous ochronosis; and may be considered a hallmark for the diagnosis of this entity. The RCM features of exogenous ochronosis have not been previously described, to our knowledge. The presence of dark, well-defined, round-to-oval and banana-shaped structures raised the suspicion of an exogenous material deposition because they do not correspond to any previously described structure of the normal skin or cutaneous disease. Pigmented lesions with lichenoid changes that exhibit blue-gray granules on dermoscopy may be distinguished using RCM by the presence of bright, plump cells throughout the upper dermis corresponding to melanophages in the absence of the newly described dermal banana-shaped dark spaces.[9,10] Confocal features of other lesions, such as melasma or Ota nevus, have not been previously reported. Nevertheless, it is difficult to conclude that these findings are specific to exogenous ochronosis. Other conditions in which foreign materials are deposited in the skin, such as argyria and chrysiasis, may have similar dermoscopic and confocal features and, thus, need to be further characterized.

Treatment of exogenous ochronosis is still challenging for the physician. There is agreement regarding the convenience of stopping the use of the causative agent. Cryotherapy and trichloroacetic acid have been proved to be ineffective, whereas retinoic acid can be beneficial in some patients. Topical corticosteroids and sunscreens have variable efficacy.[11] There have been reports of successful treatments with dermabrasion combined or not with carbon dioxide laser.[12] Bellew and Alster[13] described 2 patients with exogenous ochronosis successfully treated with Q-switched alexandrite laser. To

Downloaded from www.archdermatol.com at Universitat Pompeu Fabra, on September 28, 2010
©2010 American Medical Association. All rights reserved.

our knowledge, IPL, commonly used in the treatment of vascular stains, photoaging, pigmented lesions, and photoepilation, has not been previously reported as a treatment for exogenous ochronosis. In the present patient, only a mild improvement and scarce lightening were achieved, especially on the background of the lesion, after 6 courses of treatment. Clear-cut involution of granular and arciform structures was not achieved. Further studies are needed to define the exact therapeutic role of IPL in the treatment of exogenous ochronosis. In conclusion, we stress the usefulness of noninvasive techniques in the diagnosis of pigmented lesions on the face. The striking dermoscopic findings should arouse the clinical suspicion of exogenous ochronosis and enable the physician to avoid unnecessary skin biopsies. In this particular setting, RCM might be of interest for confirming the existence of an exogenous material. Future RCM characterization in larger series of patients with deposit skin diseases, including exogenous ochronosis, is needed.

Accepted for Publication: March 12, 2010.
Correspondence: Inmaculada Gil, MD, Department of Dermatology, Hospital del Mar-Universitat Autònoma de Barcelona, Passeig Marítim 25-29, Postal Code 08003, Barcelona, Spain (igil@imas.imim.es).
Author Contributions: Drs Gil, Segura, Puig, Pujol, and Herrero-González had full access to all the data in the study and take responsibility for the integrity of the data and the accuracy of the data analysis. *Study concept and design*: Gil, Segura, Pujol, and Herrero-González. *Acquisition of data*: Gil, Segura, Martínez-Escala, Lloreta, Puig, Vélez, and Herrero-González. *Analysis and interpretation of data*: Gil, Segura, Lloreta, Puig, Vélez, Pujol, and Herrero-González. *Drafting of the manuscript*: Gil, Segura, Martínez-Escala, Lloreta, and Herrero-González. *Critical revision of the manuscript for important intellectual content*: Gil, Segura, Puig, Vélez, Pujol, and Herrero-González. *Administrative, technical, or material support*: Gil, Segura, Martínez-Escala, Lloreta, Puig, Vélez, and Herrero-González. *Study supervision*: Gil, Segura, Lloreta, Puig, Vélez, Pujol, and Herrero-González.
Financial Disclosure: None reported.

REFERENCES

1. Rajadhyaksha M, González S, Zavislan JM, Anderson RR, Webb RH. In vivo confocal scanning laser microscopy of human skin II: advances in instrumentation and comparison with histology. *J Invest Dermatol*. 1999;113(3):293-303.
2. Dogliotti M, Leibowitz M. Granulomatous ochronosis: a cosmetic-induced skin disorder in Blacks. *S Afr Med J*. 1979;56(19):757-760.
3. Touart DM, Sau P. Cutaneous deposition diseases, part II. *J Am Acad Dermatol*. 1998;39(4, pt 1):527-546.
4. Hoshaw RA, Zimmerman KG, Menter A. Ochronosislike pigmentation from hydroquinone bleaching creams in American blacks. *Arch Dermatol*. 1985;121(1):105-108.
5. Jordaan HF, Van Niekerk DJT. Transepidermal elimination in exogenous ochronosis: a report of two cases. *Am J Dermatopathol*. 1991;13(4):418-424.
6. Kramer KE, López A, Stefanato CM, Phillips TJ. Exogenous ochronosis. *J Am Acad Dermatol*. 2000;42(5, pt 2):869-871.
7. Charlín R, Barcaui CB, Kac BK, Soares DB, Rabello-Fonseca R, Azulay-Abulafia L. Hydroquinone-induced exogenous ochronosis: a report of four cases and usefulness of dermoscopy. *Int J Dermatol*. 2008;47(1):19-23.
8. Berman B, Riccoti C, Viera M, Amini S Differentiation of exogenous ochronosis from melasma by dermoscopy. Poster presented at: American Academy of Dermatology 67th Annual Meeting; March 6-10, 2009; San Francisco, CA.
9. Segura S, Puig S, Carrera C, Palou J, Malvehy J. Dendritic cells in pigmented basal cell carcinoma: a relevant finding by reflectance-mode confocal microscopy. *Arch Dermatol*. 2007;143(7):883-886.
10. Segura S, Puig S, Carrera C, Palou J, Malvehy J. Development of a two-step method for the diagnosis of melanoma by reflectance confocal microscopy. *J Am Acad Dermatol*. 2009;61(2):216-229.
11. Levin CY, Maibach H. Exogenous ochronosis: an update on clinical features, causative agents and treatment options. *Am J Clin Dermatol*. 2001;2(4):213-217.
12. Diven DG, Smith EB, Pupo RA, Lee M. Hydroquinone-induced localized exogenous ochronosis treated with dermabrasion and CO_2 laser. *J Dermatol Surg Oncol*. 1990;16(11):1018-1022.
13. Bellew SG, Alster TS. Treatment of exogenous ochronosis with a Q-switched alexandrite (755 nm) laser. *Dermatol Surg*. 2004;30(4, pt 1):555-558.

Archives Web Quiz Winner

Congratulations to the winner of our June quiz, Dipankar De, MD, Department of Dermatology, Post Graduate Institute of Medical Education and Research, Chandigarh, India. The correct answer to our June challenge was *coccidioidomycosis*. For a complete discussion of this case, see the Off-Center Fold section in the July *Archives* (Gallo ES, Pehoushek JF, Crowson AN. An exophytic nasal nodule. *Arch Dermatol*. 2010; 146[7]:789-794).

Be sure to visit the *Archives of Dermatology* Web site (http://www.archdermatol.com) to try your hand at the interactive quiz. We invite visitors to make a diagnosis based on selected information from a case report or other feature scheduled to be published in the following month's print edition of the *Archives*. The first visitor to e-mail our Web editors with the correct answer will be recognized in the print journal and on our Web site and will also receive a free copy of *The Art of JAMA II*.

Downloaded from www.archdermatol.com at Universitat Pompeu Fabra, on September 28, 2010
©2010 American Medical Association. All rights reserved.

Anexo III: Pellacani G, Longo C, Malvehy J, Puig S, Carrera C, Segura S, et al. In vivo confocal microscopic and histopathologic correlations of dermoscopic features in 202 melanocytic lesions. Arch Dermatol. 2008;144:1597-608.

STUDY

In Vivo Confocal Microscopic and Histopathologic Correlations of Dermoscopic Features in 202 Melanocytic Lesions

Giovanni Pellacani, MD; Caterina Longo, MD; Josep Malvehy, MD; Susana Puig, MD; Cristina Carrera, MD; Sonia Segura, MD; Sara Bassoli, MD; Stefania Seidenari, MD

Objectives: To identify in vivo microscopic substrates of the dermoscopic patterns of melanocytic lesions and to correlate them with histopathologic features.

Design: Before excision, lesion areas that showed characteristic dermoscopic patterns were imaged by dermoscopy and confocal microscopy and directly correlated with histopathologic features.

Setting: Departments of Dermatology of the University of Modena and Reggio Emilia and Hospital Clínico of Barcelona, between July 2006 and March 2007.

Patients: Patients with 202 melanocytic lesions, corresponding to 76 melanomas, 114 nevi, and 12 Spitz or Reed nevi.

Main Outcome Measures: Correlation of dermoscopic patterns in melanocytic lesions with confocal microscopic findings and conventional histopathologic findings.

Results: Characteristic architectural and cytologic substrates were identified in vivo with the use of confocal microscopy and correlated with histopathologic features. Pigment network atypia was evidenced through confocal microscopy as a disarrangement of dermoepidermal junction architecture and cellular atypia. Pigmented globules consisted of cell clusters, corresponding to melanocytic nests identified on histopathologic analysis. Black dots correlated with intraepidermal reflective spots or with large pagetoid cells in nevi and melanoma, respectively. Blue structures usually consisted of numerous pleomorphic cells, corresponding to malignant melanocytes and inflammatory cells in melanomas, whereas plump bright cells, corresponding to melanophages on histopathologic analysis, characterized benign lesions. Within regression, a retiform distribution of collagen fibers, which sometimes intermingled with melanophages and rarely with nucleated cells, was observable.

Conclusions: The knowledge of the cytologic and architectural aspects of the different dermoscopic patterns, as they appear by in vivo confocal microscopy, may guide the user to the identification of specific substrates in melanocytic lesions and consequently the interpretation of the dermoscopic features.

Arch Dermatol. 2008;144(12):1597-1608

DERMOSCOPY IS A WIDELY diffused technique based on the visualization and magnification of subsurface structures, which is useful for diagnostic purposes. The identification of specific structures leads the observer to the diagnostic definition of melanocytic and nonmelanocytic skin lesions.[1-4] Although some dermoscopic features correspond to histologic findings, a direct and exact correlation is difficult to determine. A step-sectioning procedure[5,6] and micropunch technique[7] were used to correlate accurately dermoscopic features with their histopathologic counterparts. Moreover, horizontal histologic sections can be performed; however, this procedure is limited to selected features because of the risk of interference with the Breslow thickness evaluation.[8]

For editorial comment see page 1644

In vivo reflectance confocal microscopy (RCM) produces horizontal images of the skin at a cellular level resolution from the surface to the papillary dermis. It has been used for the study of normal skin and different diseases,[9,10] resulting in the differential diagnosis of malignant melanoma (MM).[11-13] Because the single image on the monitor during patient examination corresponds to a small area of approximately 0.5 mm per side at a precise depth, the interpretation of the confocal features depends strongly on the knowledge of the structure under examination. Correlations among some dermoscopic features, such as pigment network, globules, streaks, and blue structures, as determined by confocal microscopy and histologic analysis have recently been shown.[14-20]

Author Affiliations: Department of Dermatology, University of Modena and Reggio Emilia, Modena, Italy (Drs Pellacani, Longo, Bassoli, and Seidenari); and Department of Dermatology, Melanoma Unit, Hospital Clínico, Barcelona, Spain (Drs Malvehy, Puig, Carrera, and Segura).

Downloaded from www.archdermatol.com at Universidad de Cadiz, on November 16, 2009
©2008 American Medical Association. All rights reserved.

Confocal microscopy seems to be the natural link between dermoscopy and histopathologic analysis because of its high resolution, horizontal imaging, and noninvasiveness. Therefore, we aimed to identify RCM aspects that correspond to dermoscopic features of melanocytic lesions and to correlate them with histopathologic features, systematically exploring all the observable features of melanocytic lesions in a large series of cases.

METHODS

The study has been approved by the institutional review boards of the University of Modena and Reggio Emilia and Hospital Clínico of Barcelona, and the Declaration of Helsinki protocols were followed. Participants gave their written informed consent.

LESION IMAGES

This study included a total of 202 melanocytic lesions from as many patients who were recruited at the Department of Dermatology of the University of Modena and Reggio Emilia and at the Melanoma Unit of the Hospital Clínico of Barcelona, between July 2006 and March 2007 following the same protocol. The lesions corresponded to 76 MMs (22 in situ, 33 thinner than 1 mm, 14 with a thickness between 1 and 2 mm, 7 with a thickness of >2 mm), 114 melanocytic nevi (33 junctional, 70 compound, 8 intradermal, and 3 blue nevi), and 12 Spitz or Reed nevi, consecutively recorded because each dermoscopic feature was observed in at least 15 cases. Lesions were from the lower limbs in 43 cases, upper limbs in 19, chest in 28, abdomen in 24, and back in 88. No lesion from the face, palms and soles, mucosal areas, and genital regions was considered for the peculiarity of dermoscopic patterns. When centering the RCM adapter ring onto the lesion area of interest, a direct correlation among dermoscopic, confocal microscopic, and histopathologic features was obtained in all cases. Digital dermoscopic and RCM images of the ring-delimited area were acquired, and a silk suture or an ink mark at 1 pole of the specimen was positioned in all cases to make its orientation easier. All lesions were then excised, and step sections were cut for diagnostic confirmation and pattern correlation. Common nevi included in this study, which had typical dermoscopic features, were excised only for cosmetic reasons and because of a patient request. Moreover, in cases in which the dermoscopic feature of interest was limited to a small area, a 2-mm punch incisional biopsy in that particular area of the lesion was also performed to obtain a perfect histopathologic correlation.

INSTRUMENTS

Digital dermoscopy imaging was performed by high-resolution digital dermoscopes (FotoFinder; TeachScreen Software GmbH, Bad Birnbach, Germany; and DermLite Foto; 3GEN LLC, Dana Point, CA) for all cases. Moreover, in some cases a low-resolution dermoscopic camera integrated into the Vivascope software was used to allow precise confocal navigation and to look at dermoscopic images (VivaCam; Lucid Inc, Henrietta, New York, NY).

The RCM images were acquired by means of near-infrared reflectance confocal laser scanning microscopes (Vivascope 1000 and Vivascope 1500; Lucid). Instruments and acquisition procedures are described elsewhere.[9,14] A minimum area of 4 × 4 mm was acquired (block image) to visualize the corresponding area by means of dermoscopy. Subsequently, series of high-resolution images (capture and stack images) were obtained at different levels from the surface down to the papillary dermis. Each image corresponds to a horizontal section at a selected depth with a 475 × 350-µm field of view for Vivascope 1000 and a 500 × 500-µm field of view for Vivascope 1500.

Histologic pictures were acquired by means of a light microscope (Axioscope 40; Zeiss, Göttingen, Germany) equipped with a digital camera (AxioCam MRc5; Zeiss) and dedicated software.

IMAGE DESCRIPTION

Dermoscopic image description of each pattern was performed according to the definition of the literature.[1,2,4-6] The RCM images were described using the terms previously proposed and recently summarized in a consensus terminology glossary.[11,13,21,22] Histopathologic description of both architectural patterns and cytologic features was performed on several hematoxylin-eosin–stained 4-µm sections derived from the block corresponding to the dermoscopic and confocal area of interest. Histologic correlations were noted and confirmed by studying several similar cases.

RESULTS

The most relevant confocal aspects and their histologic substrates for each dermoscopic feature are listed in the **Table**.

PIGMENT NETWORK

Fifty-two lesions presented with a typical pigment network, all corresponding to melanocytic nevi, whereas an atypical pigment network was observed in 28 MMs (8 in situ, 19 thinner than 1 mm, and 1 thicker) and 27 nevi. When using RCM, a typical network was characterized in all cases by rings of bright polygonal cells surrounding roundish to oval dark areas corresponding to dermal papillae, observable at the dermoepidermal junction between 60 and 100 µm below the surface. The size and shape of the dermal papillae exactly corresponded to the ones of the network holes, whereas the network lines were correlated with 2 paired portions of adjacent rings, resulting at high-magnification dermoscopy in the bilayer structure of the network grid.[23] Routine histologic analysis revealed elongated rete ridges with an increased number of melanocytes in the basal layer and pigmented basal keratinocytes (**Figure 1**). A club-shaped elongated rete ridge with prominent basal layer pigmentation along with larger melanocytes was observed in 2 cases of junctional nevi that exhibited a lentiginous pattern, compatible with the larger size of the bright cells forming the rings on confocal microscopy. No pagetoid melanocytosis or single or clustered atypical cells were present on RCM and histologic analysis. In 8 cases, a few plump bright cells were visible within the dermal papilla, corresponding to small bluish structures within the holes of the network and melanophages on histologic analysis.

The atypical pigment network corresponded to irregular and dishomogeneous dermal papillae. These papillae did not have a demarcated rim of bright cells but were separated by loosely thick interpapillary spaces. These spaces consisted of large reflecting cells that coincided with the irregular network grid, previously defined as "nonedged papillae,"[16] on RCM. Irregular enlargements of the intrapapillary spaces were described in 19 MMs and 19 nevi. Cells were usually larger than the typical keratinocytes, although atypical cells, with highly

Downloaded from www.archdermatol.com at Universidad de Cadiz, on November 16, 2009
©2008 American Medical Association. All rights reserved.

Table. Confocal Microscopic and Histopathologic Correlations of Dermoscopic Features in Melanocytic Lesions

Dermoscopic Pattern	No. of Cases			RCM Features	Frequency of RCM Atypia, No. (%)[a]			Histopathologic Features
	Melanoma	Nevus	Spitz		Melanoma	Nevus	Spitz	
Pigment network								
Typical		52		Edged papillae: rings of bright cells surrounding roundish to oval dark areas corresponding to dermal papillae at the dermoepidermal junction.		0		Elongated regular rete ridges with an increased number of melanocytes in the basal layers and pigmented basal keratinocytes.
Atypical	28	27		Nonedged papillae: dark dermal papillae usually irregular in size and shape, without a demarcated rim of bright cells, but separated by more or less thick interpapillary spaces constituted by large reflecting cells coinciding with the irregular network grid.	27 (96)	4 (15)		Disarrangement of the rete ridge in all cases. Increased number of atypical melanocytes predominantly in melanomas.
Pigment globules								
Regular		15		Dense melanocytic clusters: compact aggregates with sharp margins, constituted by large polygonal monomorphous cells.		0		Typical and monomorphous nevocytic nests at the dermoepidermal junction and within the papillary dermis.
Irregular	27	20	3	Irregularly shaped clusters, usually showing regular cytologic features in benign lesions and atypical cells in melanomas.	22 (81)	4 (20)	2 (67)	Typical nevocytic nests corresponded to homogeneous dense clusters, whereas nonhomogeneous clusters showed up as compact aggregates of pleomorphic melanocytes.
Pigment dots	61	71	8	Single large pagetoid cells, frequently aggregated in small clusters, were predominantly observable in MMs and some Spitz nevi, whereas bright structures within an even epidermis were typical of benign lesions. Bluish dots corresponded to plump bright cells within papillary dermis.	52 (81)	9 (13)	5 (63)	Cells in superficial layers corresponded to pagetoid infiltration, whereas bright structures showed up as free melanin clumps within the epidermis. Plump bright cells corresponded to melanophages.
Streaks	27	17	8	Radial streamings: parallel series of elongated lines of basal cells projected toward the periphery. Peripheral globules: dense clusters at the lesion periphery. Pseudopods: globularlike bulging structures, similar to dense nests bridged with the lesion core.	4 (15)	0	1 (13)	Radial streamings: elongated and parallel oriented epidermal cristae at the periphery of the lesion. Peripheral globules: typical nevocytic nests at the periphery. Pseudopods: well-defined nests, located at the tip of the enlarged and parallel oriented crista.
Diffuse pigmentation								
Light brown pigmentation	36			Regular honeycombed pattern.	0			Few pigmentation and regular epidermal architecture.
Dark diffuse pigmentation and pigment blotches	36	18	5	Bright cobblestone pattern, sometimes intermingled with cells spreading upward in melanomas and Spitz nevi.	31 (58)	2 (11)	3 (60)	Pigmentation within keratinocytes and transepidermal melanin loss together with pagetoid melanocytosis in correspondence with spreading upward cells.
Blue structures								
Blue-whitish veil	20	1	1	Disarranged pattern and presence of roundish pagetoid infiltration in superficial layers, nonedged papillae and cytologic atypia in basal layer, dishomogeneous and/or cerebriform nests and nucleated and/or plump cells in dermal papillae.	10 (100)	0	1 (100)	Orthokeratosis and parakeratosis associated with pagetoid melanocytosis. Disarray of the dermoepidermal contour, marked cell atypia, and malignant cells in nests, cords, or solitary infiltrating the dermis together with melanophages and inflammatory cells.
Blue areas and blue diffuse pigmentation	3	10	2	Plump bright cells within dermal papillae. Blue nevi: no specific features.	3 (100)	0	2 (100)	Melanophages and inflammatory infiltrate in the dermis. Blue nevi: ill-defined deep dermal proliferation of elongated or dendritic dermal melanocytes.
Regression	34	3		Thin epidermis and coarse network of ill-defined grainy bundles or fibers in the dermis, sometimes intermingled with small bright reflecting spots and plump bright cells.	7 (21)	0		Thin, devoid of melanin, epidermis, covering areas of fibroplasia with inflammatory infiltrate, constituted by leukocytes and few melanophages.

Abbreviations: MM, malignant melanoma; RCM, reflectance confocal microscopy.
[a] Presence of roundish pagetoid cells, large atypical cells at the dermoepidermal junction, nucleated cells infiltrating papillary dermis, and/or clusters of pleomorphic cells.

reflective cytoplasm and occasionally with branching dendriticlike structures, located at the dermoepidermal junction and/or spreading upward in a pagetoid fashion, were observable in 27 of 28 MMs and 4 of 27 nevi on RCM. Histopathologic examination revealed a disarrangement of the rete ridge in all cases, whereas in all MMs and only 2 nevi an increased number of atypical melanocytes, sometimes forming irregular and confluent nests at the dermoepidermal junction, were observable (**Figure 2**).

Downloaded from www.archdermatol.com at Universidad de Cadiz, on November 16, 2009
©2008 American Medical Association. All rights reserved.

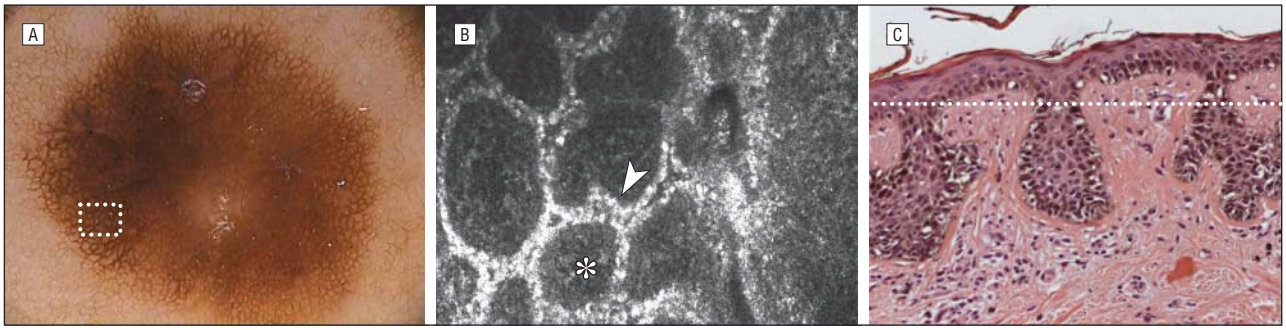

Figure 1. Routine histologic analysis revealed elongated rete ridges with an increased number of melanocytes in the basal layer and pigmented basal keratinocytes. A, Typical pigment network in a nevus on dermoscopy consisting of small, uniformly spaced network holes and thin network lines (white dotted square corresponds to the reflectance confocal microscopy [RCM] image) (original magnification ×30). This structure correlated with roundish to oval dark areas, corresponding to dermal papillae (white asterisk) rimmed by rings of bright cells (white arrowhead) on RCM (B) (original magnification ×30) and to regular elongated rete ridges on histologic analysis (white dotted line corresponds to the level of the RCM image) (C) (hematoxylin-eosin, original magnification ×100).

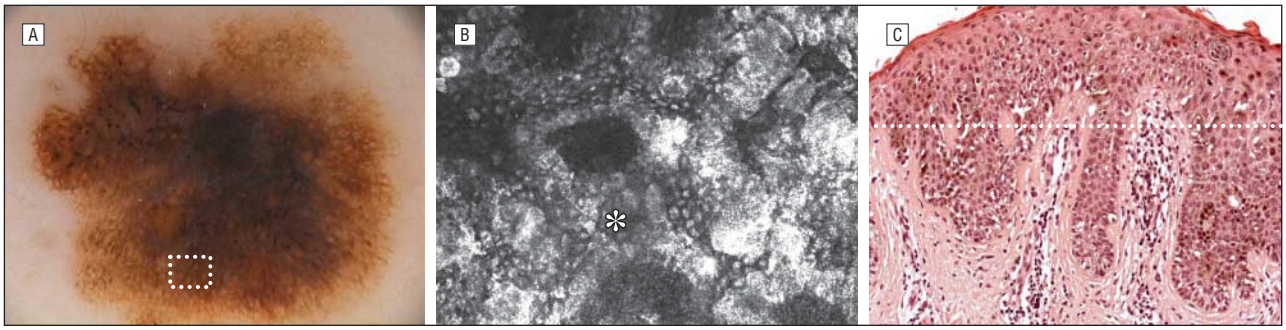

Figure 2. Histologic analysis revealed an increased number of atypical melanocytes, sometimes forming irregular and confluent nests at the dermoepidermal junction. A, Atypical pigment network with irregular holes and thick lines in a melanoma on dermoscopy (white dotted square corresponds to the reflectance confocal microscopy [RCM] image) (original magnification ×30). B, The absence of rings of bright cells (nonedged papillae) and loosely thick interpapillary spaces (white asterisk) were present on RCM (original magnification ×30). C, Histopathologic analysis revealed a disarrangement of the rete ridge (white dotted line corresponds to the level of the RCM image) (hematoxylin-eosin, original magnification ×100).

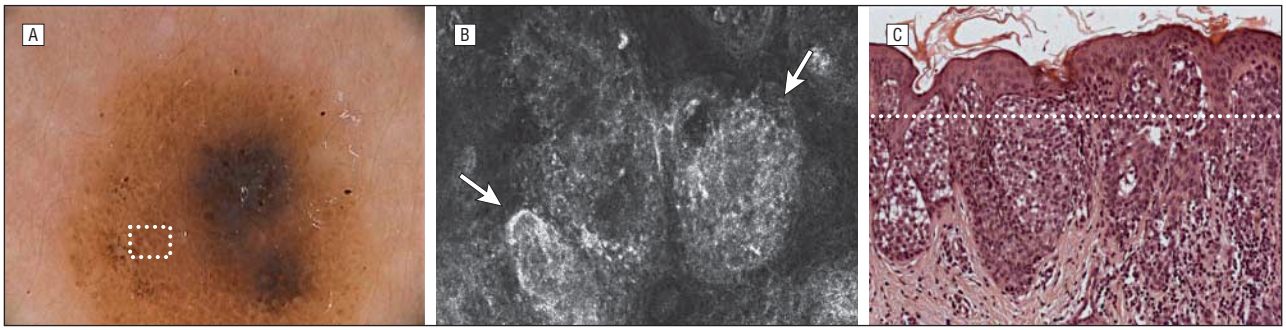

Figure 3. Histologic analysis revealed discrete melanocytic nests, composed of typical and monomorphous nevocytes, located at the dermoepidermal junction and within the papillary dermis. A, Brown globules in a nevus on dermoscopy (white dotted square corresponds to the reflectance confocal microscopy [RCM] image) (original magnification ×30). The RCM showed homogeneous dense clusters (white arrows) (B) (original magnification ×30) corresponding to regular melanocytic nests on histologic analysis (white dotted line corresponds to the level of the RCM image) (C) (hematoxylin-eosin, original magnification ×100).

PIGMENT GLOBULES

Regular homogeneous globules were studied in 15 nevi, 5 of which corresponded to dermal nevi. An exact correspondence in shape was observed between the brown globules on dermoscopy and the dense melanocytic clusters on RCM, appearing as compact aggregates with a sharp margin of large polygonal cells similar in morphologic features and reflectivity.[15] Histopathologic analysis revealed discrete melanocytic nests, composed of typical and monomorphous nevocytes, located at the dermoepidermal junction and within the papillary dermis (**Figure 3** and **Figure 4**). The large polygonal structures forming the dermoscopic cobblestone pattern in the 5 dermal nevi appeared on RCM as large aggregates of clustered cells, with enlarging dermal papillae and without connection to the basal cell layer. Some large, roundish nucleated cells loosely aggregated were sometimes visible in the upper portion of the cluster. In depth, clusters assumed a more compact and homogeneous aspect with no evident cell contours. On histologic examination, nevus cells were disposed in an orderly manner as cords and nests of cells decreasing in size with depth and separated by thin fibers (**Figure 5**).

Downloaded from www.archdermatol.com at Universidad de Cadiz, on November 16, 2009
©2008 American Medical Association. All rights reserved.

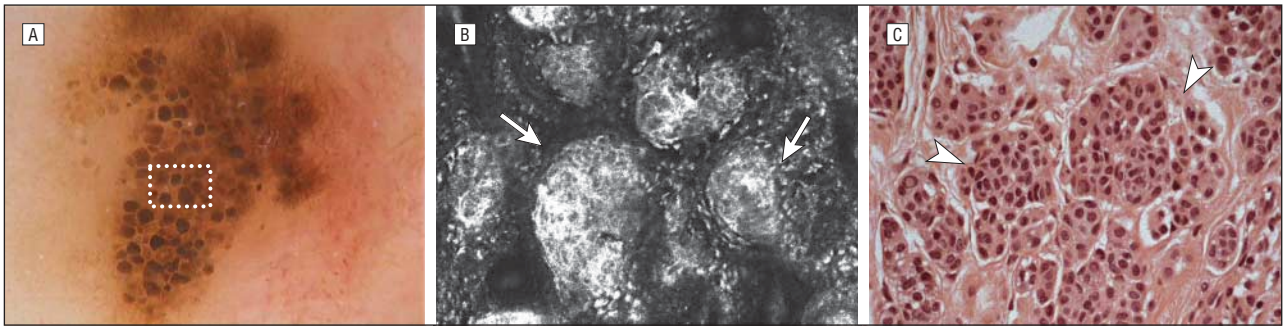

Figure 4. Histologic analysis revealed discrete melanocytic nests, composed of typical and monomorphous nevocytes, located at the dermoepidermal junction and within the papillary dermis. A, Dermoscopy of a compound nevus showing regular polygonal globules forming a cobblestone pattern (white dotted square corresponds to the reflectance confocal microscopy [RCM] image) (original magnification ×50). The RCM showed roundish to oval, large dense clusters immediately below the dermoepidermal junction (white arrows) (B) (original magnification ×30), corresponding to melanocytic nests in the papillary dermis on histologic analysis (white arrowheads) (C) (hematoxylin-eosin, original magnification ×200).

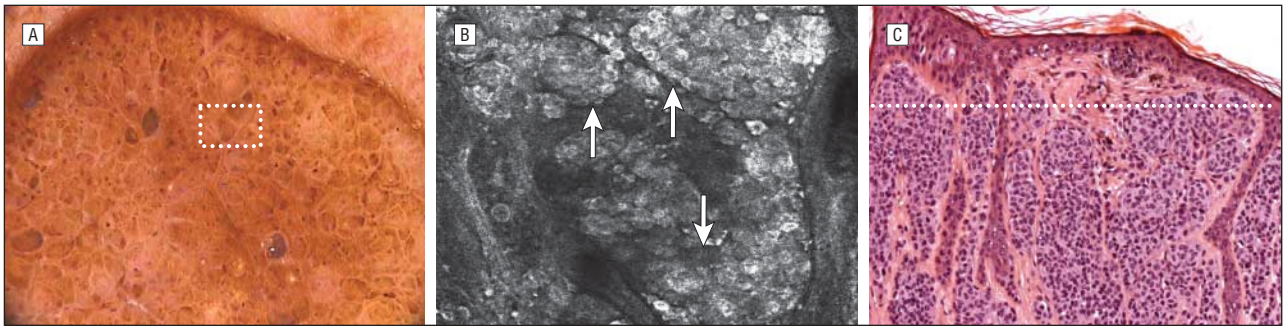

Figure 5. Histologic analysis revealed orderly nevus cells that were disposed as cords and nests of cells decreasing in size with depth and separated by thin fibers. A, Dermal nevus with a cobblestone pattern on dermoscopy (white dotted square corresponds to the reflectance confocal microscopy [RCM] image) (original magnification ×30). B, The RCM showed large, roundish, loosely aggregated cells in the upper portion of the cluster (white arrows) (original magnification ×30). C, On histologic analysis, nevus cells were disposed in an orderly manner as cords and nests of cells separated by thin fibers clearly visible in the superficial dermis, decreasing in size with depth (white dotted line corresponds to the level of the RCM image) (hematoxylin-eosin, original magnification ×100).

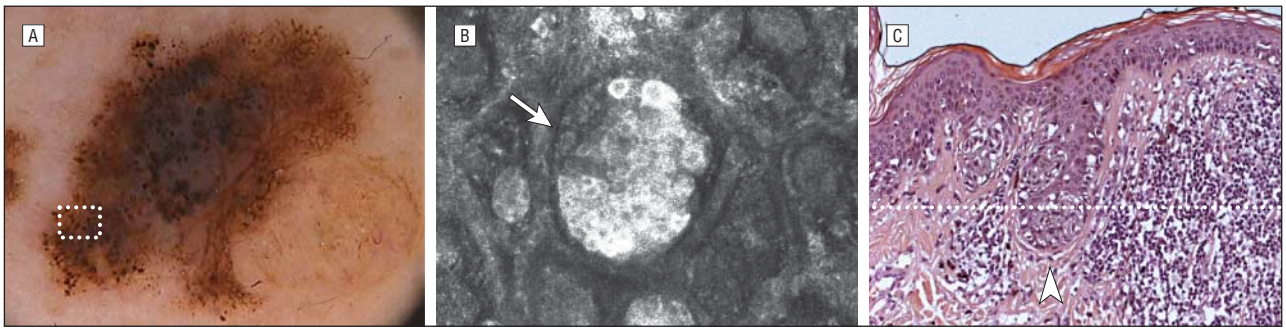

Figure 6. Histologic analysis revealed clusters of pleomorphic malignant melanocytes, predominantly distributed at the dermoepidermal junction and in the papillary dermis. A, Atypical pigment globules in a melanoma on dermoscopy (white dotted square corresponds to the reflectance confocal microscopy [RCM] image) (original magnification ×20). Irregularly shaped clusters, composed of nonhomogeneous morphologic features and reflectivity cells, were visible using RCM (white arrows) (B) (original magnification ×30) and corresponded to atypical clusters of pleomorphic melanocytes at histologic analysis (white arrowhead) (white dotted line corresponds to the level of the RCM image) (C) (hematoxylin-eosin, original magnification ×100).

Globules, irregular in size, shape, pigmentation, and/or distribution, were studied in 27 MMs, 20 melanocytic nevi, and 3 Spitz or Reed nevi. The RCM revealed irregularly shaped clusters in all lesions, with a regular dense structure in 5 of 27 MMs, 16 of 20 melanocytic nevi, and 1 of 3 Spitz nevi. Cells that are nonhomogeneous in morphologic features and reflectivity were observed in the remaining cases. On histologic analysis, atypical globules made of dense clusters of nonhomogeneous cells appeared as compact aggregates of pleomorphic melanocytes, variable in size and shape, predominantly distributed at the dermoepidermal junction and in the papillary dermis (**Figure 6**).

Pigment dots were observed in 140 lesions, belonging to 61 MMs, 71 nevi, and 8 Spitz or Reed nevi. In the superficial layers of 52 of 61 MMs, single large cells, frequently aggregated in small clusters, with reflective cytoplasm and dark nucleus spreading upward in a pagetoid fashion, were clearly visible and highly contrasted in respect to the honeycombed or cobblestone background structure of the epidermis, showing up as small aggregates of pagetoid melanocytes on histologic analy-

Downloaded from www.archdermatol.com at Universidad de Cadiz, on November 16, 2009
©2008 American Medical Association. All rights reserved.

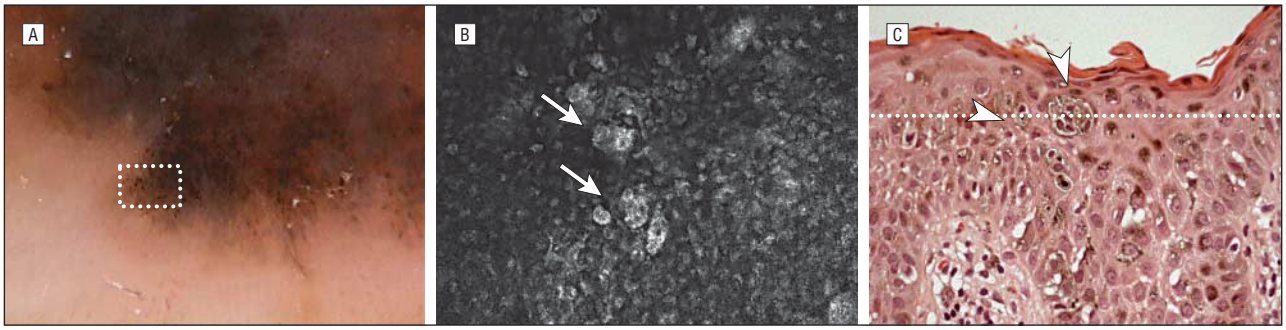

Figure 7. Histologic analysis revealed pagetoid cells. Pigment dots in a melanoma on dermoscopy (white dotted square corresponds to the reflectance confocal microscopy [RCM] image) (A) (original magnification ×50) consisting of single large cells, frequently aggregated in small clusters, with reflective cytoplasm and dark nucleus, spreading upward in a pagetoid fashion in the superficial layers on RCM (white arrows) (B) (original magnification ×30) and of aggregates of pagetoid melanocytes on histologic analysis (white arrowheads) (white dotted line corresponds to the level of the RCM image) (C) (hematoxylin-eosin, original magnification ×200).

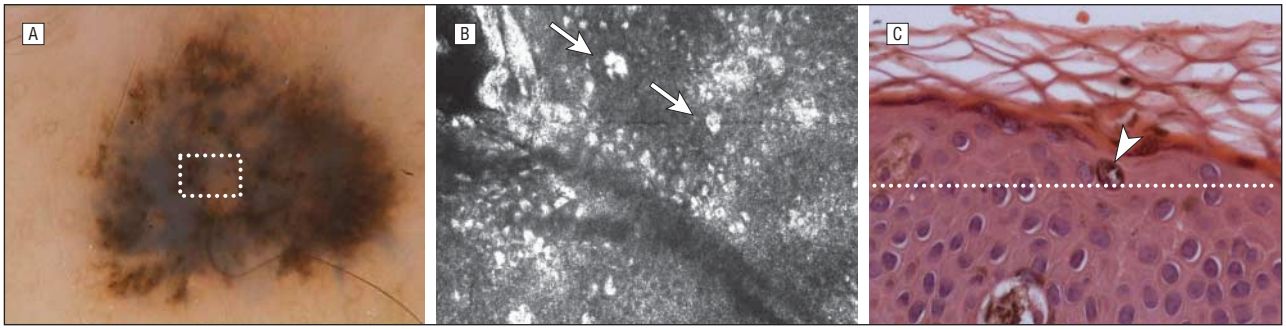

Figure 8. Histologic analysis revealed clumps of melanin in the superficial epidermal layers. Spitz nevus characterized by brown and black dots on dermoscopy (white dotted square corresponds to the reflectance confocal microscopy [RCM] image) (A) (original magnification ×70) showing a honeycombed and cobblestone pattern with the focal presence of reflecting spots on RCM (white arrows) (B) (original magnification ×30) and corresponding to melanin clumps within the epidermis on histologic analysis (white arrowhead) (white dotted line corresponds to the level of the RCM image) (C) (hematoxylin-eosin, original magnification ×400).

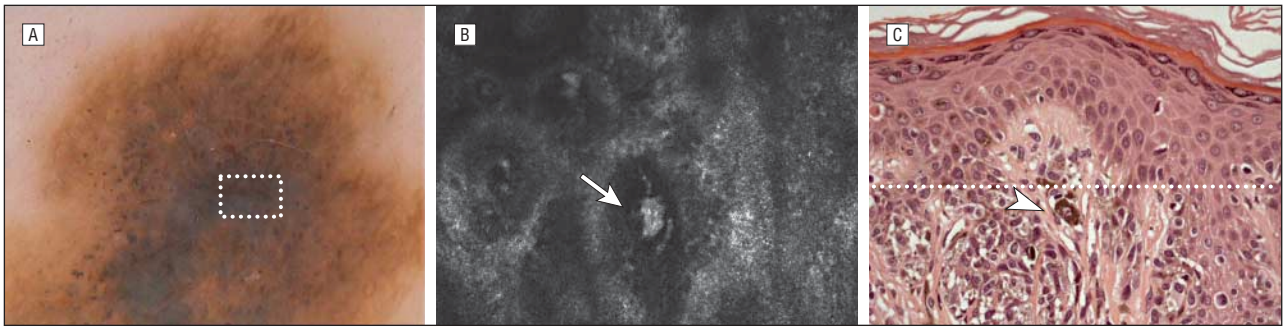

Figure 9. Histologic analysis revealed a few melanophages located in the upper part of the dermal papilla. Bluish dots in a nevus on dermoscopy (white dotted square corresponds to the reflectance confocal microscopy [RCM] image) (A) (original magnification ×50) made up of small aggregates of plump bright cells within dermal papillae visible by RCM (white arrow) (B) (original magnification ×30) and corresponding to few melanophages located in the upper part of the dermal papillae at histologic analysis (white arrowhead) (white dotted line corresponds to the level of the RCM image) (C) (hematoxylin-eosin, original magnification ×200).

sis (**Figure 7**). On the other hand, 5 of 8 Spitz nevi showed few pagetoid cells and some ovoidal, homogeneously bright structures, corresponding to free melanin clumps within the stratum corneum. Pagetoid cells were also visible in 9 nevi, whereas the remaining cases showed a honeycombed and/or cobblestone pattern with the focal presence of reflecting spots on RCM, corresponding to melanin clumps within the epidermis (**Figure 8**). On the other hand, bluish dots observed in 31 nevi were composed of small aggregates of plump bright cells within the dermal papillae. These dots corresponded to a few melanophages located in the upper part of the dermal papilla on histologic examination (**Figure 9**).

Streaks (peripheral structures) were present in 52 cases, 15 of which (8 MMs, 4 nevi, and 3 Spitz or Reed nevi) showed radial streamings,[7] 19 (8 MMs, 8 nevi, and 3 Spitz or Reed nevi) peripheral globules, and 18 (11 MMs, 5 nevi, and 2 Spitz or Reed nevi) pseudopods.[24] On RCM, radial streamings consisted of parallel series of elongated junctional thickening–like structures or of lines of interpapillary basal cells projected toward the periphery, separated by narrow elongated darker areas corresponding to dermal papillae. On histologic analysis, elongated and parallel oriented epidermal cristae were observable at the periphery of the lesion (**Figure 10**).

Downloaded from www.archdermatol.com at Universidad de Cadiz, on November 16, 2009
©2008 American Medical Association. All rights reserved.

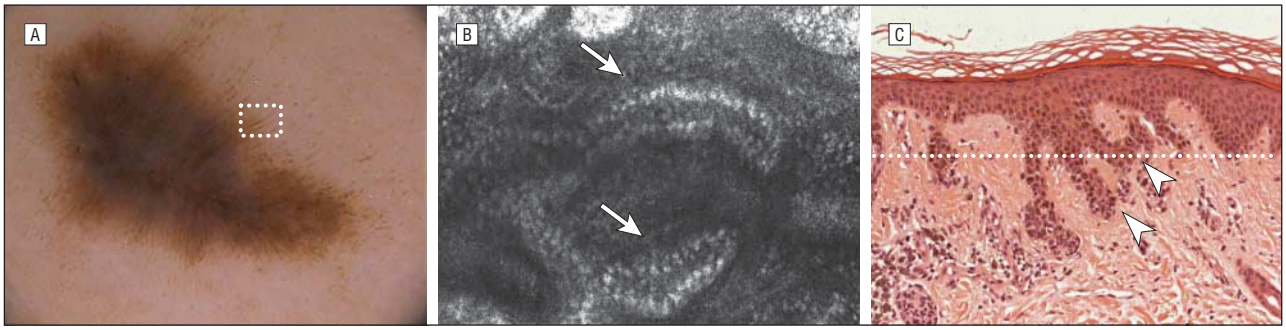

Figure 10. Histologic analysis revealed elongated and parallel oriented epidermal cristae at the periphery of the lesion. Radial streaming in a nevus on dermoscopy (white dotted square corresponds to the reflectance confocal microscopy [RCM] image) (A) (original magnification ×30), composed of parallel series of elongated lines of basal cells projected toward the periphery, separated by narrow darker areas corresponding to dermal papillae on RCM (white arrows) (B) (original magnification ×30) and correlated on histologic analysis to elongated and parallel oriented epidermal cristae at the periphery of the lesion (white arrowheads) (white dotted line corresponds to the level of the RCM image) (C) (hematoxylin-eosin, original magnification ×100).

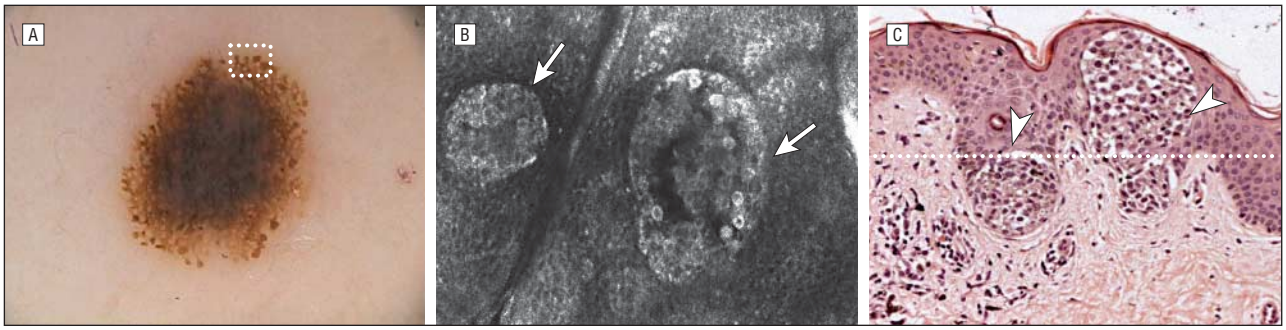

Figure 11. Histologic analysis revealed melanocytic nests at the dermoepidermal junction, sometimes pushing up the epidermis. Peripheral globules on dermoscopy (white dotted square corresponds to the reflectance confocal microscopy [RCM] image) (A) (original magnification ×30) and consisted of clusters of loosely aggregated cells with well-demarcated outlines, neatly separated by the lesion core on RCM (white arrows) (B) (original magnification ×30). Histologic analysis revealed well-defined junctional aggregates of nevus cells, sometimes pushing up the epidermis, at the periphery (white arrowheads) (white dotted line corresponds to the level of the RCM image) (C) (hematoxylin-eosin, original magnification ×200).

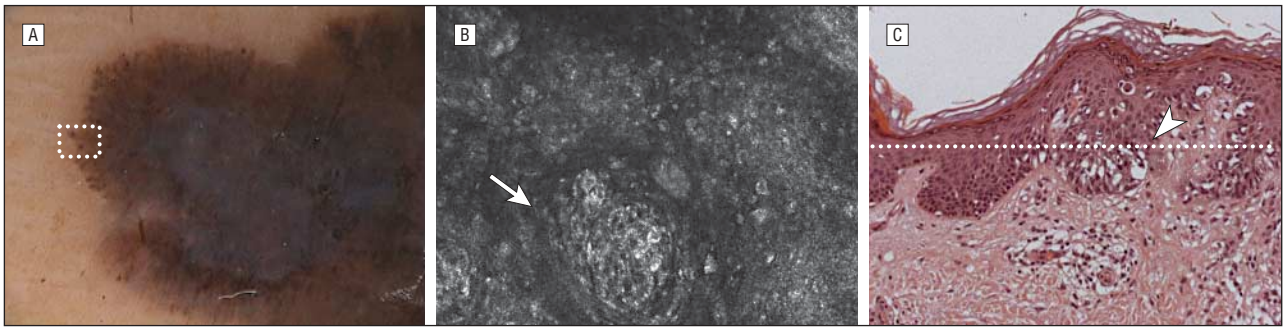

Figure 12. Histologic analysis revealed clumps of melanin in the superficial epidermal layers. Peripheral globules in a melanoma on dermoscopy (white dotted square corresponds to the reflectance confocal microscopy [RCM] image) (A) (original magnification ×30), consisting of cells irregular in size and shape that form nonhomogeneous clusters on RCM (white arrow) (B) (original magnification ×30) and of aggregates of pleomorphic malignant melanocytes on histologic analysis (white arrowhead) (white dotted line corresponds to the level of the RCM image) (C) (hematoxylin-eosin, original magnification ×100).

On the other hand, peripheral globules did not differ from brown globules, corresponding to dense or sparse cell clusters on RCM, exactly fitting in shape with dermoscopic findings. Melanocytic nests at the dermoepidermal junction, sometimes pushing up the epidermis, were observable on histologic analysis (**Figure 11**). In 4 of 8 MMs and in 1 of 3 Spitz or Reed nevi, irregular peripheral globules corresponded to aggregates of pleomorphic melanocytes on histologic analysis (**Figure 12**).

With the use of RCM, pseudopods presented a globularlike structure at the extremity, similar to a dense nest located immediately below the epidermal basal layer and characterized by sharp borders only in the outside front, but connected at the lesion core by a sheet of loosely aggregated cells, giving rise to a comet star–like appearance. On histologic analysis, a well-defined nest, located at the tip of the enlarged and parallel oriented crista, was observable (**Figure 13**).

Diffuse pigmentation was studied in 95 lesions, belonging to 36 nevi and showing a light brown pigmentation, 33 lesions (17 MMs, 11 nevi, and 5 Spitz or Reed nevi) with dark brown to black homogeneous diffuse pigmentation, and 26 lesions (19 MMs and 7 nevi) with

Downloaded from www.archdermatol.com at Universidad de Cadiz, on November 16, 2009
©2008 American Medical Association. All rights reserved.

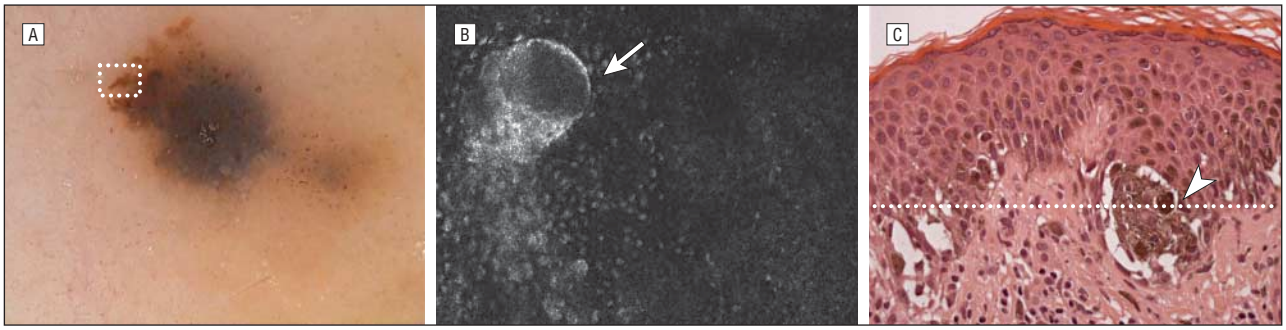

Figure 13. Histologic analysis revealed discrete nests at the edge of the lesion. Pseudopods in a nevus as shown by dermoscopy (white dotted square corresponds to the reflectance confocal microscopy [RCM] image) (A) (original magnification ×50) that correspond to dense nests bridged with the lesion core by a sheet of loosely aggregated cells, giving rise to a comet like appearance on RCM (white arrow) (B) (original magnification ×30). Histologic analysis revealed a well-defined nest, located at the tip of the enlarged and parallel oriented crista (white arrowhead) (white dotted line corresponds to the level of the RCM image) (C) (hematoxylin-eosin, original magnification ×200).

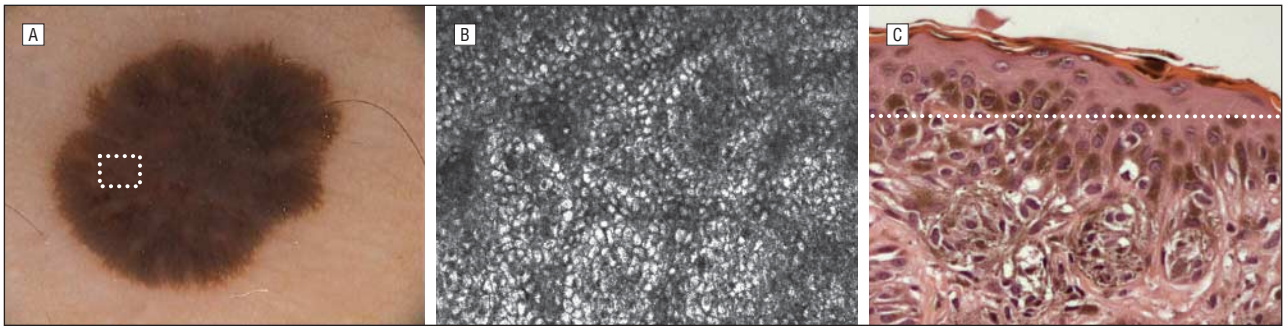

Figure 14. Histologic analysis revealed little pigmentation in the epidermal layers. Light brown homogeneous pigmentation of a nevus as observable by dermoscopy (white dotted square corresponds to the reflectance confocal microscopy [RCM] image) (A) (original magnification ×50) was characterized by a honeycombed pattern in superficial layers on RCM (B) (original magnification ×30) and corresponded to scarcely pigmented epidermal layers on histologic analysis (white dotted line corresponds to the level of the RCM image) (C) (hematoxylin-eosin, original magnification ×200).

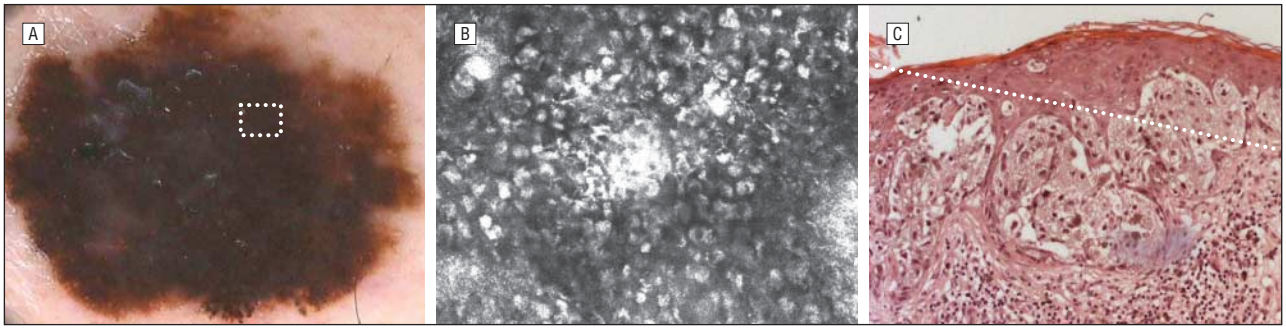

Figure 15. Histologic analysis revealed abundant transepidermal melanin dispersion. A, Dark diffuse pigmentation in a nevus on dermoscopy (white dotted square corresponds to the reflectance confocal microscopy [RCM] image) (original magnification ×30). The RCM revealed high reflective superficial layers giving rise to a bright cobblestone pattern (B) (original magnification ×30) caused by the abundant content of melanin within the keratinocytes (white dotted line corresponds to the level of the RCM image) (C) (hematoxylin-eosin, original magnification ×200).

dark pigment blotches. Light brown homogeneous pigmentation was characterized in superficial layers by a honeycombed pattern. Immediately below this area, a subtle network of small regular edged papillae, occasionally alternated with small, weakly reflecting, dense, regular nests, was observed in all cases. Histologic analysis revealed little pigmentation in the epidermal layers (**Figure 14**).

On RCM, dark diffuse pigmentation and pigment blotches showed a high reflectivity in the superficial layers owing to the abundant content of melanin within the keratinocytes, resulting in a bright cobblestone pattern (**Figure 15**). In 21 of 36 MMs and 2 of 5 Spitz or Reed nevi, the RCM cobblestone pattern was intermingled with large pagetoid cells (**Figure 16**). Immediately below the superficial layers, 31 MMs, 2 nevi, and 3 Spitz or Reed nevi showed a disarrangement of the dermoepidermal architecture and/or single or clustered atypical cells, whereas regular edged papillae and dense regular nests were usually observable in benign lesions. Plump bright cells were also present within the dermal papillae in some benign and malignant lesions. The brightness of the keratinocytes corresponded to abundant pigmentation within keratinocytes on histologic examination. Confocal pagetoid infiltration and cytologic and architectural atypia were confirmed by histopathologic analysis.

Downloaded from www.archdermatol.com at Universidad de Cadiz, on November 16, 2009
©2008 American Medical Association. All rights reserved.

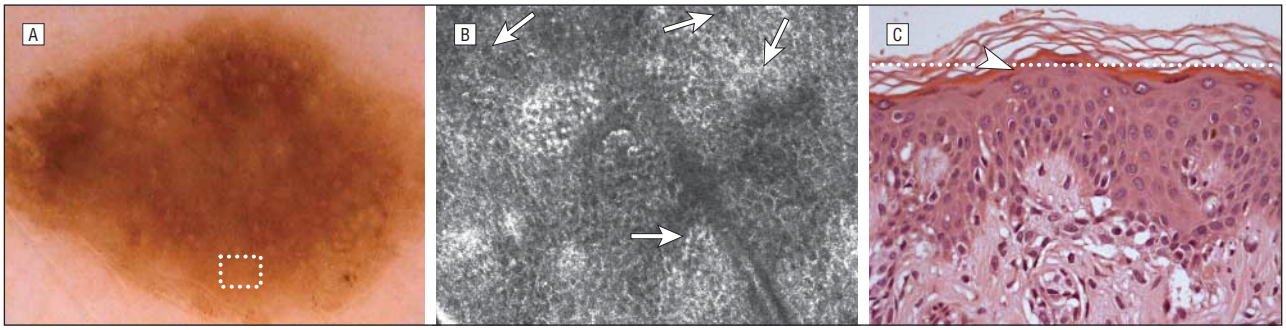

Figure 16. Histologic analysis revealed pigmented keratinocytes and numerous pagetoid cells in the epidermis. Dark diffuse pigmentation in a melanoma on dermoscopy (white dotted square corresponds to the reflectance confocal microscopy [RCM] image) (A) (original magnification ×20). The RCM showed a cobblestone pattern intermingled with large round to oval cells with bright cytoplasm and dark nucleus (white arrows) (B) (hematoxylin-eosin, original magnification ×30) that correspond to pagetoid infiltration on histologic analysis (white arrowheads) (white dotted line corresponds to the level of the RCM image) (C) (hematoxylin-eosin, original magnification ×100).

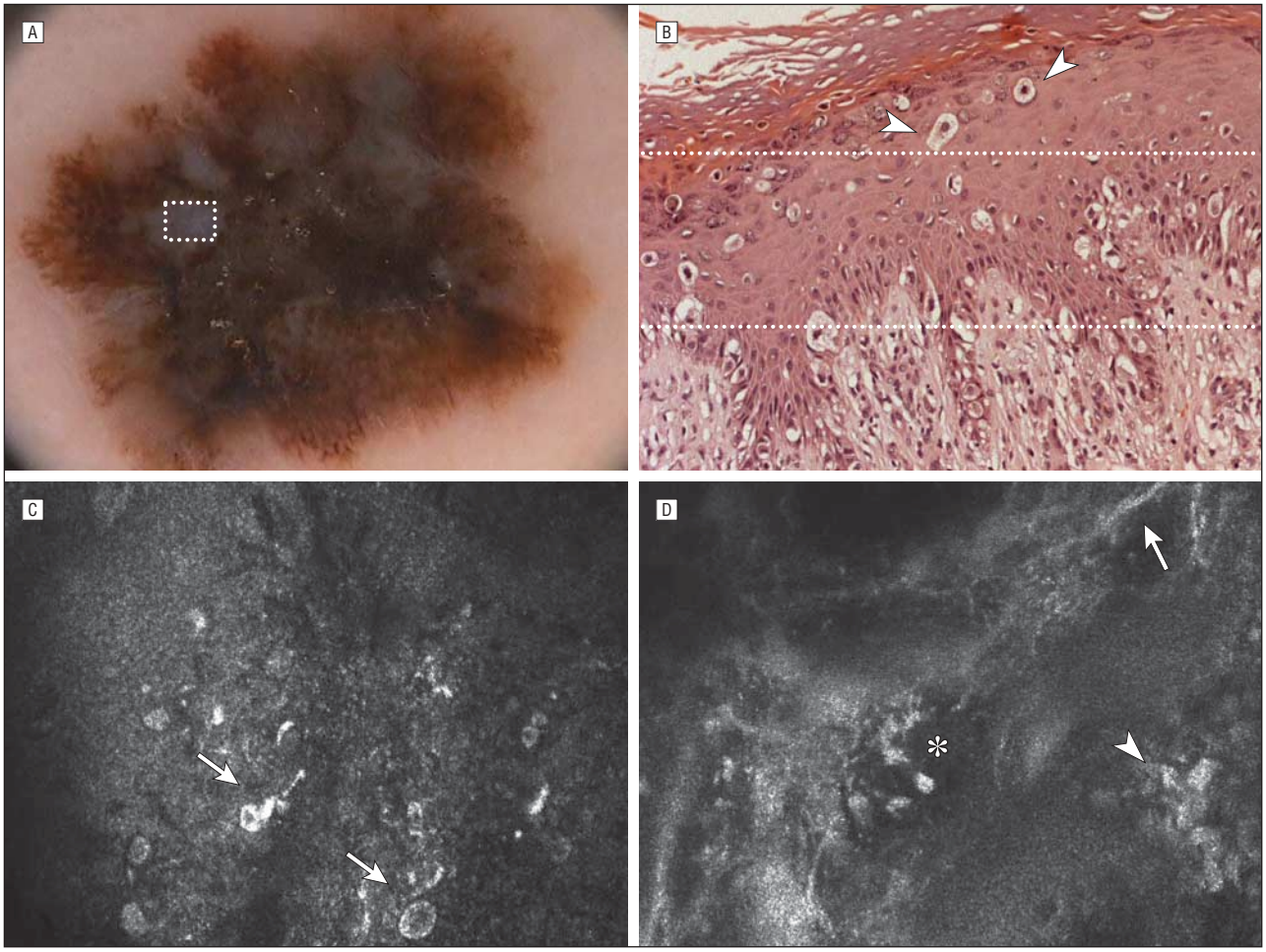

Figure 17. Histologic analysis revealed epidermal disarray and pagetoid infiltration, and nondiscrete nests, malignant melanocytes, and marked inflammatory infiltrate in the dermis. A, Blue veil in a melanoma on dermoscopy (white dotted square corresponds to the reflectance confocal microscopy [RCM] image) (original magnification ×20). B, Histologic analysis showed parakeratosis, pagetoid infiltration, and architectural disarray with marked cytologic atypia (white arrowheads) (white dotted line corresponds to the level of the RCM image) (original magnification ×200). The RCM showed a disarranged pattern and roundish pagetoid infiltration in the epidermis (white arrows) (C) (original magnification ×30) and nonedged papillae, atypical cells in the basal layer (white arrow) and in the upper dermis (white asterisk), and melanophages (white arrowhead) (D) (hematoxylin-eosin, original magnification ×30).

Blue structures were observed in 32 cases, including 20 MMs, 1 nevus, and 1 Spitz or Reed nevus with a blue-whitish veil and 3 MMs, 5 nevi, and 2 Spitz or Reed nevi with blue areas.[25] A homogeneous steel blue pigmentation was present in 5 blue nevi.

All MMs and the Spitz or Reed nevus characterized by the blue veil showed epidermal disarray, roundish pagetoid infiltration, nonedged papillae, and cytologic atypia in the basal layer. Dishomogeneous nests were preset in 12 lesions and cerebriform clusters in 8, along with nu-

Downloaded from www.archdermatol.com at Universidad de Cadiz, on November 16, 2009
©2008 American Medical Association. All rights reserved.

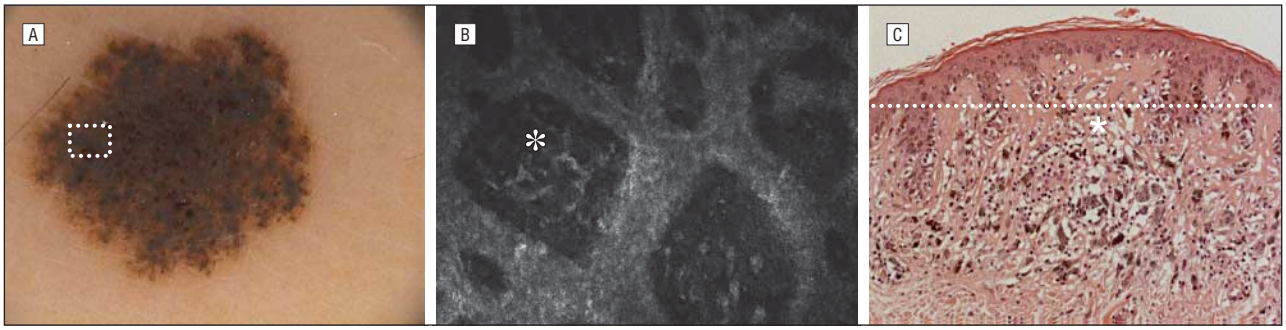

Figure 18. Histologic analysis revealed numerous melanophages corresponding to the presence of blue areas on dermoscopy and plump bright cells on reflectance confocal microscopy (RCM). Blue area in a nevus on dermoscopy (white dotted square corresponds to the RCM image) (A) (original magnification ×30) characterized by plump bright cells with ill-defined borders in the papillary dermis at RCM (white asterisk) (B) (original magnification ×30) and corresponding to melanophages at histologic analysis (white asterisk) (white dotted line corresponds to the RCM image) (C) (hematoxylin-eosin, original magnification ×100).

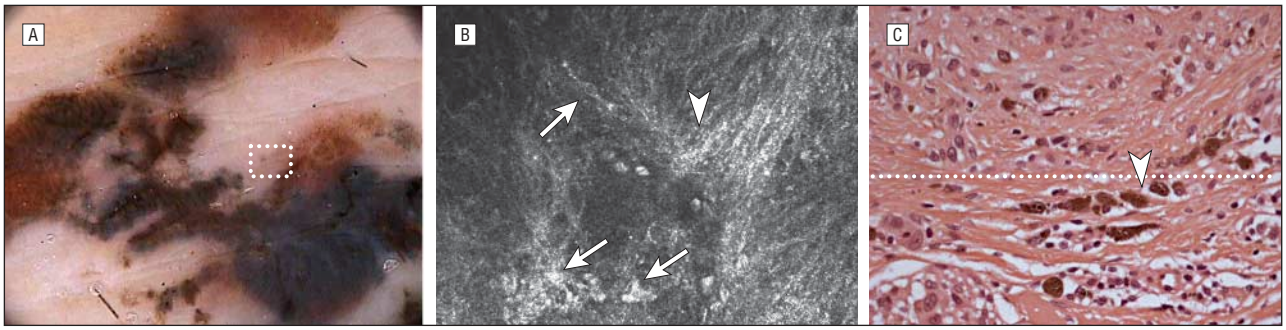

Figure 19. Histologic analysis revealed a few malignant melanocytes within marked regression. Regression in a melanoma on dermoscopy (white dotted square corresponds to the reflectance confocal microscopy [RCM] image) (A) (original magnification ×20) that corresponds to a coarse network of ill-defined grainy bundles (white arrowhead) and bright roundish or spindled reflecting cells (white arrows) using RCM (B) (original magnification ×30) and correlate to neoplastic and inflammatory infiltrate on histologic analysis (white arrowhead) (white dotted line corresponds to the level of the RCM image) (C) (hematoxylin-eosin, original magnification ×200).

merous nonaggregated cells infiltrating the dermal papillae, corresponding to a collection of plump bright and nucleated cells (**Figure 17**). On histopathologic analysis, epidermal alterations corresponded to orthokeratosis and parakeratosis associated with marked pagetoid melanocytosis. The dermoepidermal contour disappeared completely, presenting marked cytologic atypia. Nests of malignant cells crowded against the epidermis and infiltrated the dermis, along with cords and single cells deeply invading the dermis and intermingling with a marked inflammatory infiltrate and melanophages. On the other hand, the nevus with a blue veil on dermoscopy revealed a thickened epidermis and abundant melanophages in the dermis on RCM and histologic analysis.

Exploring blue areas by means of RCM, the areas were found to correlate with the presence of plump bright cells, corresponding to melanophages on histologic analysis (**Figure 18**), in all nevi but 1, which showed dense clusters in depth. Isolated nucleated cells intermingled with plump bright ones were present within dermal papillae in all MMs and correlated with infiltrating malignant melanocytes. Moreover, some RCM features suggesting an MM diagnosis, such as a disarranged epidermal pattern, roundish pagetoid cells, nonedged papillae, and cytologic atypia, as well as their histopathologic substrates, were identified in all malignant lesions and in 2 Spitz or Reed nevi, whereas they were absent in common nevi.

In the 5 blue nevi, a normal honeycombed pattern and a regular pattern composed of slight reflecting rings of cells surrounding dark empty papillae, not different from healthy skin, were observable on RCM. Histopathologic analysis showed ill-defined deep dermal proliferation of elongated or dendritic dermal melanocytes. The depth of the localization of the cellular component in blue nevi seemed to be responsible for the lack of RCM findings.

Regression was evaluated in 34 MMs and in 3 nevi; some of the cases were characterized by extensive regression areas with blue pepperlike granules. All cases showed few epidermal layers characterized by a honeycombed pattern; only 7 MMs also showed a few pagetoid cells. The dermoepidermal boundary was imperceptible, passing directly from the honeycombed epidermal layers to the dermis without the appearance of the reflective basal cells and papillary contours. The dermis consisted of a coarse network of ill-defined grainy bundles or, less frequently, of fibers oriented in the same direction. Small bright reflecting spots and plump bright cells, intermingled with collagen bundles, were usually observable in correspondence where the peppering is shown. Few nucleated cells with bright cytoplasm and well-defined borders, suggestive of malignant melanocytes infiltrating the dermis, were present in only 4 MMs (**Figure 19**). Histologic analysis revealed a thin, atrophic epidermis devoid of melanin, covering areas of fibroplasia. Inflammatory infiltrate, consisting of leukocytes and a few melanophages, was present within fibroplasia. Also on histologic analysis, malignant cells were seldom observed within the regression area.

Downloaded from www.archdermatol.com at Universidad de Cadiz, on November 16, 2009
©2008 American Medical Association. All rights reserved.

COMMENT

Dermoscopy used by experts yielded an improvement in diagnostic accuracy, in particular for thin MMs.[3] However, to rule out malignant neoplasms with high sensitivity, numerous nevi are excised owing to dermoscopic atypical features akin to MMs. Recently, the introduction of RCM in the field of skin oncology showed the capability to produce real-time in vivo sections of the skin at a nearly histologic resolution, enabling the clear and well-contrasted visualization of cells and structures at a maximum depth of approximately 250 µm. The histologic correspondence of some confocal features has been demonstrated,[14-20] although numerous patterns still have to be clearly defined. The increasing interest in using RCM in specialized skin cancer centers derives from the possibility of having a more accurate presurgical diagnosis for different skin tumors, resulting in demonstrated improvement in diagnostic accuracy, especially for basal cell carcinoma and melanocytic lesions, also with respect to dermoscopy.[13,26] The need to position a metal ring with adhesive tape for the examination of a single lesion limits RCM's application as a screening tool, and its use remains restricted to selected lesions. For this reason, RCM can be efficiently applied on dermoscopically difficult lesions, enabling the improvement of diagnostic specificity.[12,13] Recently, Scope and coworkers[18] demonstrated the good positive correlation between the global dermoscopic pattern and confocal mosaics at the dermoepidermal junction and a correspondence between confocal aspects and specific dermoscopic features, such as atypical pigment network, pigment globules, peripheral streaks, and a blue-whitish veil, on 11 lesions. Subsequently, the same authors focused their analysis on 7 cases that presented with peripheral streaks, enabling confocal-histologic relations and distinction among different morphologic subtypes on the basis of their confocal aspects.[19]

This study aimed to explore systematically the confocal substrates of the dermoscopic features of melanocytic lesions, with the exception of site-specific patterns, to obtain a comprehensive description and characterization of the underlying cytologic and architectural features and to correlate them with histopathologic features. In detail, the identification of single large, bright cells in superficial layers, the basal layer, and the papillary dermis or the presence of clusters of pleomorphic cells may help to interpret some underlying dermoscopic features that are characteristic of malignant neoplasms. The overall analysis of RCM features in a large population of dermoscopically equivocal melanocytic lesions showed the capability of this technique in improving diagnostic specificity for MM.[13] On the other hand, the present study suggests that RCM examination should be conducted focusing on specific dermoscopic features to better discover RCM diagnostic clues, whereas areas presenting with dermoscopic features that usually lack RCM diagnostic substrates should be avoided. Tight correspondence between network holes and dermal papillae, network meshes and interpapillary spaces, and pigment globules and cell clusters was confirmed.[14-20] Cytologic and architectural atypia on RCM was predominantly present in MMs and strongly correlated with histologic features. Otherwise, the observation of large cells within dense clusters in dermal nevi should not be interpreted as cytologic atypia, corresponding to larger melanocytes in the upper portion of the dermal nests or cords. Although different RCM substrates were confirmed for peripheral streaks, MM-specific aspects were not observable within these structures. Moreover, the histologic substrate of pigment dots was clearly identifiable by RCM, distinguishing between pagetoid melanocytosis, suggestive of a malignant neoplasm, and melanin clumps within the epidermis.

The presence of confocal features suggestive of malignancy, such as atypical melanocytes, pagetoid cells, or nonedged papillae, turned out to be useful for the correct interpretation of dermoscopically indeterminate aspects, such as dark pigmentation, pigment blotches, or blue structures.[2,4,27] As recently demonstrated, RCM was particularly useful for the interpretation of the bluish pigmentation, enabling the distinction between inflammatory infiltrate, predominantly constituted by plump bright cells within dermal papillae corresponding to melanophages, and malignant melanocytic cells, which singularly or in clusters infiltrate the dermis in invasive MMs.[20] On the other hand, within regression areas, RCM failed to identify MM-specific aspects in most cases.

In conclusion, the knowledge of the cytologic and architectural aspects of the different dermoscopic patterns, as they appear by means of RCM, may be useful for the detection of specific substrates in MMs and may lead to a more accurate interpretation of the dermoscopic alterations. Furthermore, the possibility of recognizing in vivo cytologic patterns and following them up over time may help to identify MM precursors and to understand the biology of melanocytic lesions.[28]

Accepted for Publication: October 29, 2007.
Correspondence: Giovanni Pellacani, MD, Department of Dermatology, University of Modena and Reggio Emilia, Via del Pozzo 71, 41100 Modena, Italy (pellacani.giovanni@unimo.it).
Author Contributions: *Study concept and design:* Pellacani, Longo, Malvehy, Puig, and Seidenari. *Acquisition of data:* Longo, Carrera, Segura, and Bassoli. *Analysis and interpretation of data:* Pellacani, Longo, Malvehy, and Puig. *Drafting of the manuscript:* Pellacani and Malvehy. *Critical revision of the manuscript for important intellectual content:* Pellacani, Longo, Malvehy, Puig, and Seidenari. *Study supervision:* Pellacani, Malvehy, Puig, and Seidenari.
Financial Disclosure: None reported.
Funding/Support: This study was partially supported by a grant from the Fondazione Cassa di Risparmio di Modena and by a Emili Letang Personal Grant from the Hospital Clinic of Barcelona to Dr Segura.
Additional Contributions: Cristina Vaschieri, PhD, Department of Dermatology, University of Modena and Reggio Emilia, provided technical assistance.

REFERENCES

1. Pehamberger H, Steiner A, Wolff K. In vivo epiluminescence microscopy of pigmented skin lesions, I: pattern analysis of pigmented skin lesions. *J Am Acad Dermatol.* 1987;17(4):571-583.

Downloaded from www.archdermatol.com at Universidad de Cadiz, on November 16, 2009
©2008 American Medical Association. All rights reserved.

2. Kenet RO, Kang S, Kenet BJ, Fitzpatrick TB, Sober AJ, Barnhill RL. Clinical diagnosis of pigmented lesions using digital epiluminescence microscopy: grading protocol and atlas. *Arch Dermatol*. 1993;129(2):157-174.
3. Bafounta ML, Beauchet A, Aegerter P, Saiag P. Is dermoscopy (epiluminescence microscopy) useful for the diagnosis of melanoma? results of a meta-analysis using techniques adapted to the evaluation of diagnostic tests. *Arch Dermatol*. 2001;137(10):1343-1350.
4. Argenziano G, Soyer HP, Chimenti S, et al. Dermoscopy of pigmented skin lesions: results of a consensus meeting via the Internet. *J Am Acad Dermatol*. 2003; 48(5):679-693.
5. Yadav S, Vossaert KA, Kopf AW, Silverman M, Grin-Jorgensen C. Histopathologic correlates of structures seen on dermoscopy (epiluminescence microscopy). *Am J Dermatopathol*. 1993;15(4):297-305.
6. Soyer HP, Kenet RO, Wolf IH, Kenet BJ, Cerroni L. Clinicopathological correlation of pigmented skin lesions using dermoscopy. *Eur J Dermatol*. 2000;10 (1):22-28.
7. Braun RP, Kaya G, Masouye I, Krischer J, Saurat JH. Histopathologic correlation in dermoscopy: a micropunch technique. *Arch Dermatol*. 2003;139(3): 349-351.
8. Rezze GG, Scramim AP, Neves RI, Landman G. Structural correlations between dermoscopic features of cutaneous melanomas and histopathology using transverse sections. *Am J Dermatopathol*. 2006;28(1):13-20.
9. Rajadhyaksha M, Grossman M, Esterowitz D, Webb RH, Andersson RR. In vivo confocal scanning laser microscopy of human skin: melanin provides strong contrast. *J Invest Dermatol*. 1995;104(6):946-952.
10. González S, Swindells K, Rajadhyaksha M, Torres A. Changing paradigms in dermatology: confocal microscopy in clinical and surgical dermatology. *Clin Dermatol*. 2003;21(5):359-369.
11. Langley RGB, Rajadhyaksha M, Dweyer PJ, Sober AJ, Flotte TJ, Andersson RR. Confocal scanning laser microscopy of benign and malignant melanocytic skin lesions in vivo. *J Am Acad Dermatol*. 2001;45(3):365-376.
12. Pellacani G, Cesinaro AM, Seidenari S. Reflectance-mode confocal microscopy of pigmented skin lesions–improvement in melanoma diagnostic specificity. *J Am Acad Dermatol*. 2005;53(6):979-985.
13. Pellacani G, Guitera P, Longo C, Avramidis M, Seidenari S, Menzies S. The impact of in vivo reflectance confocal microscopy for the diagnostic accuracy of melanoma and equivocal melanocytic lesions. *J Invest Dermatol*. 2007;127 (12):2759-2765.
14. Pellacani G, Cesinaro AM, Grana C, Seidenari S. In vivo confocal scanning laser microscopy of pigmented Spitz nevi: comparison of in vivo confocal images with dermoscopy and routine histopathology. *J Am Acad Dermatol*. 2004;51(3): 371-376.
15. Pellacani G, Cesinaro AM, Seidenari S. In vivo assessment of melanocytic nests in nevi and melanomas by reflectance confocal microscopy. *Mod Pathol*. 2005; 18(4):469-474.
16. Pellacani G, Cesinaro AM, Longo C, Grana C, Seidenari S. Microscopic in vivo description of cellular architecture of dermoscopic pigment network in nevi and melanomas. *Arch Dermatol*. 2005;141(2):147-154.
17. Marghoob AA, Charles CA, Busam KJ, et al. In vivo confocal scanning laser microscopy of a series of congenital melanocytic nevi suggestive of having developed malignant melanoma. *Arch Dermatol*. 2005;141(11):1401-1412.
18. Scope A, Benvenuto-Andrade C, Agero AL, Halpern AC, Gonzalez S, Marghoob AA. Correlation of dermoscopic structures of melanocytic lesions to reflectance confocal microscopy. *Arch Dermatol*. 2007;143(2):176-185.
19. Scope A, Gill M, Benveuto-Andrade C, Halpern AC, Gonzalez S, Marghoob AA. Correlation of dermoscopy with in vivo reflectance confocal microscopy of streaks in melanocytic lesions. *Arch Dermatol*. 2007;143(6):727-734.
20. Pellacani G, Bassoli S, Longo C, Cesinaro AM, Seidenari S. Diving into the blue: in vivo microscopic characterization of the dermoscopic blue hue. *J Am Acad Dermatol*. 2007;57(1):96-104.
21. Busam KJ, Charles C, Lee G, Halpern AC. Morphological features of melanocytes, pigmented keratinocytes, and melanophages by in vivo confocal scanning laser microscopy. *Mod Pathol*. 2001;14(9):862-868.
22. Scope A, Benvenuto-Andrade C, Agero AL, et al. In vivo reflectance confocal microscopy imaging of melanocytic skin lesions: consensus terminology glossary and illustrative images. *J Am Acad Dermatol*. 2007;57(4):644-658.
23. Puppin D, Salomon D, Saurat JH. Amplified surface microscopy: preliminary evaluation of a 400-fold magnification in the surface microscopy of cutaneous melanocytic lesions. *J Am Acad Dermatol*. 1993;28(6):923-927.
24. Menzies SW, Crotty KA, McCarthy WH. The morphologic criteria of the pseudopod in surface microscopy. *Arch Dermatol*. 1995;131(4):436-440.
25. Massi D, De Giorgi V, Carli P, Santucci M. Diagnostic significance of the blue hue in dermoscopy of melanocytic lesions: a dermoscopic-pathologic study. *Am J Dermatopathol*. 2001;23(5):463-469.
26. Nori S, Rius-Diaz F, Cuevas J, et al. Sensitivity and specificity of reflectance-mode confocal microscopy for in vivo diagnosis of basal cell carcinoma: a multicenter study. *J Am Acad Dermatol*. 2004;51(6):923-930.
27. Kreusch J, Rassner G. Structural analysis of melanocytic pigment nevi using epiluminescence microscopy: review and personal experiences. *Hautarzt*. 1990; 41(1):27-33.
28. Zalaudek I, Hofmann-Wellenhof R, Soyer HP, Ferrara G, Argenziano G. Naevogenesis: new thoughts based on dermoscopy. *Br J Dermatol*. 2006;154(4): 793-794.

Correction

Error in Byline and Author Contributions. In the Study by Scope et al titled "Correlation of Dermoscopy With In Vivo Reflectance Confocal Microscopy of Streaks in Melanocytic Lesions," published in the June 2007 issue of the *Archives* (2007;143[6]:727-734), the last name of the third author in the byline on page 727 and in the Author Contributions on page 733 was misspelled. The author's name should have read as follows: Cristiane Benvenuto-Andrade, MD.

Downloaded from www.archdermatol.com at Universidad de Cadiz, on November 16, 2009
©2008 American Medical Association. All rights reserved.

Anexo IV: Carrera C, Palou J, Malvehy J, Segura S, Aguilera P, Salerni G, et al. Early stages of melanoma on the limbs of high-risk patients: clinical, dermoscopic, reflectance confocal microscopy and histopathological characterization for improved recognition. Acta Derm Venereol. 2011;91:137-46.

INVESTIGATIVE REPORT

Early Stages of Melanoma on the Limbs of High-risk Patients: Clinical, Dermoscopic, Reflectance Confocal Microscopy and Histopathological Characterization for Improved Recognition

Cristina CARRERA[1], Josep PALOU[1,2], Josep MALVEHY[1,3], Sonia SEGURA[5], Paula AGUILERA[1], Gabriel SALERNI[1], Louise LOVATTO[1], Joan A. PUIG-BUTILLÉ[3,4], Llùcia ALÓS[2] and Susana PUIG[1,3]

Departments of [1]Dermatology, [2]Pathology and [4]Genetics, Melanoma and Dermatopathology Units, Hospital Clínic de Barcelona, [3]Institut d'Investigacions Biomèdiques August Pi i Sunyer (IDIBAPS), Universitat de Barcelona, Spain, CIBER de Enfermedades Raras, Instituto de Salud Carlos III (ISCIII), and [5]Department of Dermatology, Hospital del Mar, Parc de Salut Mar, Barcelona, Spain

Early stages of 36 melanomas on limbs were morphologically characterised. Most occurred in high-risk patients (multiple and/or familial melanoma) attending a referral unit for melanoma and pigmented lesions. None of the tumours was clinically suspicious for melanoma (mean diameter of 4.3 mm). The tumours were classified into four dermoscopic groups: (*i*) prominent network (*n* = 16); (*ii*)delicate network (*n* = 5); (*iii*) hypo-pigmentation with dotted vessels (*n* = 10); and (*iv*) diffuse light pigmentation with perifollicular pigmentation (*n* = 5). Confocal microscopy performed in 12 cases allowed the identification of atypical, single cells within epidermal layers. Histopathology showed marked large atypical cells in a pagetoid spreading pattern in most cases. Significant associations were detected between the third dermoscopic group and naevoid histological appearance and delay in detection, and between the fourth group and lentigo-maligna-like features. Dermoscopy allowed an increase in the suspicious threshold in these difficult melanomas in high-risk patients and enabled the subclassification of early melanomas on the limbs, with a correct confocal and histopathological correlation. Although the biological behaviour of these incipient tumours remains uncertain, the most appropriate treatment seems to be recognition and proper excision. ***Key words: atypical mole syndrome; dermoscopy; dermatoscopy; familial melanoma; melanoma; naevus; reflectance confocal microscopy.***

(Accepted June 23, 2010.)

Acta Derm Venereol 2011; 91: XX–XX.

Cristina Carrera, Department of Dermatology, Melanoma Unit, Hospital Clínic Barcelona, IDIBAPS, Villarroel 170, ES-08036 Barcelona, Spain. E-mail: criscarrer@yahoo.es

There is only one effective treatment for malignant melanoma (MM): complete excision of early stage tumours. *In situ* MMs are the only cases with a 100% cure rate after proper surgery, decreasing to 80–85% in thin MM (under 1 mm Breslow). MMs on the limbs are not well characterised in the literature, especially in the early stages, although they appear to be related to different epidemiological settings (e.g. women with intermittent sun-exposure on the lower limbs) (1, 2).

Atypical mole syndrome (AMS), defined by the presence of more than 100 naevi, and/or more than 10 clinical and dermoscopically atypical naevi, and/or previously excised dysplastic naevi, is the most important independent risk marker for developing MM. In addition, naevi are both possible MM precursors and early MM simulators. In fact, the most difficult task in early detection of MM is to differentiate them from the more frequent benign melanocytic lesions. However, systematic excision of atypical naevi has no benefit in preventing MM in these high-risk patients (3, 4).

It is estimated that 10% of cases of MM occur in a familial setting as an autosomal dominant trait. In approximately 50% of these familial multiple melanoma (FamMM) cases a responsible gene can be found, being *CDKN2A* and *CDK4* the two major susceptibility genes most commonly identified. FamMM cases and their relatives, especially when they are affected by AMS and/or are mutation carriers have a very high risk of MM development, even up to 1000 times over general population. To date, no clinical, dermoscopic, or histopathological special feature has been related to tumours in FamMM (5–7). Polymorphisms in *melanocortin 1 receptor (MC1R)* gene, especially the red hair variants (RHV), are considered low susceptibility genes to MM development, increasing the MM risk up to 10 times in respect to wild type (8). We studied the interaction between these low-risk variants among FamMM cases, and found that they can increase the genetic risk in *CDKN2A* (high-risk gene) mutation carriers by up to 14 times and contribute to a less suspicious clinical and dermoscopic appearance of tumours, less colour, and fewer structures (9).

The clinical ABCDE rule fails to recognise MMs that are small (less than 6 mm in diameter) or that exhibit regular shape and homogeneous colour, are symmetrical or undergo unnoticed changes (10, 11). Dermoscopy is now well accepted as a non-invasive technique that improves the accuracy of skin tumour diagnosis (12–14), and is especially useful in the differential diagnosis of MM simulators or hypopigmented MM, avoiding unnecessary excisions (15–17).

© 2011 The Authors. doi: 10.2340/00015555-1021
Journal Compilation © 2011 Acta Dermato-Venereologica. ISSN 0001-5555

In vivo reflectance-mode laser scanning confocal microscopy (RCM) is a non-invasive imaging technique that allows real-time skin examination at high resolution and thus improves the diagnostic accuracy in MM and other non-melanocytic tumours (18–20).

We performed a retrospective study of 36 very early MMs on limbs. The objectives of this study were: (*i*) to describe the dermoscopic and *in vivo* RCM features in order to improve their future recognition; (*ii*) to correlate these findings with histopathological characteristics of the tumours that could suggest different types of early MM on the limbs in these very early stages.

MATERIALS AND METHODS

A systematic retrospective review of all thin MMs located on limbs diagnosed in a specialised Pigmented Lesion Unit of a referral hospital between 2005 and 2008.

The inclusion criteria were: (*i*) thin MM (< 1 mm Breslow) proven by histopathological examination, located on limbs; (*ii*) clinical, dermoscopic and histopathological data available; and (*iii*) clinically unsuspicious for MM, defined by no clinical ABCD criteria fulfilled.

Complete clinical patient history was recorded, including familial history, previous melanocytic lesions excised and other MM-associated risk factors. Genetic studies were performed when DNA was available. Exons 1alfa, 1beta, 2 and 3, intronic changes IVS2-105 and –34G>T in the *CDKN2A* promoter, and exon 2 from *CDK4* were studied by PCR single-strand conformation polymorphism (PCR-SSCP) analysis and sequencing (7). *MC1R* was studied by direct sequencing (9).

Clinical and dermoscopic images were taken using digital cameras (Olympus Camedia, Canon G7 and/or Nikon Coolpix 4500) and a polarised dermatoscope (DermlitePhoto®; 3 GEN, LLC.Dana Point, CA, USA). In the case of the high-risk patients included in our digital follow-up protocol (21), Mole Max II (Dermamedical Instruments®), able to detect digital clinical and/or dermoscopic changes in a 6-month follow-up, was an additional tool used in the study. Clinical evaluation was based on ABCDE criteria and dermoscopic pattern analysis (22).

Whenever possible, *in vivo* RCM examination was performed with near-infrared reflectance confocal laser scanning microscopes (Vivascope 1500®; Lucid Inc., Henrietta, NY, USA). The instruments and acquisition procedures, as well as the features studied, have been described previously (23).

Conventional haematoxylin-eosin staining and immunohistochemistry (Melan A, HMB45, Ki67) were performed whenever it was considered necessary. Histopathologically, MMs were classified into one of the following groups according to their characteristics:

- Naevoid MM: predominance of nesting pagetoid invasion of the upper layers of epidermis over solitary cells.
- Paget's disease-like MM: characterised by atypical large

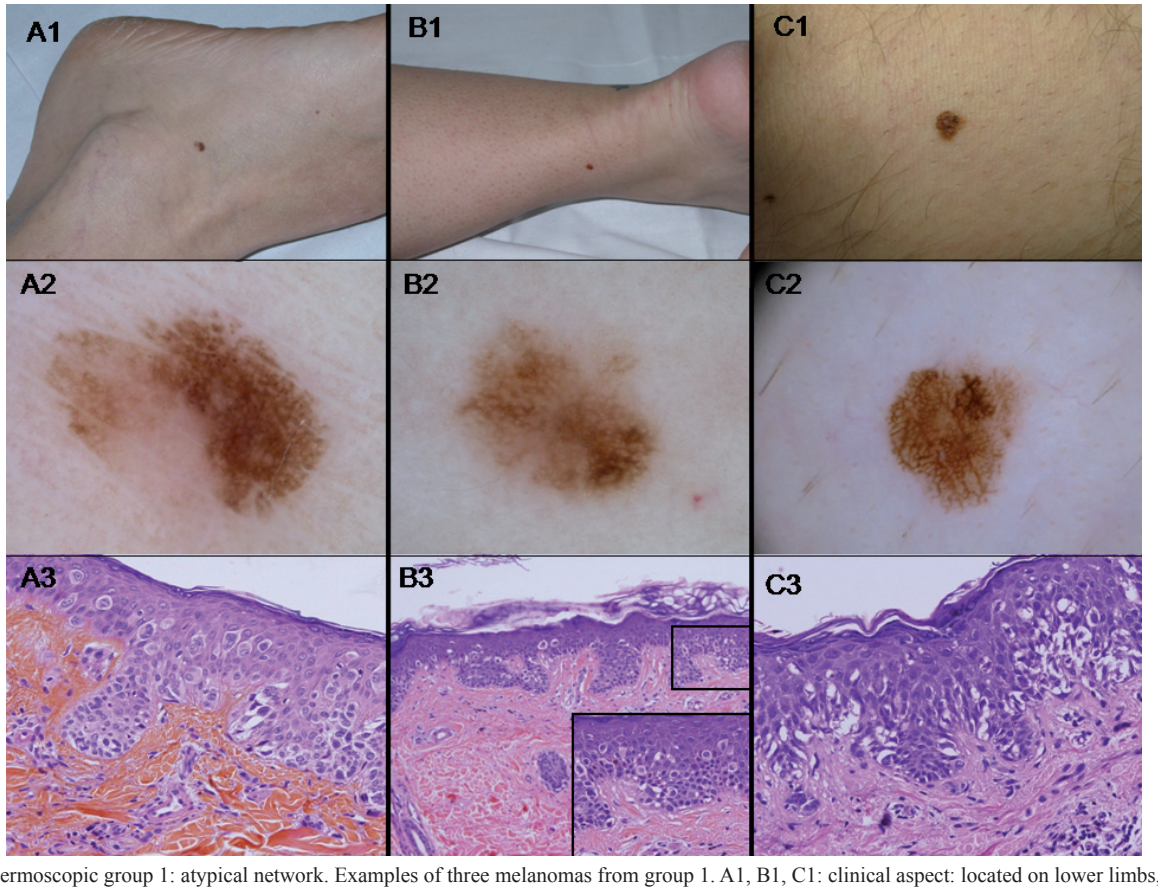

Fig. 1. Dermoscopic group 1: atypical network. Examples of three melanomas from group 1. A1, B1, C1: clinical aspect: located on lower limbs, small dark brown lesions, with no malignant criteria A2, B2, C2: dermoscopic images (original magnification × 30). Prominent network pattern, with two colours and asymmetrical pigment distribution. Case A is completely asymmetrical in one axis. A3, B3, C3: histopathological examination (× 20 (B3) and × 40 (A3, B3 inset and C3)). Proliferation of atypical large melanocytes, both solitary and forming discrete nests, in junctural and intraepidermal layers. These three cases were *in situ* malignant melanoma.

epithelioid cells invading the whole epidermis resembling genuine Paget's disease.
- Lentiginous MM: melanocytic hyperplasia, with severe architectural atypia and intraepidermal spreading. Small nests can be found on the bottom of rete ridges.
- Lentigo maligna-type: atypical melanocytic proliferation along a faded dermal-epidermal junction and flattened epidermis, with solitary and small nests invading the upper epidermis and characteristic follicular involvement. It may be associated with marked actinic damage.

Statistical evaluation was carried out using SPSS statistical software package for Windows (version 16.0; SPSS Inc., Chicago, IL, USA). A chi-square test was applied for all category features, and Fischer's exact test was applied if any expected cell value in the 2×2 table was < 5. Each group was compared with the other three. Mean and median values were determined for quantitative variables and compared using the Student's *t* test.

RESULTS

Patient data

Thirty-six tumours from 35 patients in our high-risk patient-set were reviewed. Tumours were assigned, based on overall appearance in dermoscopic analyses, to one of four groups (for details see below – Dermoscopic examintion): 1, Prominent network (16 tumours, 46%) (Fig. 1); 2, Delicate network with no specific MM dermoscopic features (5 tumours, 14%) (Fig. 2). Melanomas were detected by changes in digital follow-up; 3, Hypopigmented with atypical vessels (10 tumours, 28%), (Fig. 3); and Group 4, Diffuse light pigmentation and perifollicular pigmentation (5 tumours, 14%), (Fig. 4). Patient clinical characteristics are summarised in Table I.

The most remarkable feature was the predomination of women ($n = 29$) over men ($n = 6$), and the presence of high-risk MM history, since 40% had familial MM history, 49% personal MM history, and 17% had multiple primary MMs (MPM) before the current MM diagnosis. The majority of patients (75%) were affected by atypical mole syndrome. Eighteen had been included in our digital follow-up high-risk surveillance programme, which involves total-body photography mapping and digital dermoscopy of atypical lesions every 6 months, as described previously by our group (21).

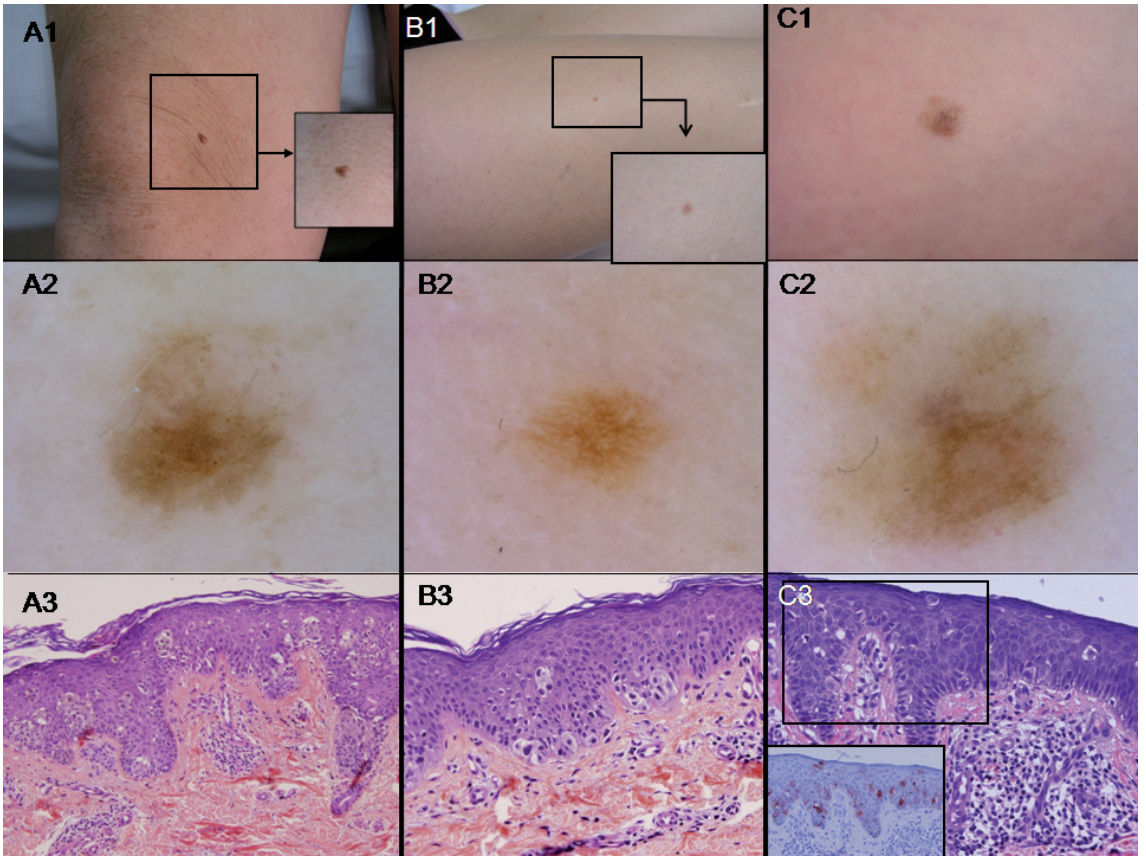

Fig. 2. Dermoscopic group 2: delicate network with changes on digital follow-up. Examples of three melanomas from group 2. A1, B1, C1: clinical aspect: located on lower limbs, the smallest lesions had a completely unremarkable aspect. Case A1 and B1 are mother and daughter, both of them CDKN2A mutation and double-red-hair-variant-MC1R carriers, affected by multiple primary malignant melanoma (MM). A2, B2, C2: dermoscopic images (original magnification ×30). Light-brown very delicate network pattern, with a slight asymmetrical light-brown structureless area in cases A2 and C2 due to a pre-existing naevus. In all cases the lesions were excised due to changes seen in digital follow-up of a very high-risk patient setting. A3, B3, C3 histopathological examination (×20). Proliferation of atypical large melanocytes, both solitary and forming nests, in junctural and intraepidermal layers. All were *in situ* MM. Note the immunohistochemical study in C3 with a more evident pagetoid spreading of Melan-A positive cells.

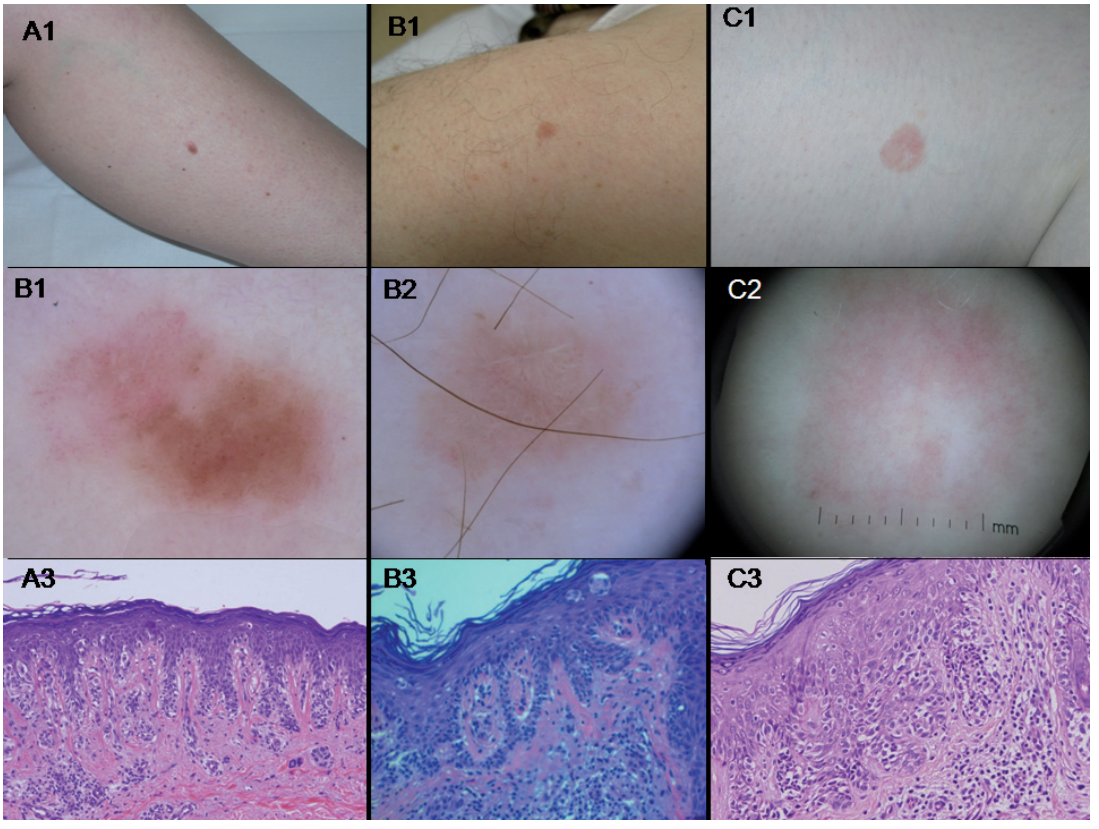

Fig. 3. Dermoscopic group 3: atypical vascular pattern. Examples of three melanomas from group 3. A1, B1, C1: clinical aspect: located on lower limbs, all achromic lesions with erythema. Case C1: albinism type OCA1 in a 34-year-old woman, the largest lesion in the series. A2, B2, C2: dermoscopic images (original magnification × 30). Homogeneous or unspecific pattern, only remarkable by vessels and a light-brown structureless pigmentation. Dotted vessels and whitish linear structures (chrysalides-like) are the only noteworthy features. A3, B3, C3: histopathological examination (× 20). Lentiginous hyperplasia of atypical melanocytes, with mild pagetoid spreading and marked vascular hyperplasia.

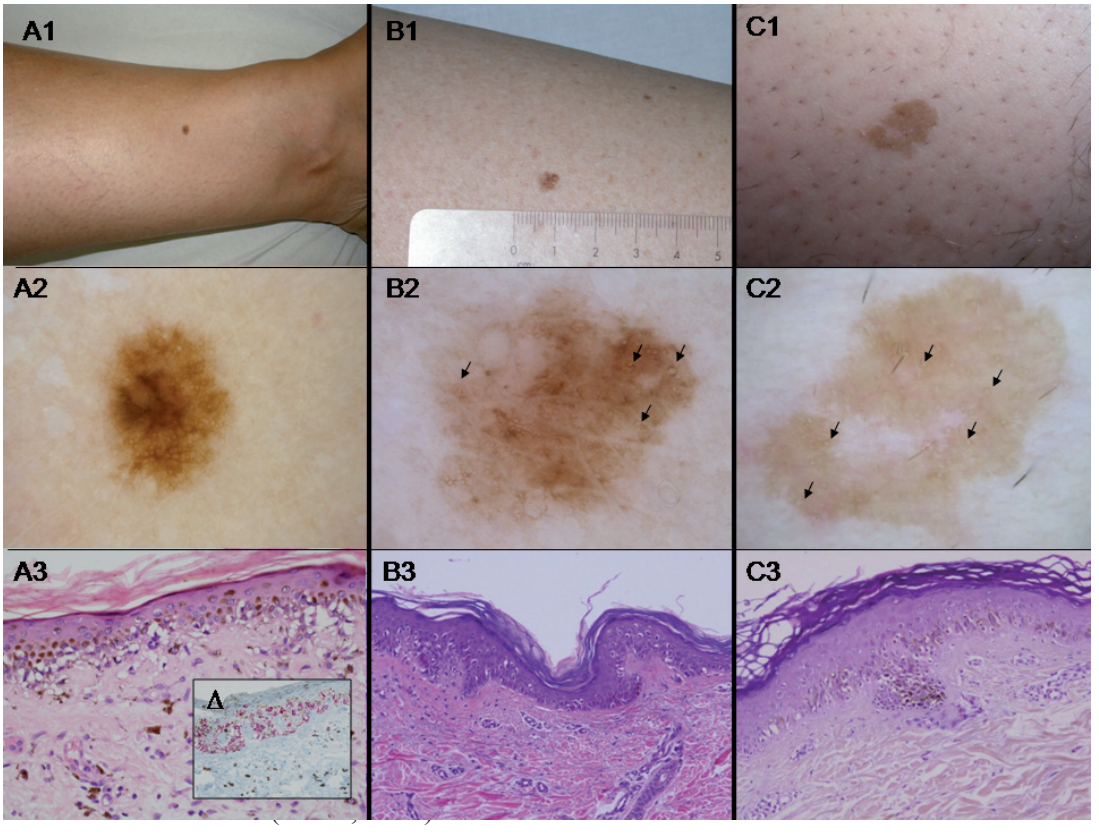

Fig. 4. Dermoscopic group 4: perifollicular pigmentation. Examples of three *in situ* melanomas. A1, B1, C1: clinical aspect: located on lower limbs, the only remarkable feature was irregular borders. A2, B2, C2: dermoscopic images (original magnification × 30). Light-brown structureless pigmentation, with thin and broken pigmented network, and focal hyperpigmentation in case 2. Note some irregular follicular openings (*arrows*). A3, B3, C3: histopathological examination (× 20). Flattened epidermis, with variable elastosis, and proliferation of dendritic melanocytes in both the basal and suprabasal layers. Note the remarkable pagetoid spreading in immunohistochemistry image (Δ) (Melan-A staining).

Table I. *Clinical features of the 35 patients included in this series. Patients were assigned to one of four groups based on the dermoscopic characteristics of their tumours: 1, "Prominent network"; 2, "Delicate network with no specific MM dermoscopic features"; 3, "Hypopigmented with atypical vessels"; and 4, "Diffuse light pigmentation and perifollicular pigmentation". CDKN2A/CDK4 mutation status was assessed in 21 of the 35 patients. MC1R variants were studied in 20 patients. Multiple malignant melanoma (MM): two or more melanomas diagnosed before the present case. Familial MM: two or more melanoma cases among first-degree relatives.*

Patient characteristics	Group 1 $n=16$	Group 2 $n=4$	Group 3 $n=10$	Group 4 $n=5$	Total $n=35$
Sex, *n* (%)					
Female	15 (94)	4 (100)	6 (60)	4 (80)	29 (83)
Male	1 (6)	0 (0)	4 (40)	1 (20)	6 (17)
Age (years), mean ± SD	44.7 ± 14.0	40.4 ± 14.7	49 ± 19.3	50 ± 8.3	46 ± 15.4
Atypical mole syndrome, *n* (%)	12 (75)	4 (100)	8 (80)	2 (40)	26 (75)
Previous MM, *n* (%)	7 (44)	3 (75)	6 (60)	1 (25)	17 (49)
Digital follow-up, *n* (%)	8 (50)	4 (100)	4 (40)	2 (40)	18 (51)
Multiple MM, *n* (%)	2 (12)	3 (75)	1 (10)	0 (0)	6 (17)
Familial MM, *n* (%)	6 (37)	4 (100)	2 (20)	2 (40)	14 (40)
Genetic studies performed, *n* (%)	8 (50)	4 (100)	8 (80)	2 (50)	21 (38)
CDKN2A/CDK4 mutation/studied, *n* (%)	4/8 (50)	3/4 (75)	1/7 (14)	0/2 (0)	8/21 (38)
MC1R/studied, *n* (%)					
Any variant	6/8 (75)	3/3 (100)	8/8 (100)	1/1 (100)	18/20 (90)
Red hair variants	4/8 (50)	3/3 (100)	5/8 (62)	1/1 (100)	10/20 (50)
More than one variant	0/8 (0)	2/3 (66)	5/8 (62)	0/1 (0)	7/20 (35)

SD: standard deviation; MM: malignant melanoma. Note: one patient in group 2 presented with two tumours.

lower limbs, mainly below the knee ($n=28$, 78%). All were less than 6 mm in diameter (except for two lesions, 7 and 8 mm in diameter, both lacking pigment, one of them in a patient affected by oculo-cutaneous albinism type 1). The median diameter was 4.3 mm (SD 1.12 mm, range 3–8 mm). On clinical examination none of them fulfilled ABCD criteria for MM suspicion. Only 15 lesions showed mild asymmetry; none presented more than two colours, and borders were slightly irregular in seven cases.

Dermoscopic examination

Most of the tumours showed two colours and asymmetry in one axis. However, 14 were completely symmetrical and 7 were monochromic. The most frequent overall pattern was reticular pigmented (21 tumours), and no lesion showed a multi-component pattern. An atypical pigmented network was detected in 15 cases, irregular pigment distribution was observed in 20 cases, and atypical vessels in 10 cases. Other worrying, but infrequent, dermoscopic features observed are detailed in Table II.

Based on overall appearance in dermoscopic analyses, tumours were classified into four groups (see above):

- Prominent network, characterised by atypical prominent pigmented network with broadened lines and narrow holes.
- Delicate network with no specific MM dermoscopic features.
- Hypopigmented with atypical vessels, with no classical features of MM, but little or no pigment, and dotted vessels and inverse network in several cases.
- Diffuse light pigmentation and perifollicular pigmentation, simulating solar lentigo but with irregular pigmentation of follicule-openings.

Reflectance confocal microscopy (RCM) examination

All the evaluated lesions ($n=12$) were suspicious for melanoma using the second-step algorithm previously described by our group (24). Positive criteria for melanoma were the presence of a pagetoid spread of atypical cells in eight cases, being roundish in six cases, and dendritic in four (two cases showed both cell types) (Fig. 5); the presence of non-edged papillae in eight cases; and the presence of atypical cells in the basal layer in four cases and in the dermal papilla in three.

In the dermis, non-nucleated dermal cells (plump cells) were observed in four cases, related to the presence of blue regression (peppering) or melanophages in intense pigmented lesions. Vessels were identified in two cases, with tortuous morphology corresponding to atypical vessels seen under dermoscopy.

Dermoscopic features were the main reason for excision in 31 cases; the remaining five cases (dermoscopic group 2) were excised due to minimal changes on digital follow-up in a very-high-risk patient set, despite an unsuspicious clinical and dermoscopic appearance.

Histopathological study

All lesions were evaluated, by two independent pathologists (JP and LA).

Twenty-eight tumours (80%) were *in situ* MMs, and the remaining eight were micro-invasive MMs, Clark II in five cases and Clark III in three cases. The median Breslow index in these was 0.5 mm. There were only

Table II. *Clinical and dermoscopic examination of 36 tumours classified by dermoscopic group.*

	Group 1 $n=16$	Group 2 $n=5$	Group 3 $n=10$	Group 4 $n=5$	Total $n=36$
Clinical tumour features					
Site, *n* (%)					
Lower limbs	16 (100)	5 (100)	7 (70)	5 (100)	33 (92)
Upper limbs	0 (0)	0 (0)	3 (30)	0 (0)	3 (7)
In situ malignant melanoma, *n* (%)	13 (72)	5 (100)	5 (50)	5 (100)	28 (78)
Ugly duckling sign, *n* (%)	1 (6)	0 (0)	1 (10)	0 (0)	2 (5)
Size, mm, mean ± SD	4.12 ± 0.9	3.6 ± 0.9	5 ± 1.4	4.4 ± 0.9	4.3 ± 1.12
Clinical asymmetry, *n* (%)	9 (56)	3 (60)	2 (20)	1 (20)	15 (42)
One colour, *n* (%)	4 (25)	2 (40)	7 (70)	3 (60)	16 (45)
Two colours, *n* (%)	12 (75)	3 (60)	3 (30)	2 (40)	20 (56)
Irregular borders, *n* (%)	4 (25)	0 (0)	0 (0)	3 (60)	7 (20)
Dermoscopic tumour features, n (%)					
Asymmetry in one axis, *n* (%)	11 (70)	3 (60)	5 (50)	3 (60)	22 (60)
Only one colour, *n* (%)	0 (0)	2 (40)	4 (40)	1 (20)	7 (20)
Two colours, *n* (%)	13 (72)	3 (60)	5 (50)	4 (80)	25 (69)
More than two colours, *n* (%)	3 (18)	0 (0)	1 (10)	0 (0)	4 (11)
Reticular pattern, *n* (%)	14 (88)	5 (100)	0 (0)	2 (40)	21 (58)
Globular pattern, *n* (%)	1 (6)	0 (0)	1 (10)	0 (0)	2 (5)
Non-specific global pattern, *n* (%)	1 (6)	0 (0)	9 (90)	3 (60)	13 (35)
Atypical network, *n* (%)	14 (88)	0 (0)	1 (10)	0 (0)	15 (42)
Irregular globules, *n* (%)	5 (31)	0 (0)	3 (30)	0 (0)	8 (22)
Radial streaks /pseudopods, *n* (%)	4 (25)	0 (0)	1 (10)	0 (0)	5 (16)
Hyper/hypopigmented irregular areas, *n* (%)	7 (44)	2 (40)	7 (70)	4 (80)	20 (56)
Irregular blotches, *n* (%)	3 (18)	0 (0)	0 (0)	4 (80)	7 (20)
Dotted vessels, *n* (%)	1 (6)	0 (0)	9 (90)	0 (0)	10 (29)
Regression features, *n* (%)	3 (18)	1 (20)	1 (10)	1 (20)	6 (17)
Perifollicular pigmentation, *n* (%)	1 (6)	0 (0)	0 (0)	5 (100)	5 (16)
Negative/inverse network, *n* (%)	0 (0)	0 (0)	3 (30)	0 (0)	3 (8)

five cases of MM witn a melanocytic neavus associated in histopathological examination..

Based on the histopathological classification of incipient MMs explained in the Materials and Methods, we were able to divide our cases into groups and to study their possible associations with different dermoscopic groups (Table III). Thirteen cases were classified as naevoid-like MM, with statistically significant associations with marked nesting ($p<0.001$) and marked vascular hyperplasia ($p<0.05$). Eleven cases were classified as pagetoid MM-type, with marked pagetoid invasion of the epidermis, and association with very large roundish atypical cells in most cases ($p<0.03$). Six cases were considered lentiginous MM-type, with

Table III. *Histopathological examination of 36 tumours classified by dermoscopic group. Column headings indicate total numbers and percentages. Note that it was not possible to review the histopathological features of one tumour in group 1 (total of 35 tumours examined), unlike in the clinical/dermoscopic diagnosis (all 36 tumours studied).*

Histopathological features	Group 1 $n=15$	Group 2 $n=5$	Group 3 $n=10$	Group 4 $n=5$	Total $n=35$
Histological classification					
Naevoid malignant melanoma	4 (27)	2 (40)	7 (70)	0 (0)	13 (38)
Pagetoid malignant melanoma	8 (54)	2 (40)	1 (10)	0 (0)	11 (31)
Lentiginous malignant melanoma	3 (20)	1 (20)	2 (20)	0 (0)	6 (17)
Lentigo malignant melanoma-like	0 (0)	0 (0)	0 (0)	5 (100)	5 (14)
Naevus-associated	2 (13)	1 (20)	2 (20)	0 (0)	5 (14)
Marked nest tendency	5 (33)	3 (60)	9 (90)	1 (20)	18 (51)
Marked lentiginous melanocytic hyperplasia	5 (33)	1 (20)	4 (40)	3 (60)	13 (37)
Marked pagetoid spreading	10 (66)	4 (80)	6 (60)	3 (60)	23 (66)
Marked vascular hyperplasia	1 (7)	1 (20)	4 (40)	0 (0)	11 (31)
Marked inflammatory infiltrates	4 (27)	1 (20)	7 (70)	0 (0)	12 (34)
Atypical large cells	6 (40)	2 (40)	2 (20)	1 (20)	11 (31)
Atypical epithelioid-like cells	11 (73)	3 (60)	8 (80)	3 (60)	25 (72)
Histological diagnosis					
Clark I	13 (90)	5 (100)	5 (50)	5 (100)	28 (80)
Clark II	2 (14)	0 (0)	3 (30)	0 (0)	5 (14)
Clark III	1 (7)	0 (0)	2 (20)	0 (0)	2 (6)
Mean Breslow thickness (8 cases), mm	0.41 ± 0.1	–	0.56 ± 0.05	–	0.50 ± 0.1

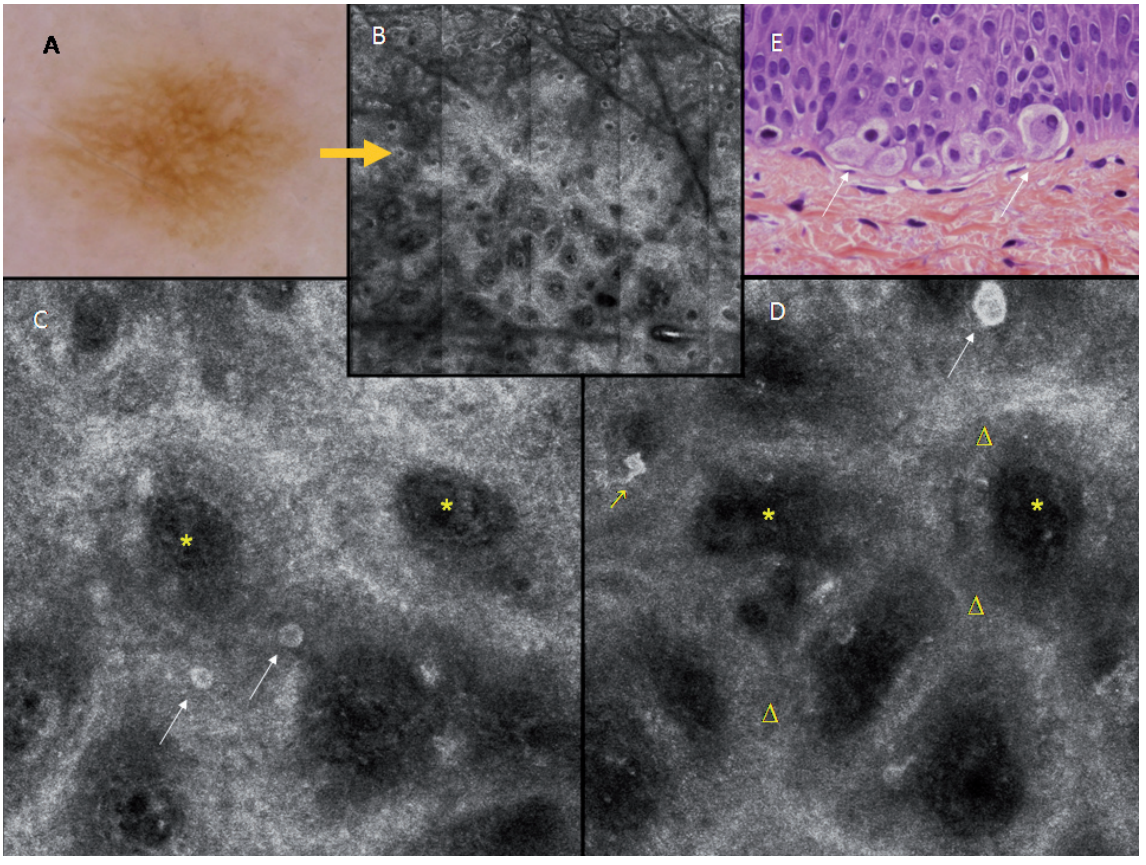

Fig. 5. A: Dermoscopic image of a new pigmented lesion on the knee of a group 2 patient (original magnification × 50). Light-brown, symmetrical pigmented network. B: *In vivo* RCM image sequence in a 4 × 4 mm mosaic: ringed architecture at the dermo-epidermal junction, with (× 30) irregular elongated regular rete ridges with an increased number of refractive cells in the basal layer. C and D: 500 × 500 µm RCM images. Non-edged papillae: dark dermal papillae irregular in size and shape (*), without a demarcated rim of bright cells, separated by interpapillary spaces of different thicknesses (Δ). Scattered atypical junctional nucleated roundish cells at layer (*white arrows*), with a single dendritic cell (*thin yellow arrow*). E: Histopathological examination (original magnification × 200). Atypical large and roundish melanocytes in the dermo-epidermal layer corresponding to the highlighted cells in the RCM and histopathological images.

this characteristic architecture as the most remarkable feature. And the remaining five cases were classified as lentigo-maligna-like MMs. However, not all of these five cases showed signs of elastosis.

Defining features of each dermoscopic group

The first group (atypical prominent network) was associated with lesions that were clinically and dermoscopically more pigmented and polychromic ($p < 0.05$). *In vivo* RCM demonstrated that four lesions presented striking pagetoid spreading of atypical cells. Histopathologically, group 1 was associated with the most marked pagetoid spreading of atypical solitary cells, so-called Pagetoid-type MM (eight cases, 54% of this group, $p = 0.02$). The diagnosis was *in situ* MM in 13 cases (90%) (Table IV).

The second group (delicate light-brown pigmented network) contained the smallest tumours (mean diameter 3.6 mm), with weak pigmentation, which explains in part the unremarkable aspect of these incipient tumours, and is congruent with *MC1R* variants status. The three patients studied had red hair and multiple variants in *MC1R*. Confocal detection of pagetoid cells within the upper epidermis aided the diagnosis in three cases. All were *in situ* MMs (Table IV).

The third group (hypopigmented or achromic lesions with atypical vasculature) was the second most frequent pattern, and the only **one** detected in MM located on upper limbs (30% vs. 0%). The mean size of lesions was slightly larger than the other groups (5 mm ± 1.4 mm), and in two cases the tumour was the reason for consultation because of erythema and pruritus. Most lesions (90%) showed an unspecific overall dermoscopic pattern ($p < 0.001$) and atypical vascularisation, with dotted vessels ($p < 0.001$). In addition three cases (30%) presented an inverse network ($p < 0.05$). This group comparing with the other 3, contains the most invasive tumours (*in situ* MM: 50% vs. 88% in the remaining groups, $p < 0.03$; Clark II/III: 50% vs. 9% in the other groups, $p < 0.01$). The third group was statistically associated with the histopathological naevoid MM type ($p = 0.01$), and it was also possible to observe a marked vascular hyperplasia and inflammatory infiltrates (Table IV).

Table IV. *Characterisation of each malignant melanoma (MM) subgroup. For each group, the most remarkable features are listed.*

Characteristic features	*n* (%)*	Significance (Fisher's exact test)
Group 1 (16 patients, 16 tumours)		
Female	15 (94)	NS
>1 colour clinically	12 (75)	0.04
>1 colour dermoscopically	16 (100)	<0.05
Network global pattern	14 (88)	0.01
Atypical network	14 (88)	0.01
In situ MM	13 (90)	NS
Pagetoid-type MM (histopathological)	8 (54)	0.02
Group 2 (4 patients, 5 tumours)		
Female	4 (100)	NS
Multiple primary MM	3 (75)	<0.01
Familial multiple MM	4 (100)	<0.03
Diameter (mm), median (SD)	3.6 (0.09)	NS (Student's *t*-test)
Network global pattern	5 (100)	<0.01
Diagnosed by changes in digital FU	5 (100)	<0.001
In situ MM	5 (100)	NS
Group 3 (10 patients, 10 tumours)		
Male	4 (40)	0.04
Multiple *MC1R* variants	5 (62)†	0.05
Upper limbs	3 (30)	0.02
Only one colour clinically	7 (70)	<0.05
Only one colour dermoscopically	4 (40)	<0.05
Non-specific global pattern	9 (90)	0.01
Dotted vessels	9 (90)	0.01
Inverse negative network	3 (30)	<0.05
Invasive MM	5 (50)	0.03
Naevoid-type MM	7 (70)	0.01
Marked nested tendency	9 (90)	<0.05
Marked vascular hyperplasia	4 (40)	0.05
Marked inflammatory infiltrates	7 (70)	0.01
Group 4 (5 patients, 5 tumours)		
Female	4 (80)	NS
Irregular borders clinically	3 (60)	0.03
Irregular blotches dermoscopically	4 (80)	0.01
Perifollicular pigmentation	5 (100)	<0.001
In situ MM	5 (100)	NS
Lentigo-type MM (histopathological)	5 (100)	<0.001

*Unless otherwise indicated

†Five cases out of eight studied.

NS: not significant in Fisher's exact test analysis. FU: follow-up.

In the fourth group (light-brown structureless and perifollicular pigmentation), a solar lentigo appearance with irregular borders (three cases) was the most remarkable clinical feature. The dermoscopy criterion for suspicion was pigmentation of the perifollicular openings over a lighter brown structureless pigmentation. These five tumours were *in situ* MM with atypical cells invasion of follicles similar to lentigo-maligna-MM but without extensive elastosis (Table IV).

DISCUSSION

Based on this review, mainly dermoscopy, sometimes aided by digital follow-up (DFU) and/or RCM, allowed the excision of 36 early MMs on limbs with unsuspicious clinical aspects.

Our aim was to characterise *in vivo* and *ex vivo* thin MMs on limbs diagnosed over the last 3 years in our unit. A large proportion of the patients in this series belong to a very high-risk MM setting: 49% were affected by previous MPM, 40% had a FamMM syndrome and 75% were affected by AMS. These data are consistent with a population attending a specific pigmented lesions unit in a referral hospital such as ours. The proportion of female patients cannot be explained on the basis of FamMM or MPM (7) and is consistent with the predominant incidence of melanoma on the lower limb in females and on the trunk in males in our general population, as is the case in most countries.

Both primary and secondary prevention strategies are especially important in these families, as the risk of MM may reach 1000 times that in the general population. Early detection of MM without an increase in unnecessary excisions is important in these cases (4–7). To date, the only way to identify this population is through their medical history. However, it would be of great interest to find special clinical, dermoscopic or histopathological features for tumours that form as a result of genetic factors. It has been demonstrated that dermatological surveillance programmes involving total-body photography, digital dermoscopy and *in vivo* RCM are feasible and allow early diagnosis of most *in situ* or micro-invasive MMs, thus avoiding unnecessary excision of benign lesions (optimal ratio benign/malignant) (4, 20, 21, 25). Genetic studies in MM families facilitate the identification of high-risk non-affected individuals who may benefit from specific surveillance programmes. FamMM is a potential pathological candidate for genetic counselling (5–7).

The gender and location of the tumours in this series agree with the well-established higher prevalence of MM on the lower limbs in women (26–28). We also found a higher proportion of male cases among the few upper limb MMs included.

Clinically all lesions were very small and not intensely pigmented, and the clinical "ugly duckling" sign only helped to identify them in only two cases. Our series showed that incipient MMs do not usually present the classical malignant appearance and therefore do not fulfil the ABCD criteria. We should, however, assume it is a feasible and useful tool for MM screening among the general population and for use by general practitioners, but not acceptable for use by dermatologists. This clinically unremarkable appearance and the lack of the "ugly duckling" sign in the majority of cases, reminds us that it is important not to clinically pre-select lesions for dermoscopy (29), especially in high-risk patients. Recently, Zalaudek et al. (30) demonstrated that the time needed for complete skin examination aided by dermoscopy is only one minute longer than for that without, and complete

examination with dermoscopy, even in cases with a high naevi count, took approximately 3 min.

In dermoscopic analysis none of our cases showed a multi-component pattern, or marked asymmetry in structure or pigmentation, which are considered clues for recognising MM. This emphasises the importance of finding other dermoscopy features in these early and difficult lesions, such as those we propose in this series, for small, symmetrical and hypopigmented lesions (15–17, 31, 32).

The main open question regards the potential malignant behaviour of these tumours. Obviously, the only way to truly demonstrate the malignant nature of a melanocytic lesion is through the development of metastasis. However, the clinical/dermoscopic and histopathological morphological features of a tumour are usually sufficient to make a diagnosis. As we are now detecting tumours at such an early stage, it is difficult to observe the classical and marked malignant features of more advanced MM. On the other hand, it may be possible that these lesions would never evolve to more invasive MM. Khalifeh et al. (33) reported a series of 11 atypical melanocytic lesions on distal lower limbs, especially on the ankle, which they consider as benign tumours that could be misdiagnosed as MM *in situ*. They concluded that these were benign lesions based on mild cytological atypia, no pagetoid spreading, and no recurrence after a follow-up period of between 4 months and 13 years. These cases showed some similarities to ours, but we found pagetoid invasion in the epidermis in all cases. A benign outcome in such lesions is possible. However; observation of only 11 cases is not sufficient to confirm a benign behaviour.

In agreement with previous studies on RCM in MM, the most frequent features associated with malignancy are the partial or total loss of the honeycomb pattern, pagetoid spreading of roundish or dendritic cells, and irregular or non-edged papillae (24, 34, 35). In our series, despite the unremarkable clinical appearances of the 36 tumours, we were able, based on dermoscopic classification, to establish good correlations between dermoscopic presentation and confocal and histopathological features. In at least two cases in which clinical and dermoscopic features were suggestive of benign lesions or inconclusive, confocal examination according to a two-step algorithm recently described by our group (24) increased our suspicion and led us to decide on excision instead of follow-up.

Based on our experience, we propose a dermoscopic classification of the early stages of MM on the limbs that could help the further investigation of possible different origins, such as has been proposed in recent observations regarding cutaneous stem cells (36, 37) and MM pathways.

The distribution of *in situ* MMs among the dermoscopic groups was not uniform. Between 90% and 100% of cases in groups 1, 2 and 4 were *in situ* MMs, whereas 50% of MM in group 3 (hypopigmented with atypical vessels) were *in situ* MMs. This may be explained by a delay in diagnosis for more deeply invasive lesions with lesions with greater diameters, which agrees with our observation in a study of MC1R polymorphisms, and which could contribute to a hypopigmented MM aspect with fewer dermoscopic features, thus implying a more difficult early diagnosis (9).

In conclusion, we reviewed 36 cases of very early MMs on the limbs. None of these cases could have been diagnosed by clinical examination alone. Dermoscopy aided by digital follow-up and occasionally by confocal microscopy encouraged us to excise these clinically unsuspicious lesions. The limitation of this retrospective series is that it is not possible to compare these morphological features with those of excised benign lesions, or to confirm the future malignant behaviour of these incipient tumours. Obviously not all thin MMs will disseminate, and not all *in situ* and micro-invasive MMs will become invasive and life-threatening. However, several of the present patients belong to families affected by FamMM, and unfortunately some relatives had died from MM-associated metastasis. Therefore, our aim must be for all MMs in these high-risk patients to be diagnosed at the *in situ* stage. Finally, we can conclude that, despite a banal clinical aspect, melanocytic lesions on the limbs can present some dermoscopic or confocal features that raise suspicion. All of these tumours should be removed or have a short-term follow-up, especially in the case of the very high-risk population attending a referral pigmented lesions unit.

ACKNOWLEDGEMENTS

This work is dedicated to all our willing patients, who have always collaborated and helped us to improve our knowledge of their disease. We are indebted to our dermatologist colleagues, biologists and nurses, who work together on a daily basis and whose effort is not always reflected in investigative papers. We also thank Gillian Randall for her help with the text edition.

This project has been partially supported by Fondo de Investigaciones Sanitarias (FIS), grant 06/0265; Red de Centros de Cáncer C03/10, ISCIII, and the European Union Network of Excellence: 018702 and "The Melanoma Genetic Consortium", National Cancer Institute (National Institute of Health) USA.

The authors declare no conflicts of interest.

REFERENCES

1. Leiter U, Buettner PG, Eigentler TK, Garbe C. Prognostic factors of thin cutaneous melanoma: an analysis of the central malignant melanoma registry of the German Dermatological Society. J Clin Oncol 2004; 22: 3660–3667.
2. Garbe C, Leiter U. Melanoma epidemiology and trends. Clin Dermatol 2009; 27: 3–9.
3. Tsao H, Bevona C, Goggins W, Quinn T. The transformation rate of moles (melanocytic naevi) into cutaneous melanoma. A population-based estimate. Arch Dermatol

2003; 139: 282–288.
4. Carli P, De Giorgi V, Crocetti E, Mannone F, Massi D, Chiarugi A, Giannotti B. Improvement of malignant/benign ratio in excised melanocytic lesions in the 'dermoscopy era': a retrospective study 1997–2001. Br J Dermatol 2004; 150: 687–692.
5. Bishop JN, Harland M, Randerson-Moor J, Bishop DT. Management of familial melanoma. Lancet Oncol 2007; 8: 46–54.
6. Bergman W, Gruis NA. Phenotypic variation in familial melanoma consequences for predictive DNA testing. Arch Dermatol 2007; 143: 525–526.
7. Puig S, Malvehy J, Badenas C, Ruiz A, Jimenez D, Cuellar F, et al. Role of the CDKN2A locus in patients with multiple primary melanomas. J Clin Oncol 2005; 23: 3043–3051.
8. Goldstein AM, Chaudru V, Ghiorzo P, Badenas C, Malvehy J, Pastorino L, et al. Cutaneous phenotype and MC1R variants as modifying factors for the development of melanoma in CDKN2A G101W mutation carriers from 4 countries. Int J Cancer 2007; 121: 825–831.
9. Cuéllar F, Puig S, Kolm I, Puig-Butille J, Zaballos P, Martí-Laborda R, et al. Dermoscopic features of melanomas associated with MC1R variants in Spanish CDKN2A mutation carriers. Br J Dermatol 2009; 160: 48–53.
10. Wolf IH, Smolle J, Soyer HP, Kerl H. Sensitivity in the clinical diagnosis of malignant melanoma. Melanoma Res 1998; 8: 425–429.
11. Goldsmith SM, Solomon AR. A series of melanomas smaller than 4 mm and implications for the ABCDE rule. J Eur Acad Dermatol Venereol 2007; 21: 929–934.
12. Bafounta ML, Beauchet A, Aegerter P, Saiag P. Is dermoscopy (epiluminescence microscopy) useful for the diagnosis of melanoma? Results of a meta-analysis using techniques adapted to the evaluation of diagnostic tests. Arch Dermatol 2001; 137: 1343–1350.
13. Kittler H, Pehamberger H, Wolff K, Binder M. Diagnostic accuracy of dermoscopy. Lancet Oncol 2002; 3: 159–165.
14. Carli P, de Giorgi V, Chiarugi A, Nardini P, Weinstock MA, Crocetti E, et al. Addition of dermoscopy to conventional naked-eye examination in melanoma screening: a randomized study. J Am Acad Dermatol 2004; 50: 683–689.
15. Argenziano G, Zalaudek I, Ferrara G, Johr R, Langford D, Puig S, et al. Dermoscopy features of melanoma incognito: indications for biopsy. J Am Acad Dermatol 2007; 56: 508–513.
16. Puig S, Argenziano G, Zalaudek I, Ferrara G, Palou J, Massi D, et al. Melanomas that failed dermoscopic detection: a combined clinicodermoscopic approach for not missing melanoma. Dermatol Surg 2007; 33: 1262–1273.
17. Menzies SW, Kreusch J, Byth K, Pizzichetta MA, Marghoob A, Braun R, et al. Dermoscopic evaluation of amelanotic and hypomelanotic melanoma. Arch Dermatol 2008; 144: 1120–1127.
18. Pellacani G, Cesinaro AM, Seidenari S. Reflectance-mode confocal microscopy of pigmented skin lesions-improvement in melanoma diagnostic specificity. J Am Acad Dermatol 2005; 53: 979–985.
19. Gerger A, Koller S, Weger W, Richtig E, Kerl H, Samonigg H, et al. Sensitivity and specificity of confocal laser-scanning microscopy for in vivo diagnosis of malignant skin tumors. Cancer 2006; 107: 193–200.
20. Pellacani G, Guitera P, Longo C, Avramidis M, Seidenari S, Menzies S. The impact of in vivo reflectance confocal microscopy for the diagnostic accuracy of melanoma and equivocal melanocytic lesions. J Invest Dermatol 2007; 127: 2759–2765.
21. Malvehy J, Puig S. Follow-up of melanocytic skin lesions with digital total-body photography and digital dermoscopy: a two-step method. Clin Dermatol 2002; 20: 297–304.
22. Argenziano G, Soyer HP, Chimenti S, Talamini R, Corona R, Sera F et al. Dermoscopy of pigmented skin lesions: results of a consensus meeting via the Internet. J Am Acad Dermatol 2003; 48: 679–693.
23. Scope A, Benvenuto-Andrade C, Agero AL, Malvehy J, Puig S, Rajadhyaksha M, et al. In vivo reflectance confocal microscopy imaging of melanocytic skin lesions: consensus terminology glossary and illustrative images. J Am Acad Dermatol 2007; 57: 644–658.
24. Segura S, Puig S, Carrera C, Palou J, Malvehy J. Development of a two-step method for the diagnosis of melanoma by reflectance confocal microscopy. J Am Acad Dermatol 2009; 61: 216–229.
25. Kittler H, Guitera P, Riedl E, Avramidis M, Teban L, Fiebiger M, et al. Identification of clinically featureless incipient melanoma using sequential dermoscopy imaging. Arch Dermatol 2006; 42: 1113–1119.
26. Clark LN, Shin DB, Troxel AB, Khan S, Sober AJ, Ming ME. Association between the anatomic distribution of melanoma and sex. J Am Acad Dermatol 2007; 56: 768–773.
27. Cho E, Rosner BA, Colditz GA. Risk factors for melanoma by body site. Cancer Epidemiol Biomarkers Prev 2005; 14: 1241–1244.
28. Silva Idos S, Higgins CD, Abramsky T, Swanwick MA, Frazer J, Whitaker LM, et al. Overseas sun exposure, naevus counts, and premature skin aging in young english women: a population-based survey. J Invest Dermatol 2009; 129: 50–59.
29. Seidenari S, Longo C, Giusti F, Pellacani G. Clinical selection of melanocytic lesions for dermoscopy decreases the identification of suspicious lesions in comparison with dermoscopy without clinical preselection. Br J Dermatol 2006; 154: 873–879.
30. Zalaudek I, Kittler H, Marghoob AA, Balato A, Blum A, Dalle S, et al. Time required for a complete skin examination with and without dermoscopy: a prospective, randomized multicenter study. Arch Dermatol 2008; 144: 509–513.
31. Fikrle T, Pizinger K. Dermatoscopic differences between atypical melanocytic naevi and thin malignant melanomas. Melanoma Res 2006; 16: 45–50.
32. Pizzichetta MA, Talamini R, Stanganelli I, Puddu P, Bono R, Argenziano G, et al. Amelanotic/hypomelanotic melanoma: clinical and dermoscopic features. Br J Dermatol 2004; 150: 1117–1124.
33. Khalifeh I, Taraif S, Reed JA, Lazar AF, Diwan AH, Prieto VG. A subgroup of melanocytic naevi on the distal lower extremity (ankle) shares features of acral naevi, dysplastic naevi, and melanoma in situ: a potential misdiagnosis of melanoma in situ. Am J Surg Pathol 2007; 31: 1130–1136.
34. Scope A, Benvenuto-Andrade C, Agero AL, Halpern AC, Gonzalez S, Marghoob AA. Correlation of dermoscopic structures of melanocytic lesions to reflectance confocal microscopy. Arch Dermatol 2007; 143: 176–185
35. Pellacani G, Longo C, Malvehy J, Puig S, Carrera C, Segura S, et al. In vivo confocal microscopic and histopathologic correlations of dermoscopic features in 202 melanocytic lesions. Arch Dermatol 2008; 144: 1597–1608.
36. Zalaudek I, Marghoob AA, Scope A, Leinweber B, Ferrara G, Hofmann-Wellenhof R, et al. Three roots of melanoma. Arch Dermatol 2008; 144: 1375–1379.
37. Grichnik JM. Melanoma, nevogenesis, and stem cell biology. J Invest Dermatol 2008; 128: 2365–2380.

Anexo V: Definición de los criterios de microscopía confocal de reflectancia en tumores cutáneos

A. LESIONES MELANOCÍTICAS

Criterio confocal	**Descripción**	**Lesión asociada**
Epidermis		
Patrón en panal de abejas	Cél. poligonales de 10-20 μm con núcleo oscuro y citoplasma delgado brillante	Piel normal, nevus
Patrón en empedrado	Cél. poligonales pequeñas con citoplasma brillante separado por un reborde menos reflectante	Piel normal, nevus
Patrón desestructurado	Pérdida de la arquitectura normal de la epìdermis con presencia de células y partículas granulares distribuidas de forma irregular y ausencia de patrón en panal o empedrado	Melanoma
Crecimiento pagetoide	Presencia de cél. nucleadas con núcleo oscuro y citoplasma brillante en las capas suprabasales	Melanoma, nevus Spitz
Morfología	La morfología de las cél. puede ser redonda o con proyecciones dendríticas	
Densidad	Densidad leve si ≤ 3 cél. por campo visión 0,5x0,5 mm, mod-intenso si >3	
Tamaño	Pequeño si el tamaño celular medio es <20μm, grande si es mayor de 20μm	

Unión dermo-epidérmica		
Papilas con contorno	Papilas dérmicas rodeadas por un reborde de células brillantes dando aspecto de anillos reflectantes	Piel normal, nevus
Papilas sin contorno	Papilas dérmicas sin reborde de células brillantes pero separadas por células grandes reflectantes	Melanoma, nevus displásico
Atipia de las cél. basales	Evaluación de la atipia citológica de la capa basal (cél. típicas: cél. pequeñas monomorfas; atipia leve: cél. grandes esporádicas; atipia marcada: cél. irregulares en tamaño, forma y reflectividad)	Nevus displásico, melanoma
Células en sábana	Cél. no agregadas localizadas en la transición de la epidermis y la dermis que ocupan la unión dermo-epidérmica sin poderse visualizar las papilas dérmicas	Melanoma nodular, melanoma en fase de crecimiento vertical
Agregados juncionales	Agregados compactos ovalados de células reflectantes conectados con la capa basal	Nevus juncional
Dermis superficial		
Nidos dérmicos densos	Agregados cel. compactos con márgenes bien definidos y cél. regulares en morfología y reflectividad	Nevus
Nidos dishomogéneos	Agregados celulares irregulares en morfología y reflectividad	Nevus displásico, melanoma
Nidos cerebriformes	Agregados amorfos confluentes formados por cél. de baja reflectividad de bordes mal definidos formando estructuras que remedan las convoluciones cerebrales	Melanoma nodular, melanoma en fase de crecimiento vertical
Cél. dérmicas nucleadas	Cél. no agregadas de redondas a ovaladas con citoplasma brillante y núcleo oscuro visible. Atípicas: más de 20 µm y pleomórficas en tamaño y forma	Nevus, melanoma

Cél. "rellenas" brillantes	Cél. brillantes de forma irregular y bordes mal definidos normalmente con núcleo no visible, a veces agrupadas dentro de las papilas dérmicas	Lesión con melanofagia
Partículas y cél. pequeñas brillantes	Puntos y cél. pequeñas de citoplasma reflectante distribuidas de forma irregular en la dermis	Lesión con inflamación
Vasos dérmicos agrandados	Espacios vasculares visibles con un diámetro superior a los capilares dérmicos de la piel normal, en ocasiones formando tortuosidades	Melanoma, algunos nevus

B. LESIONES NO MELANOCÍTICAS

Criterio confocal	Descripción	Correlación histológica
Carcinoma basocelular		
Patrón epidérmico desestructurado	Pérdida parcial del patrón en panal de abejas de la piel normal	Displasia epitelial en relación daño solar crónico
Islotes tumorales	Islotes tumorales dérmicos hiporeflectantes conectados con la epidermis, rodeados de un espacio oscuro	Nidos de células basaloides (hendiduras peritumorales)
Polarización	Células tumorales con núcleos alargados orientados en el mismo axis	Empalizadas de las células tumorales
Estructuras dendríticas	Estructuras dendríticas reflectantes delgadas o gruesas en el interior de los islotes tumorales a menudo asociadas a una célula nucleada	Melanocitos dendríticos en el interior del tumor
Células "rellenas" brillantes	Cél. brillantes de forma irregular y bordes mal definidos, normalmente sin núcleo visible, distribuidas por el interior y alrededor de los nódulos tumorales	Melanófagos
Vascularización prominente	Vasos capilares agrandados, de disposición horizontal y frecuentemente tortuosos con fenómeno de *rolling* (desplazamiento de leucocitos a lo largo de la pared del vaso)	Neo-vascularización dérmica asociada al tumor

Queratosis seborreica		
Tapones y quistes córneos	Estructuras brillantes en capas de cebolla en la superficie epidérmica (tapones) y estructuras homogéneas redondeadas brillantes intraepidérmicas(quistes)	Invaginaciones de la epidermis rellenas de queratina
Criptas	Pliegues hiporeflectantes profundos en estratos epidérmicos	Invaginaciones en la superficie de la lesión
Cordones epiteliales reflectantes (QS reticuladas y lentigos solares)	Estructuras hiperreflectantes en la unión de dermo-epidérmica formando cordones interconectados, constituidos por agregados celulares de bordes mal definidos	Hiperplasia lentiginosa de la epidermis con pigmentación de la capa basal
Tumor vascular		
Espacios vasculares	Espacios oscuros de contorno reflectante ocupando toda la dermis, por donde circulan células sanguíneas	Proliferación de estructuras vasculares en la dermis
Dermatofibroma		
Papilas con contorno	Papilas dérmicas rodeadas por un reborde de células brillantes dando aspecto de anillos reflectantes	Hiperplasia epitelial con elongación de los procesos interpapilares y pigmentación de la basal
Colágeno dérmico engrosado	Estructuras brillantes fibrilares en dermis de tamaño más grueso al de la piel normal	Densificación del colágeno dérmico y proliferación fuso-celular

Queratosis actínica		
Escama	Material amorfo de reflectividad variable	Hiperqueratosis
Células nucleadas poligonales en la capa córnea	Células bien delimitadas con un contorno fino reflectante que rodea un núcleo oscuro	Paraqueratosis
Patrón en panal de abejas atípico/desestructurado	Diversos grados de desestructuración del epitelio y pérdida de la arquitectura en panal de abejas de la piel normal	Atipia epitelial
Células nucleadas redondas en estrato espinoso-granuloso	Células bien delimitadas con un contorno fino reflectante que rodea un núcleo oscuro	Queratinocitos atípicos o cél. disqueratósicas
Vasos capilares redondos atravesando las papilas dérmicas	Células sanguíneas en el interior de papilas dérmicas	Capilares dilatados en dermis papilar